AD NUMBER

AD861021

NEW LIMITATION CHANGE

TO

Approved for public release, distribution unlimited

FROM

Distribution authorized to U.S. Gov't. agencies only; Administrative/Operational Use; OCT 1969. Other requests shall be referred to Space and Missile Systems Organization, Attn: SMEA, AF Unit P.O. Los Angeles, CA 90045.

AUTHORITY

SAMSO ltr, 16 Apr 1973

AEDC-TR-69-152

EFFECTS AND CONTROL OF CONTAMINATION FROM A SCALED MOL TRANSLATIONAL THRUSTER IN A LONGITUDINAL ORIENTATION

David W. Hill, Jr. and Dale K. Smith
ARO, Inc.

October 1969

This document may be further distributed by any holder only with specific prior approval of the MOL Project Office (SAFSL-3), AF Unit Post Office, Los Angeles, California 90045.

AEROSPACE ENVIRONMENTAL FACILITY
ARNOLD ENGINEERING DEVELOPMENT CENTER
AIR FORCE SYSTEMS COMMAND
ARNOLD AIR FORCE STATION, TENNESSEE

NOTICES

EFFECTS AND CONTROL OF CONTAMINATION FROM A SCALED MOL TRANSLATIONAL THRUSTER IN A LONGITUDINAL ORIENTATION

David W. Hill, Jr. and Dale K. Smith
ARO, Inc.

FOREWORD

The work reported herein was performed at the request of Space and Missile Systems Organization (SAMSO), Air Force Systems Command (AFSC), under Program Element 35121F, Program Area 632A.

The rocket engine and simulated vehicle skin were designed and fabricated by Marquardt Corporation and McDonnell Douglas Corporation, Missiles and Space Systems Division (MSSD), respectively.

The test results were obtained by ARO, Inc. (a subsidiary of Sverdrup & Parcel and Associates, Inc.), contract operator of the Arnold Engineering Development Center (AEDC), AFSC, Arnold Air Force Station, Tennessee, under Contract F40600-69-C-0001. The tests were conducted from May through December 21, 1968, under ARO Project No. SB0721, and the manuscript was submitted for publication on June 9, 1969.

This technical report has been reviewed and is approved.

Robert T. Otto
Major, USAF
AF Representative, AEF
Directorate of Test

Roy R. Croy, Jr.
Colonel, USAF
Director of Test

ABSTRACT

A test was conducted to determine the effects and control of contamination produced by a 1-lb scaled Manned Orbital Laboratory thruster. The test required firing the 1-lb translational thruster for 205 sec continuously and pulsing in its longitudinal position and determining the effects of contaminates from the thruster impinging on optical and thermal control surface test specimens located on a flat plate exposed to the thruster exhaust plume. The contamination ejected from the thruster in steady-state operation was much less than that of pulse-mode operation. Fences were used on the test plate to shield specimens from the thruster exhaust plume. In situ reflectance, emittance, and transmittance measurements were made on the optical and thermal control surface test specimens surfaces under vacuum conditions and at atmospheric pressure. Pretest and posttest laboratory measurements were made at atmospheric conditions. Contamination deposited on the plate was focused along and near the axis of the thruster. Contamination was ejected from the thruster at the startup of the engine in the steady-state operation. A 1.5-in.-high by 24-in.-long fence shielded specimens on the panel satisfactorily as opposed to a ¾-in.-high fence. The in situ reflectance and transmittance measurements on the specimens at the simulated altitude were more realistic of the contamination encountered by the specimens from the thruster exhaust than the atmospherical posttest laboratory measurements.

CONTENTS

APPENDIXES

I. ILLUSTRATIONS

Figure | Page

Figure | Page

Figure | Page

NOMENCLATURE

h	Distance from center of nozzle exit plane to the plate
J	Solar spectral irradiance as defined by Johnson
P_c	Combustion chamber pressure, psia
P_F	Fuel inlet pressure, psia
P_{ox}	Oxidizer inlet pressure, psia
R	Spectral reflectance
$\overline{R}$	Average visible reflectance
S	Calibration factor
T	Spectral transmittance
$\overline{T}$	Average visible transmittance
Tem	Temperature of emissometer

T_o	Initial prefire spectrum
T_s	Temperature of specimen
t_s	Relative solar transmittance
Vem	Voltage of emissometer
x	Distance from thruster exit plane
y	Transverse distance from thruster axis
z	Distance from detector to surface of panel
α	Angle between thruster axis and surface of plate, deg
α_s	Solar absorptance
ϵ	Emittance
θ	Angle of instrument rotation
μ	Wavelength, microns
ν	Wav number, cm^{-1}

SECTION I
INTRODUCTION

The exhaust plumes from attitude control rocket engines fired at orbital attitudes expand to the extent that the exhaust products strike spacecraft surfaces and externally mounted components located within a large envelope extending downstream from the nozzle exit plane. The impingement of the gas results in local surface heating, surface pressures, and possible contamination of spacecraft surfaces. These effects may cause malfunctions of apparatus mounted on or inside the spacecraft. It is, therefore, important to identify and understand the conditions that cause these effects so that they may be properly considered in the design and operation of the spacecraft. There have been several analytical predictions of exhaust plume behavior (Refs. 1 and 5) and some limited experimental tests at high altitude (Refs. 1 through 5). These tests have been limited to short durations with transient altitudes from 400,000 to 200,000 ft.

A series of tests was conducted at AEDC in a 10-ft-diam chamber to determine plume symmetry (Ref. 6); heat flux, and surface pressures (Ref. 7); and effects of contamination (Ref. 8) from a 1-lb thruster plume impinging on flat plates at an altitude of 400,000 ft. The 1-lb thruster is scaled to simulate both the 100-lb (longitudinal orientation) translational thruster, and the 22-lb (tangential and radial orientation) attitude control thrusters of the Manned Orbital Laboratory (MOL) as shown in Fig. 1, Appendix I. The flat plate simulates the MOL surface. The purpose of this test was to determine if contamination is produced by the 1-lb scaled translational thruster in its longitudinal orientation, to identify any contaminate produced, and to determine the performance degradation, if any, of optical and thermal control surfaces that have been exposed to contamination. The test required that the 1-lb scaled thruster be fired in pulses with pulse durations from 20 to 1000 milliseconds (msec) with 1000-msec off times and fired continuously up to 205 sec while maintaining a minimum simulated altitude of 400,000 ft.

SECTION II
TEST FACILITY

The test was conducted in the Aerospace Research Chamber (ARC) (8V) of the Aerospace Environmental Facility. The stainless steel chamber (Fig. 2) is 20 ft long and 10 ft in diameter. The cryopumping surfaces were designed (Ref. 9) for removing gas products from rocket engines and low density nozzles of high enthalpy. The 620 ft^2 of liquid-nitrogen (LN_2)-cooled surfaces, 800 ft^2 of gaseous-helium (GHe)-cooled surfaces, and 50 ft^2 of liquid-helium (LHe)-cooled surfaces were arranged to remove 16 kw from the exhaust gas products in an optimum manner.

The sketch below and Fig. 2 show the arrangement of the cryosurfaces to pump the high enthalpy exhaust gas products. The gas leaving the engine passes through the radially arranged, forward GHe surfaces and impinges on the annular LN_2 cryosurface where 8 kw is removed. The cooled gas is then either cryopumped by the LN_2 surface or reflected onto the GHe cryosurface where it is condensed. There is a total GHe refrigeration capacity of 8 kw—7 kw for the front GHe cryopump and the remaining 1 kw for the rear section. Since hydrogen (H_2) has a high vapor pressure (10^{-4} torr) on 15°K GHe surfaces, LHe (4.2°K) was used to remove the H_2 in the plume. The H_2 and nitrogen (N_2) exhaust gases moving axially down the chamber impinge on the LN_2 precooler, where energy is removed, and then are cryopumped on the LHe cryosurfaces.

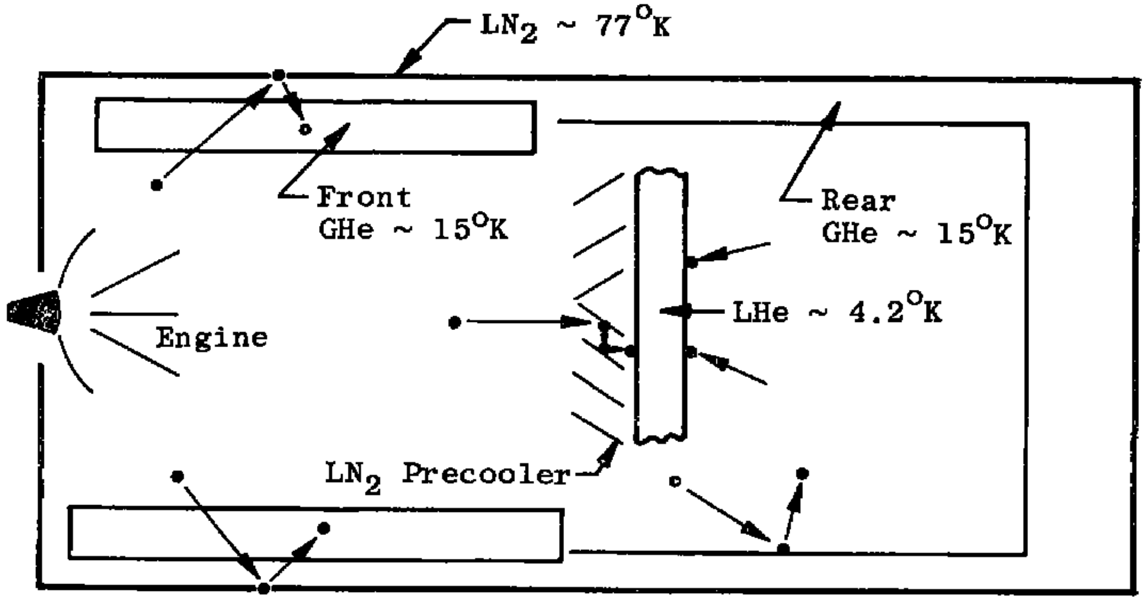

The front GHe cryosurfaces consist of fifty-two 8- by 1-ft panels positioned in a radial array about the axis of the chamber. The rear GHe cryosurface is 8 ft long and 6 ft in diameter. The supply of the gas to the front or rear GHe cryosurfaces could be distributed by externally operated valves.

The LHe was made in the Aerospace Environmental Facility. A 30-liter/hr He liquefier was used in conjunction with a 4-kw GHe refrigerator as a precooler for the gas. A 1000-liter dewar located on top of the chamber housed a Joule-Thompson valve for the final stages of liquefaction and stored the LHe.

SECTION III
TEST ARTICLES

3.1 1-LB-THRUST SCALED THRUSTER

The 1-lb-thrust MOL scaled thruster used in the test was supplied by Marquardt Corporation. The bipropellant, monomethylhydrazine and nitrogen-tetroxide ($MMH-N_2O_4$) thruster (Fig. 3) was designed for both steady and pulsing operation. The performance of the engine was investigated by Marquardt Corporation personnel who found that the lower thrust level resulted in lower combustion efficiency and pulsing performance. During the firing, the propellant valves and injectors were held at 60°F with cooling water.

The thruster design parameters and performance are shown below.

Thrust	1.0 lb
Fuel	MMH (Monomethylhydrazine)
Oxidizer	N_2O_4
Chamber Pressure	90 psi
Mixture Ratio	1.65 ± 1.5
Nozzle Expansion Ratio	40:1
Nozzle Geometry	Contoured
Chamber Temperature	4000°F
Throat Diameter	0.090 in.
Nozzle Exit Diameter	0.569 in.
Combustion Efficiency	0.830

Shown in Fig. 3 is the assembled 1-lb thruster. It consists of a water-cooled, single-doublet injector head, two fast response solenoid valves, and two 5-micron (μ) nominal filters upstream of each valve. The nozzle and combustion chamber are an integral part, machined from molybdenum.

Figure 4 shows the 1-lb thruster propellant system. The system consists mainly of three parts: the engine N_2 purge, high-point bleeds, and propellant supply system. Each propellant tank has a capacity of 2 liters. The propellants were pressurized with dry N_2. The propellant lines were 0.180-in.-ID stainless steel tubing.

3.2 TEST PANELS

There were two test panels (Figs. 5 and 6) used during the test. Panel 1 is 22.5 in. wide by 34 in. long, and panel 2 is 16 in. wide by 34 in. long. Panel 2 is mounted to panel 1, as shown in Fig. 6, on a pivot point so it could be remotely controlled and rotated flush with the panel 1 for in situ measurements. Figure 6, side view, illustrates the position of panel 2 during thruster firings. Panel 1 was mounted in a vertical plane parallel to the chamber centerline, offset 1.14 in. from the thruster centerline at the exit.

There are twenty-eight 1-in.-diam holes and six 1.5-in.-diam holes drilled through panel 1 for the purpose of inserting specimens (Fig. 6). There were also ten 1-in.-diam holes drilled through panel 2 for the same purpose.

3.3 SPECIMENS

Eleven types of specimens were used during the test to simulate the thermal control coatings and optical surfaces on the outside of the MOL vehicle. They are the following:

Type	Description	Use on MOL Vehicle
A	Zinc Oxide and Potassium Silicate ($ZNO + K_2SiO_3$)	Radiator Coating
B	Aluminum Silicone Paint (ALS_i)	Laboratory Module Coating
C	Schjeldahl Mylar® Tape (Adhesive Back Surface)	Forward Unpressurized Compartment Coating
D	Polished Aluminum	Thermal Control
G	Fused Quartz (High Efficiency Anti-reflective Coating)	View Port Window
H	Germanium Glass/Fluoride Coating	Horizon Sensor Window
J	Zinc Oxide and Potassium Silicate (with Alpo Coating)	Radiator Coating
K	Black Spinal (Potassium Silicate)	Laboratory Module Coating
T_1	Silicon Paint (K_2 SiO_3)	Thermal Control
T_2	Silicon Oxide (SiO_2)	Thermal Control
M	High Quality Mirror (Optical Grade)	Startracker
W	Quartz (Optical Grade)	Window

The above thermal control and optical specimens were each applied or attached to a 15/16-in.-diam disk which was mounted on a specimen holder (Fig. 7). The holder was threaded so it could be inserted into holes of the test panels (Fig. 8). The holders contained a heater tape with a thermocouple for maintaining the specimens at 60°F while in the vacuum.

SECTION IV
TEST INSTRUMENTATION

4.1 THRUSTER INSTRUMENTATION

The thruster was instrumented with three Taber® 500-psia pressure transducers. Two were used on the inlet side of the injector head for monitoring oxidizer and fuel pressures. One transducer was located on the engine combustion chamber. The response time of the transducers is less than 1 sec.

4.2 CHAMBER INSTRUMENTATION

There were four Bayard-Alpert-type ionization pressure gages located at various positions in the chamber. One gage was located behind the thruster for measuring the pressure during firings. The remaining gages were positioned near the LHe cryopump in order to evaluate its performance. One Alphatron® and one Baratron® were installed behind the thruster for monitoring pressures above 10^{-3} torr.

4.3 SCANNER MECHANISM

A scanner mechanism was installed in the test chamber (Figs. 9 and 10) to mount and position instrumentation for in situ measurements. The scanner mechanism provided the instruments four degrees of movement: three linear–x, y and z; and one angular–θ. Each movement was driven by a gear train and motor which could be controlled from outside the chamber. A light source was placed behind and adjacent to each specimen and transmitted a light beam through an appropriately located small hole in the panel. A photocell was mounted on each of the in situ measuring instruments. When the instrument was properly positioned relative to the desired specimen, the light beam impinged on the photocell and gave positive indication that the test instrument on the scanner mechanism was correctly located for the measurement.

4.4 IN SITU MEASUREMENTS

A Block Engineering, Inc. Model P-4 interferometer spectrometer and a locally fabricated emissometer (Ref. 10) were mounted on the scanner mechanism for making in situ measurements. The P-4 spectrometer was equipped with a locally designed and fabricated integrating sphere attachment (Ref. 10). The P-4 instrument is a quartz-polarization interferometer spectrometer which measures spectra in the range of 4,000 to 27,000 cm^{-1} (0.27 to 2.5 μ). The P-4 was used to measure in situ absolute spectral reflectance, $R(\nu)$, for the thermal control surface and mirror specimens, and relative spectra, $T(\nu)$, of the light transmitted through the window specimens from a tungsten lamp. The emissometer was used for making in situ total emittance, ϵ, measurements on selected thermal control surface specimens during the test. The raw data were reduced for analysis and presentation as described in Section 5.2.

4.5 LABORATORY MEASUREMENTS

The spectral reflectance of the specimens before and after each test were measured with a Beckman DK-2A spectroreflectometer in the 0.25- to 2.5-μ wavelength region. The instrument had been modified (Ref. 11) to measure absolute, directional-hemispherical spectral reflectance. For the present tests, the instrument was installed and operated in an airtight box which was purged with dry N_2. All postfire measurements were taken before the samples were exposed to air.

4.6 DATA SYSTEM

Figure 11 shows a schematic of the test data system which was used during the test. The specimen temperatures, P-4 spectrometer signals, emissometer, and engine flow rate data went into signal conditioning equipment, a commutator, analog-to-digital converter, digital tape, and then to the computer and/or data printout. In addition, for rapid analysis, the engine pressures and flow rates were recorded directly on an oscillograph.

SECTION V
PROCEDURE

5.1 TEST PROCEDURE

Before and after each test, DK-2A reflectance measurements were made on selected test specimens in the laboratory. White gloves were used in handling the specimens. After completing installation of specimens in the test panels, the proper scanner mechanism movement at each specimen location was checked by remote operation using position indicators (x, y, z, and θ) located outside the chamber.

After the thruster position was set, the chamber was purged with N_2 and then evacuated, first by means of a 140-cfm mechanical pump, and then by a 6-in. diffusion pump. These pumps evacuated the chamber to 10^{-4} torr pressure. At this time, the LN_2 and GHe liners were cooled down. With the cryosystems at the desired temperatures, the chamber pressure stabilized at approximately 10^{-7} torr. In situ reflectance, transmittance, and emittance measurements were then taken on selected specimens. Panel 2 was positioned so that its surface was flush with panel 1, allowing measurements to be made on the specimens. After completing the measurements, the scanner mechanism was moved to the parking position for firing (Fig. 9). The propellant tanks and lines were then pressurized, panel 2 was positioned at 45 deg relative to panel 1, and the LHe cryopump was cooled down to 4.2°K. After a selected number of firings, in situ measurements were repeated on the specimens. After completion of the firings, the chamber was pressurized to atmosphere with dry N_2 where, in some cases, sea-level in situ measurements were repeated on the specimens.

In order to prevent exposure of the specimens to air, following the test, personnel entered the dry N_2 atmosphere chamber with special breathing apparatus and placed the specimens in special containers for transmittal to the laboratory.

5.2 DATA REDUCTION

Laboratory measurements of absolute spectral reflectance and transmittance resulted in continuous curves drawn by an x-y plotter as the measurement was made at each wavelength.

In situ measurements for spectral reflectance and transmittance also resulted in plots by an x-y plotter, but the curves were not continuous and were not drawn as the measurement was made. Data reduction for the in situ spectrometer was done by a computer which produced a series of discrete values from which the curves were plotted. These discrete values were stored in computer memory before plotting and hence were available for further computation.

The absolute spectral reflectance data, $R(\nu)$, for the mirror and thermal control surface specimens were reduced by computer to obtain the average visible reflectance, $\overline{R}$, which is defined by

$$\overline{R} = \frac{\int_{12,500}^{27,000} R(\nu)\, d\nu}{\int_{12,500}^{27,000} d\nu}$$

The absolute spectral reflectance curves are included in the figures of Appendix I, and the corresponding computed values for the average visible reflectance, $\overline{R}$, are included in the data tabulated in Appendix III.

The absolute spectral reflectance data, $R(\nu)$, were also used to compute values for the solar absorptance, α_s, in accord with

$$\alpha_s = \frac{\int_{4,000}^{27,000} [1 - R(\nu)]\, J(\nu)\, d\nu}{\int_{4,000}^{27,000} J(\nu)\, d\nu}$$

where $J(\nu)$ is the generally accepted Johnson solar spectral irradiance. The values of α_s calculated for the mirror and thermal control surface samples are included in the data tabulated in Appendix III.

Spectral curves of the transmittance lamp, modified by the transmittance of the window samples and attenuation in the spectrometer, which were obtained during testing, were used with initial, pretest spectra to compute the relative spectral transmittance, $T/T_o\ (\nu)$, which is plotted in the figures of Appendix I. These values were used, in turn, to compute values of average visible relative transmittance, $\overline{T}$, defined by

$$\overline{T} = \frac{\int_{12,500}^{27,000} [T/T_o(\nu)]\, d\nu}{\int_{12,500}^{27,000} d\nu}$$

The computed values of $\overline{T}$ are tabulated in Appendix III with the other reduced data.

The relative spectral transmittance was also used to compute the relative solar transmittance, t_s, which is defined by

$$t_s = \frac{\int_{4,000}^{27,000} [T/T_o(\nu)] J(\nu) d\nu}{\int_{4,000}^{27,000} J(\nu) d\nu}$$

where, again, $J(\nu)$ is the Johnson solar spectral irradiance. The values of t_s are also tabulated in Appendix III.

In situ measurements of emittance for the thermal control surface specimens resulted in a value, ϵ, calculated from the emissometer voltage, Vem, the specimen temperature, T_s, and the emissometer temperature, Tem, in accord with

$$\epsilon = \frac{Vem}{(T_s^4 - Tem^4)S}$$

where S is a calibration factor. Values of ϵ are also tabulated in Appendix III.

In addition to the preceding values which were calculated directly from measured data, the ratio α_s/ϵ, was computed for the thermal control surface specimens; and values of the ratio are included with the other data tabulated in Appendix III.

SECTION VI
DISCUSSION AND RESULTS

The effects of rocket exhaust plume impingement on surface coatings in the contamination tests conducted can be categorized into the following (Refs. 8 and 12):

a. Erosion or ablation of the coatings as a results of aerodynamic heating.
b. Chemical corrosion of the coatings as a result of unburned propellants reacting with the coatings.
c. Condensation or deposition on the coatings.

In the previous tests (Ref. 8) (tangential orientation), the aerodynamic heating effect was insignificant because of the short duration of firing (1000 msec or less) as compared to 1000 msec off time. For this duty cycle, the maximum observed temperature on the panel was 150°F. Most surface coatings are designed to withstand temperatures greater than 150°F. The heating effect is more evident in the steady-state thruster operation (greater than 1000 msec) in the longitudinal orientation where the maximum observed temperature on the panel is 650°F (Ref. 7). Chemical corrosion occurs when the unburned propellants deposited on the surface coatings react with the coatings and create permanent damage. Since the rocket exhaust plume composition is approximately 30-percent water vapor by weight (Ref. 12), condensation is more likely to occur on the low temperature coatings. This condensation would be temporary contamination since it would evaporate with higher operational surface temperatures.

Since the contamination tests of the longitudinal, radial, and tangential orientation were not conducted in sequence, the test numbers reported for this phase (longitudinal orientation) will not be consecutive. There was a total of 13 tests with the thruster angle fixed at 18 deg and 1.14 in. from the surface of panel 1 (see Fig. 9) and one test with the thruster angle at 0 deg and 1.14 in. from the surface of panel 1. Within each test, the objective, results, test hardware, measurements, and number of firings varied, as indicated in Appendixes II and III.

The thruster was fired continuously up to 205 sec and pulsed with durations of 20-, 50-, 100-, and 1000-msec and up to 3000-msec off time between pulses. Figure 12 shows typical results of engine combustion chamber, oxidizer-to-fuel ratio and oxidizer flow rate versus engine firing time. These quantities are practically constant after initial transients.

Figure 13 shows the ARC 8V predicted chamber performance as a function of engine thrust level. From the figure it can be seen that the 1-lb thruster can be fired indefinitely (more than 100 sec) maintaining 8 x 10^{-5} torr ARC 8V chamber pressure. For thruster pulsing, the ARC 8V chamber pressure would be lower than for steady-state firing. For pulse durations of 20 to 1000 msec, the altitude decreases from 600,000 to 400,000 ft, respectively. Figure 14 shows the measured chamber pressure with time for a typical 1-lb engine firing. The continuous rise in chamber pressure is because of the thermal loading of the front GHe (20°K) cryopump.

The full-scale 22- and 100-lb thrusters use multiple hole injectors for providing optimum combustion. The injector holes have to introduce and meter the flow to the combustion chamber and atomize and mix the propellants by impingement in such a manner that a correctly proportioned, homogenious fuel-oxidizer mixture will result, one that can be readily vaporized and burned. Only the nozzle of the 1-lb thruster and mass flow rate were scaled from the full-scale thrusters. The valves were the same as for the 22- and 100-lb engines. Because of the relatively small mass flow rate of the 1-lb scaled thruster, a single doublet injector design resulted (Fig. 3). In such a simple design, misalignment of either the oxidizer or fuel injector hole can result in incomplete combustion, especially in the pulse-mode operation. The accumulated unburned propellants in the combustion chamber would be blown out of the nozzle.

Another possibility for the formation of the unburned propellants in the combustion chamber is from the "dribble volume" located between the valve seat and the exit of the injector holes. When the valves are closed, the propellants within this volume flow into the combustion chamber; when the thruster is again fired, the residue is blown out of the combustion chamber into the nozzle. Therefore, more contamination would be expected in the pulse-mode than in the steady-state operation. In addition, since this engine had an abnormally large dribble volume to combustion chamber size, the likelihood of contamination formation is large.

Two fences or shields were used in an attempt to shield specimens located on the panel from the thruster exhaust plume. Because of the generally random distribution of contamination on the test panel, visual observation rather than optical measurements were used to evaluate the effectiveness of the fences or shields for controlling contamination on the specimens.

6.1 TEST 3

The objective of test 3 was to determine if contamination is produced by the 1-lb thruster in the pulse-mode operation. During the thruster firings, large quantities of brownish-red liquid contamination collected at the thruster exit momentarily and then were blown by the thruster exhaust onto the panel and specimens. The appearance of this contamination occurred continuously after the first 10 or 15 pulses (20- and 50-msec durations). In Ref. 8 various controls were used on the thruster and test panel to minimize the contamination in the pulse-mode operation.

It was noticed from high-speed photography that contamination appeared to form in the nozzle after the first 10 to 15 pulses. The results of the motion-picture film illustrated that the contamination left the engine both as a mist and as a liquid.

Figures 15 to 22 show typically the change in reflectance, depending on the type and location of the specimen, as a result of the contamination produced by the thruster and environmental cycle of the specimens. As reported in Ref. 8, the mangitudes or trends of the data were influenced by the conditions under which the measurements were made (i.e., in a vacuum or in the laboratory). The results of this test were consistent with the results of the pulse firing tests in Ref. 8.

Figure 20 illustrates typically the effect of the environmental cycle on the reflectance of a type A speciman located at S_{16}. Of interest is curve 5 which shows the reflectance values after the test return to almost the values before the test.

6.2 TESTS 4B and 4C

In tests 4B and 4C, the contamination from the 1-lb thruster in steady-state mode firing was evaluated.

In the steady-state thruster operation, contamination was noticed only at the startup of the thruster (first 2 sec) at the thruster exit and then was blown by the thruster exhaust onto the panel.

The contamination produced by the thruster in steady-state operation (longitudinal orientation) was much less than that of the pulse firing (tangential orientation) reported in Ref. 8. The contaminates impinged along and near the centerline of the plate on specimens located at S_8, S_{11} to S_{17}, V_1, H_1, G_3, and G_8. Outside of this region of the plume, there was little evidence of impingement because of the rarefaction of the plume. Therefore, most of the data presented in this report are for locations on the plate in the vicinity of the thruster centerline.

Figure 23 shows the contamination that accumulated on specimen at location H_1 after being exposed to the rocket exhaust plume.

Figures 24 through 37 show not only the effect of the contamination but also the effects of changes in the chamber environment on the reflectance of the specimens. The specimens apparently became contaminated when the ARC 8V chamber was evacuated. The specimens are again contaminated when they are exposed to the rocket exhaust plume and when the ARC 8V chamber is returned to atmosphere. The contamination leaves or evaporates from the specimens when they are placed in the laboratory atmosphere. As a result, the reflectance measurements before and after the test are very similar. Therefore, the in situ measurements are more realistic of the contamination that might be encountered in space.

The contamination on the specimens was found (Ref. 8) to be by weight—MMH (30.5 per cent), H_2O (31.7 percent) and $-NO_3$ (37.8 percent). Because of the low vapor pressure of the constituents, they will solidify on the plate and specimens in the vacuum and evaporate at atmospheric conditions.

Specimen locations S_{12}, S_{13}, S_{15}, and S_{16} are in the stagnation region of the plume where the plate temperature and heat flux are maximum (Ref. 7). Therefore, corrosion occurs at a much greater rate than for specimens outside of this region. Figures 26, 28, 31, and 33 illustrate the corrosion on the specimens in the stagnation region. Type A specimens change to a brownish-yellow, type K from black to grey, and type C from silver to grey after being exposed to the plume.

6.3 TEST 5A

In test 5A, a 3/4-in.-high fence (Fig. II-1, Appendix II) was used in an attempt to shield specimens located at V_1, H_1, S_{14}, G_8, and G_3 from the plume contamination. The test was aborted after firing 5A-3 because of propellant system problems. The fence did not significantly reduce the contamination on specimens located at V_1, H_1, S_{14}, G_3, and G_8.

6.4 TEST 5B

The objective in test 5B was the same as in test 5A. The 3/4-in.-high fence did not reduce significantly the contamination on specimens at V_1 and H_1.

Figures 38 through 50 illustrate the changes of reflectance and show selected specimens after being subjected to the environmental cycle. Figures 43, 46, and 48 illustrate the corrosion effect on the specimens in the stagnation region of the plume on the plate. Figure 40 shows the specimen at location S_{10} without evidence of contamination. This is to be expected, since the specimen is located outside the dense region of the plume.

Figures 51 and 52 illustrate the insignificant change in transmittance on specimens at V_1 and G_7 after being exposed to the plume. There is doubt that these measurements are correct because it was visually observed that contamination existed on the specimens during the test.

6.5 TEST 6

In test 6 the effect of the thruster exhaust plume on a operational monopole directional antenna (Fig. II-1) was evaluated.

Figure 53 shows the effect the plume had on the Teflon®-coated antenna. During the test, there was a large contamination buildup on the end of the antenna. Because of the high heat flux, the Teflon on the base of the antenna was ablated; and the antenna was separated from ground plate. The impedance of the antenna did not change during the thruster operation.

6.6 TEST 13

The purpose of test 13 was to investigate the effectiveness of a 1.5-in.-high by 24-in.-long fence (Fig. II-1) to shield specimens located on panel 2, and to determine the effectiveness of heating the panel to reduce contamination.

Heating the specimens and plate to approximately 100°F reduced the amount of contamination that had deposited during the test. The use of a 1.5-in.-high fence between panels 1 and 2 reduced the amount of contamination impinging on panel 2.

Figures 54 through 61 illustrate the change of reflectance on the specimens during the test. Figures 61 and 62 show the decrease in transmittance of specimens located at startracker and G_8 after being exposed to the plume and ARC 8V chamber environment.

6.7 TEST 14

The purpose of test 14 was to evaluate the amount of contamination deposited on panel 2, startracker sled, and the flush-mounted startracker. There were significant amounts of contamination noticed on the above surfaces after thruster firings 14-1 through 14-5. The horizon sensor specimen appeared also to be contaminated. There was a significant amount of MMH ejected onto the panel as a result of the oxidizer line freezing during firing 14-6.

Figures 63 through 72 show the change in reflectances on some of the specimens located along and near the centerline of the thruster.

6.8 TEST 15

In test 15 the contamination on the short covered cavity and thermal coating cube was evaluated. There was no noticeable contamination on the cover of the short cavity during the test.

Figures 73 through 80 show the change in reflectance on various types of specimens as a result of the environmental cycle to which they were exposed. Figure 78 shows the cube after being exposed to the plume. The distinct erosion line as a result of plume impingement can be seen in the photograph. Figure 79 shows plots of reflectance measurements made before and after the test on specimen at location T_1, on the cube. There is a significant decrease in reflectance after the specimen was exposed to the plume. Figure 81 shows a plot of the transmittance measurements made on the view port specimen, location V_1, after being exposed to the environmental cycle.

6.9 TEST 20

The horizon sensor window, location H_1, was heated in test 20 in an attempt to reduce the contamination that had accumulated during the environmental cycle. A white frost was noticed on the horizon sensor window during the test. A brownish-red contamination appeared on the panel near the thruster exit. The frost evaporated when the chamber was pressurized to atmosphere.

Figures 82 to 86 show the change in reflectance measurements which were made on various specimens located at various positions on panel 1. Figure 87 shows the decrease in the transmittance measurement made before and after the test.

6.10 TEST 21

The amount of white frost contamination on the 100°F heated panel 1 with the horizon sensor window specimen was less than that in test 20. The brownish-red contamination near the thruster exit remained on the panel during the test.

Figures 88 through 92 show the change in reflectance on various specimens on panel 1 as result of the environmental cycle. Figure 93 shows the decrease in transmittance on the view port specimen, V_1, after being exposed to the environmental cycle.

6.11 TEST 22

There was no noticeable contamination on the covered short cavity (Fig. II-1) with the additional baffle. The brownish-red contamination still appeared on the panel near the thruster exit.

Figures 94 through 99 show the change in reflectance on various specimens located along and near the thruster centerline as a result of being exposed to the environmental cycle. Figure 100 shows the decrease in the transmittance measurements and the view port specimen, location V_1, after being exposed to the environmental cycle.

6.12 TEST 23

In test 23, the amount of contamination ejected from the thruster at low altitudes (250,000 ft) was evaluated. As a result of the thruster exhaust plume collapsing at the low altitudes, the contamination that was ejected from the thruster onto the test panel was distributed further along and nearer to the thruster centerline than was observed at the higher altitudes (400,000 ft). There was more contamination observed on panel 2 than observed in previous tests.

Figures 101 through 105 show the decrease in reflectance measurements made on various specimens located along and near the centerline of the thruster as a result of being exposed to the environmental cycle.

6.13 SUMMARY

Most of the specimens near and along the centerline of the thruster became significantly contaminated when exposed to the plume; therefore, the radiative properties changed significantly. The following is a list of various specimens with the maximum change in reflectance and the wavelength for which the maximum change occurred.

Specimen Type	Location	Percent Change in Reflectance	Wavelength, μ
A	S_{15},S_{16},S_{17}	80 – Decrease	0.36
B	S_{17}	60 – Decrease	0.25
C	S_8	45 – Decrease	0.30
D	S_8	28 – Decrease	0.25
J	S_{15},S_{16}	60 – Decrease	0.38
K	S_{13}	30 – Increase	0.5 to 0.70
		30 – Decrease	2.0
M	G_4	10 – Decrease	0.76
T_1	S_{14}	60 – Decrease	0.40
T_2	Startracker	25 – Decrease	0.60

All the specimens listed above show the largest change in reflectance at the lower wavelength (ultraviolet and visible) region after being exposed to the plume. The reflectance changes significantly in the ultraviolet and visible region because of the interference effect of the small particles of contamination with the shorter wavelength.

The tests indicated that the contamination occurred at the nozzle exit during the startup (first 2 sec) of the thruster firing and then was blown by the thruster exhaust onto the test panel. In the pulse-mode operation, the contamination appeared to form in the nozzle exit after the first 10 or 15 pulses and occurred continuously thereafter. The contamination on the test panel (approximately half a cup after 605 pulses in test 3) in the pulse-mode operation was much greater than in the steady-state (approximately one-fifth of a cup after test 4C) thruster operation. The results of the chemical analysis of the contamination in Ref. 8 were found to be by weight–MMH (30.5 percent), H_2O (31.7 percent), and -NO_3 (37.8 percent).

Since the tests indicate that the contamination originated in the injector and combustion chamber of the 1-lb thruster, future test work should be conducted on various injectors to minimize the contamination. One possibility is to adapt the scaled nozzle to the full-scale injector and combustion chamber. The excess combustion gas, not required for thruster operation, could then be vented from the combustion chamber to outside the vacuum chamber.

SECTION VII
CONCLUSIONS

The results from the test for the control and effect of contamination ejected from a 1-lb scaled translational thruster in its longitudinal orientation are summarized by the following observations, conclusions, and recommendations:

1. The tests indicated that a high degree of contamination resulted from the specific injector and combustion chamber configuration.

2. The contamination ejected from the thruster in the steady-state operation occurred in the startup of the thruster, and the contamination that accumulated on the test panel was much less than that in the pulse-mode operation.

3. Most of the contamination accumulated on the panel near and along the thruster axis.

4. The thruster exhaust contaminants that impinged on the panel had a corrosive effect on some of the specimens.

5. The Teflon on the monopole directional antenna was ablated after being exposed to the plume. However, the impendence of the antenna did not change.

6. Specimens A, B, C, D, E, K, M, T_1, and T_2 showed as much as an 80-percent change in reflectance in the ultraviolet and visible region after being exposed to the plume.

7. The reflectance and transmittance measurements illustrate that the measurement environment (i.e., measurements in vacuum or atmosphere) affected the magnitude or trends of the measurements made. The in situ measurements at the simulated altitudes are believed to be more representative of the true contamination on the panel than are the laboratory measurements.

8. Of the contamination controls used during this test (i.e., 0.75-, 1.5-in.-high fence, etc.) for shielding specimens from the thruster exhaust, the 1.5-in.-high fence proved most effective.

9. Further tests should be conducted to determine the variation in contamination production with varied injector and combustion chamber configurations.

REFERENCES

1. Llinas, J., Sheeran, J., and Hendershot, K.C. "A Short Duration Experimental Technique for Investigating Solid Propellant Rocket Plume Impingement Effects At High Altitudes." Cornell Aeronautical Laboratory, Buffalo, New York, ICRPG/AIAA 3rd Solid Propulsion Conference, No. 68-517, June 4-6, 1968.

2. Bauer, R.C. and Schlumpf, R.L. "Experimental Investigation of Free Jet Impingement on a Flat Plate." AEDC-TN-60-223 (AD253229), March 1961.

3. Barebo, R.L. and Ansley, R.C. "Effects of Rocket Exhaust Jet Impingement on a Movable Flat Plate at Pressure Altitudes above 200,000 Feet." AEDC-TDR-63-214, January 1964.

4. Llinas, J. "Electron Beam Measurements of Temperature and Density in the Base Region of a Clustered Rocket Model." Cornell Aeronautical Laboratory, Buffalo, New York, AIAA 2nd Flight Test Simulation and Support Conference, No. 68-236, March 25-27, 1968.

5. Burch, B.A. "Effect of Contamination on Spacecraft Surfaces Exposed to Rocket Exhausts." AEDC-TR-68-23 (AD831624L), April 1968.

6. Hill, D.W., Jr. "Investigation at High Altitudes of Rocket Exhaust Plume Symmetry and Interaction with a Plate with a Scaled MOL Thruster." AEDC-TR-69-75, April 1969.

7. Hill, D.W., Jr. and Smith, D.K. "Flat Plate Heat Flux and Pressure Measurement in an MOL Scaled Thruster Plume at 400,000-ft Altitude." AEDC-TR-69-84, May 1969.

8. Hill, D.W., Jr. and Smith, D.K. "Effects and Control of Contamination from a Scaled MOL Attitude Control Thruster in a Tangential Orientation." AEDC-TR-69-146, October 1969.

9. Heald, J.H., Jr., Dawbarn, R., and Arnold, F. "Test Chamber Concept Development for Very High Altitude Rocket Plume and Space Vehicle Systems Testing." AEDC-TR-68-205 (AD841628), October 1968.

10. Frazine, D.F. and Cox, G.S. "Instrumentation for Evaluating Effects of Plume Contamination on Optical Properties of MOL Spacecraft Surfaces." AEDC-TR-69-188, to be published.

11. Cox, George S. "Absolute Reflectance Measurements with a Ratio Recording Spectroreflectometer." AEDC-TR-69-123, to be published.

12. Borson, E.N. and Landsbaum, E.M. "A Review of Available Rocket Contamination Results." Aerospace Report No. TR-0200 (4250-20)-2.

APPENDIXES

I. ILLUSTRATIONS
II. TEST LOG
III. TABLES OF OPTICAL MEASUREMENTS

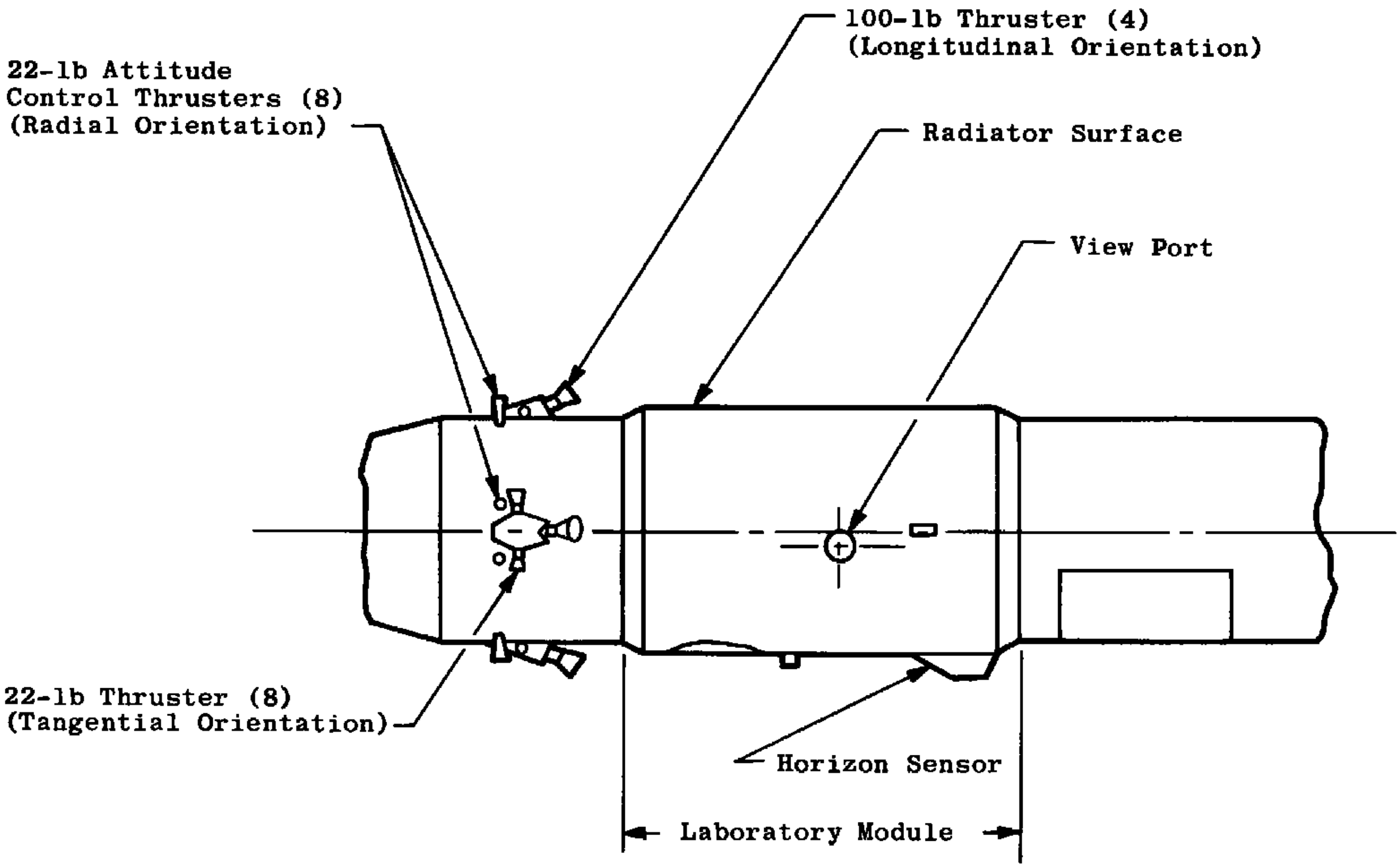

Fig. 1 Manned Orbital Laboratory with Thrusters

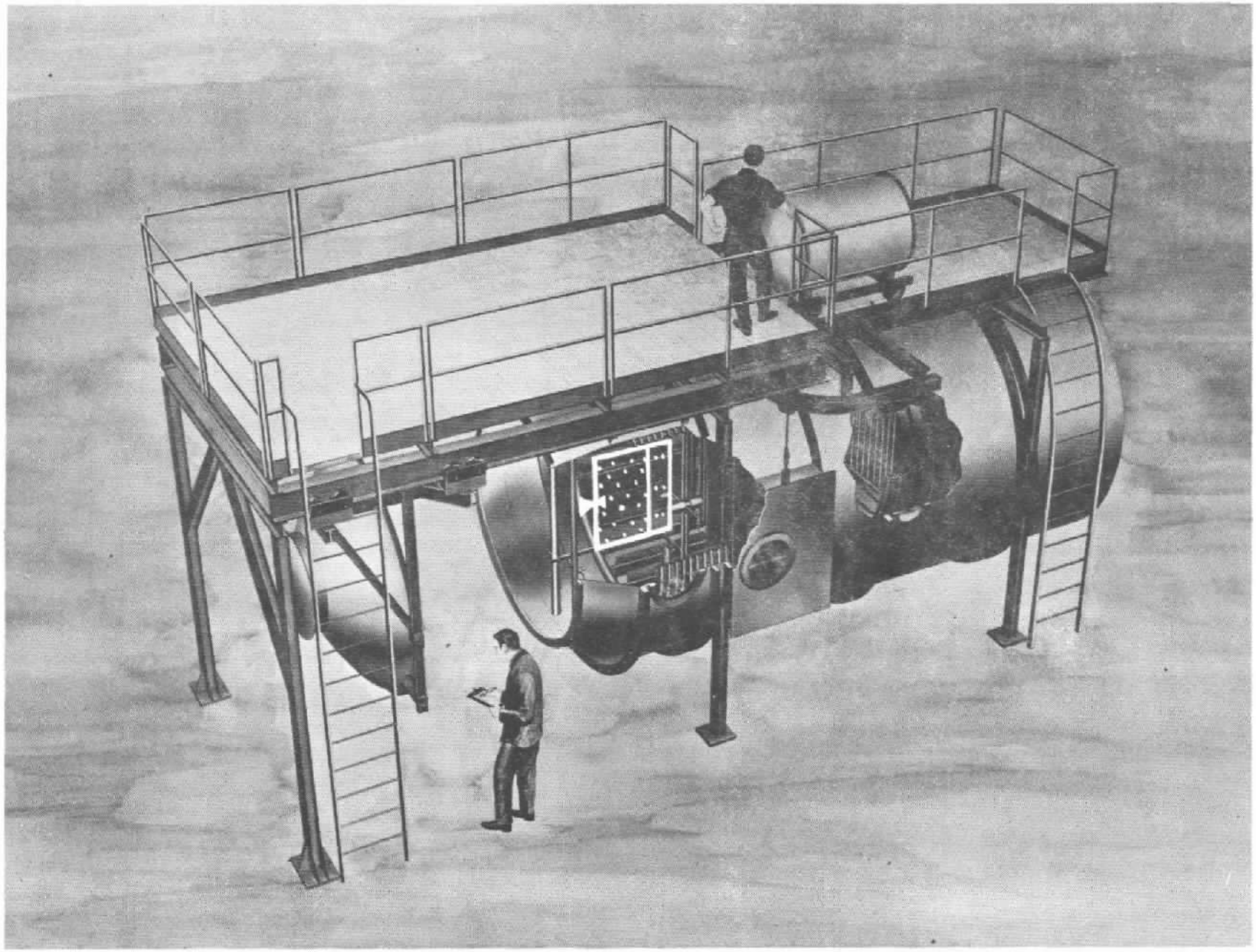

Fig. 2 Aerospace Research Chamber (ARC)(8V)

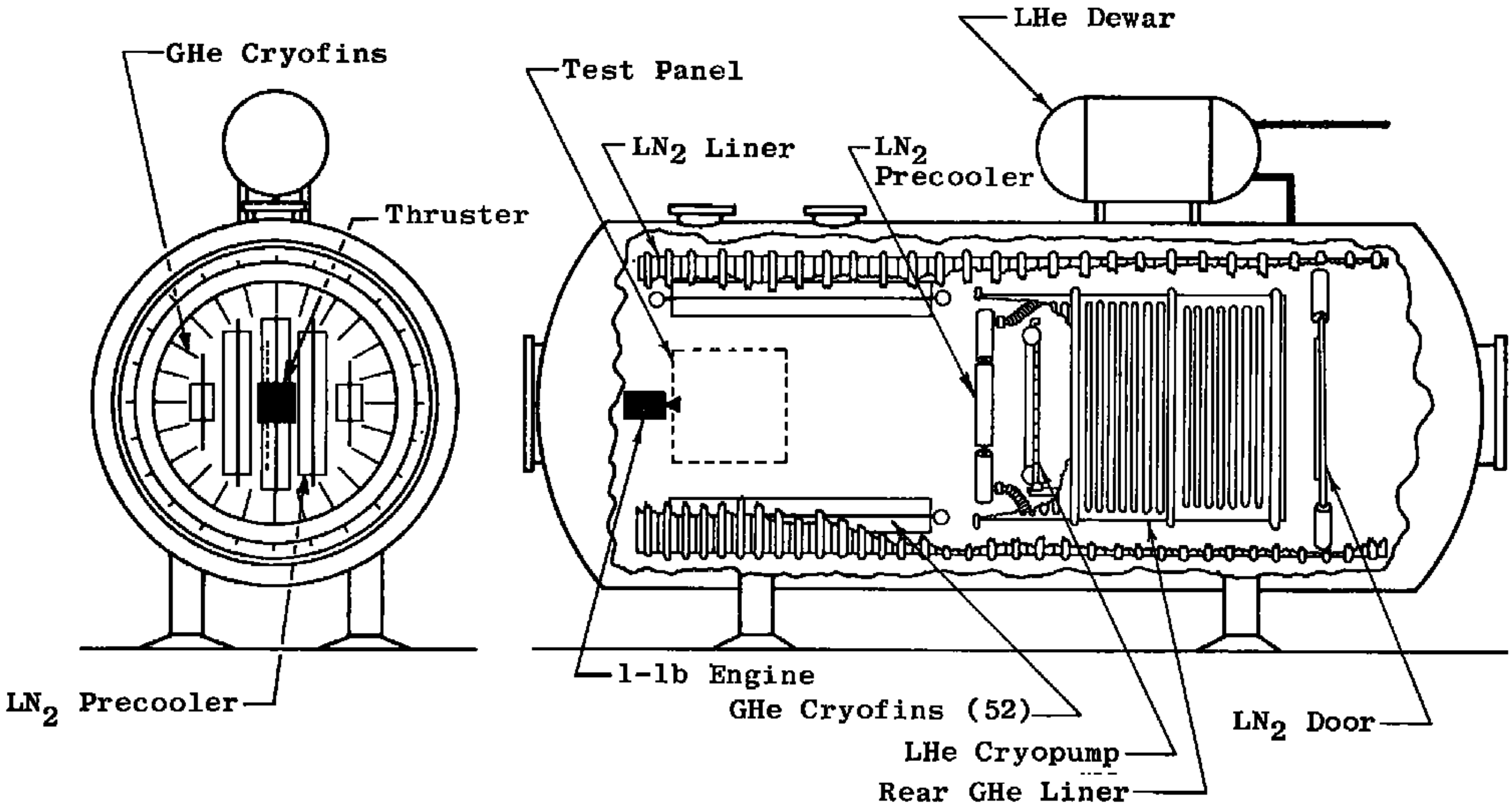

Fig. 2 Concluded

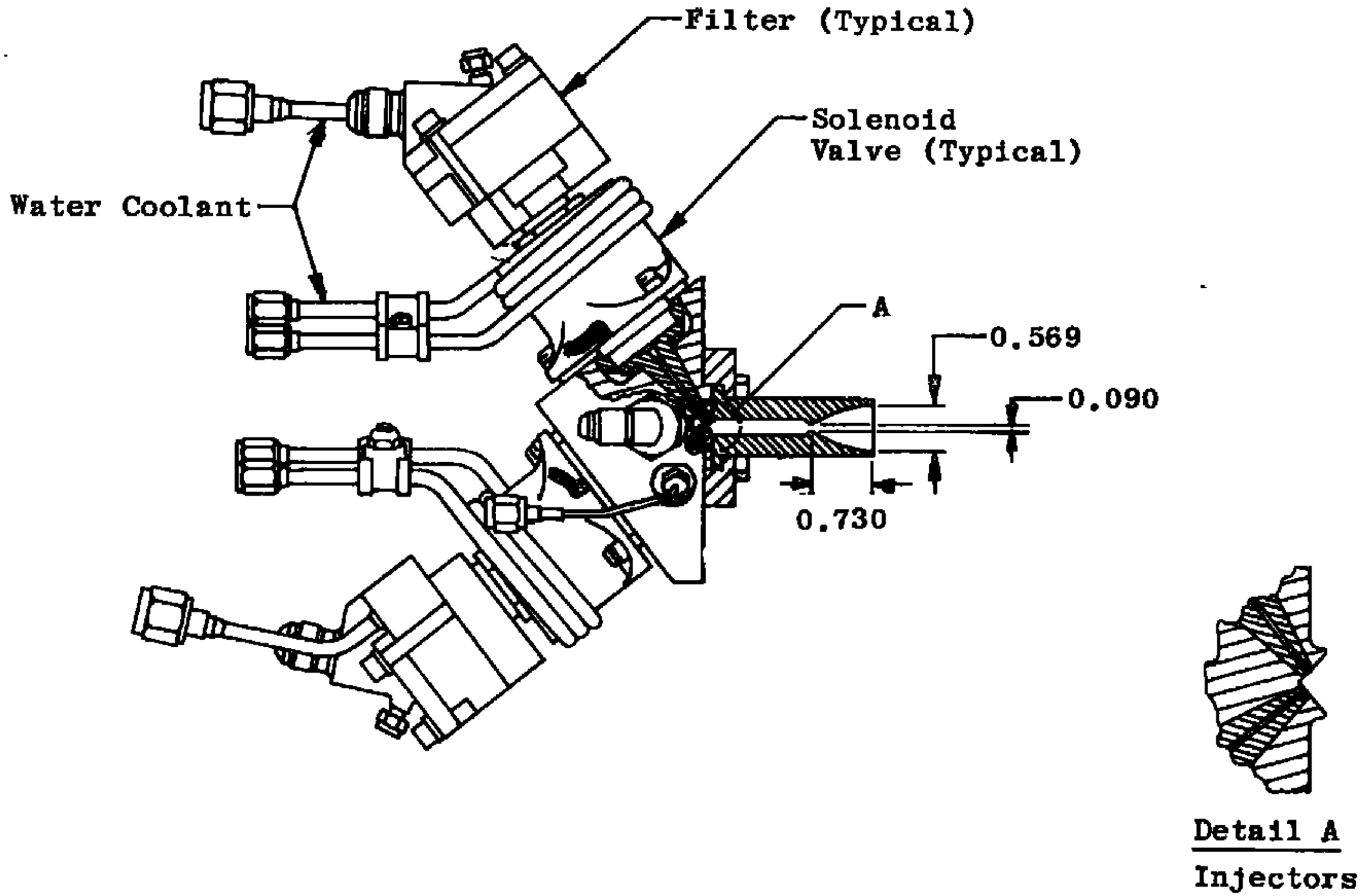

Fig. 3 1-lb-Thrust Engine and Components

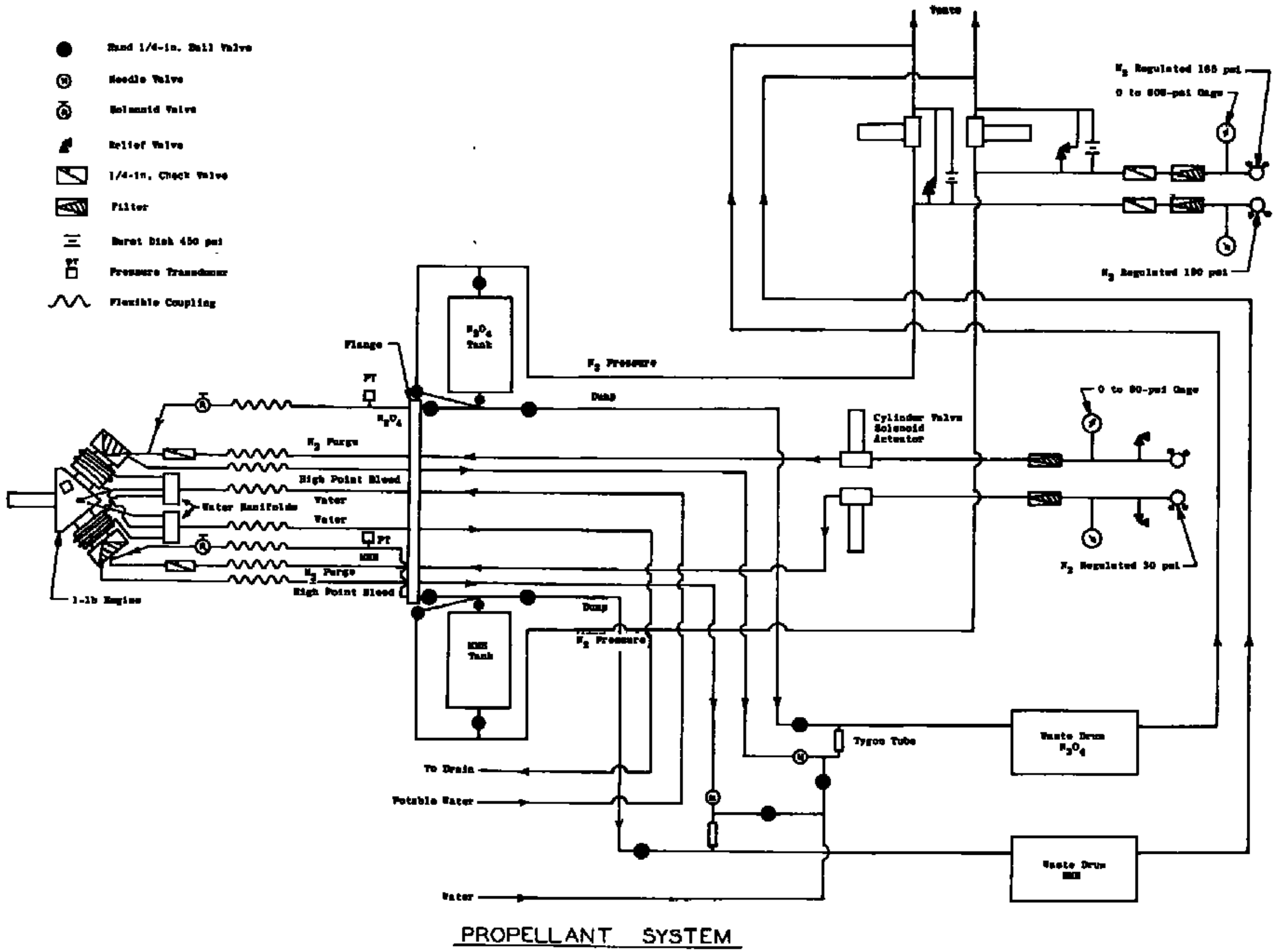

Fig. 4 Propellant System

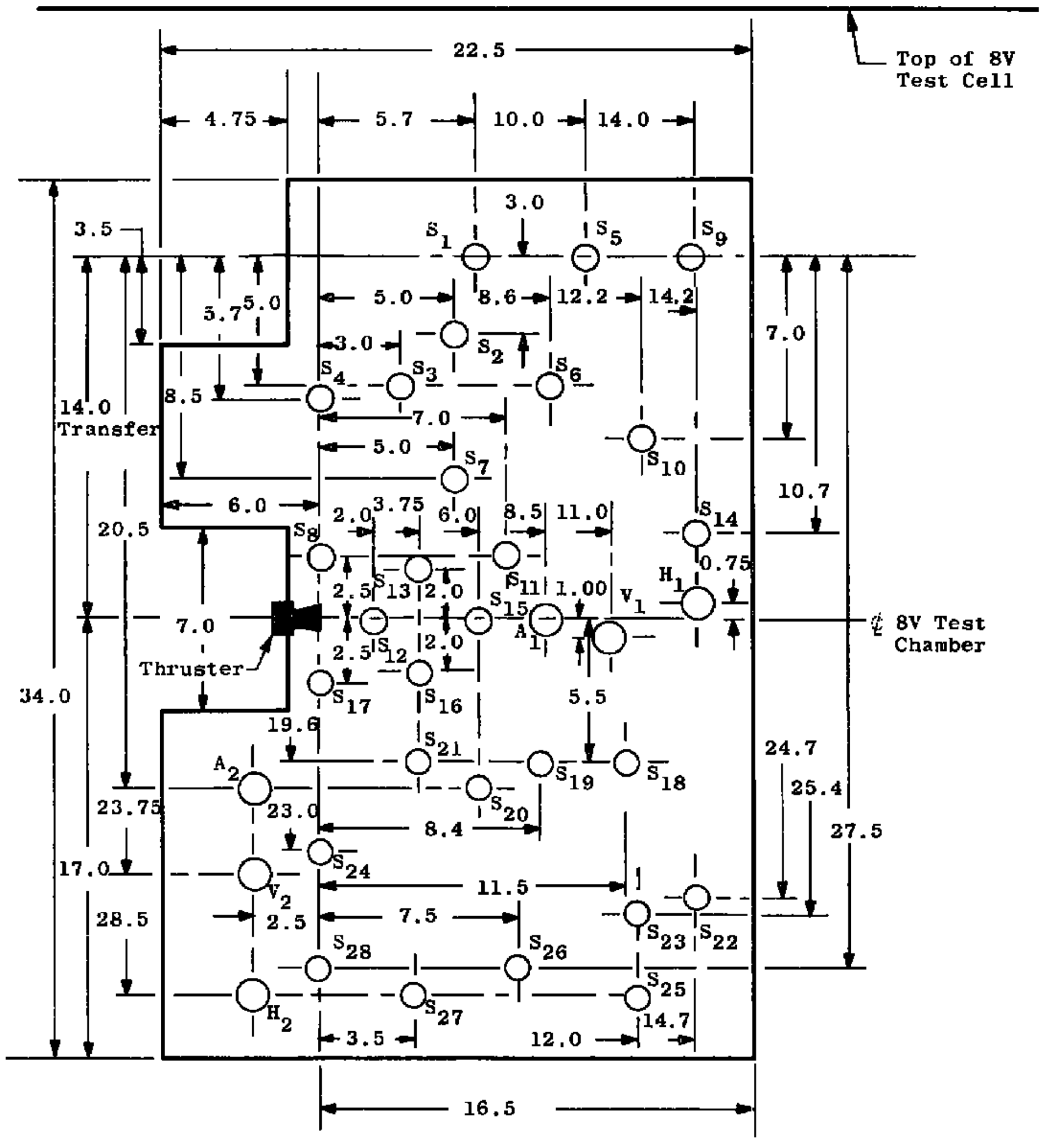

All Dimensions in Inches

Fig. 5 Detail Dimensions of Panel 1

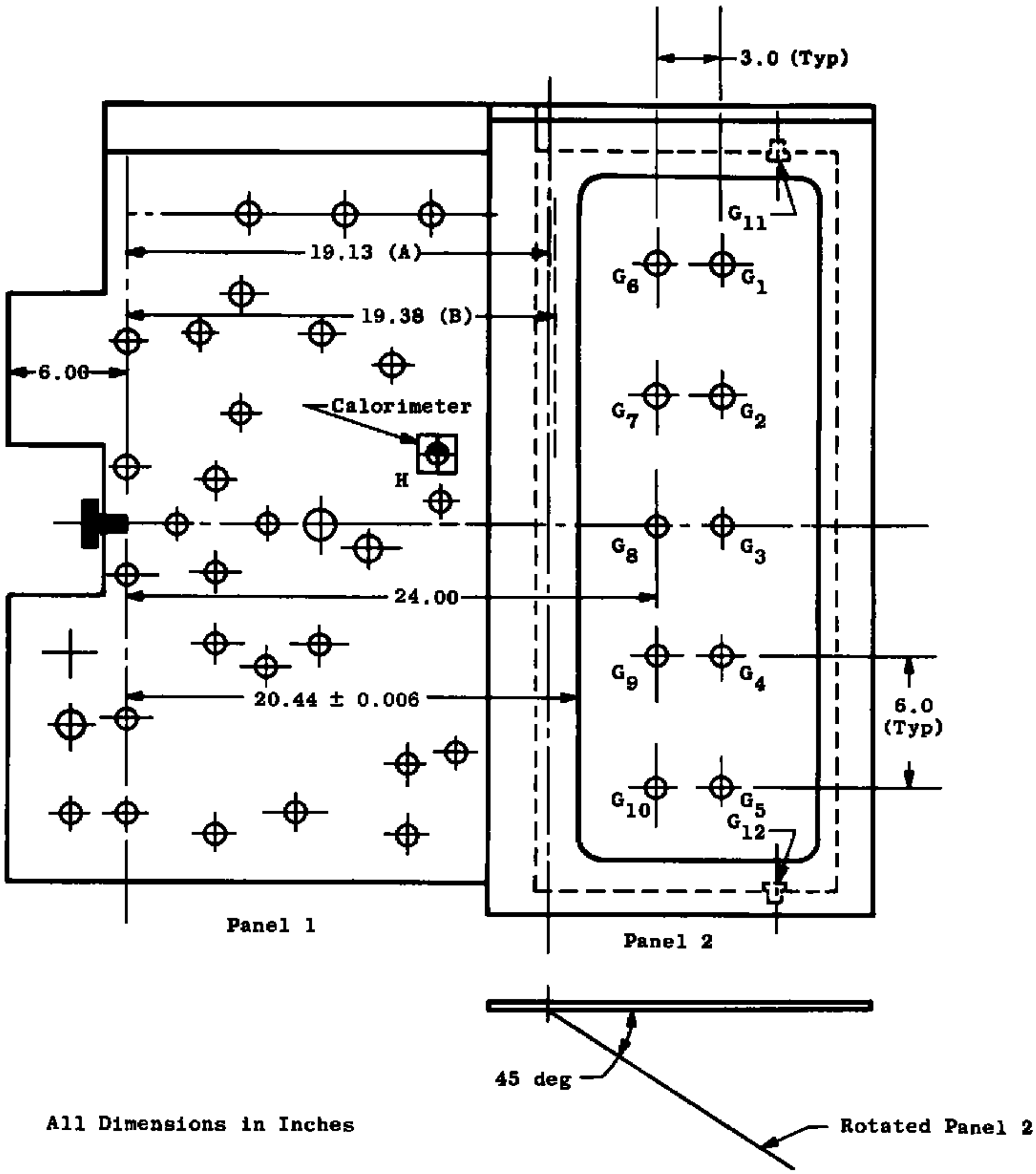

Fig. 6 Detail Dimensions of Panels 1 and 2

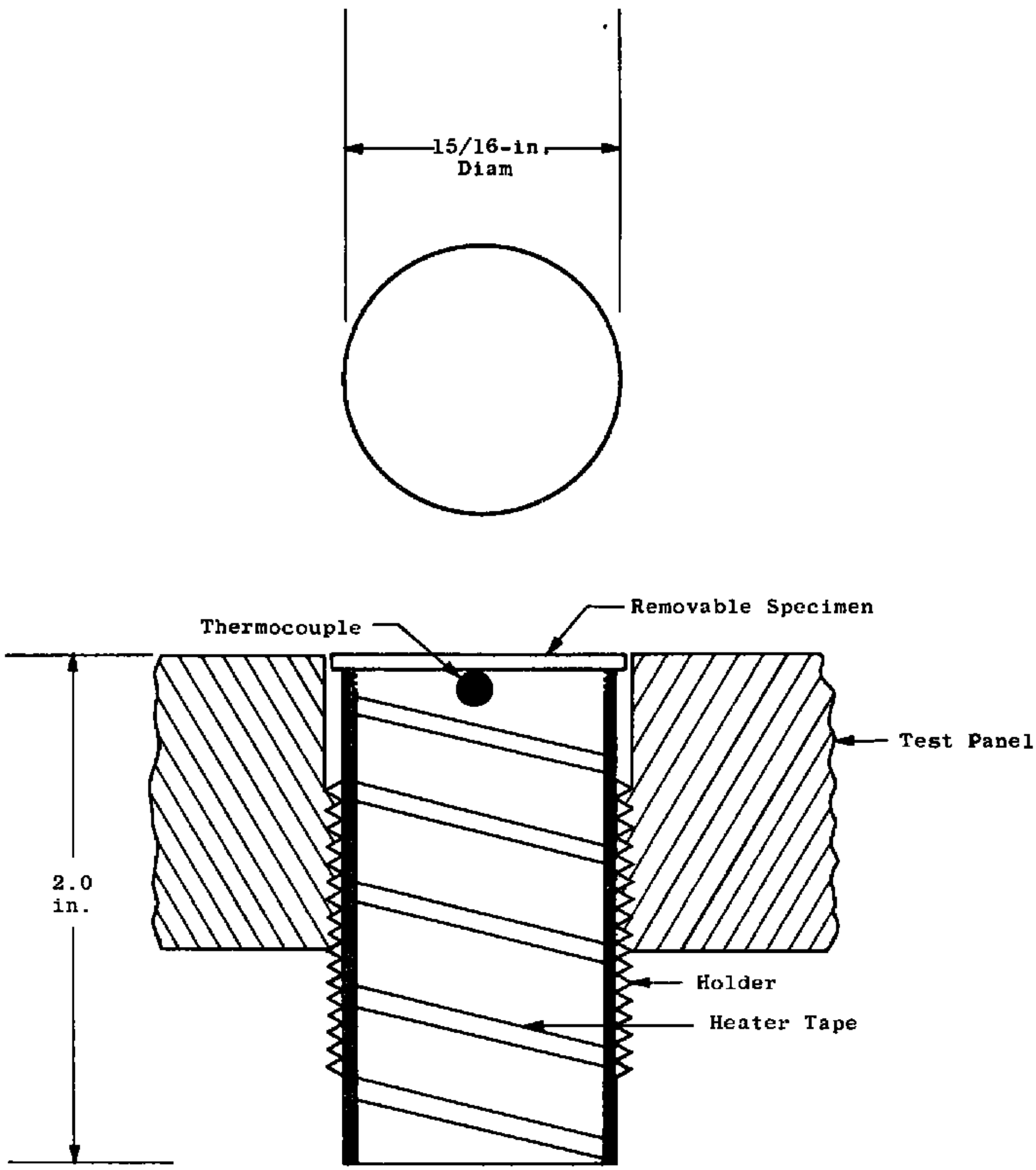

Fig. 7 Test Specimen and Holder

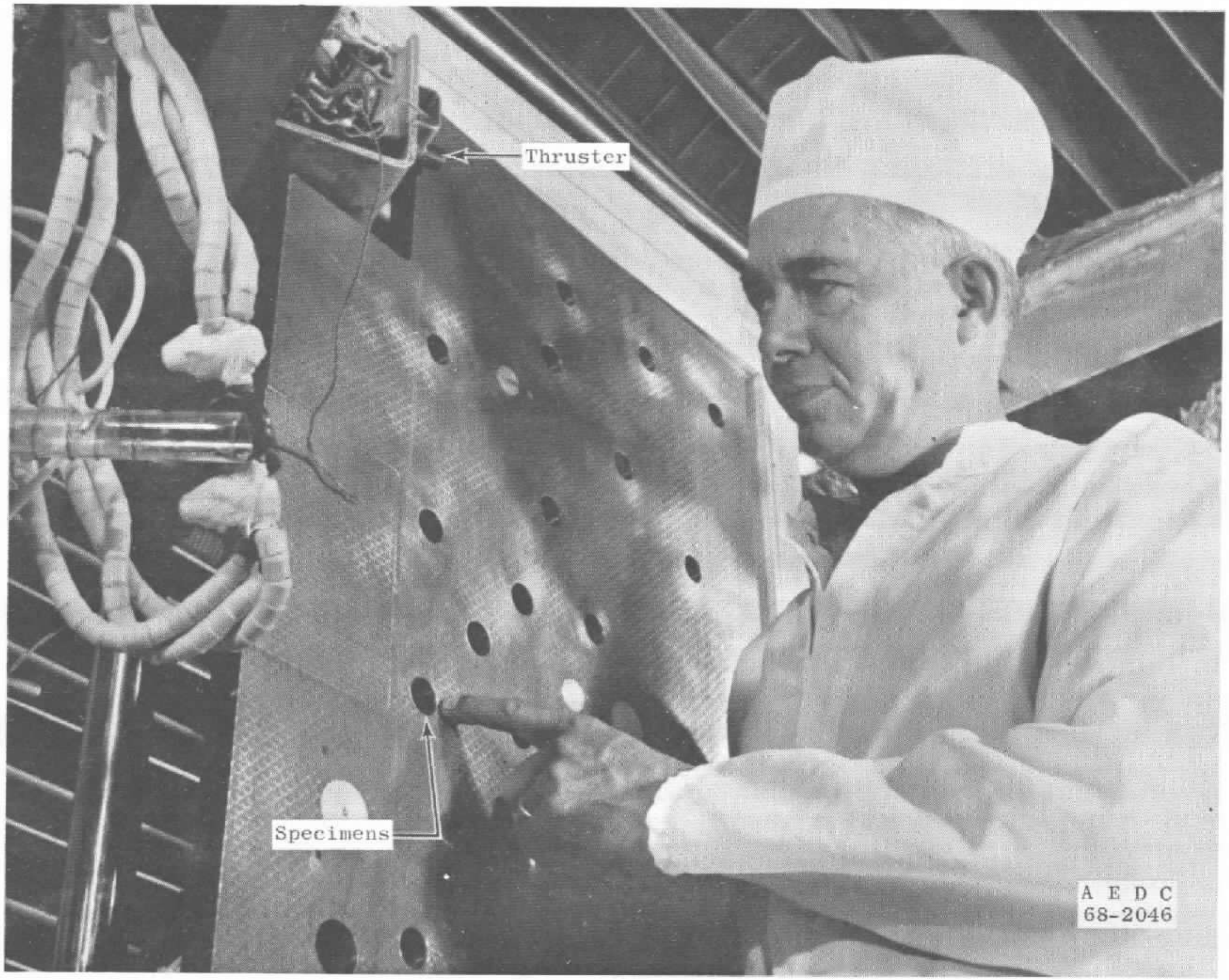

Fig. 8 Test Installation of Thruster and Specimens

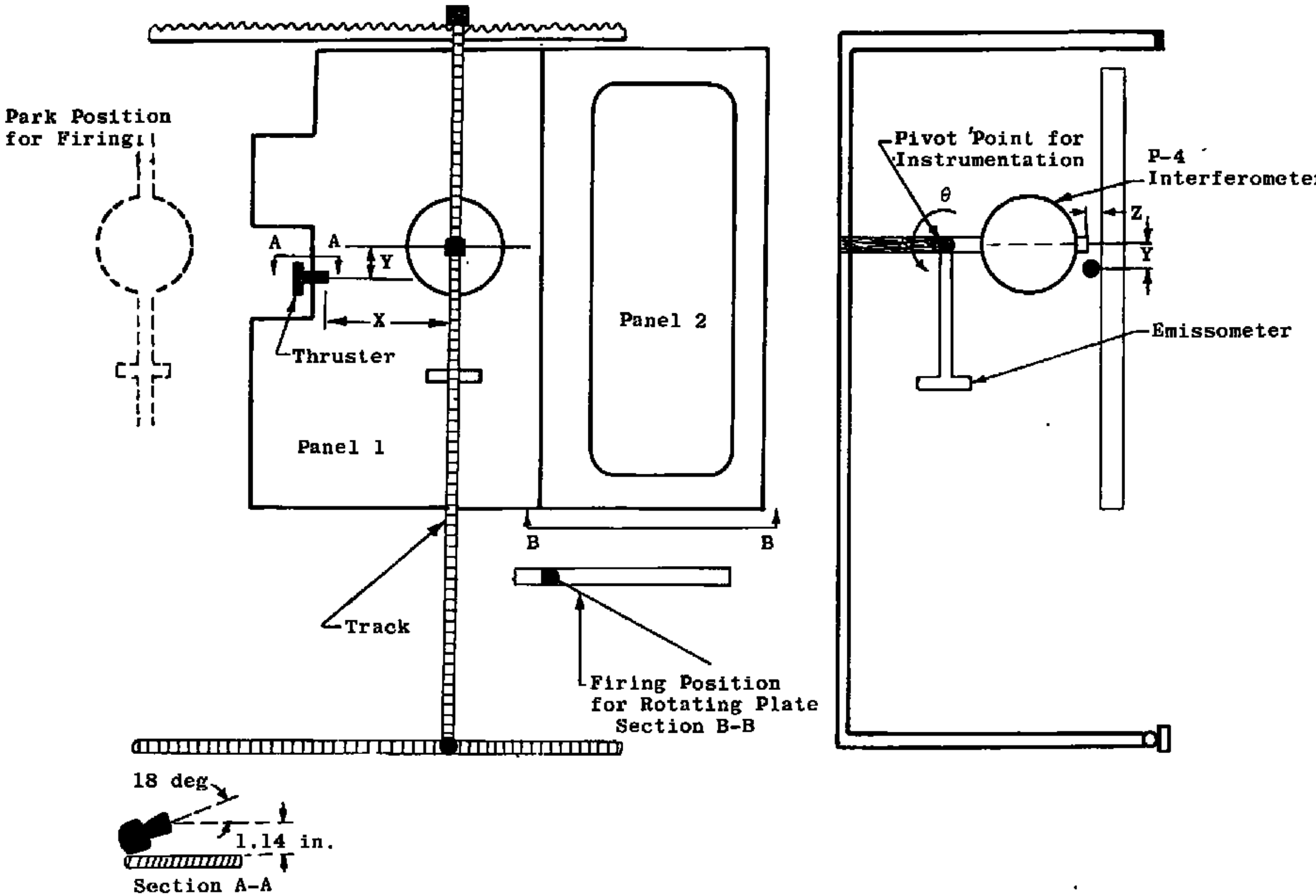

Fig. 9 Scanner Mechanism with Instrumentation and Panel

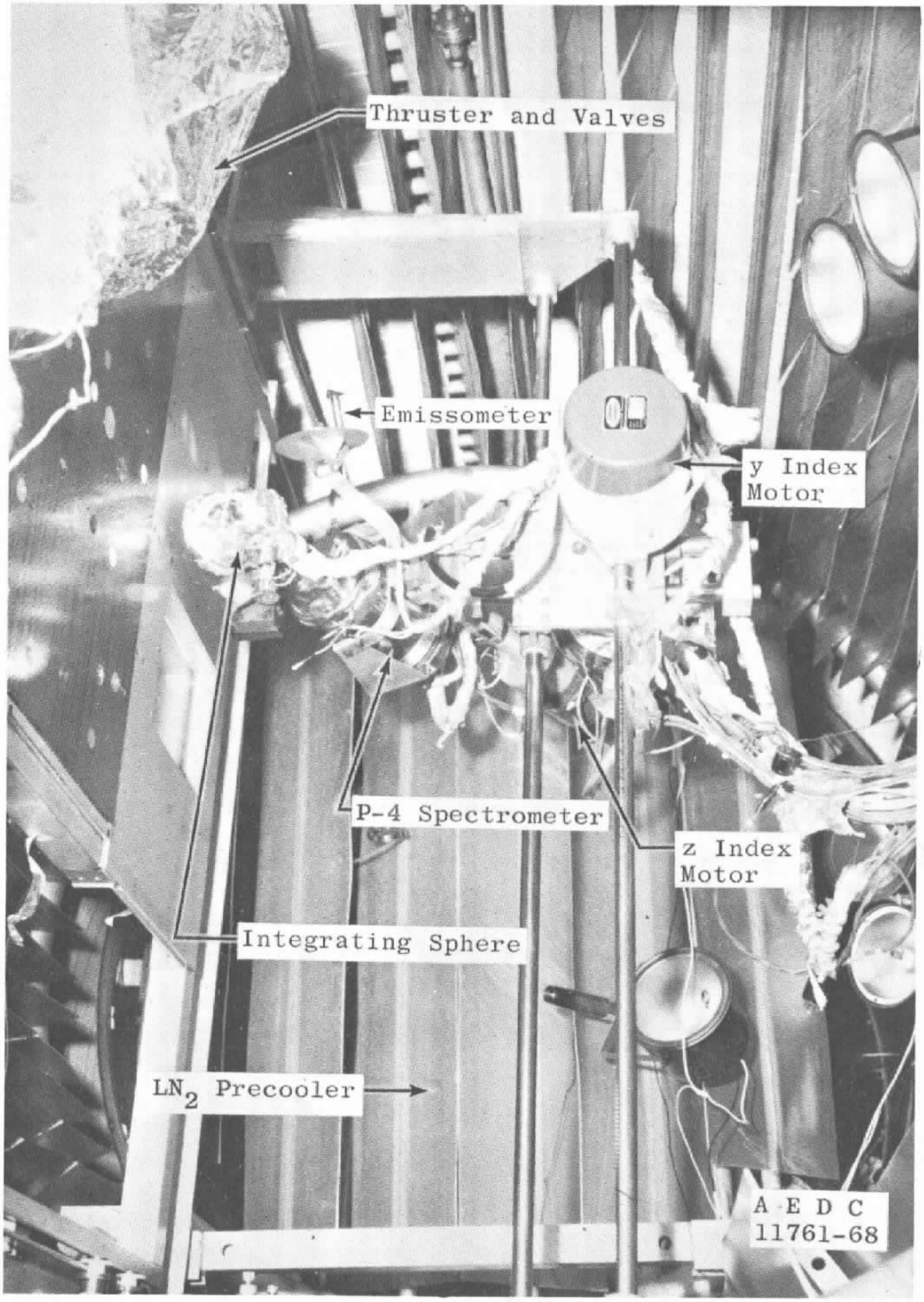

Fig. 10 Test Installation of In Situ Instrumentation

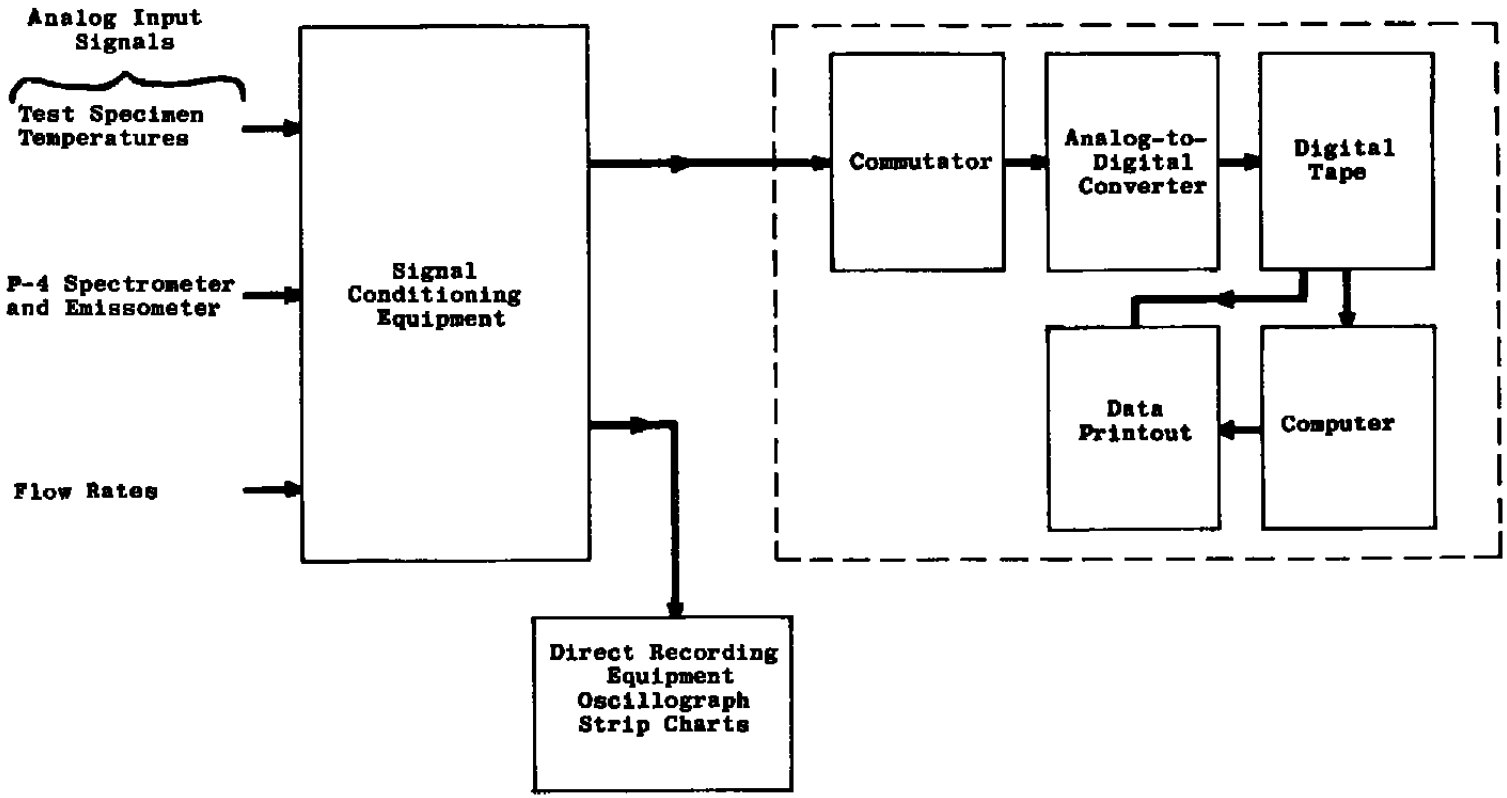

Fig. 11 Test Data System

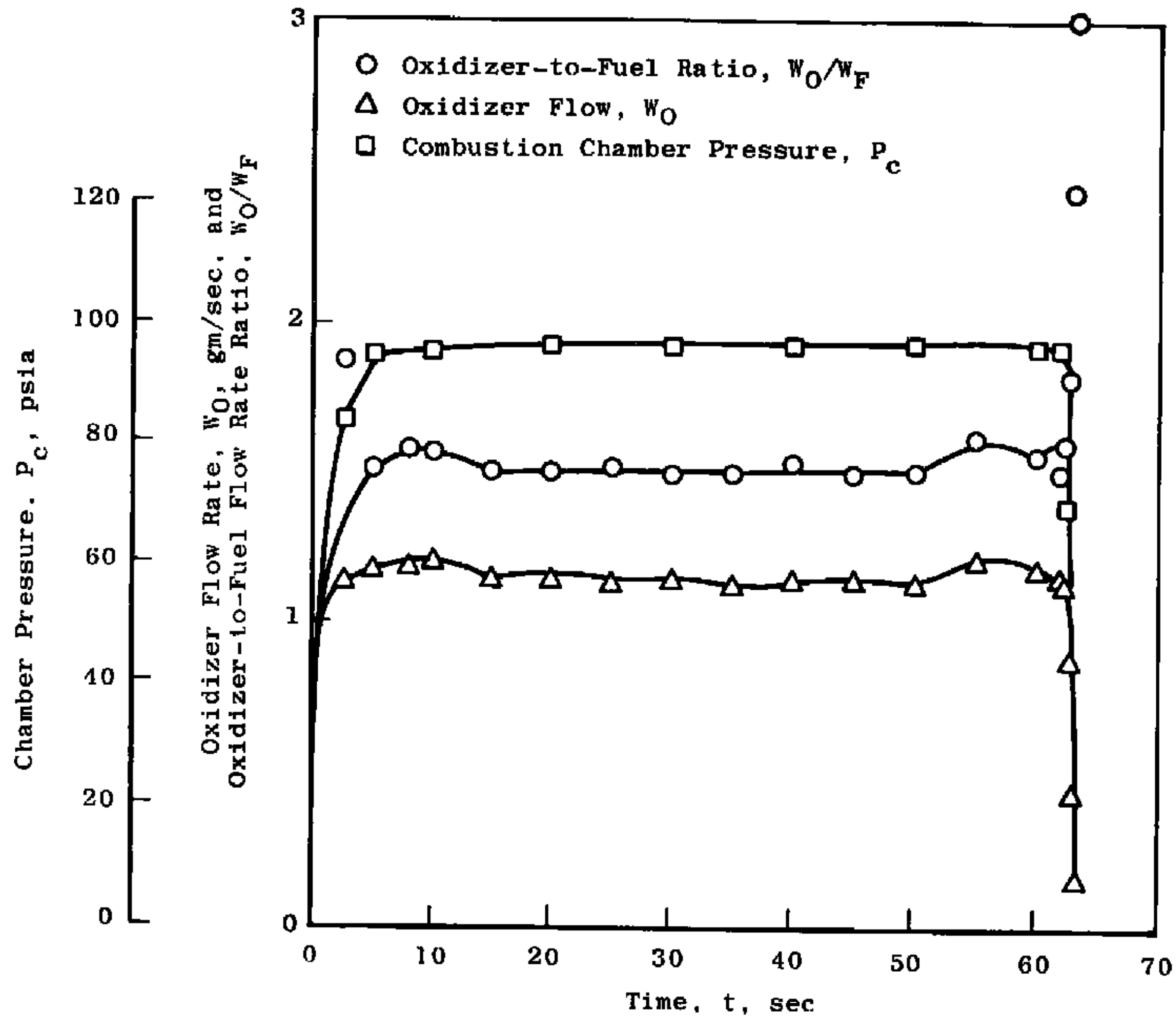

Fig. 12 Engine Pressures and Flow Rates

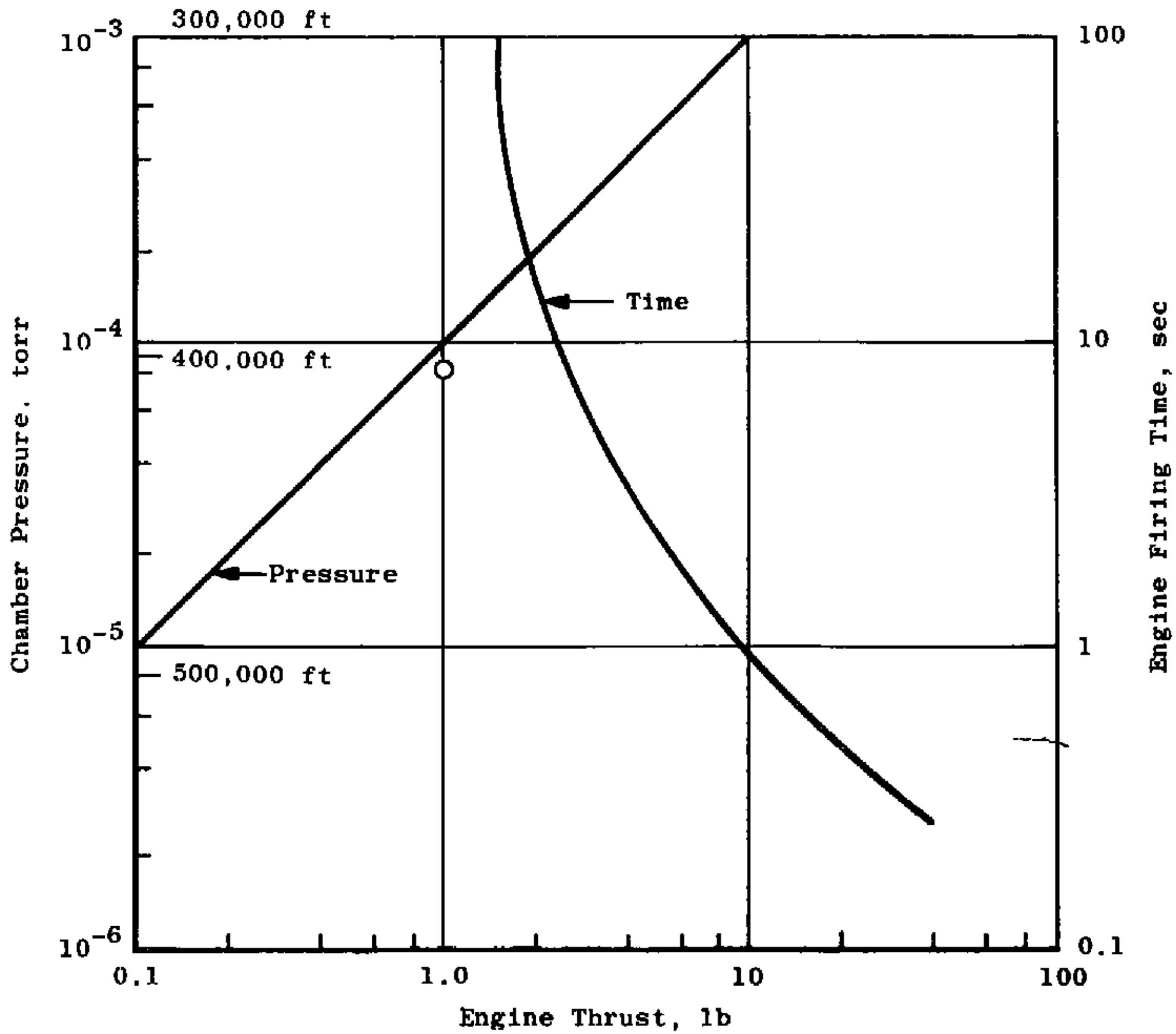

Fig. 13 Predicted ARC 8V Chamber Performance

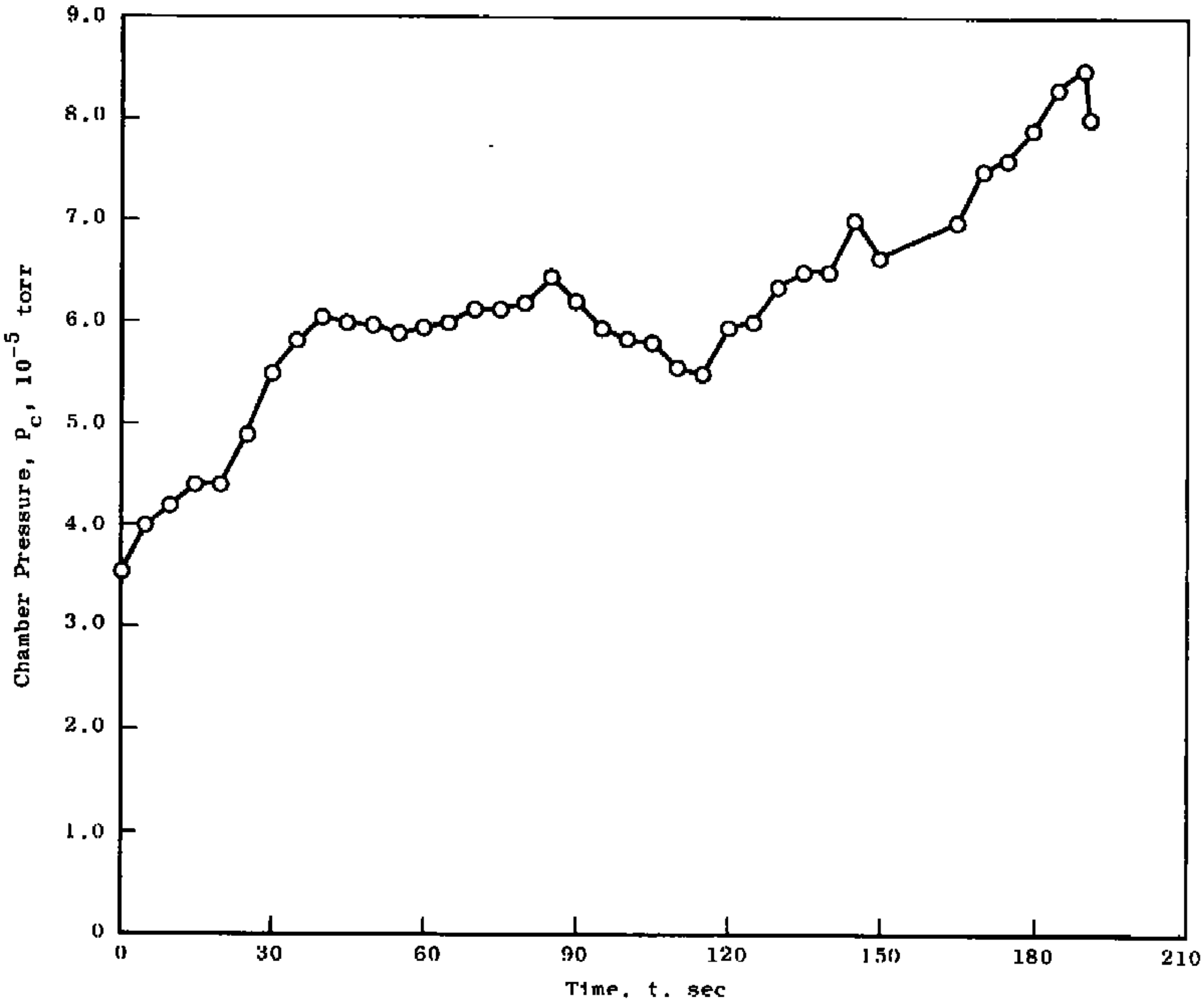

Fig. 14 ARC 8V Chamber Pressure versus Thruster Firing Time

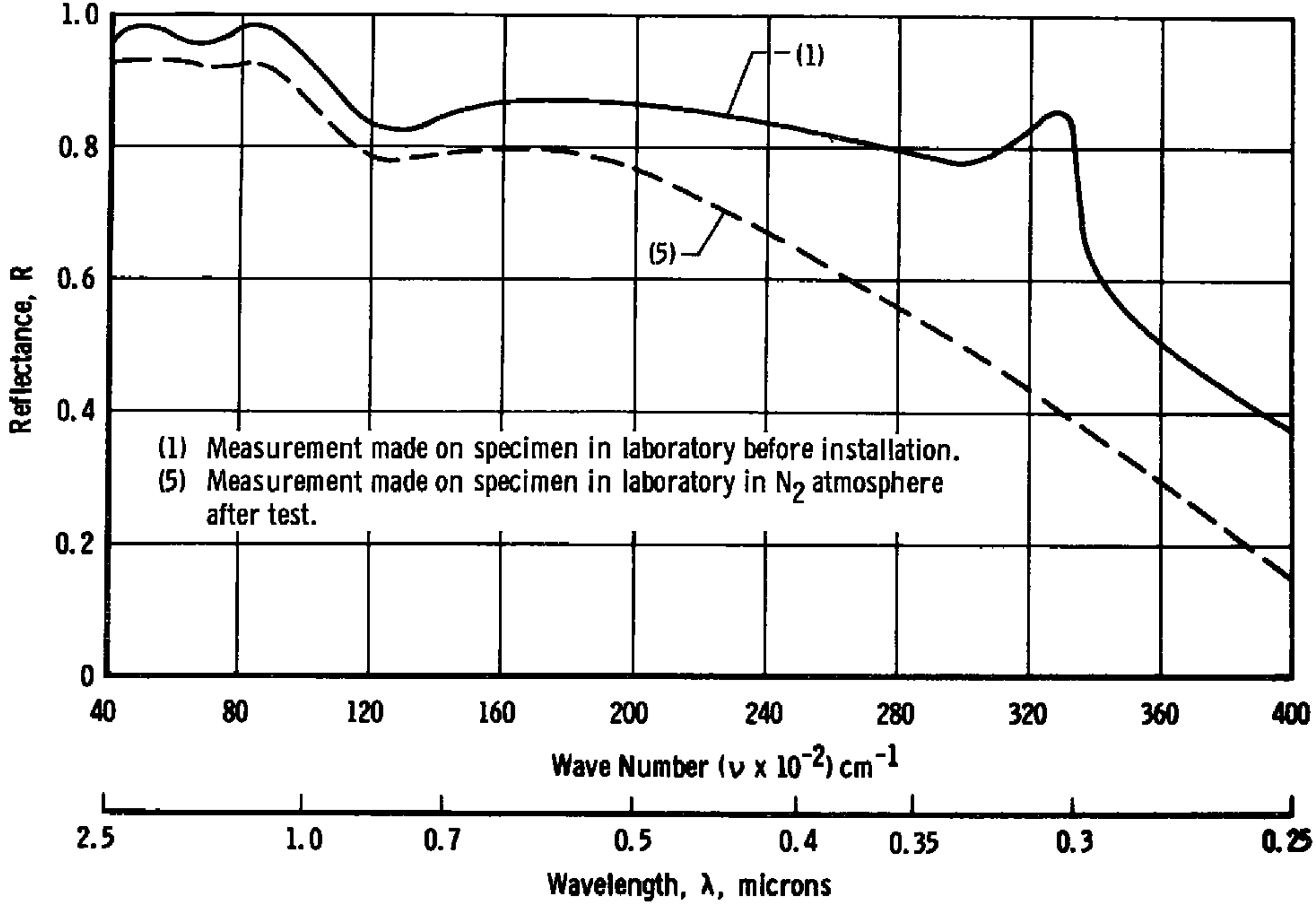

Fig. 15 Test 3—Reflectance Measurements on Specimen, Location S_8, Type C

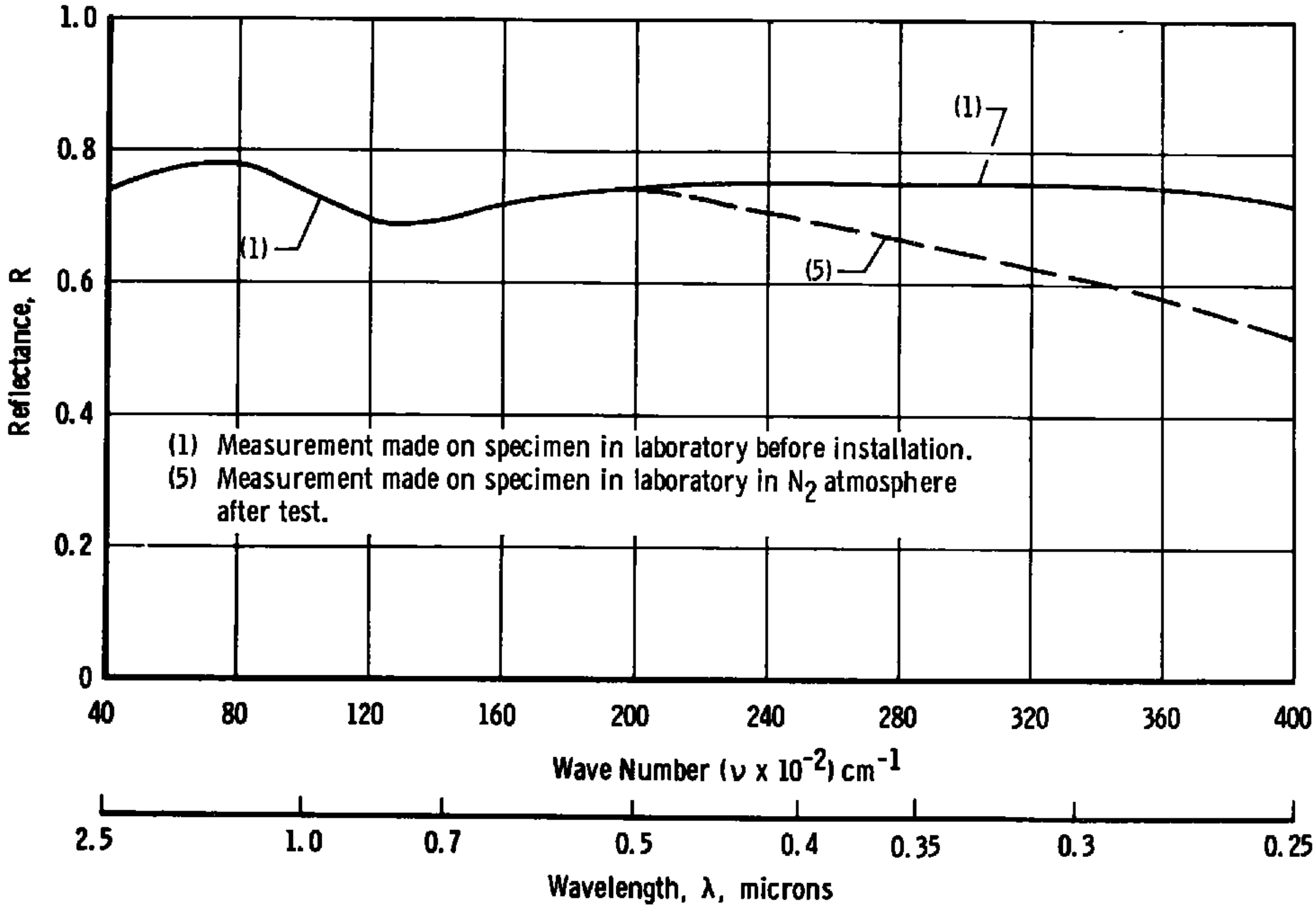

Fig. 16 Test 3—Reflectance Measurements on Specimen, Location S_{11}, Type B

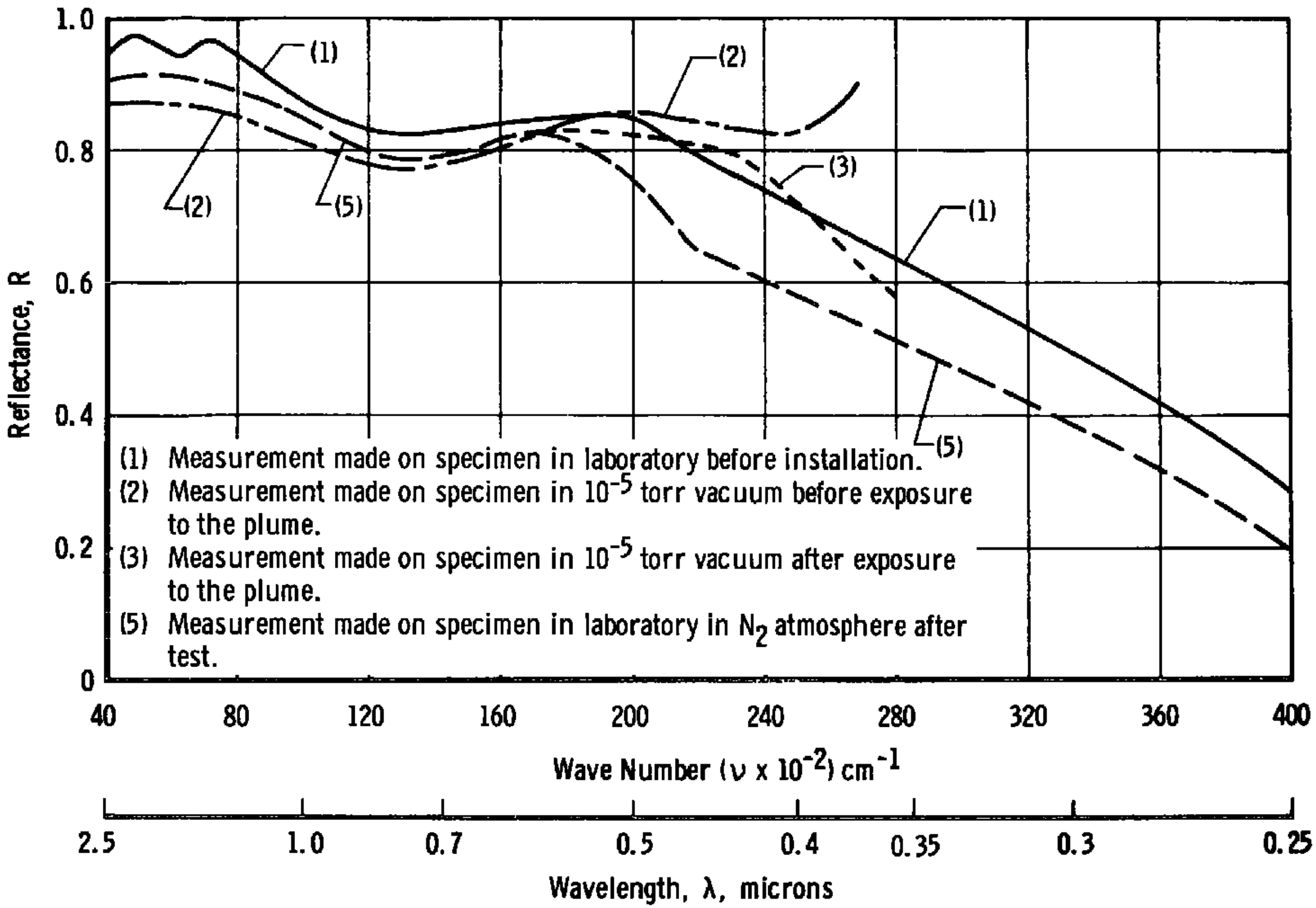

Fig. 17 Test 3—Reflectance Measurements on Specimen, Location S_{12}, Type C

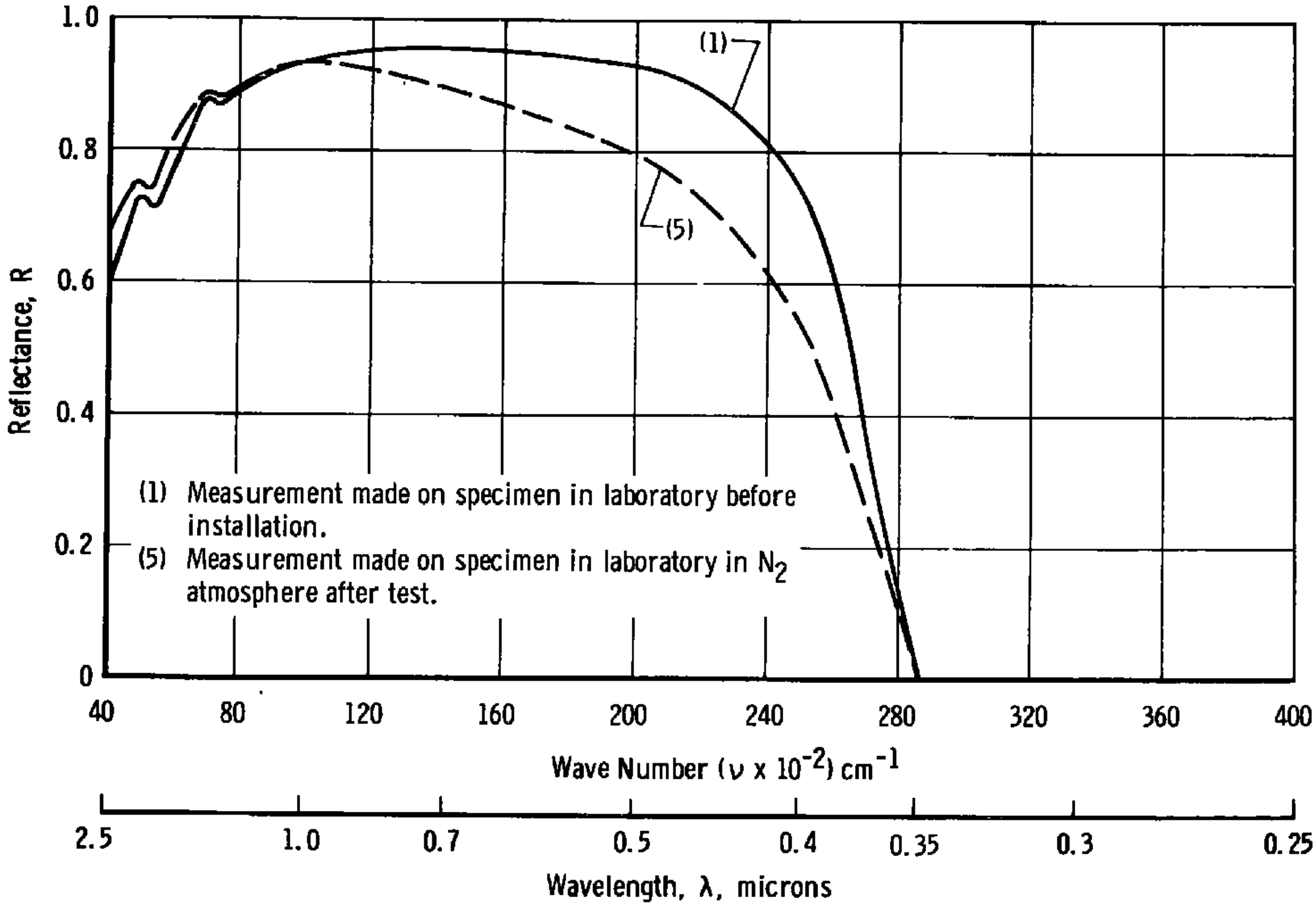

Fig. 18 Test 3—Reflectance Measurements on Specimen, Location S_{13}, Type A

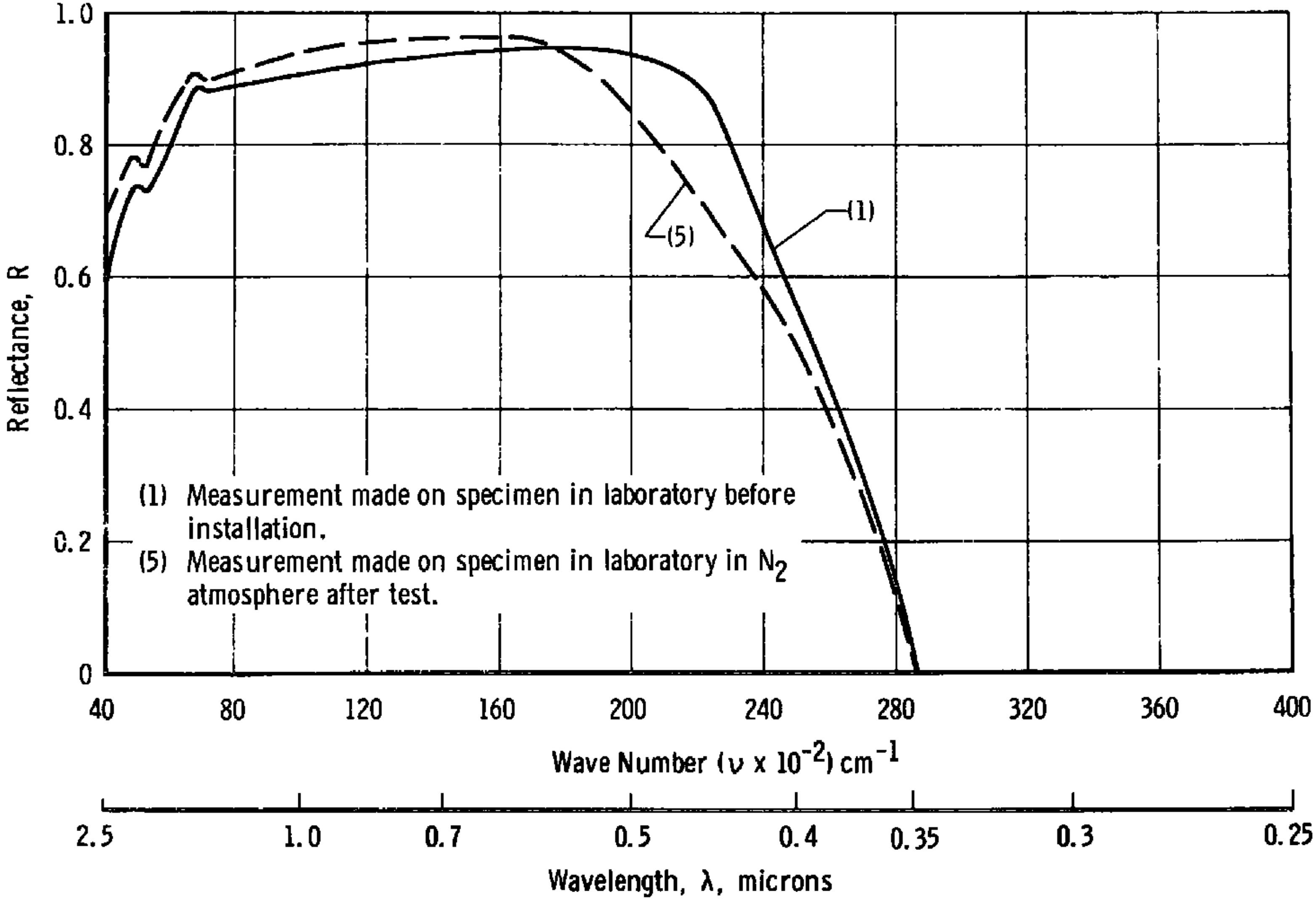

Fig. 19 Test 3—Reflectance Measurements on Specimen, Location S_{15}, Type A

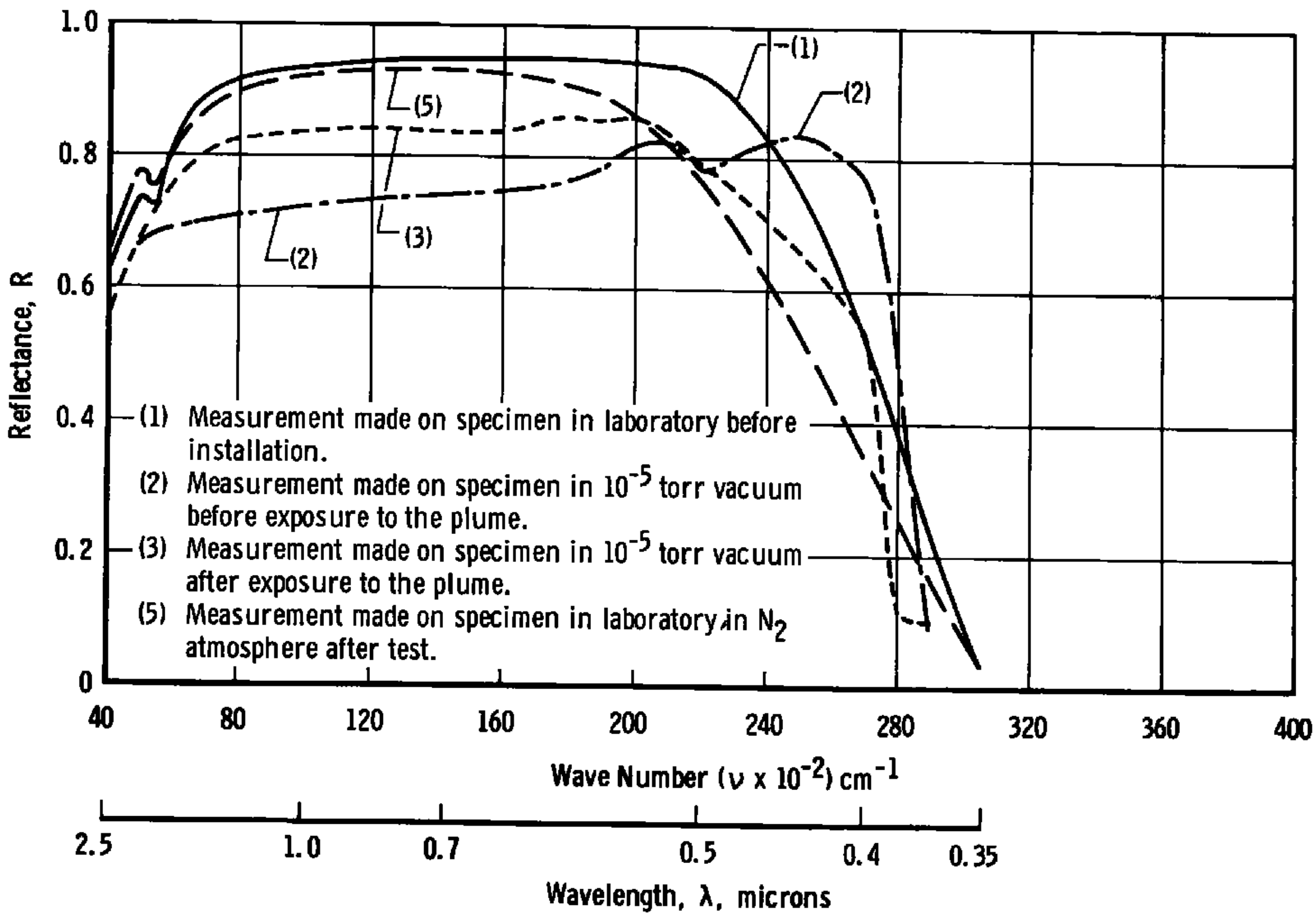

Fig. 20 Test 3—Reflectance Measurements on Specimen, Location S_{16}, Type A

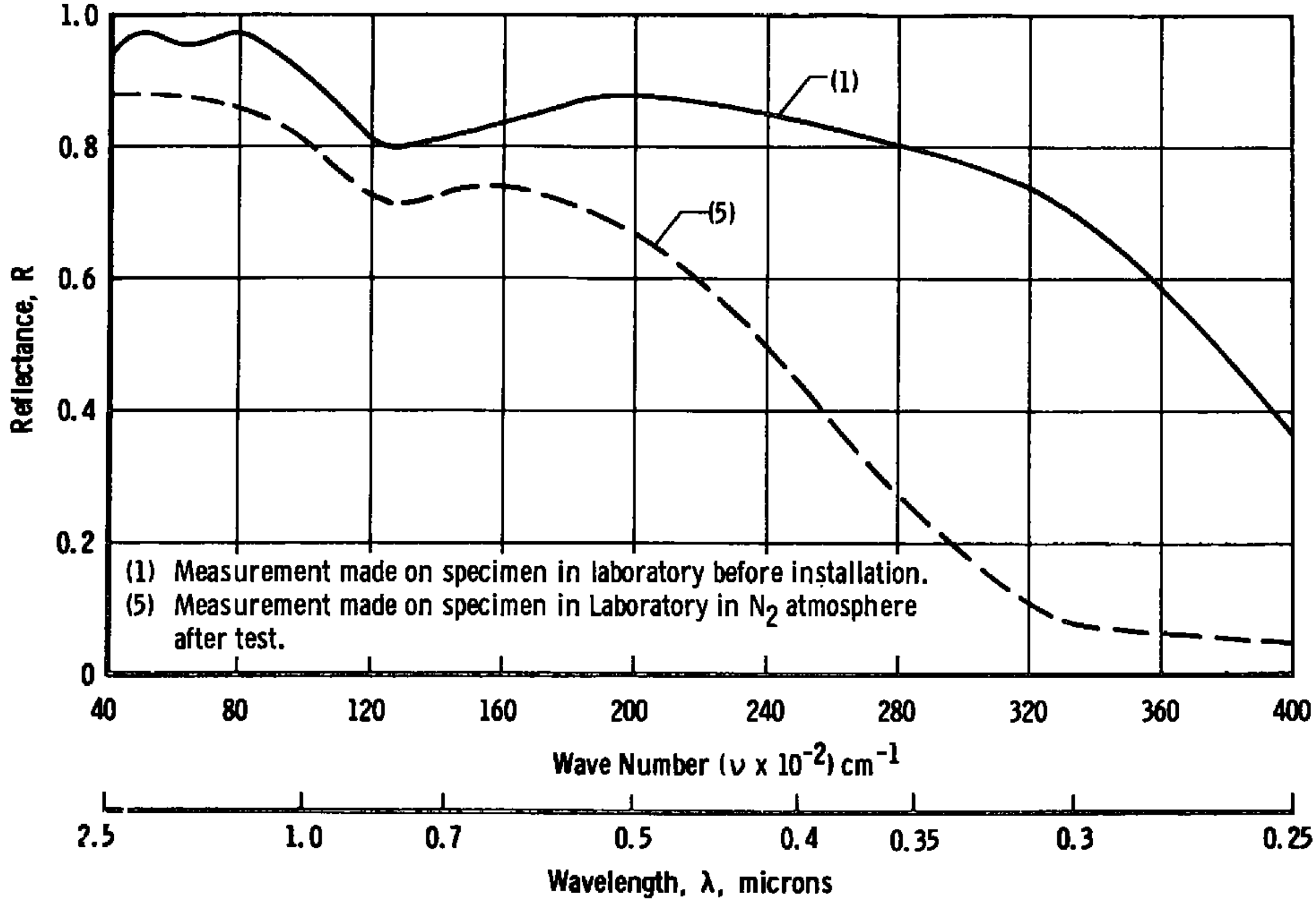

Fig. 21 Test 3—Reflectance Measurements on Specimen, Location S_{17}, Type C

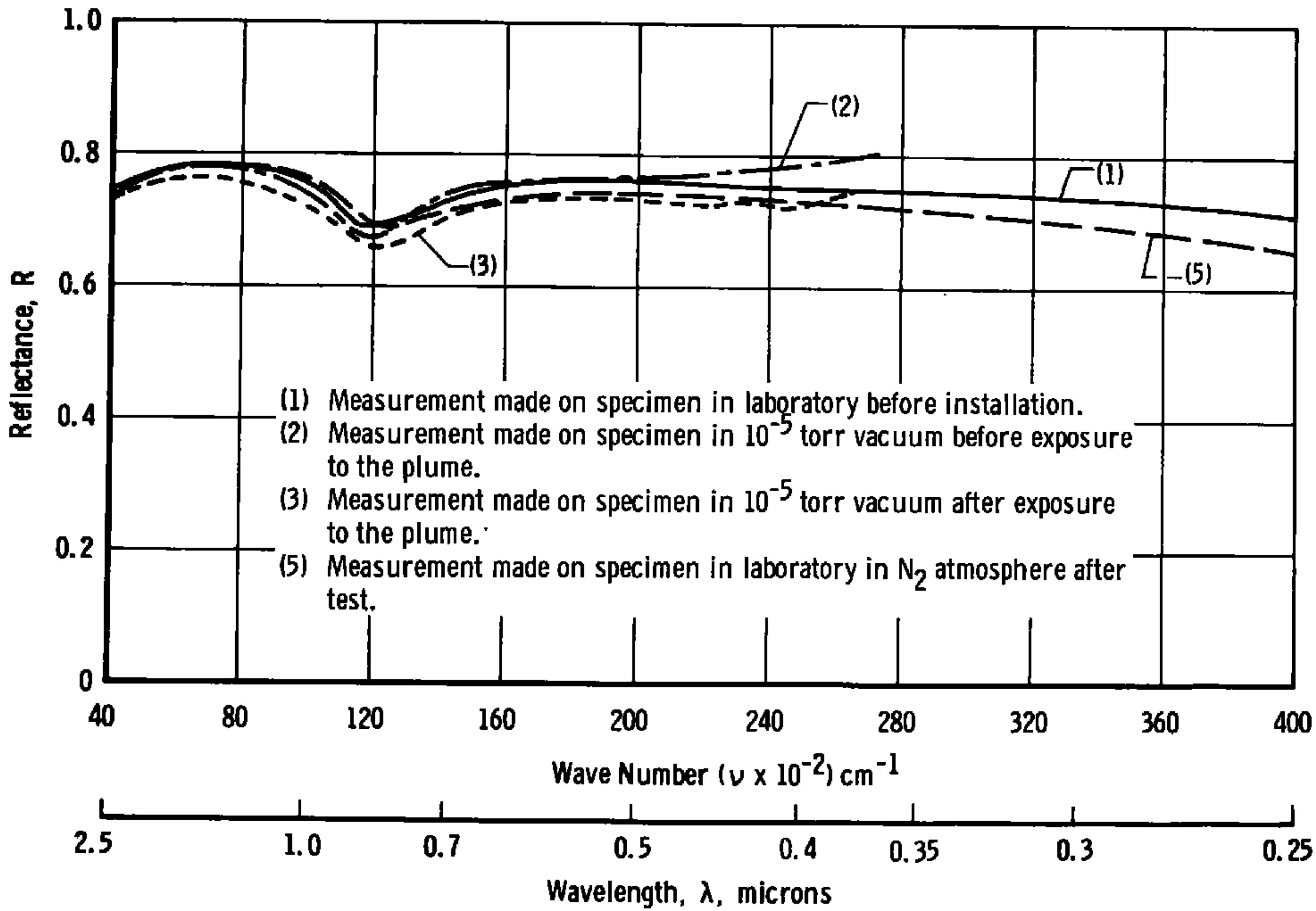

Fig. 22 Test 3—Reflectance Measurements on Specimen, Location S_{20}, Type B

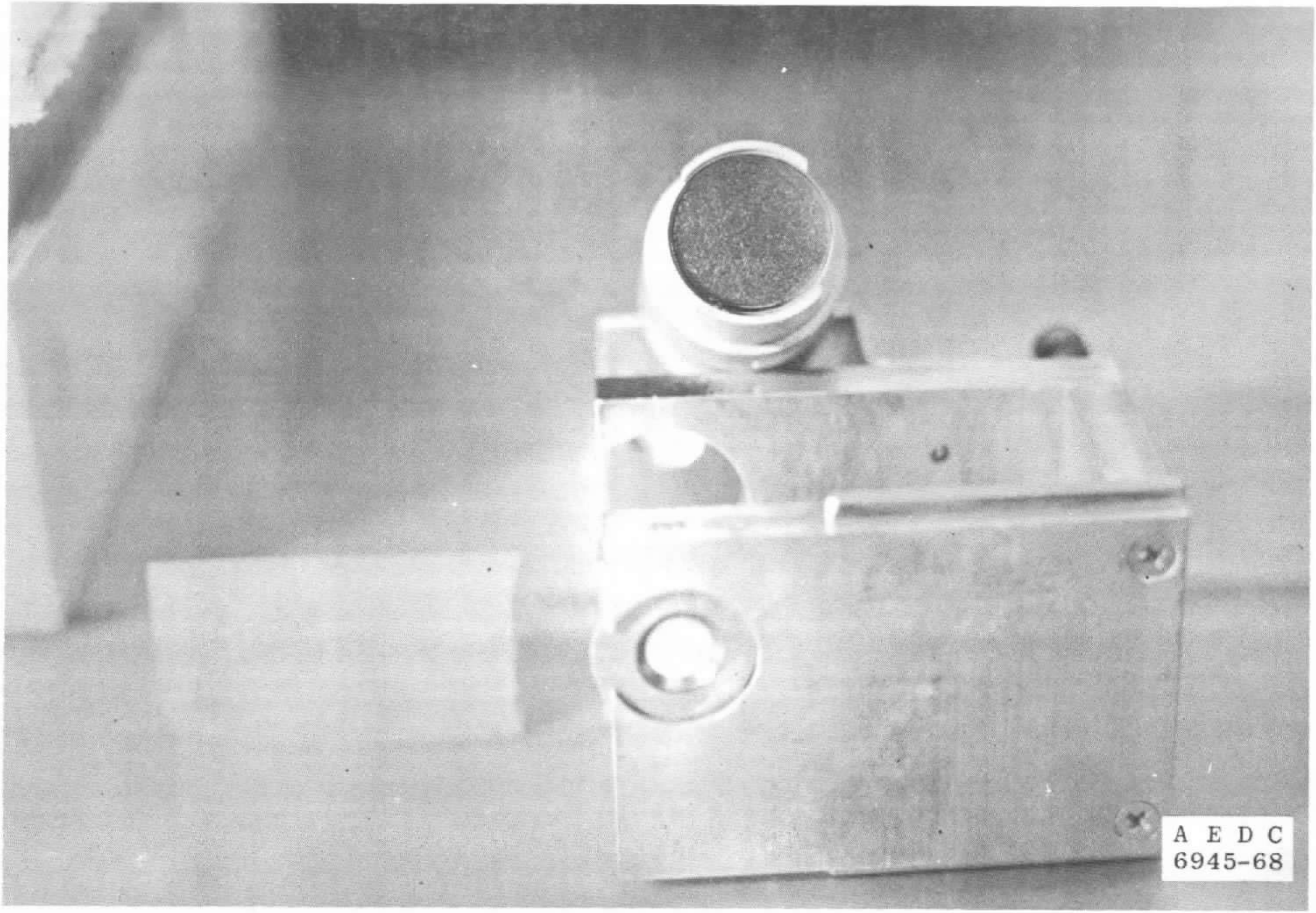

Fig. 23 Contamination on Specimen, Location H_1, after Test 4C

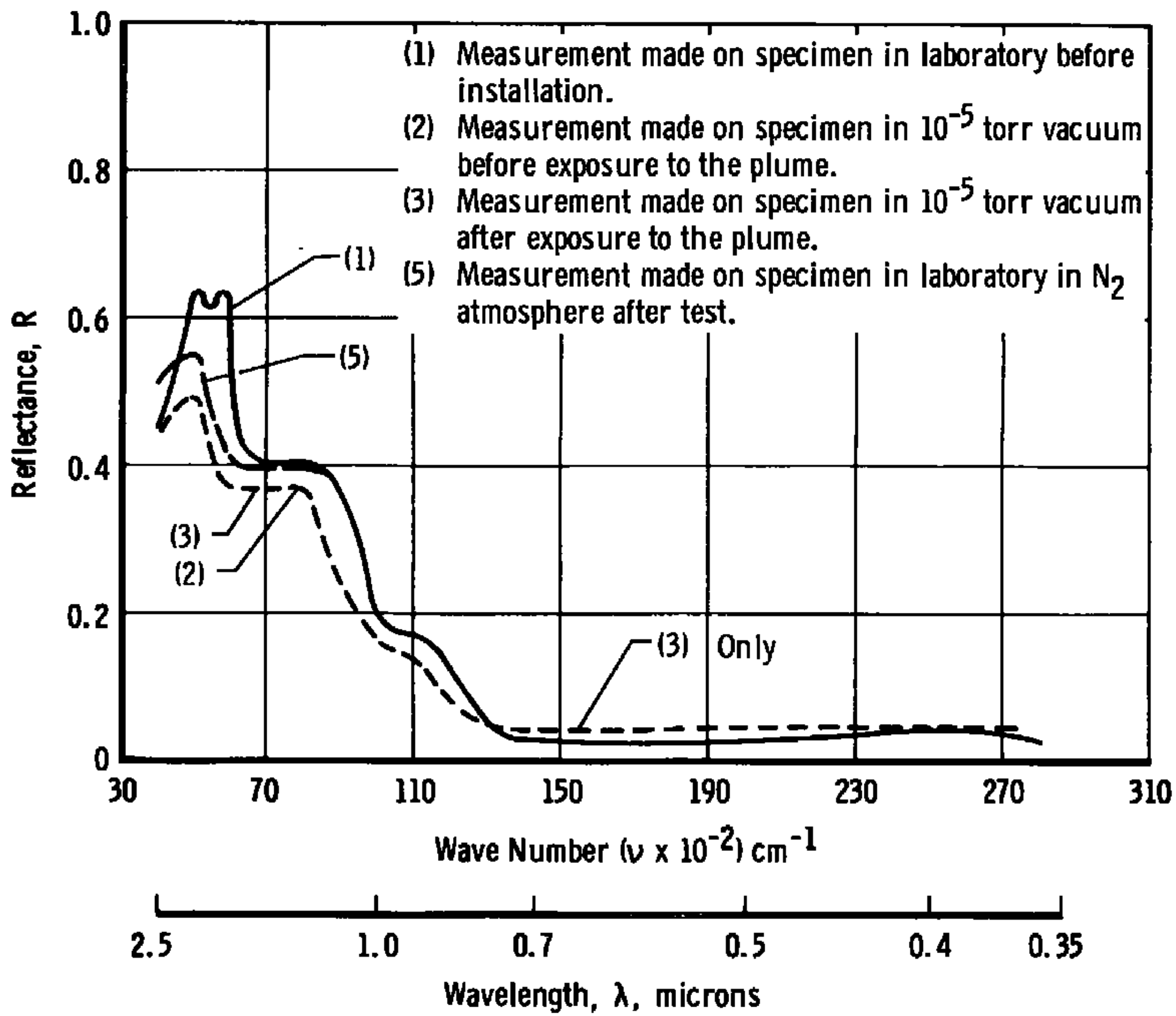

Fig. 24 Test 4C—Reflectance Measurements on Specimen, Location S_7, Type K

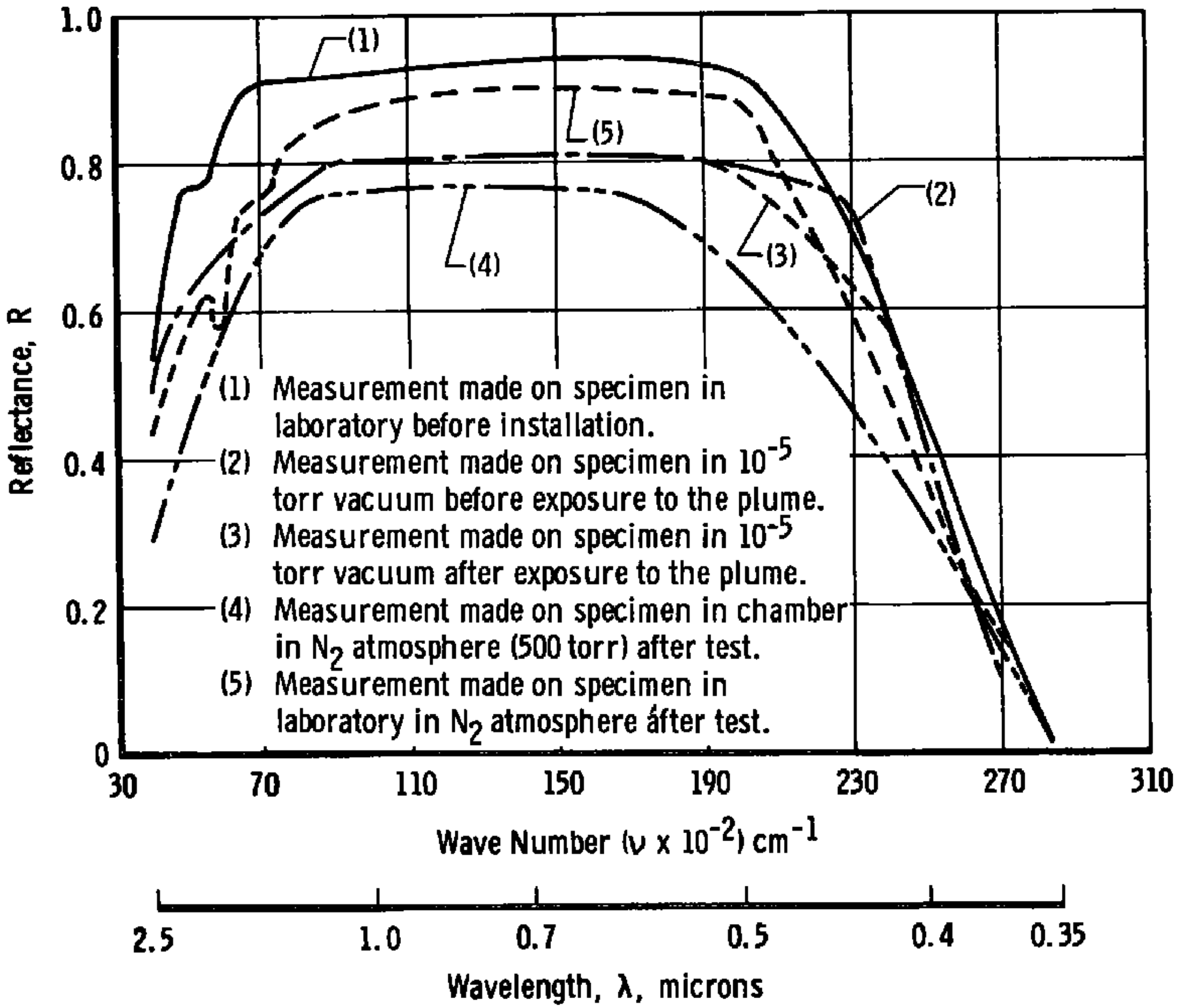

Fig. 25 Test 4C—Reflectance Measurements on Specimen, Location S_{11}, Type A

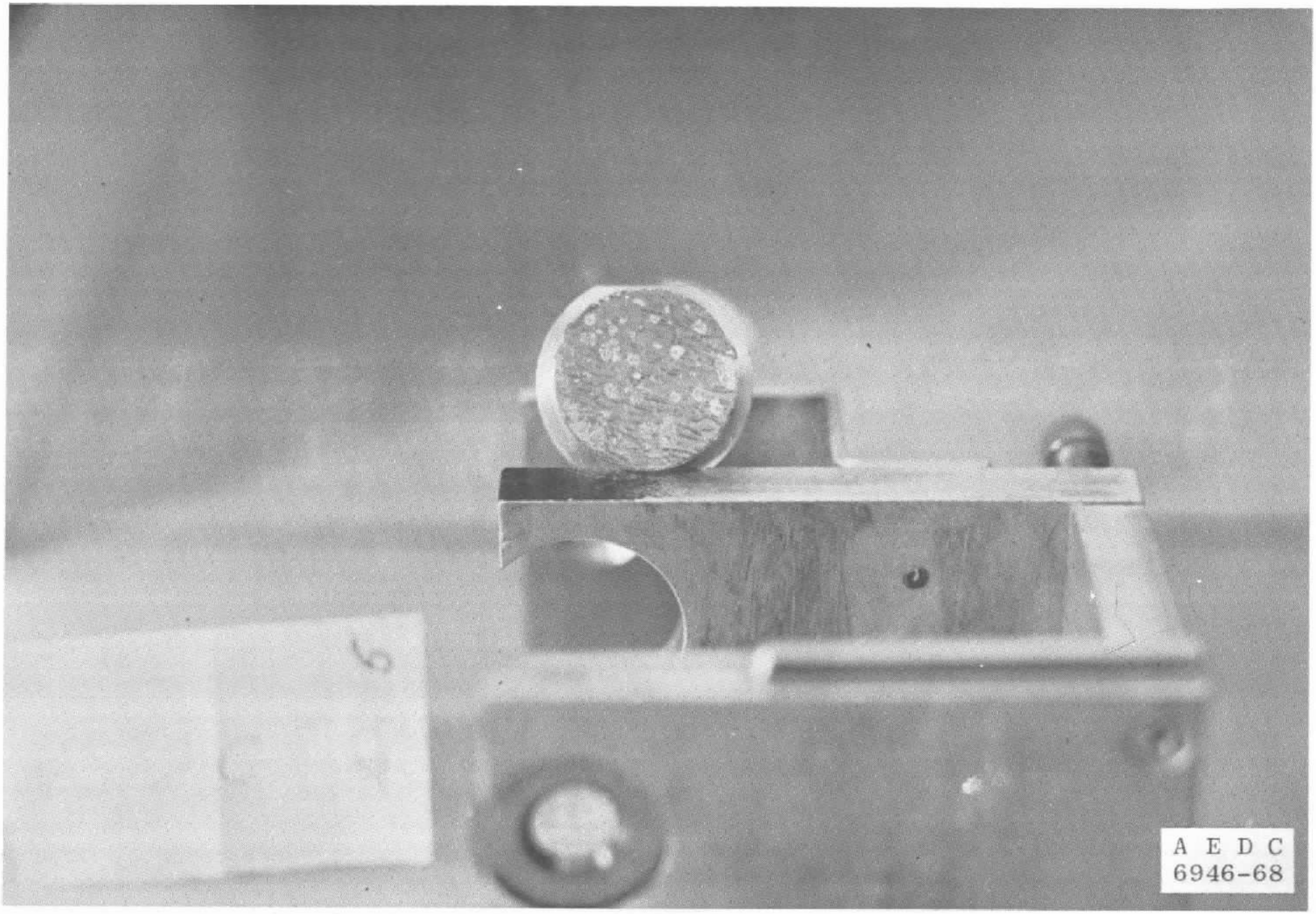

Fig. 26 Corrosion on Specimen, Location S_{12}, Type C, after Test 4C

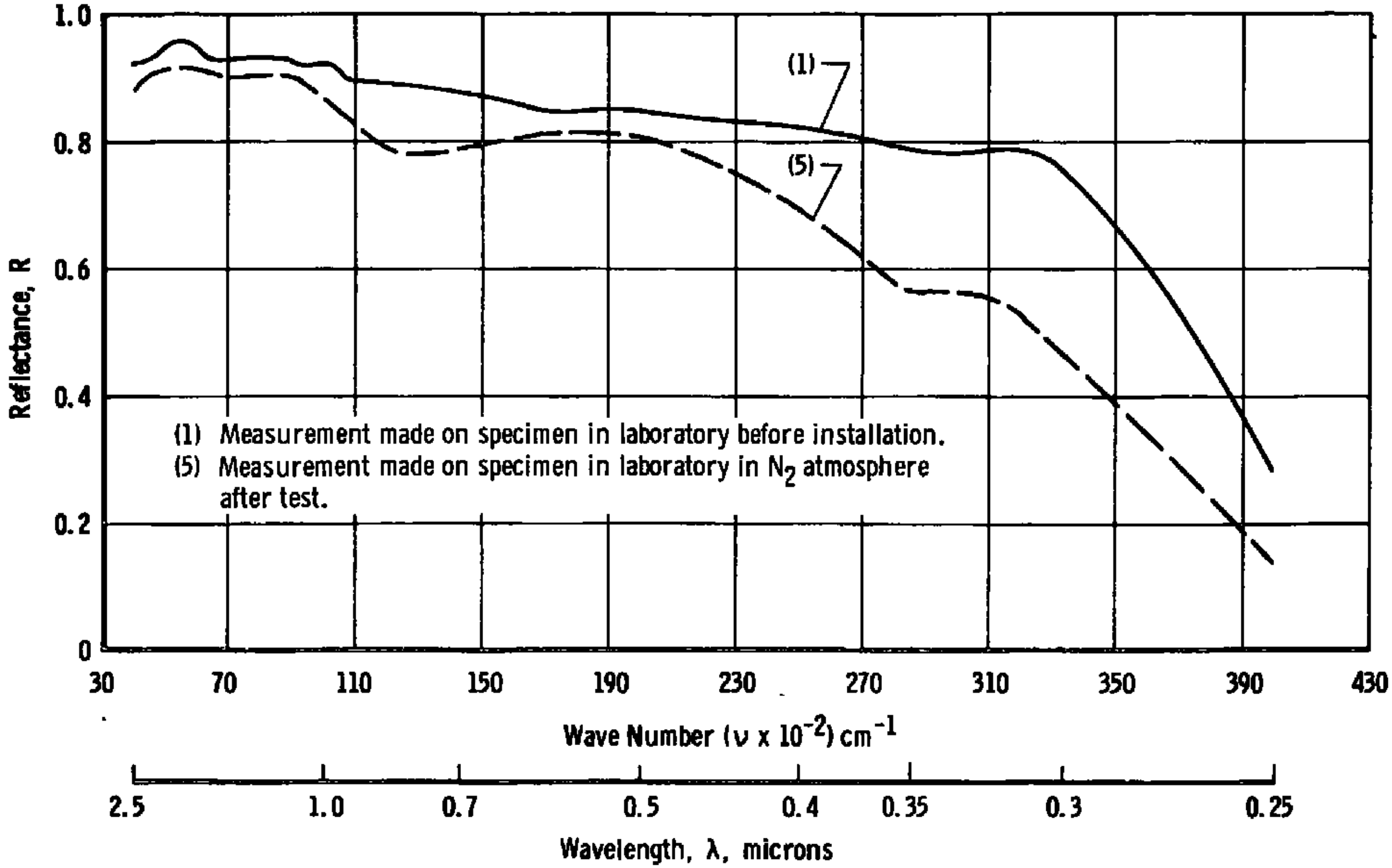

Fig. 27 Test 4C—Reflectance Measurements on Specimen, Location S_{12}, Type C

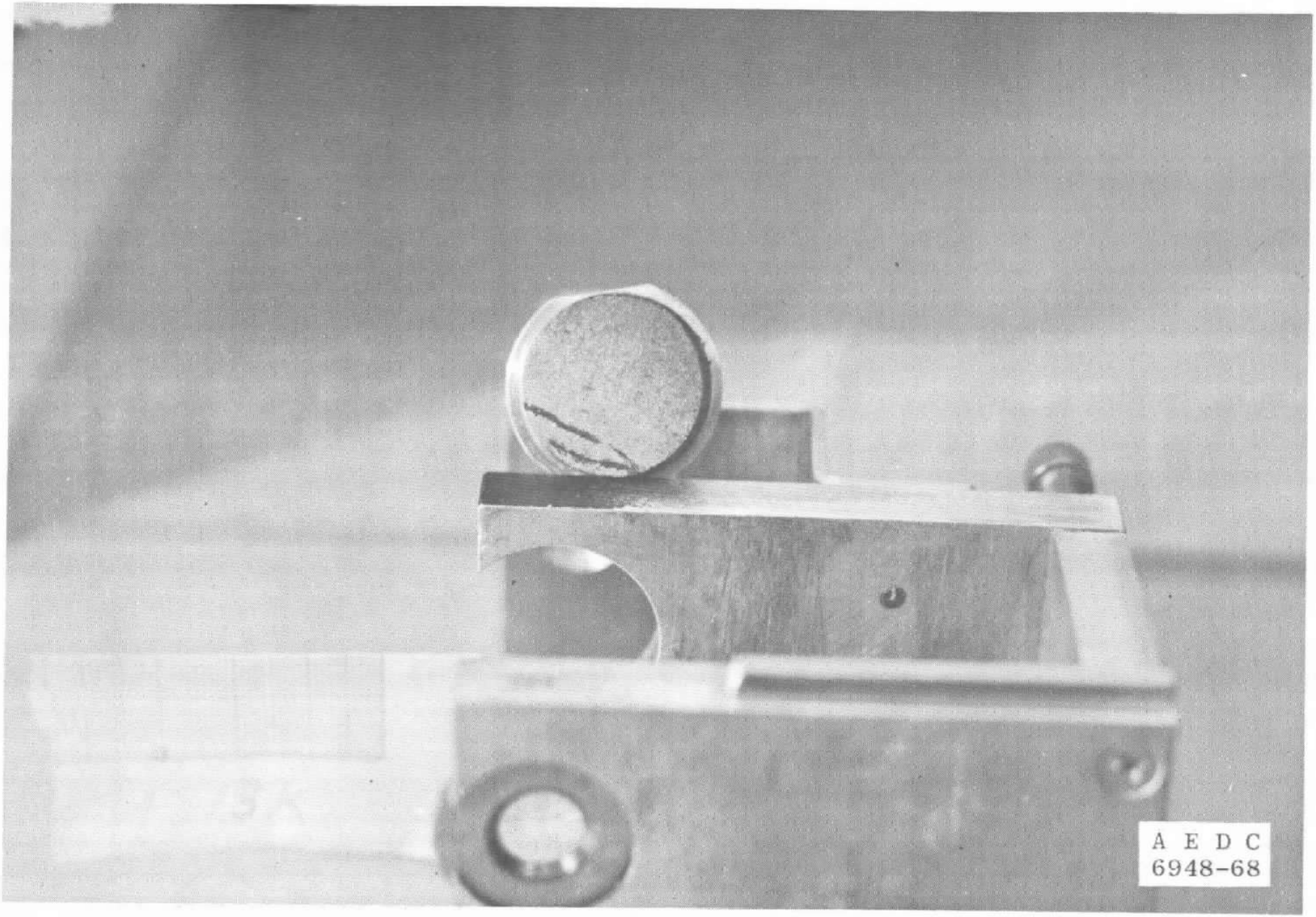

Fig. 28 Corrosion on Specimen, Location S_{13}, Type K, after Test 4C

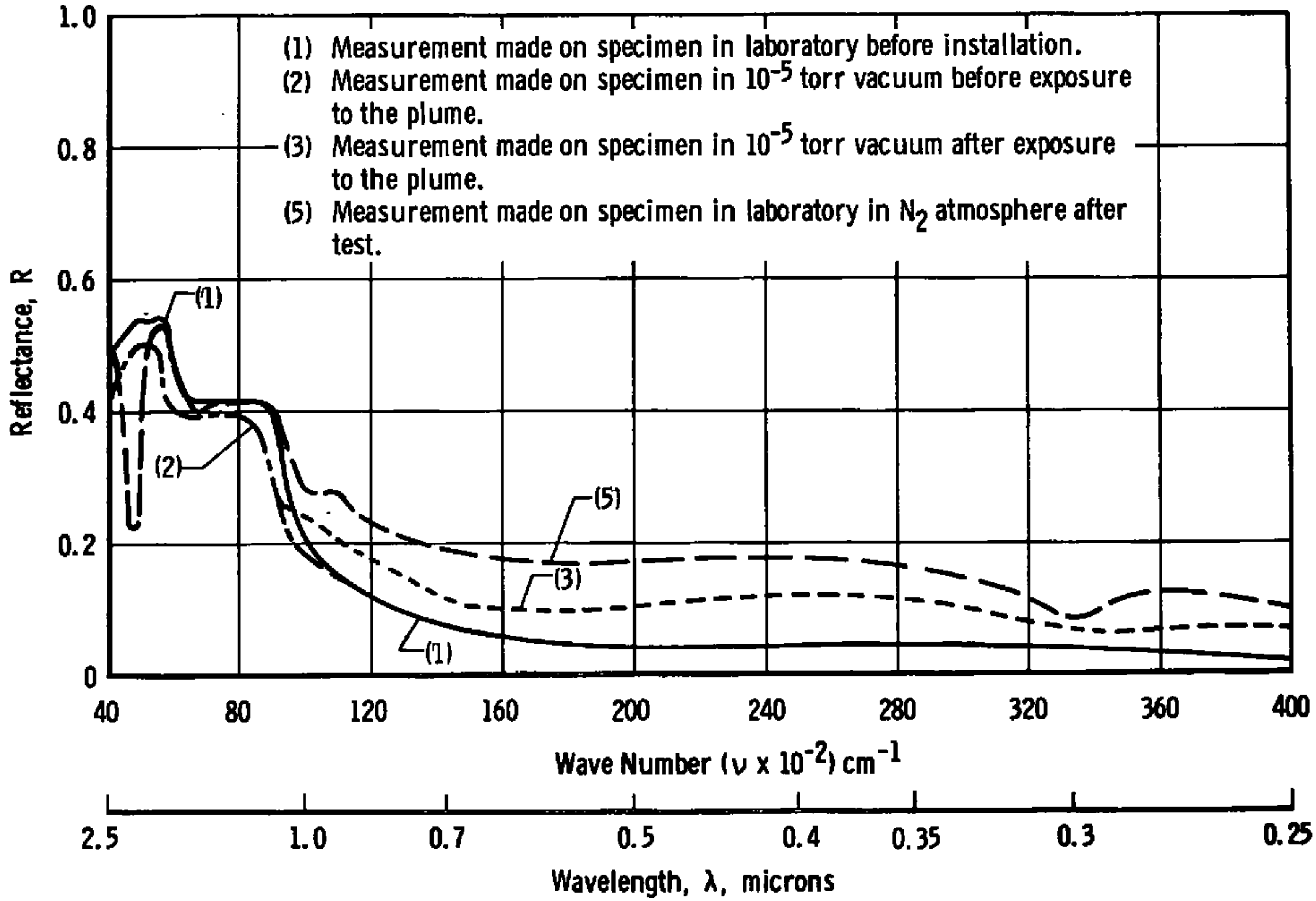

Fig. 29 Test 4C—Reflectance Measurements on Specimen, Location S_{13}, Type K

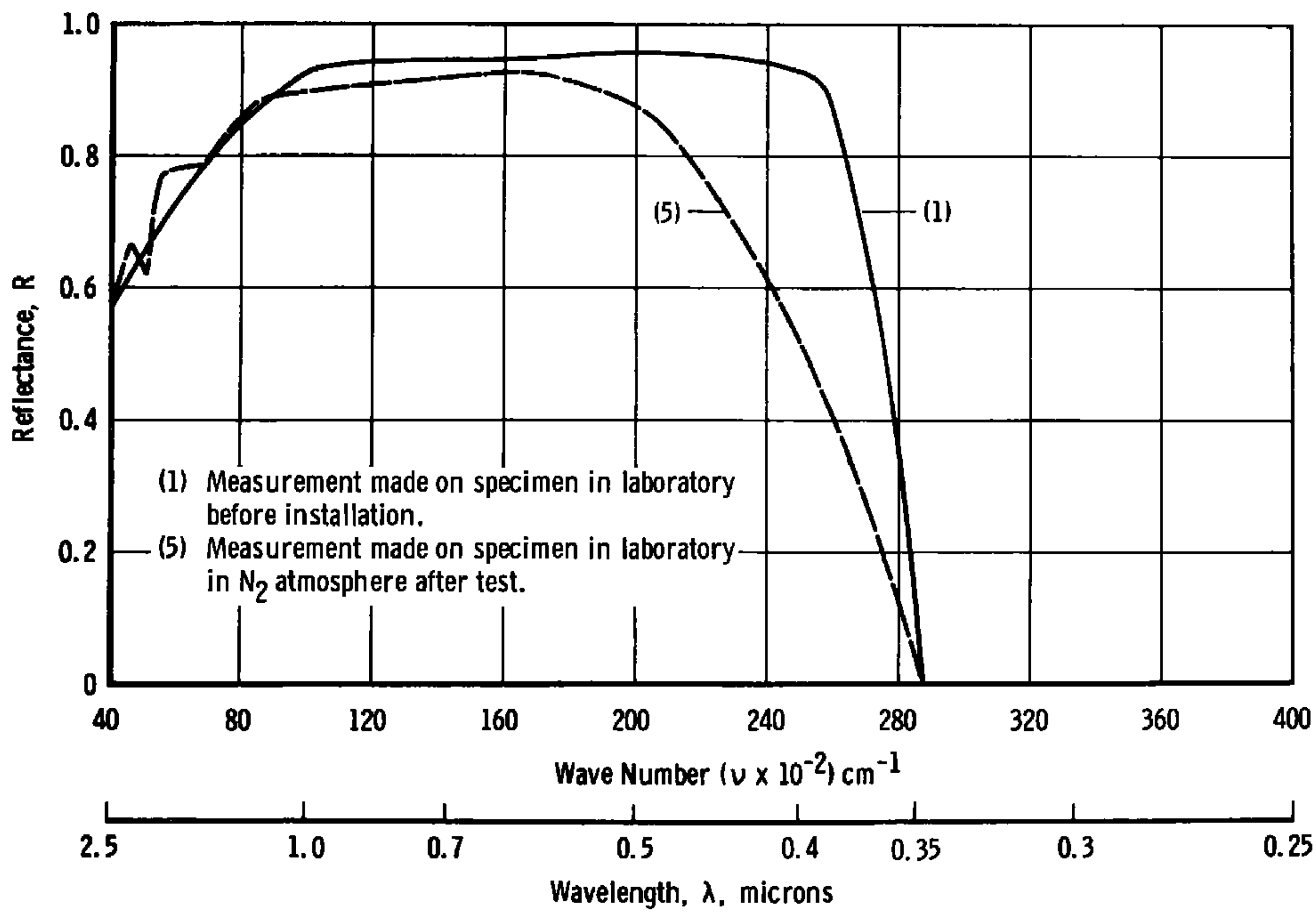

Fig. 30 Test 4C—Reflectance Measurements on Specimen, Location S_{14}, Type A

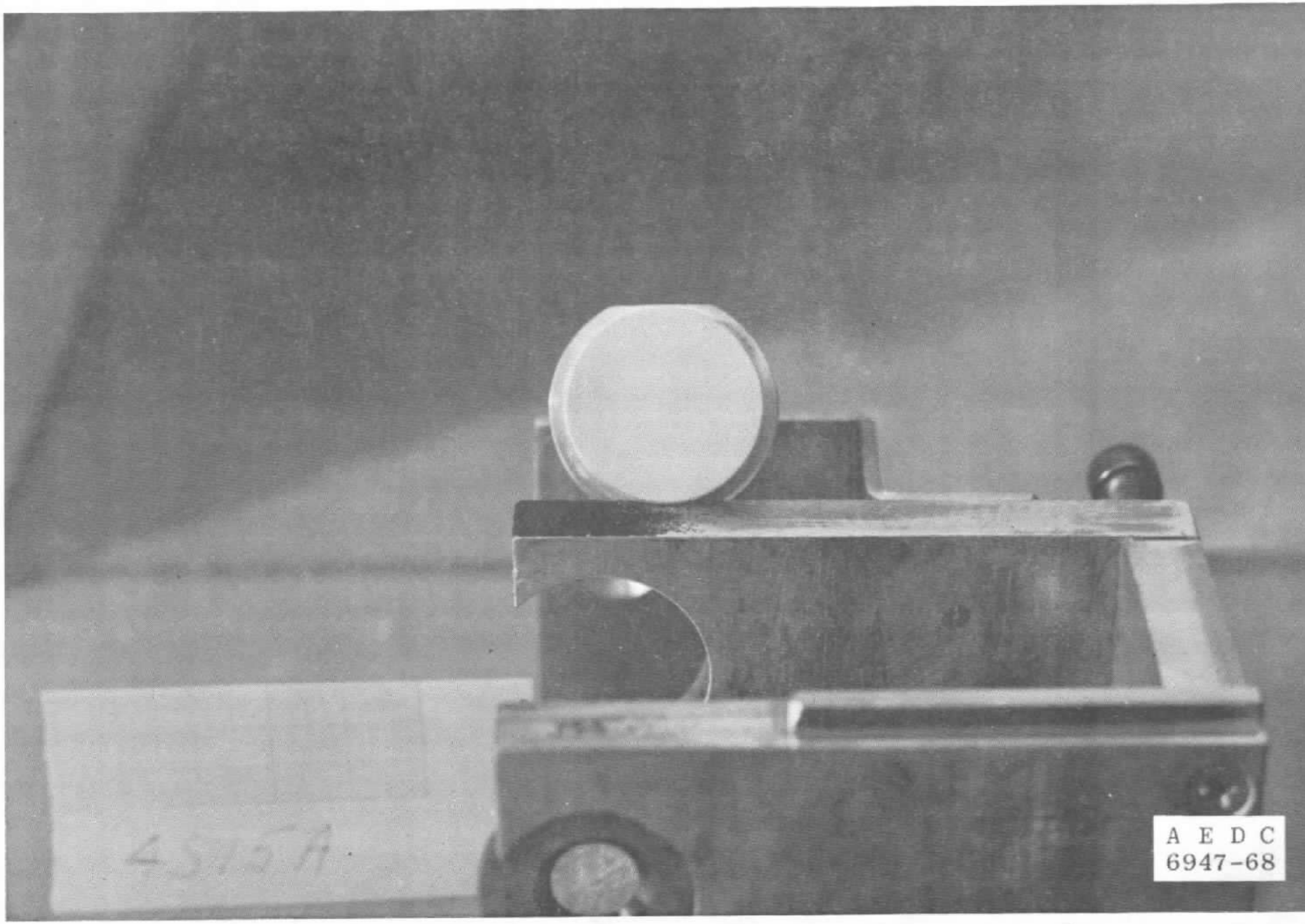

Fig. 31 Corrosion on Specimen, Location S_{15}, Type A, after Test 4C

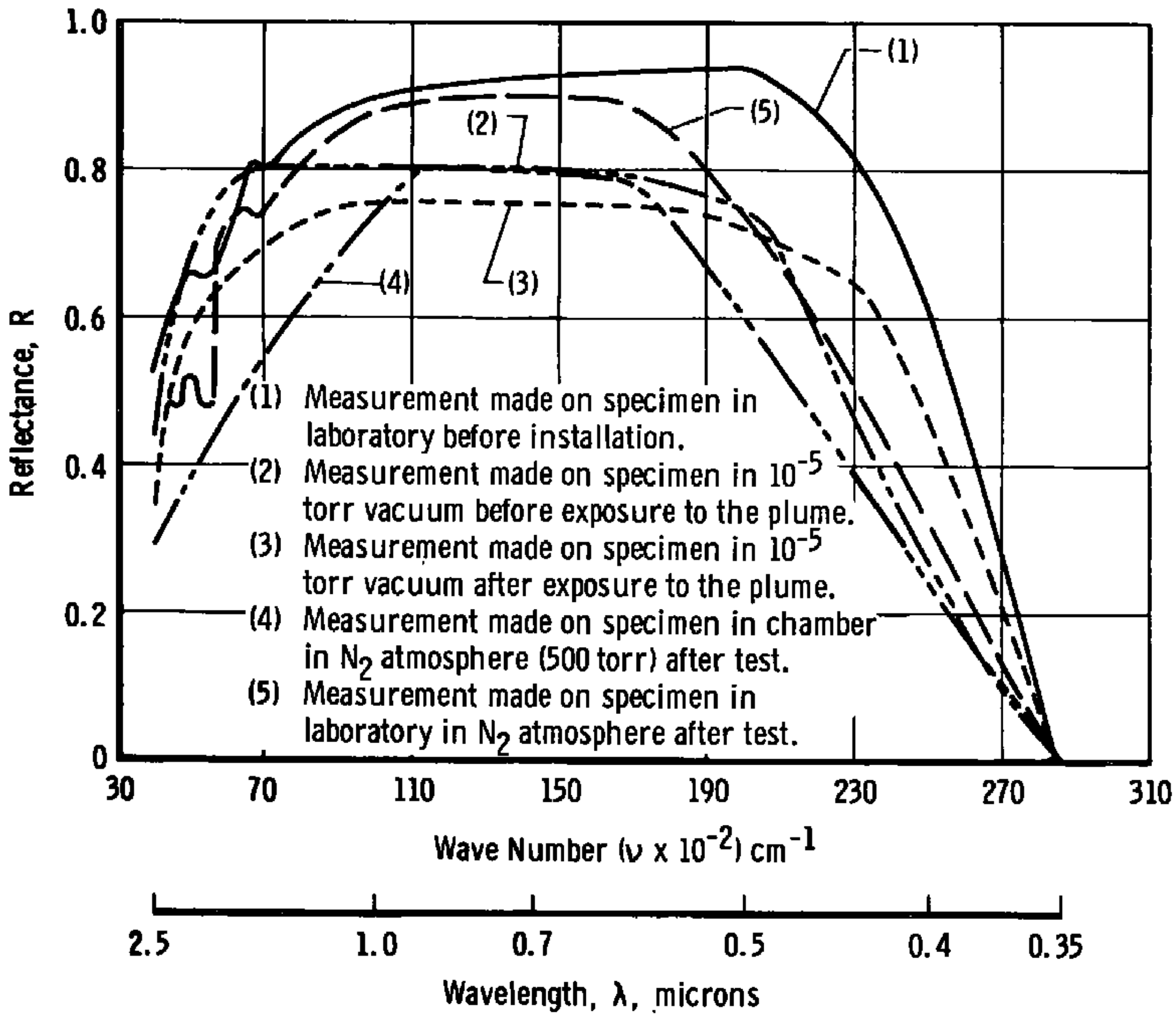

Fig. 32 Test 4C—Reflectance Measurements on Specimen, Location S_{15}, Type A

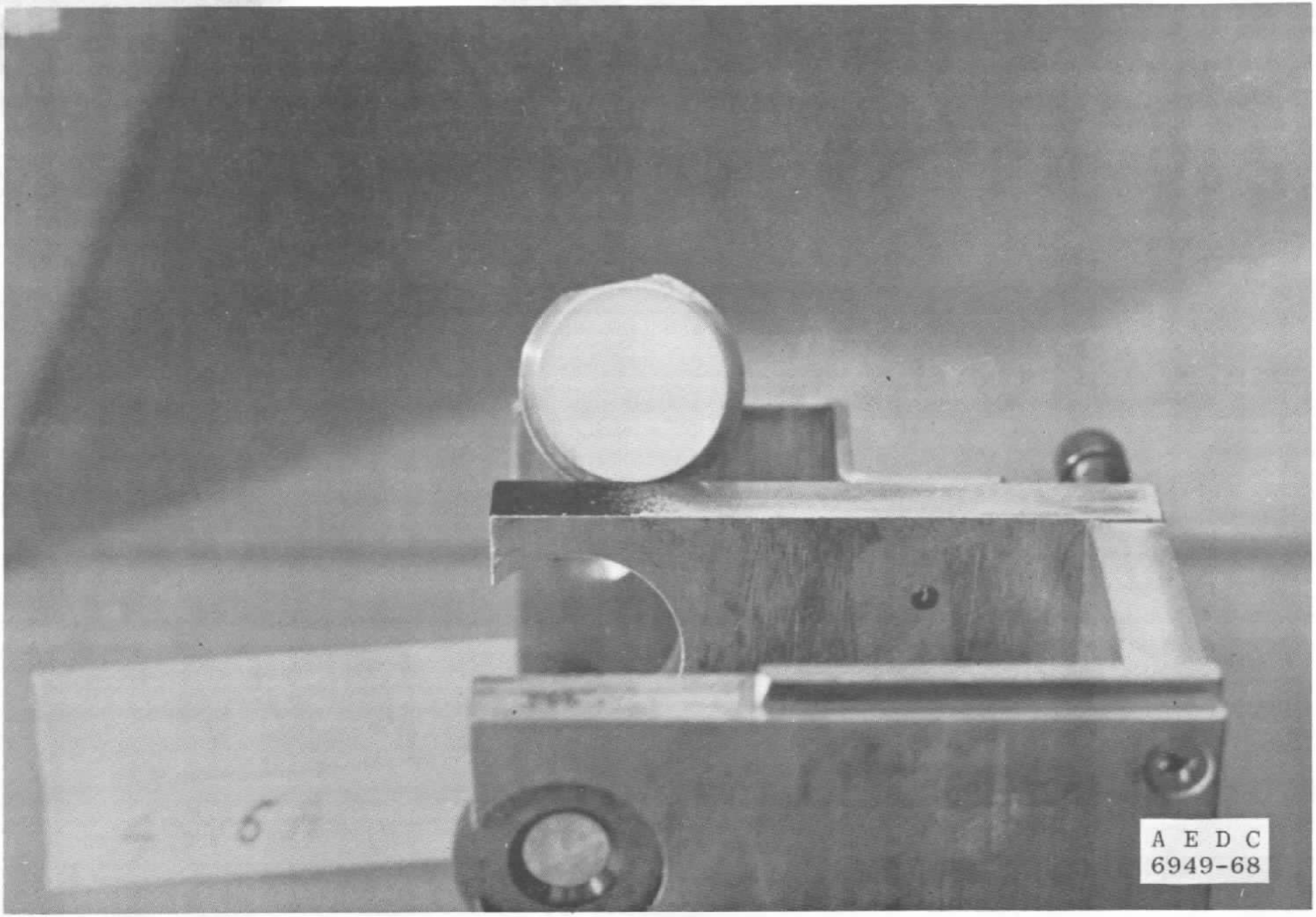

Fig. 33 Corrosion on Specimen, Location S_{16}, Type A, after Test 4C

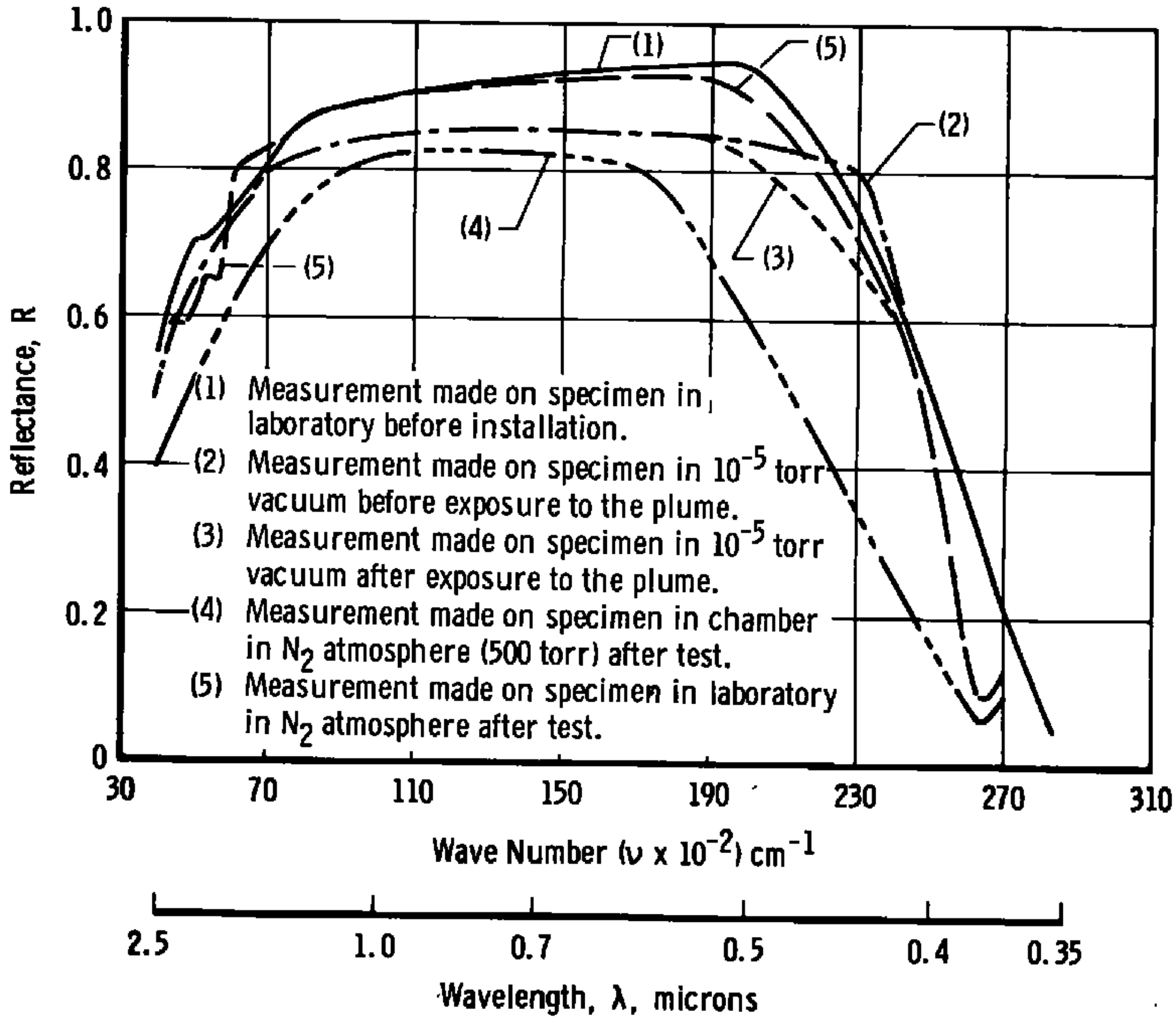

Fig. 34 Test 4C—Reflectance Measurements on Specimen, Location S_{16}, Type A

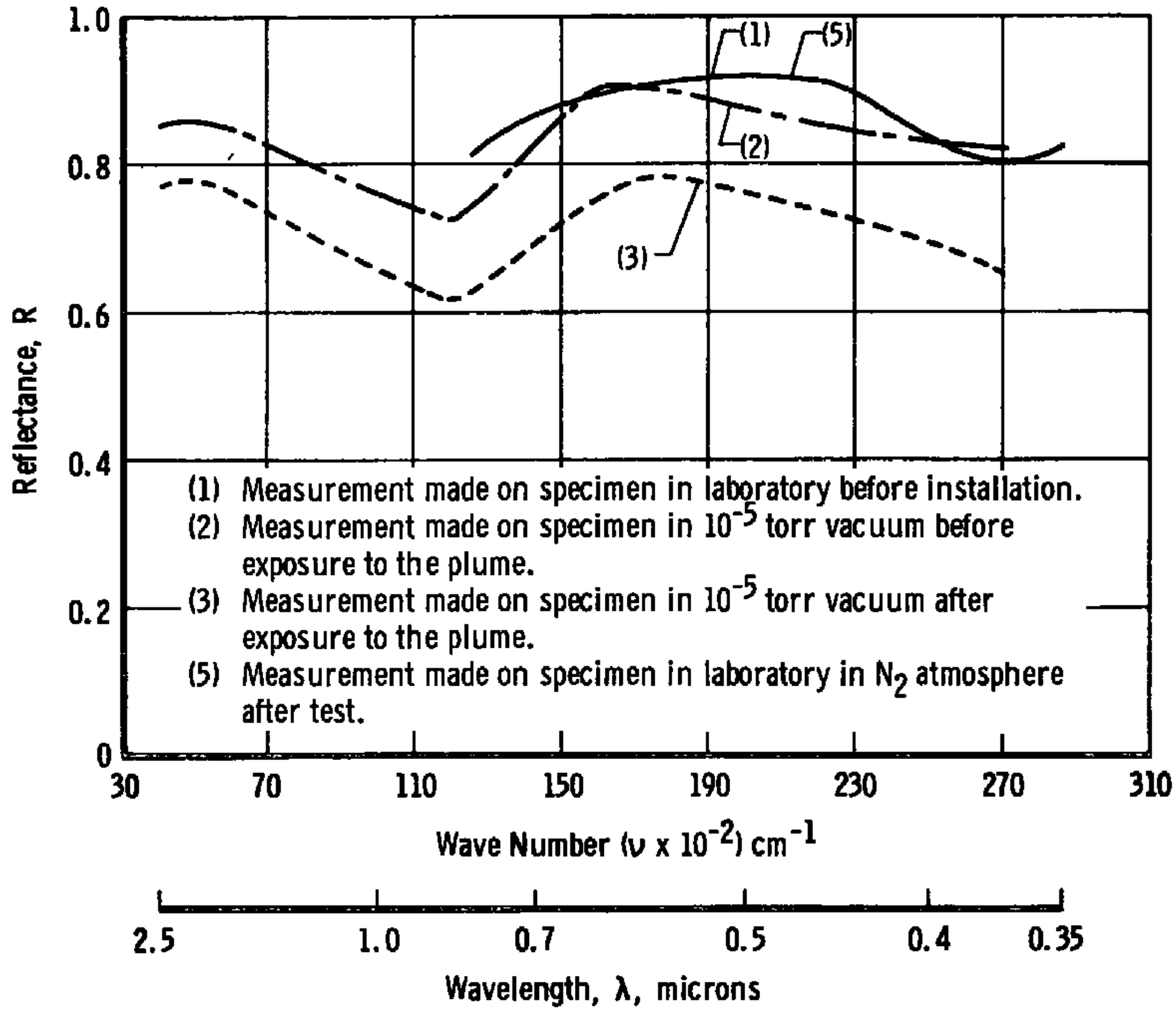

Fig. 35 Test 4C—Reflectance Measurements on Specimen, Location G_3, Mirror

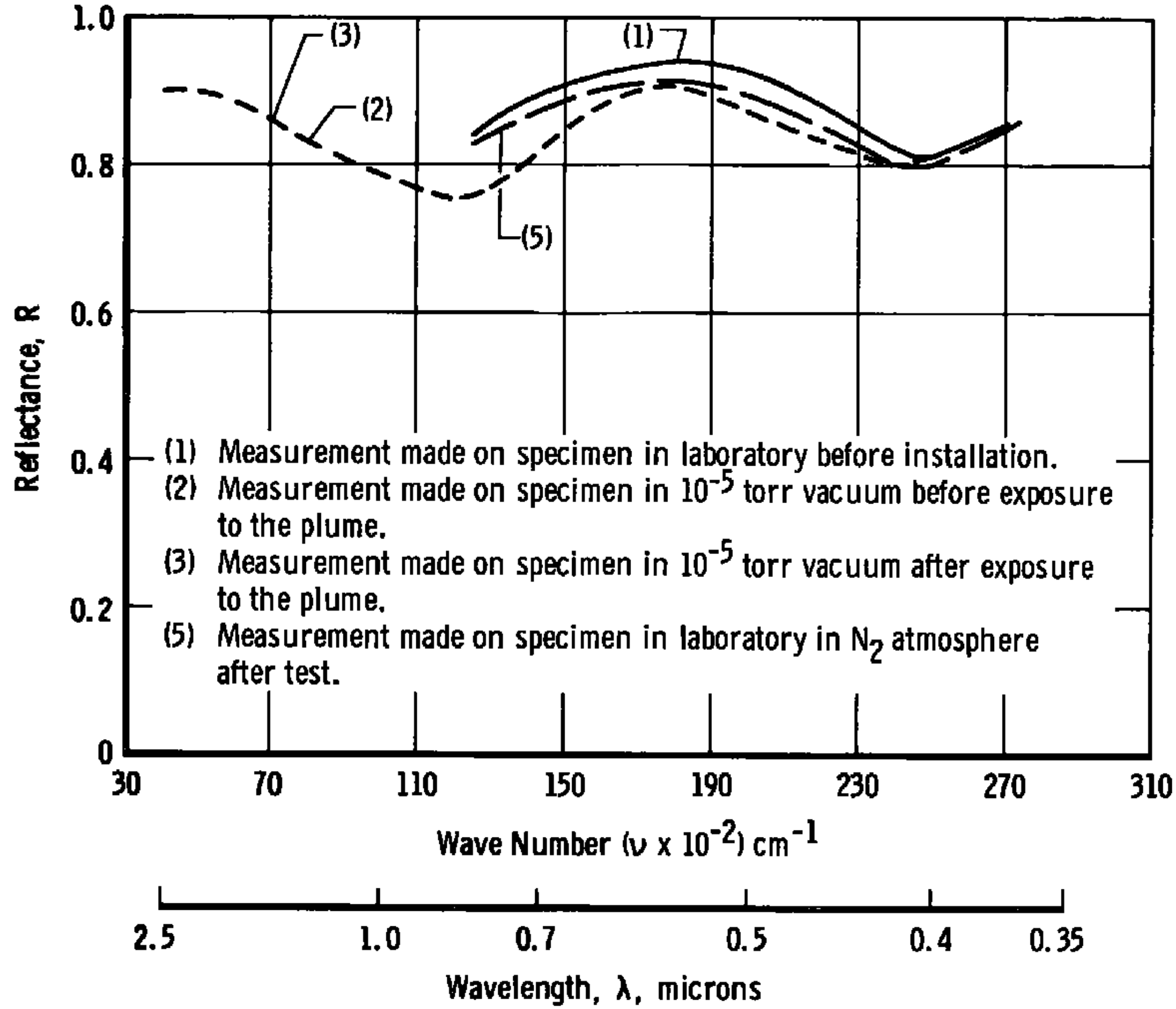

Fig. 36 Test 4C—Reflectance Measurements on Specimen, Location G_4, Mirror

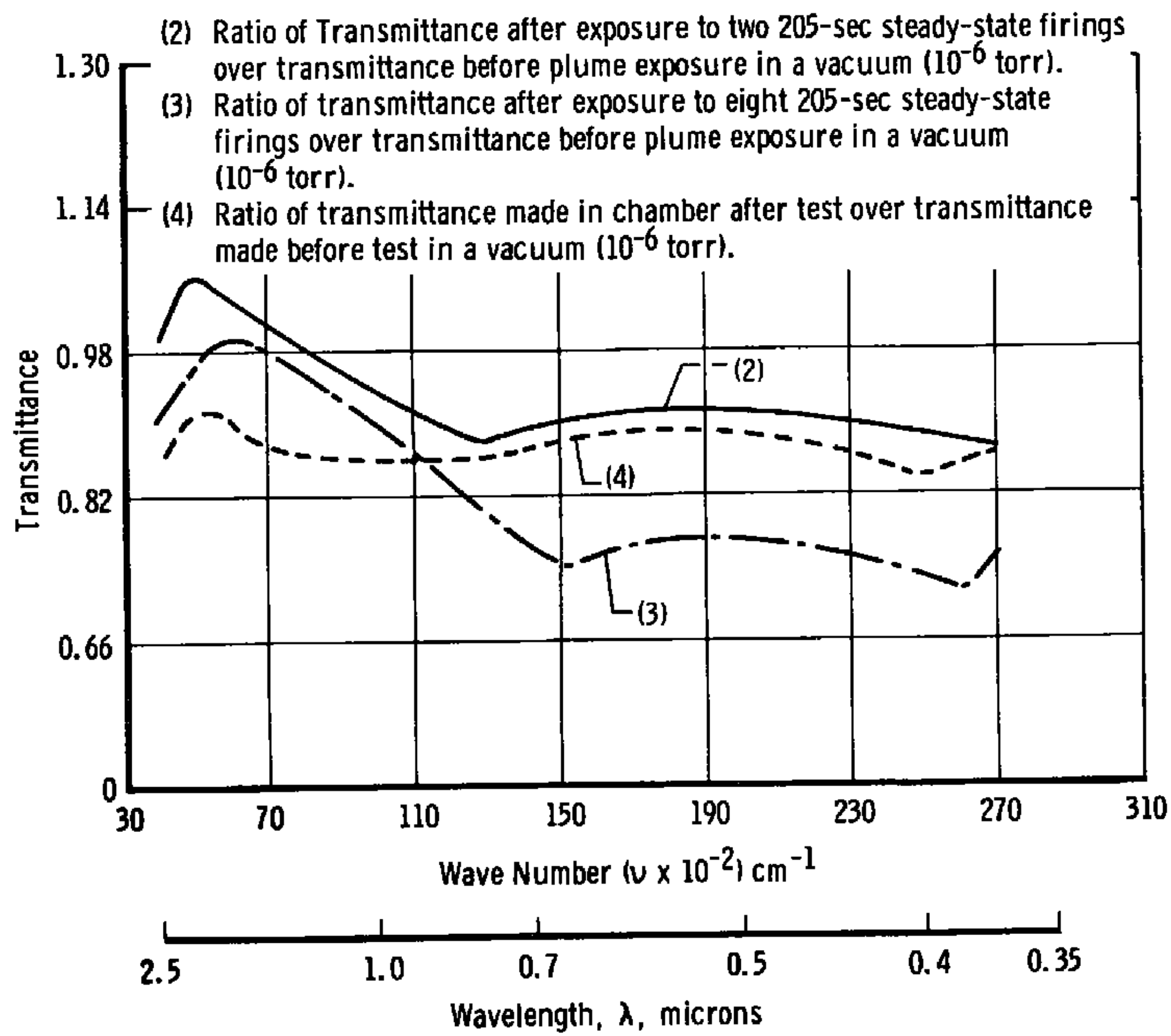

Fig. 37 Test 4C—Transmittance Measurements on Specimen, Location V_1, View Port

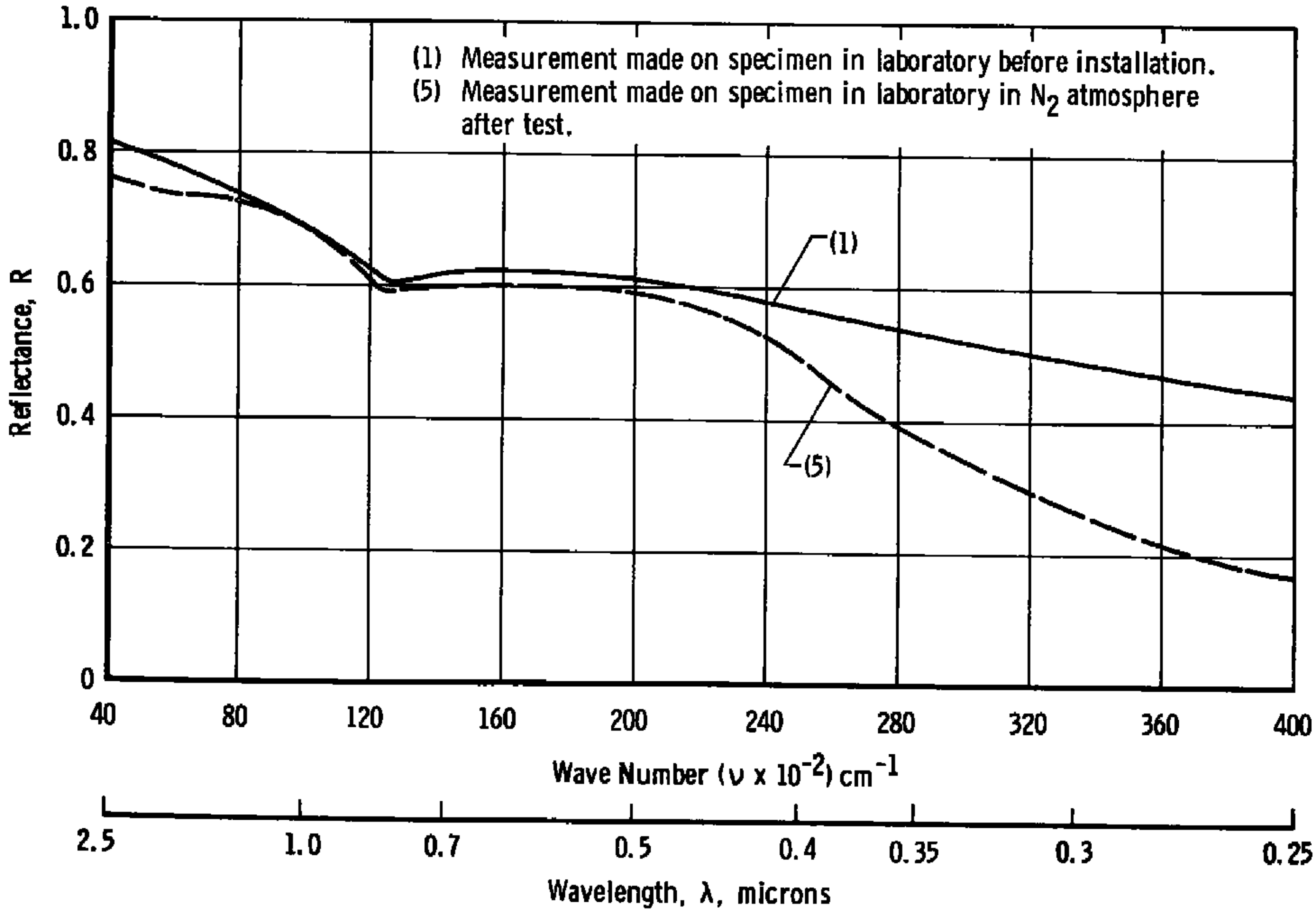

Fig. 38 Test 5B—Reflectance Measurements on Specimen, Location S_8, Type D

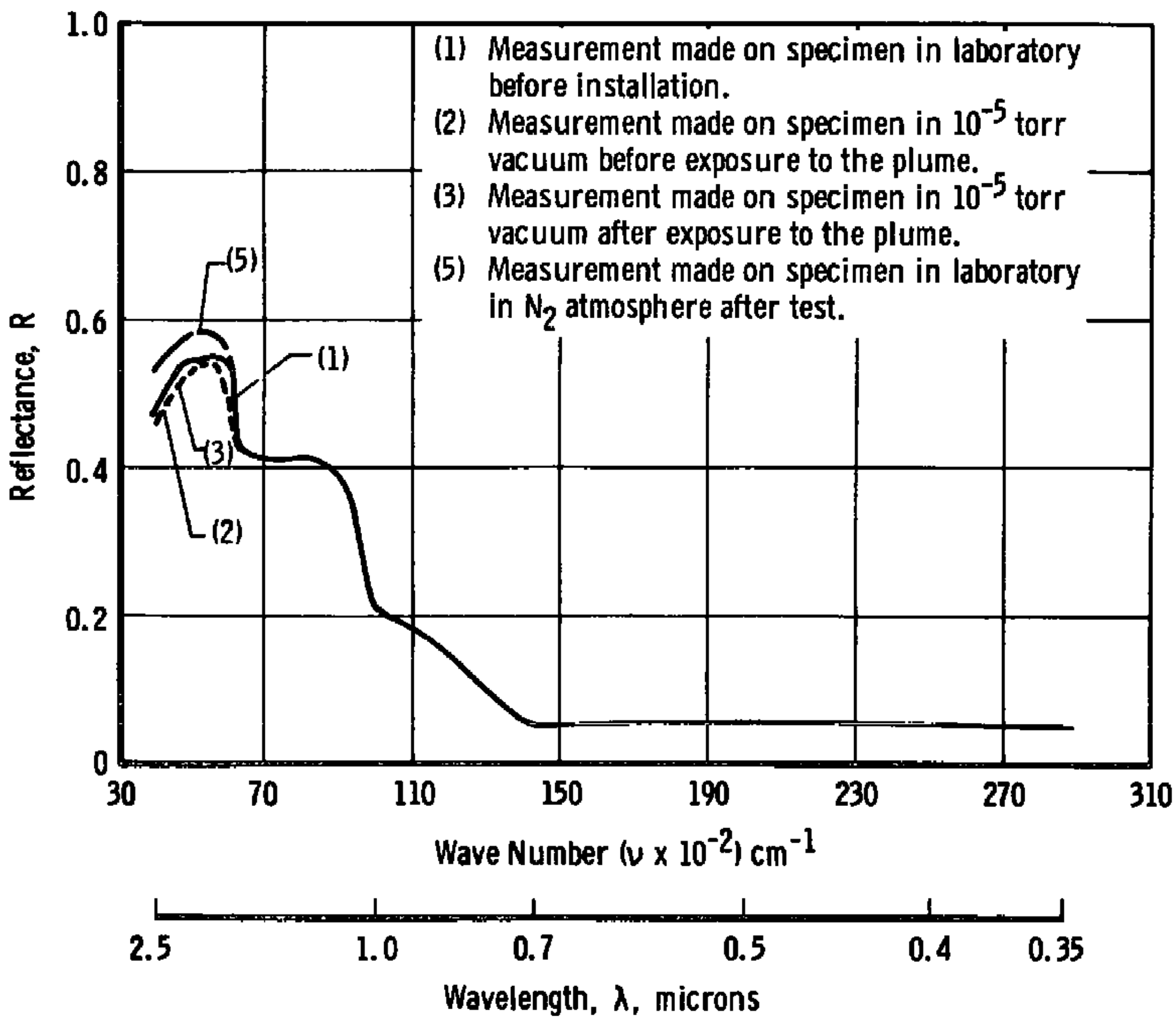

Fig. 39 Test 5B—Reflectance Measurements on Specimen, Location S_7, Type K

Fig. 40 Specimen, Location S_{10}, Mirror, after Test 5B

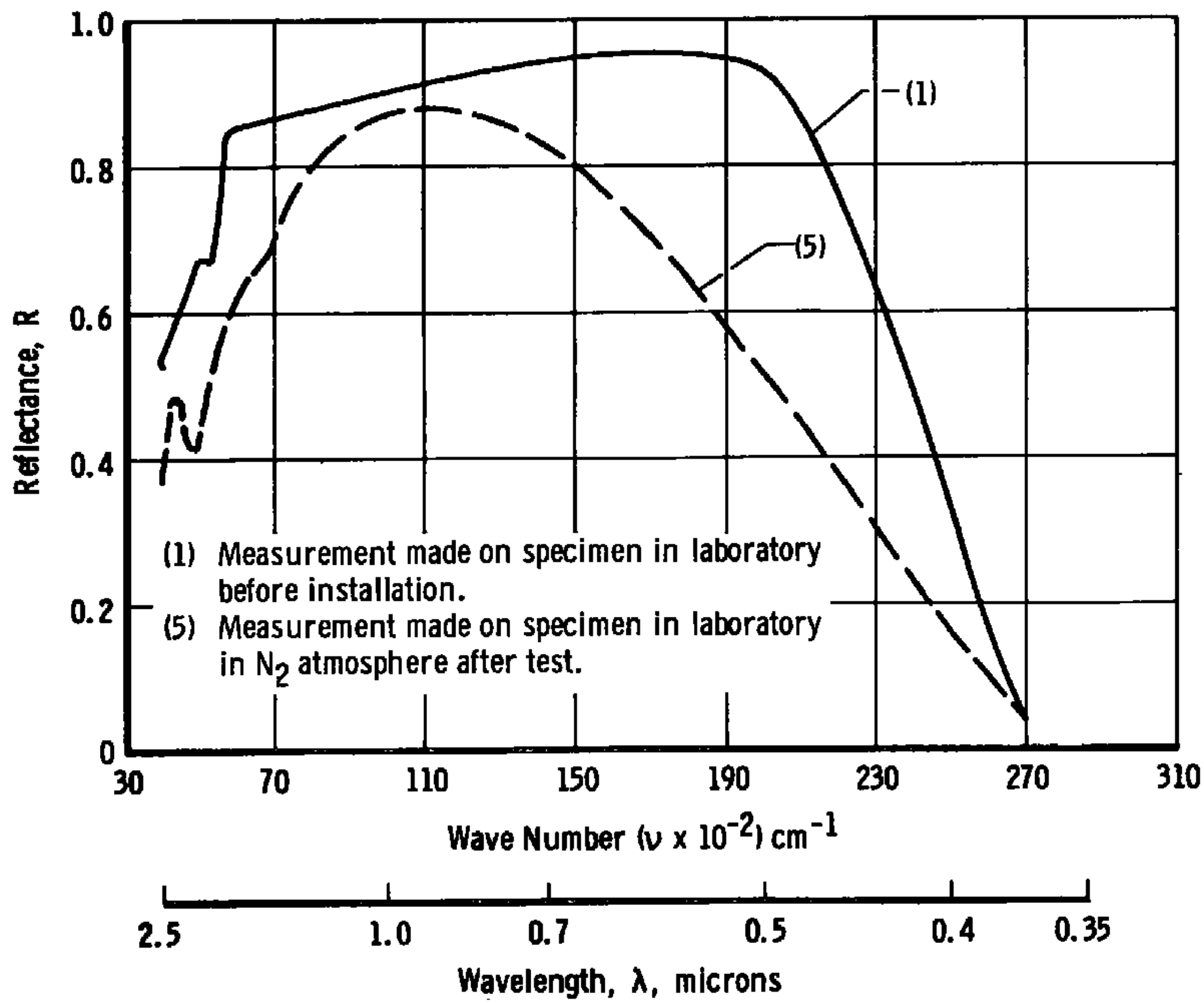

Fig. 41 Test 5B—Reflectance Measurements on Specimen, Location S_{11}, Type A

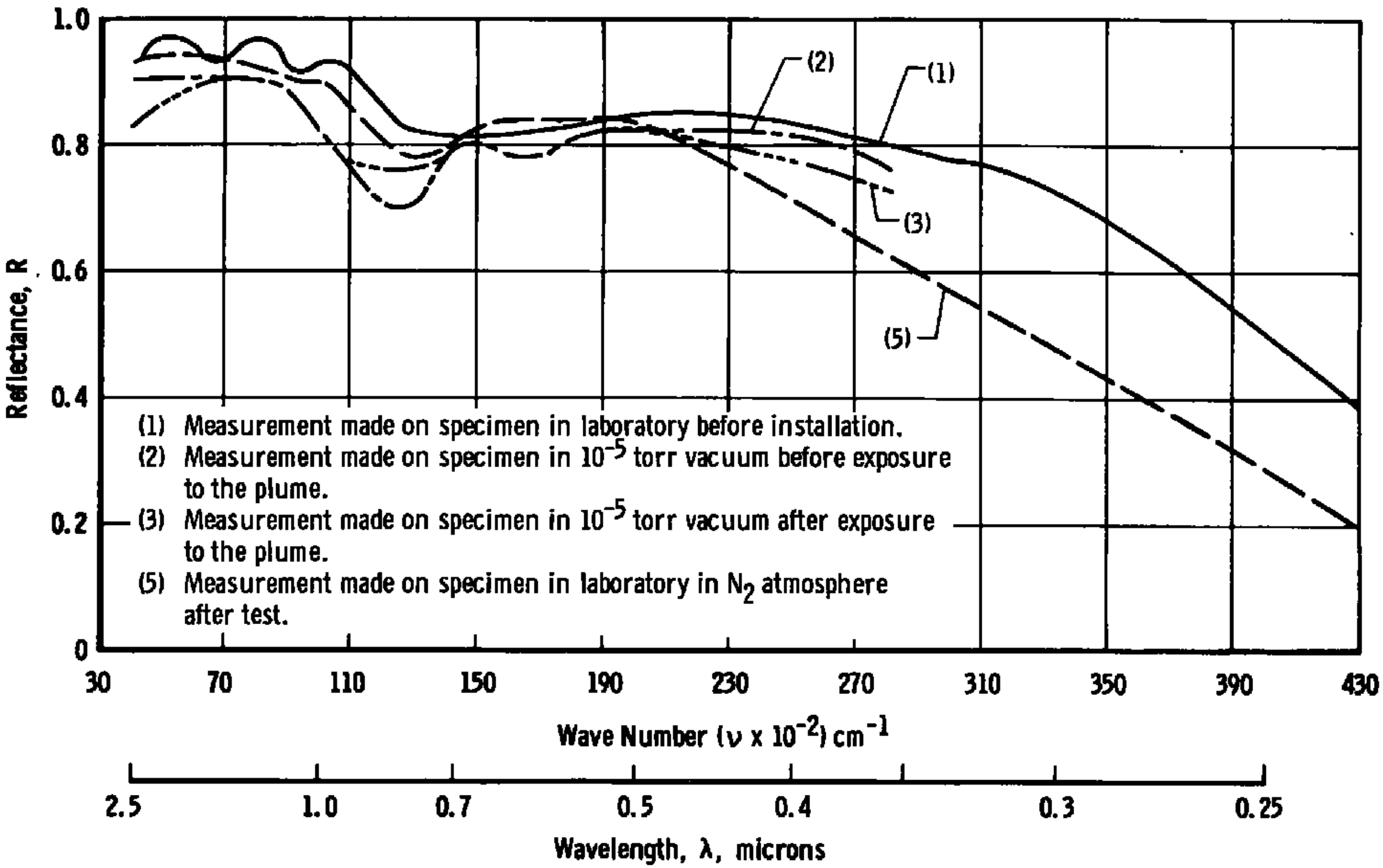

Fig. 42 Test 5B—Reflectance Measurements on Specimen, Location S_{12}, Type C

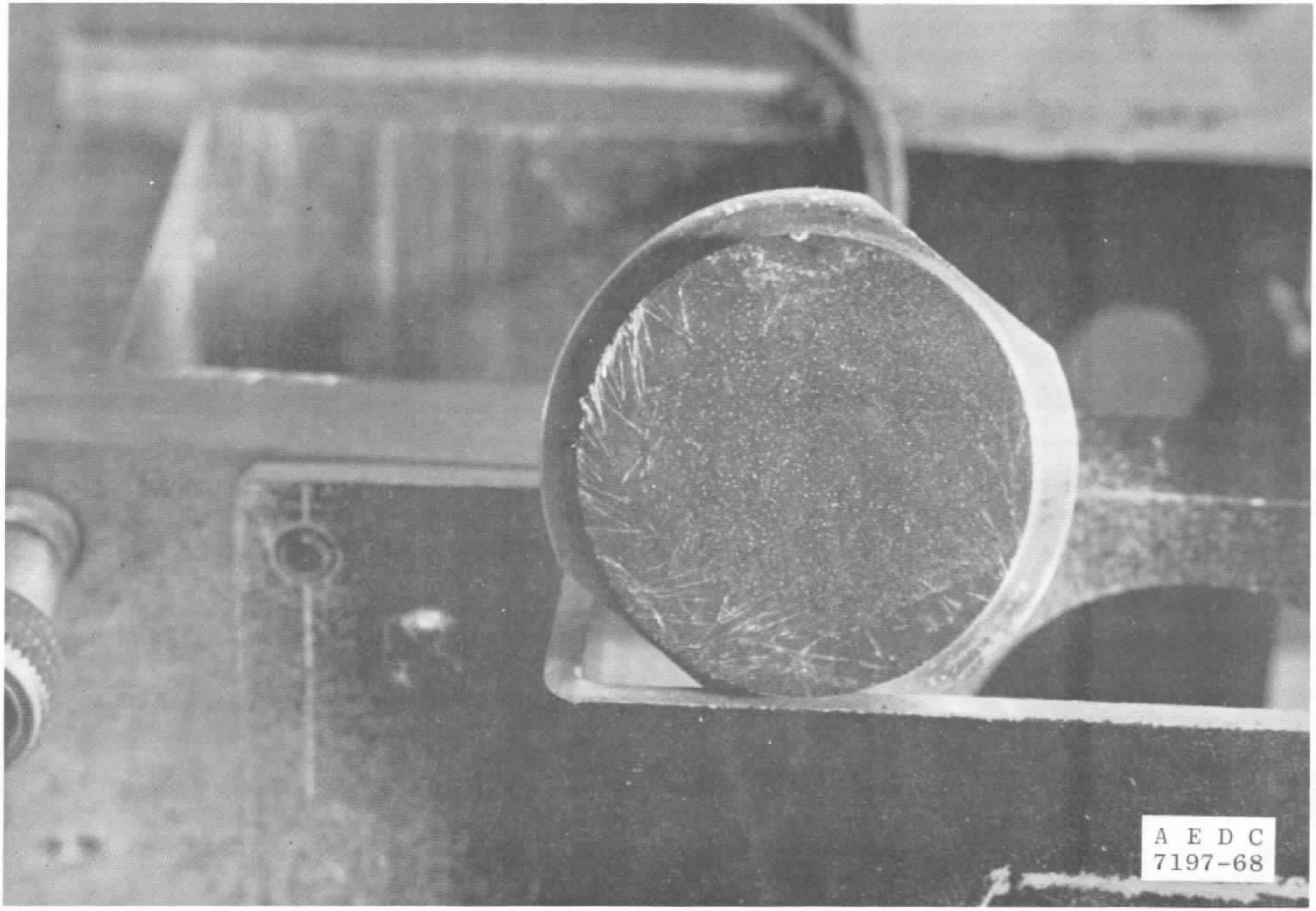

Fig. 43 Corrosion on Specimen, Location S_{13}, Type K, after Test 5B

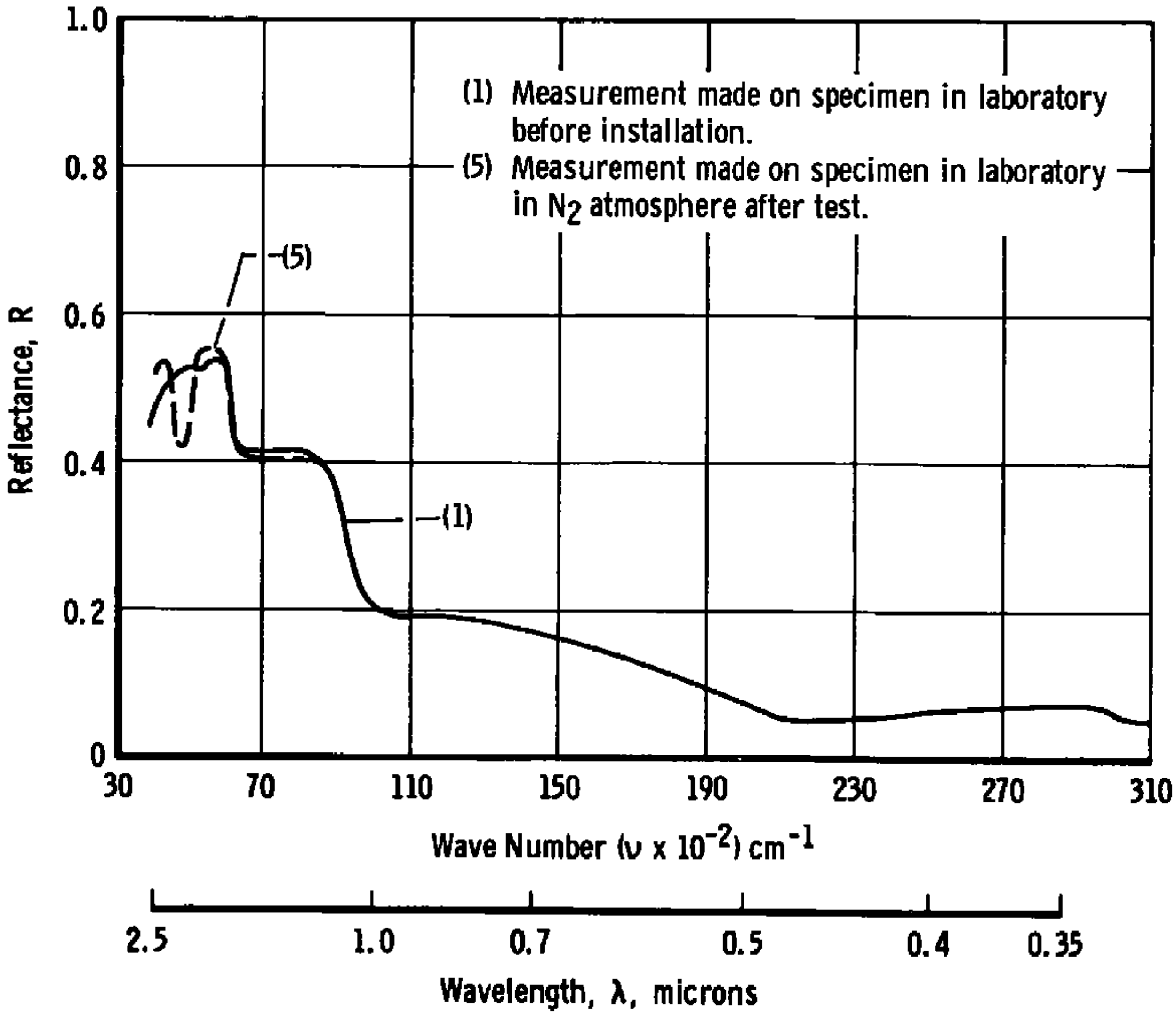

Fig. 44 Test 5B—Reflectance Measurement on Specimen, Location S_{13}, Type K

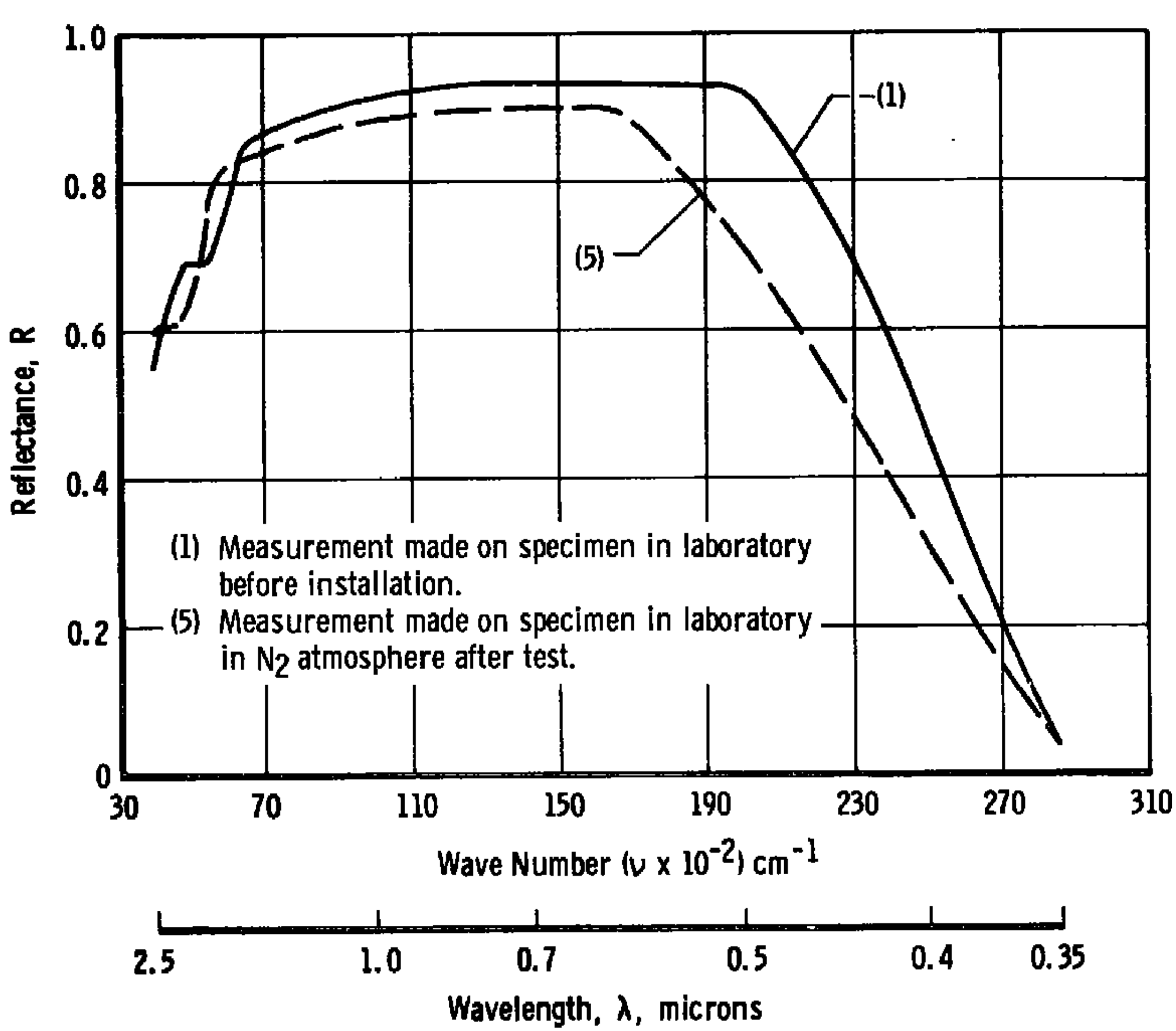

Fig. 45 Test 5B—Reflectance Measurement on Specimen, Location S_{14}, Type A

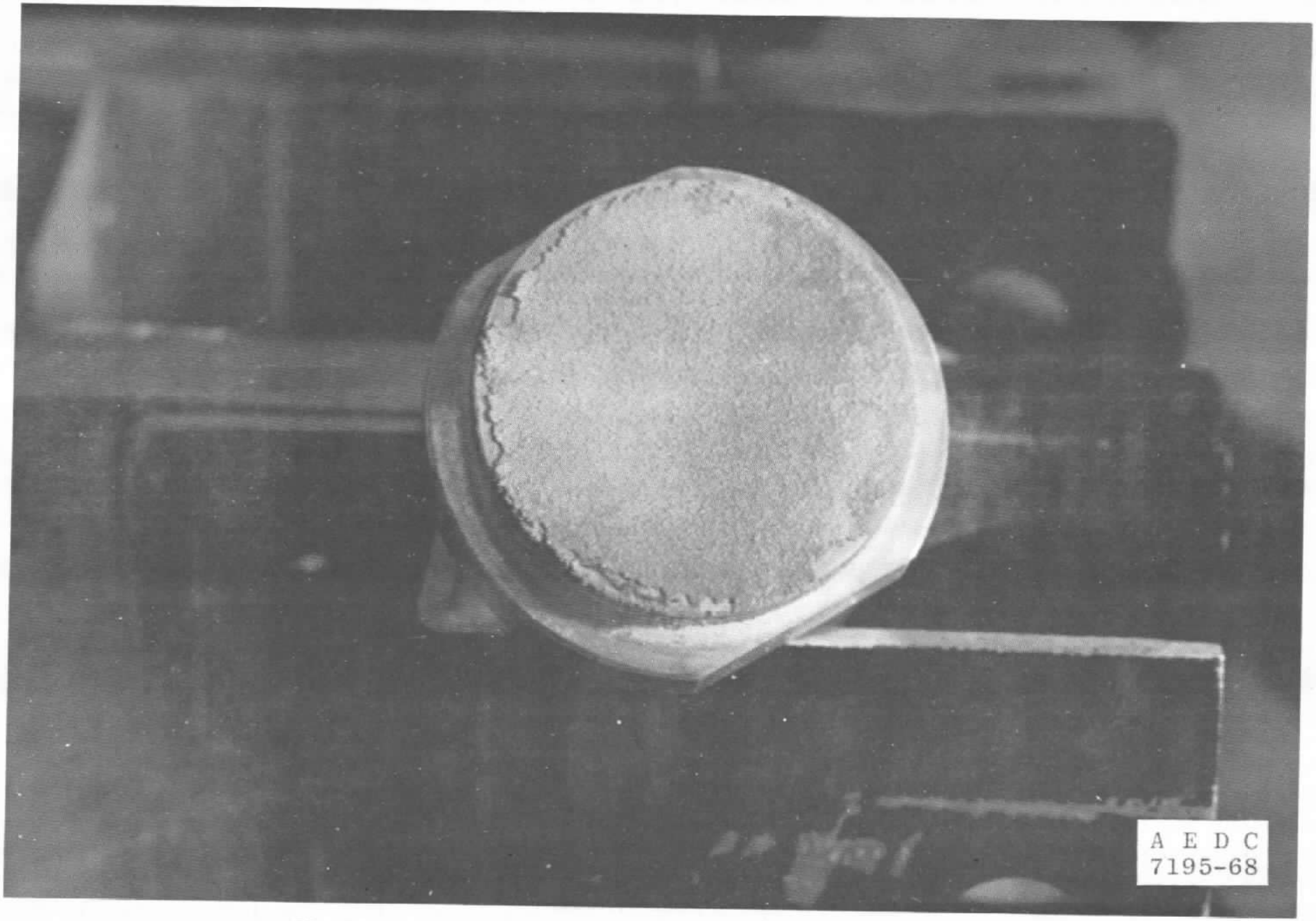

Fig. 46 Corrosion on Specimen, Location S_{15}, Type J, after Test 5B

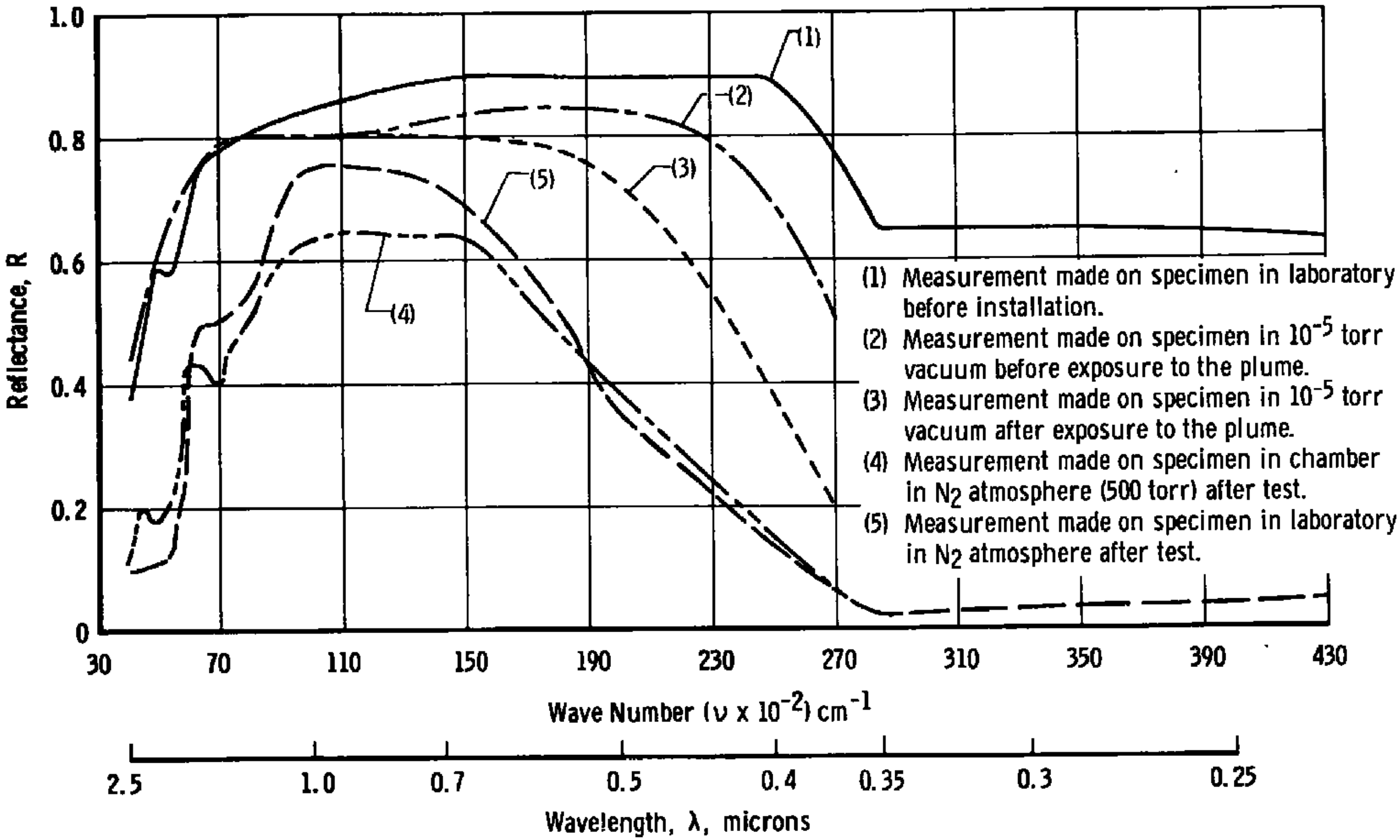

Fig. 47 Test 5B—Reflectance Measurements on Specimen, Location S_{15}, Type J

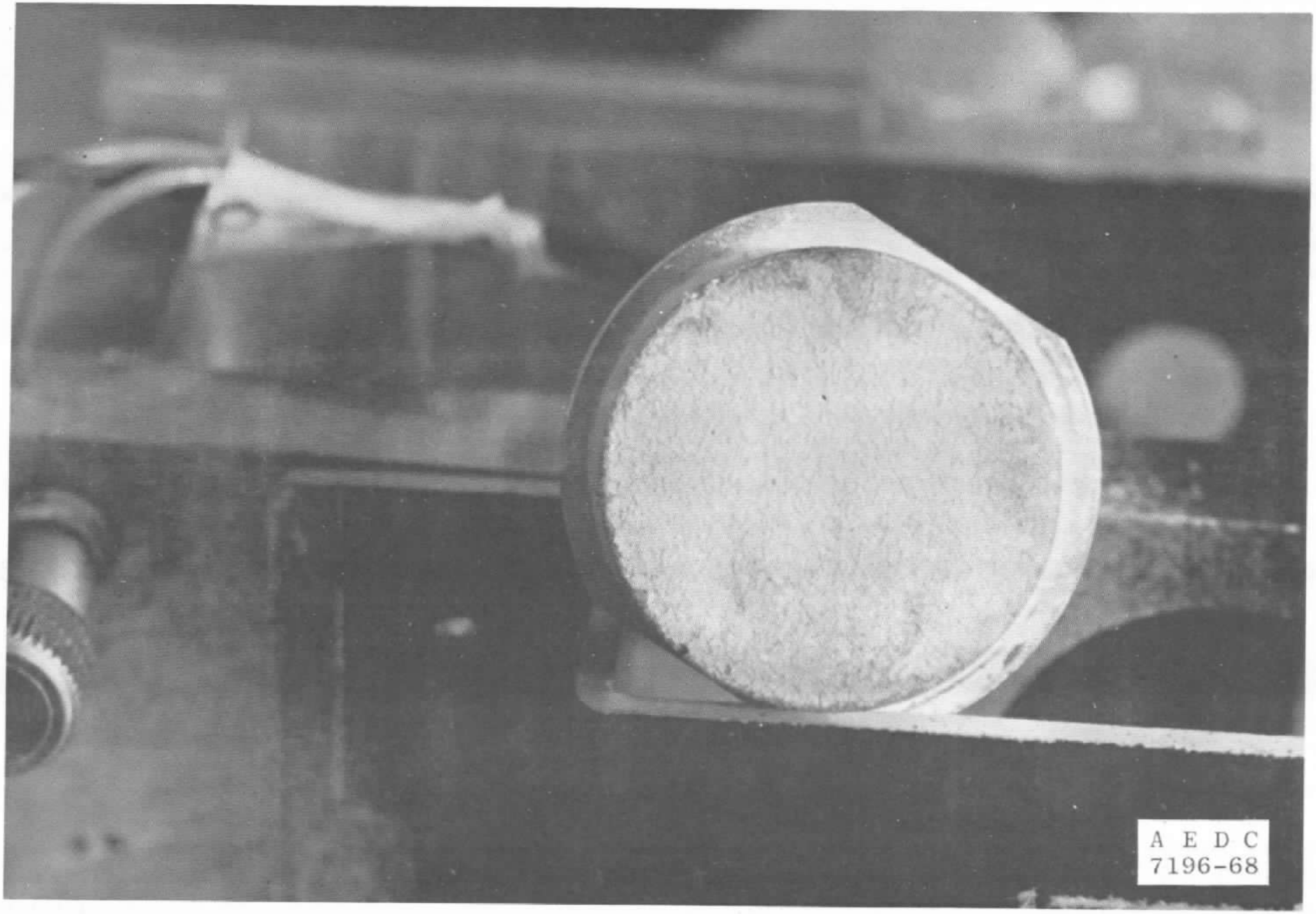

Fig. 48 Corrosion on Specimen, Location S_{16}, Type J, after Test 5B

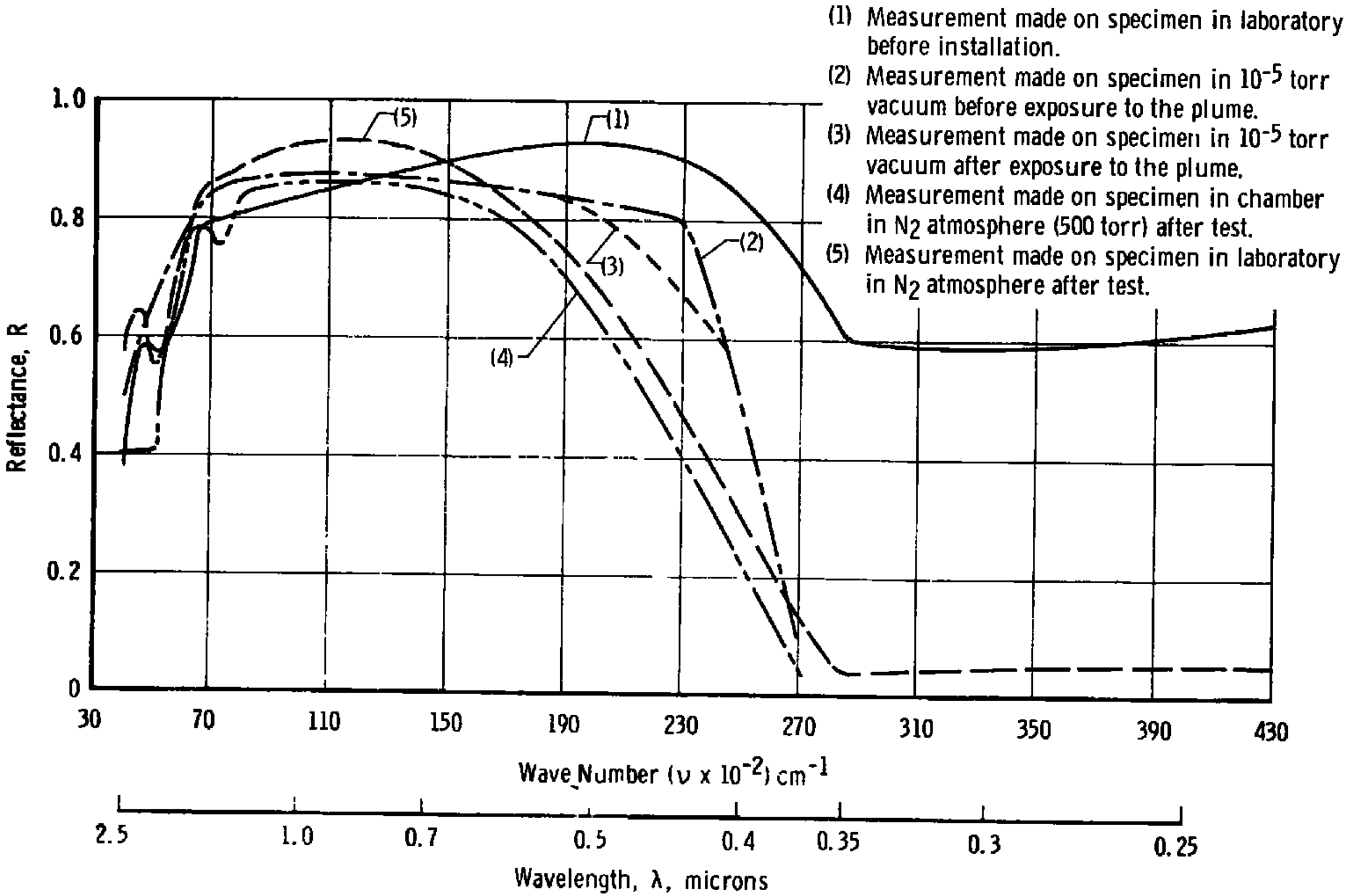

Fig. 49 Test 5B—Reflectance Measurements on Specimen, Location S_{16}, Type J

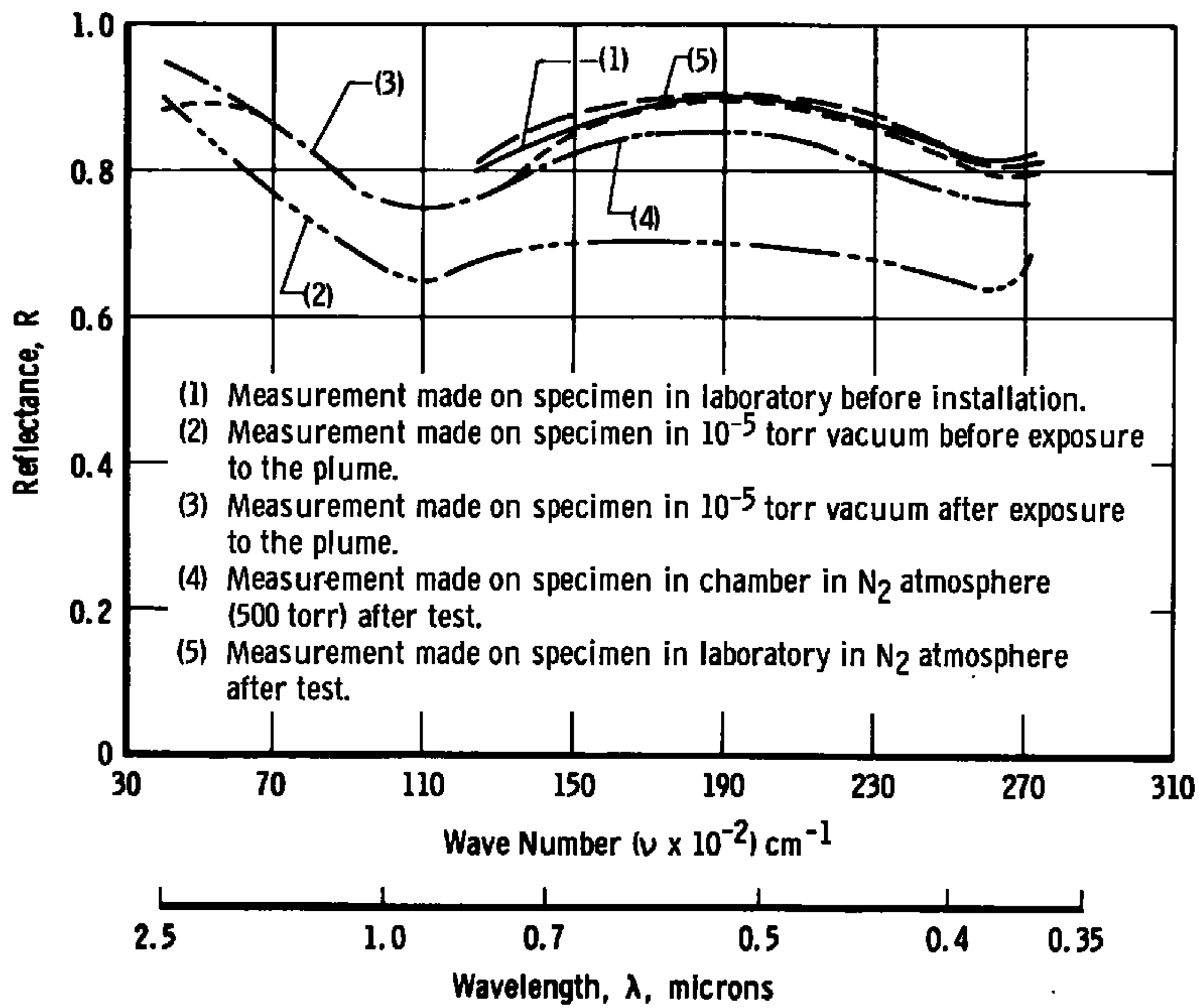

Fig. 50 Test 5B—Reflectance Measurements on Specimen, Location G_3, Mirror

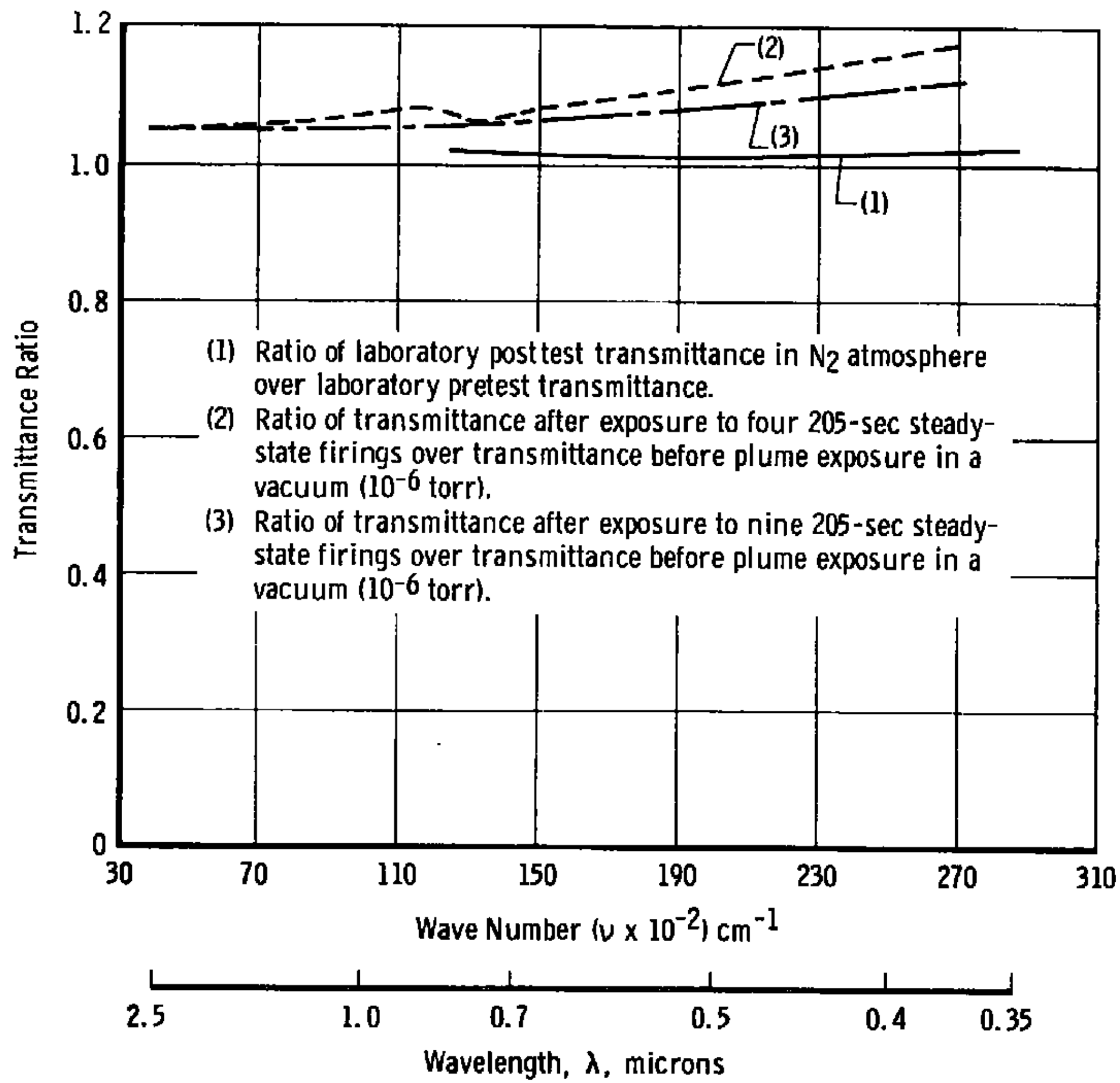

Fig. 51 Test 5B—Transmittance Measurements on Specimen, Location G_7, Window

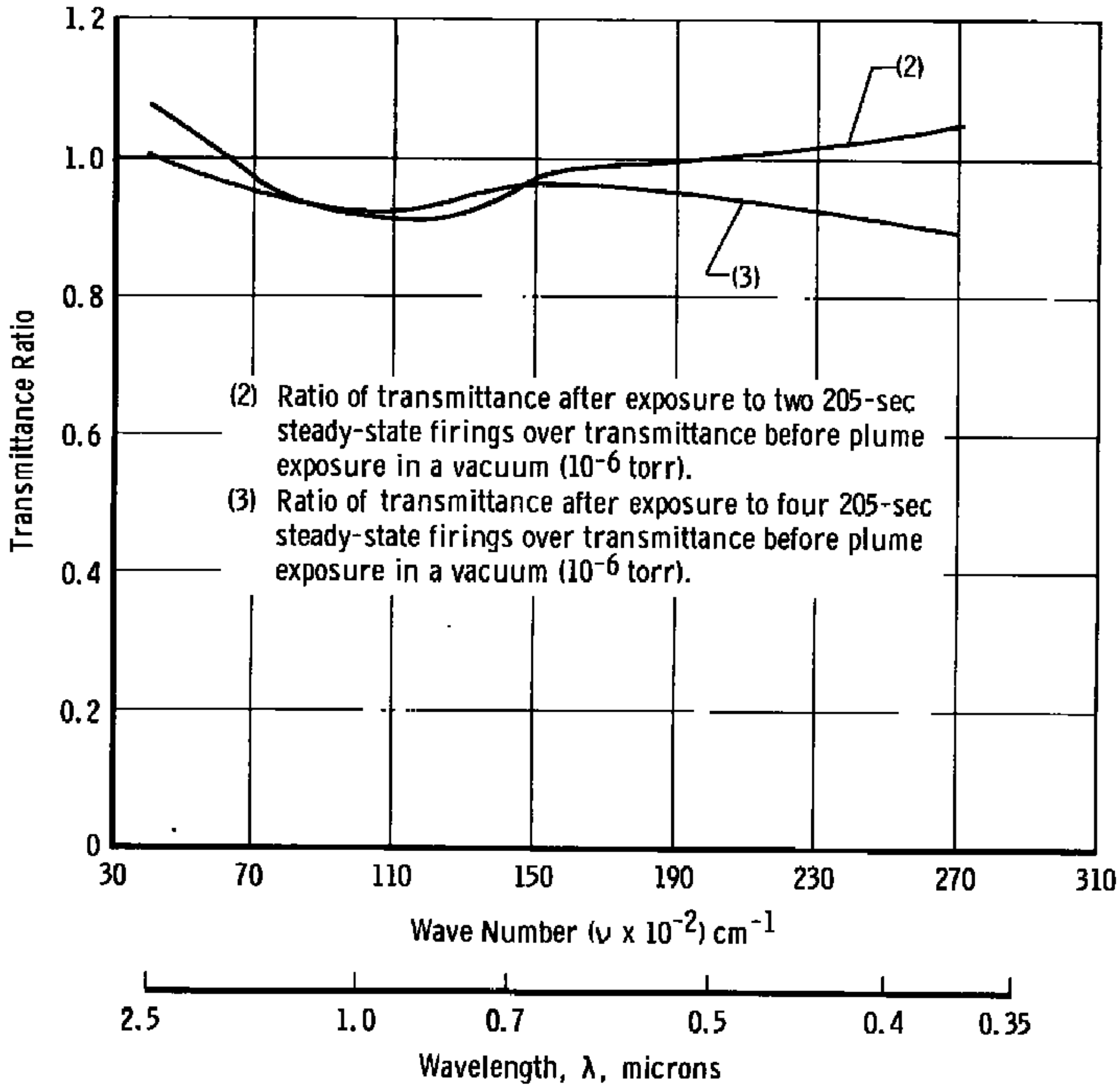

Fig. 52 Test 5B—Transmittance Measurements on Specimen, Location V_1, View Port

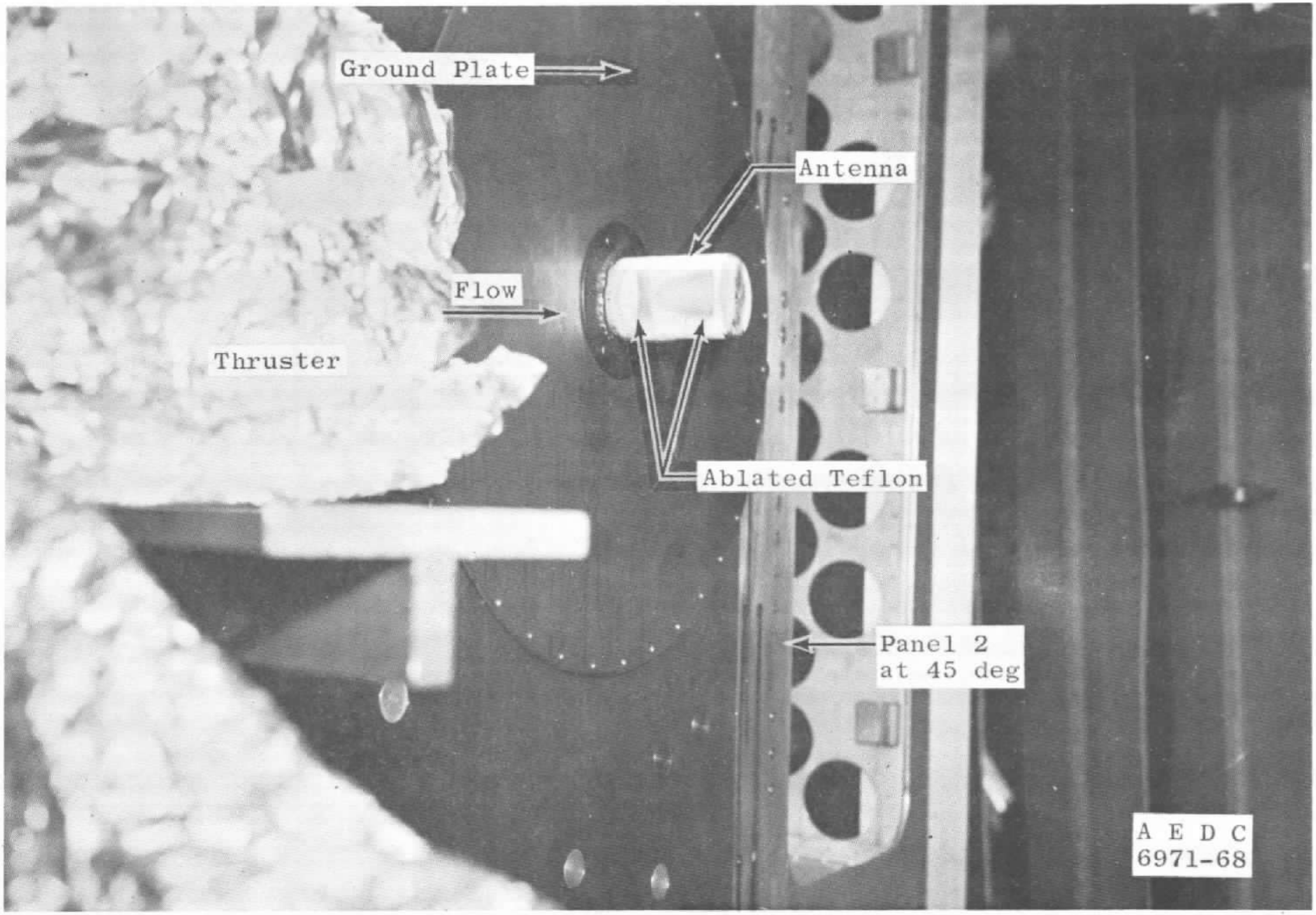

Fig. 53 Installation of Thruster, Antenna, and Panels—Test 6

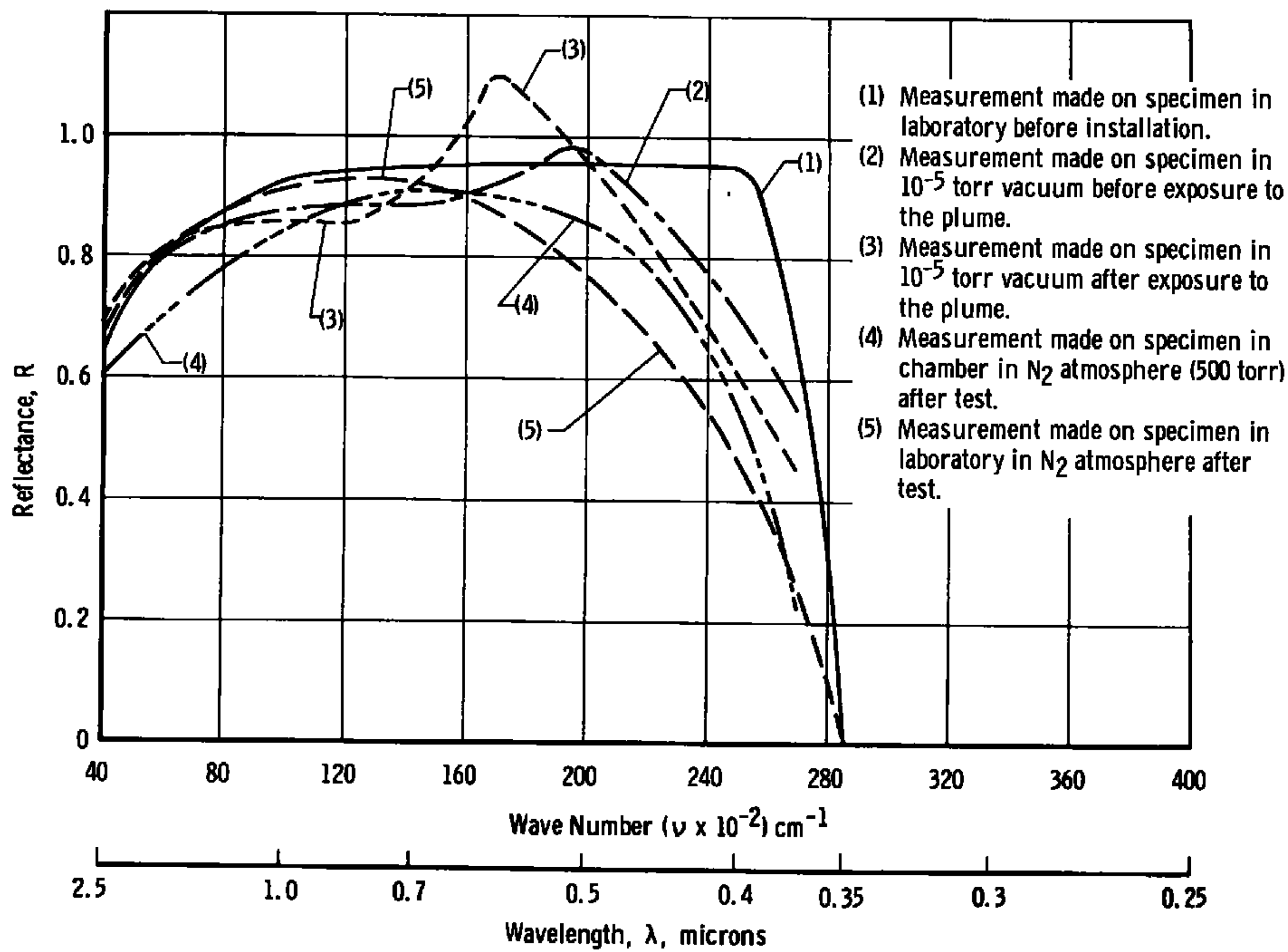

Fig. 54 Test 13—Reflectance Measurements on Specimen, Location S_{11}, Type A

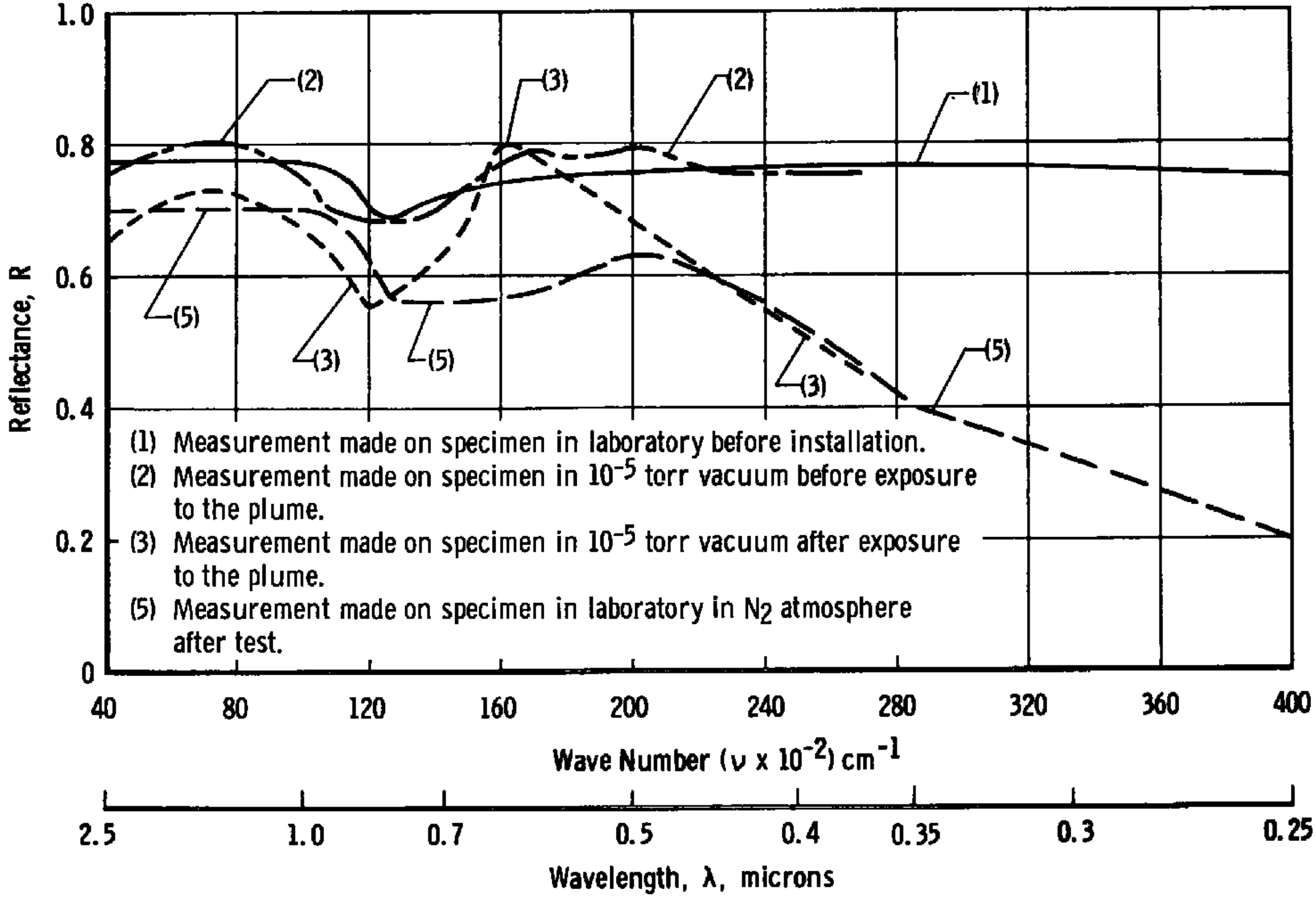

Fig. 55 Test 13—Reflectance Measurements on Specimen, Location S_{12}, Type B

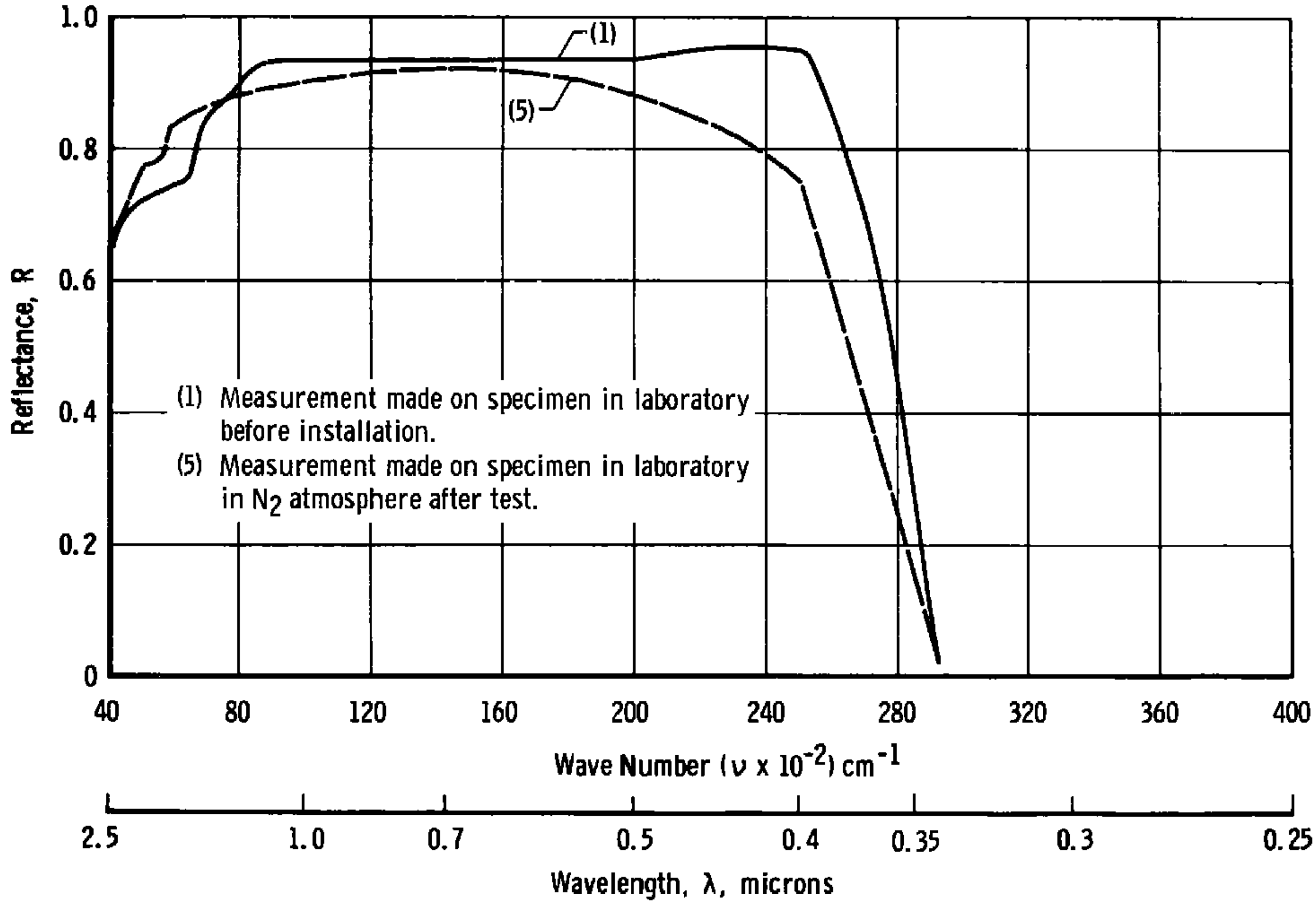

Fig. 56 Test 13—Reflectance Measurements on Specimen, Location S_{14}, Type A

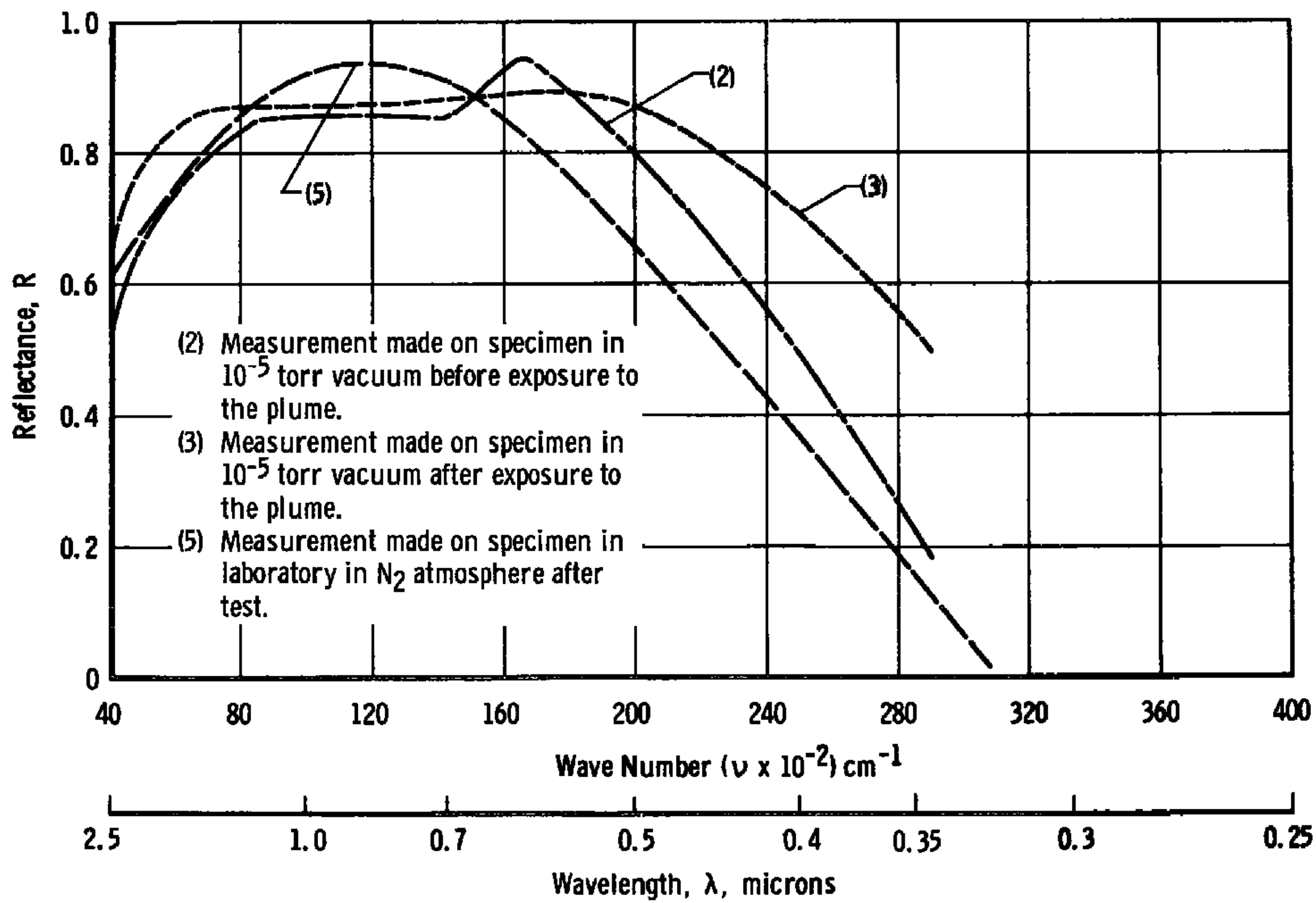

Fig. 57 Test 13—Reflectance Measurements on Specimen, Location S_{15}, Type A

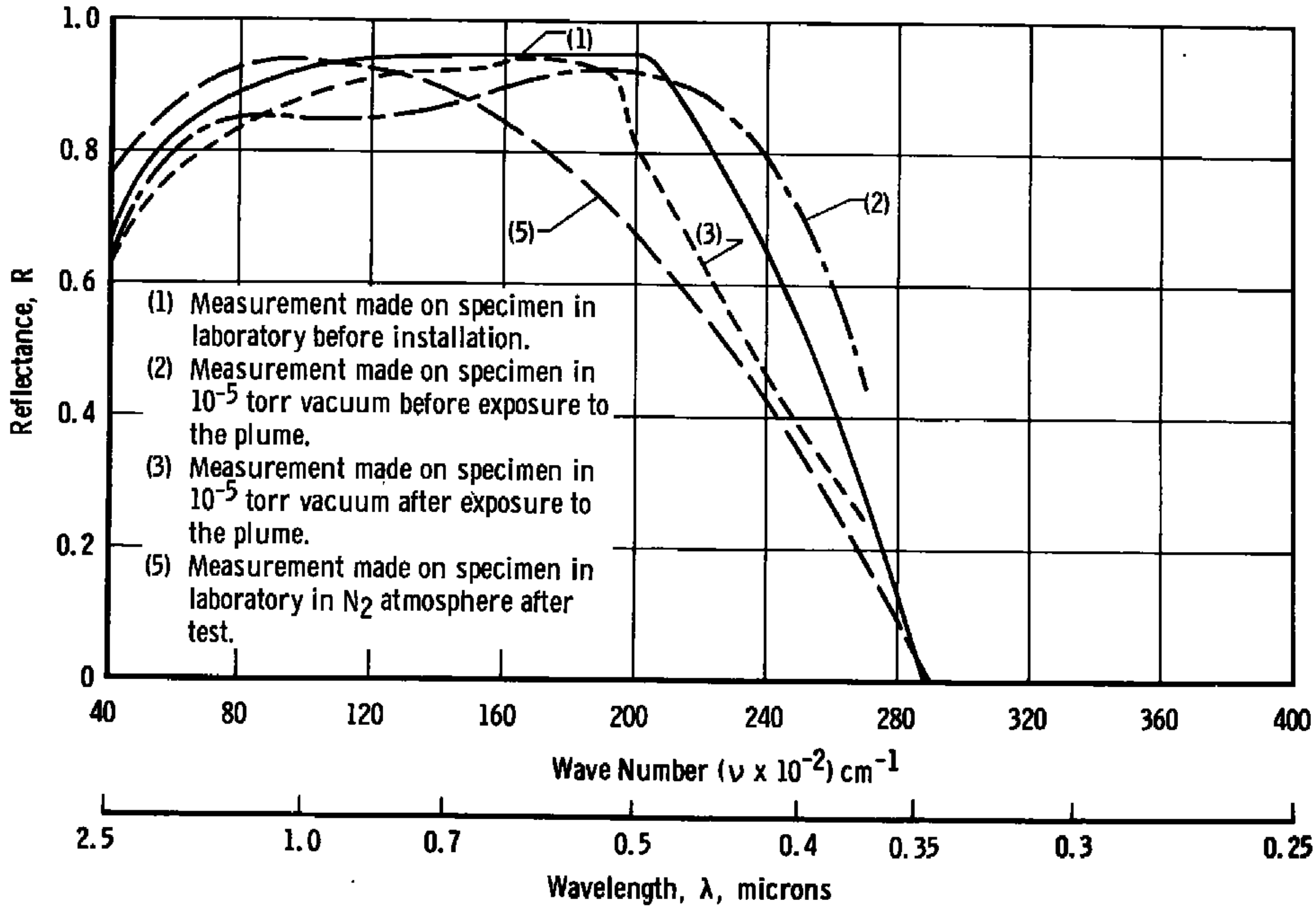

Fig. 58 Test 13—Reflectance Measurements on Specimen, Location S_{16}, Type A

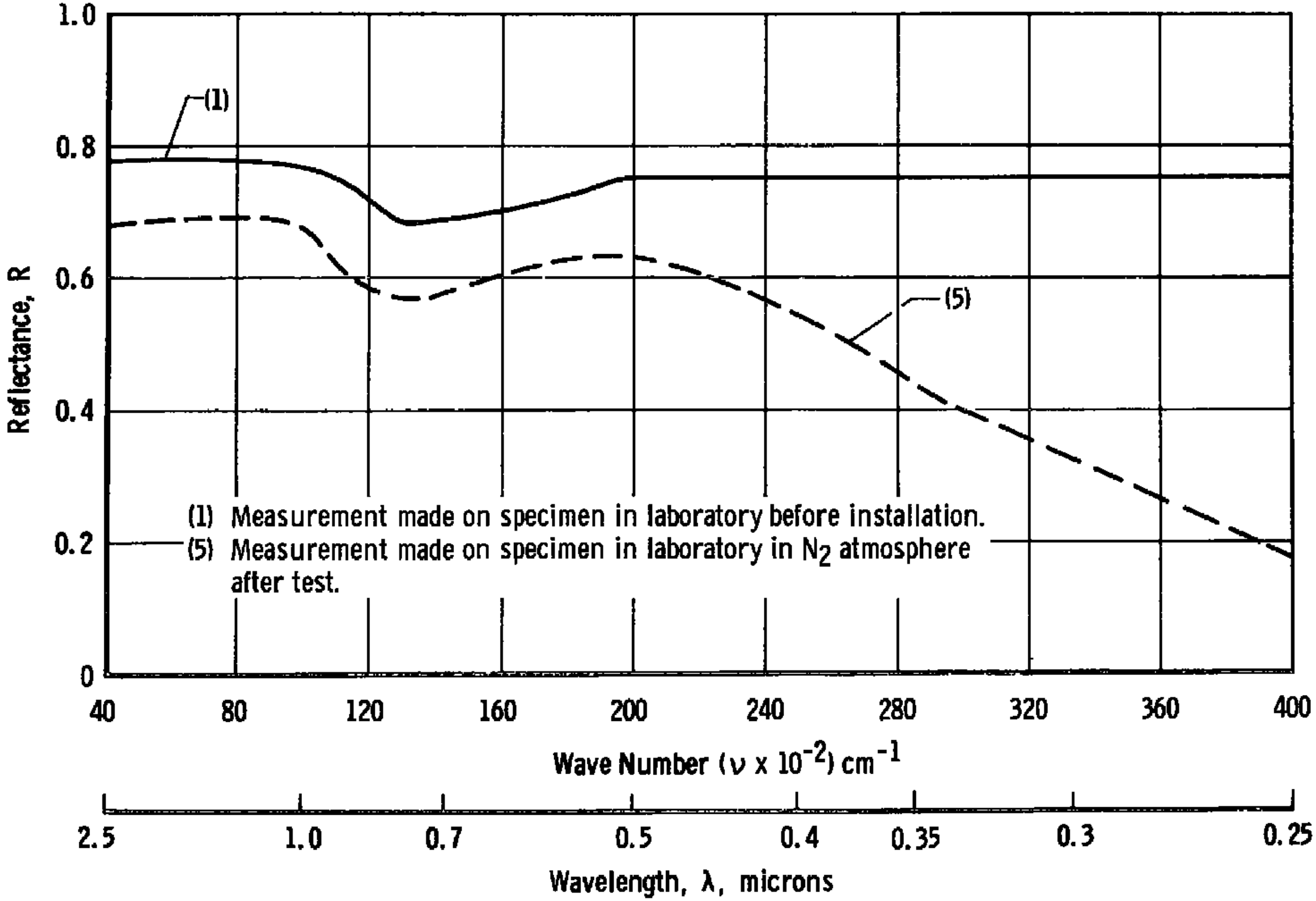

Fig. 59 Test 13—Reflectance Measurements on Specimen, Location S_{17}, Type B

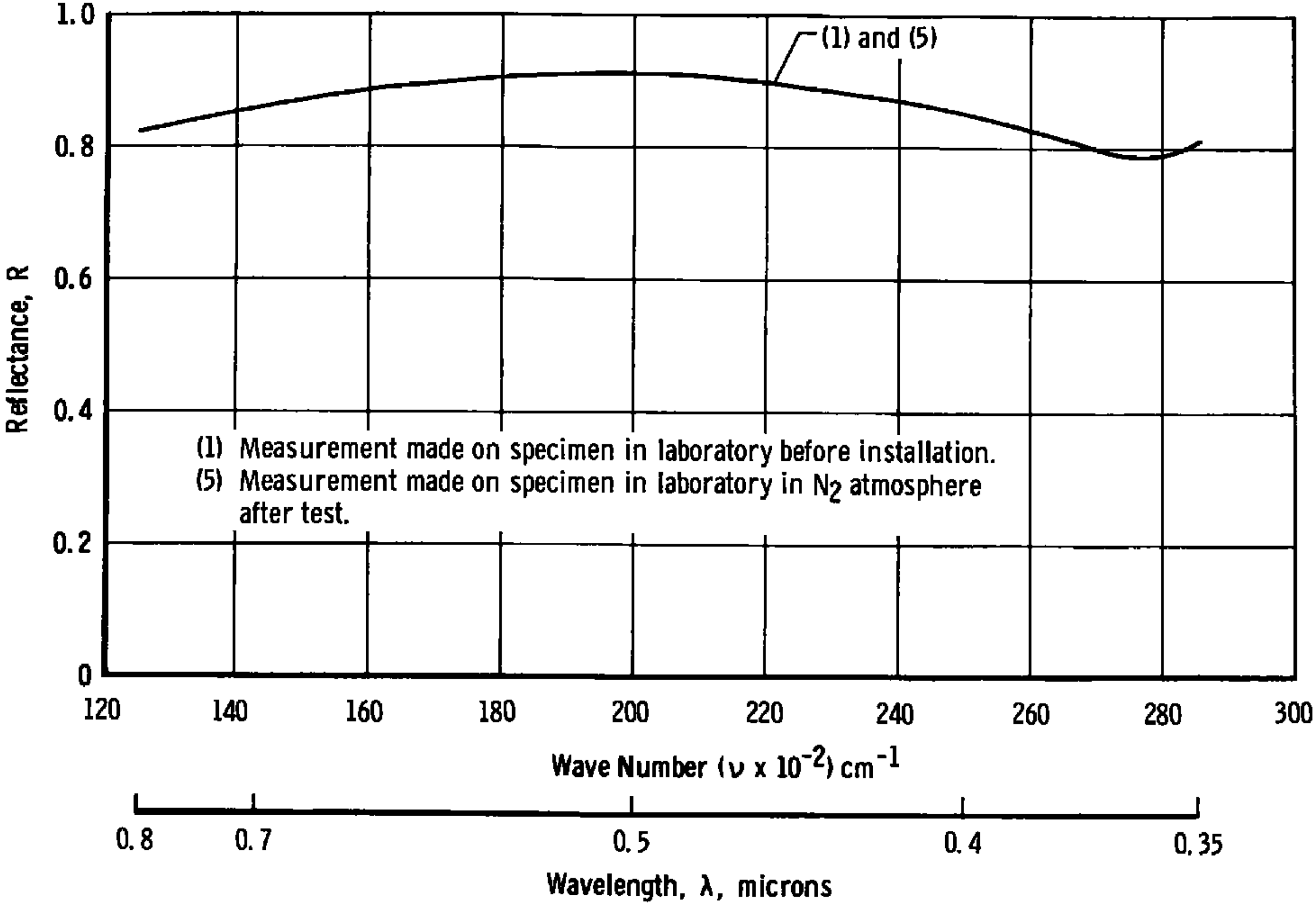

Fig. 60 Test 13—Reflectance Measurements on Specimen, Location G_3, Mirror

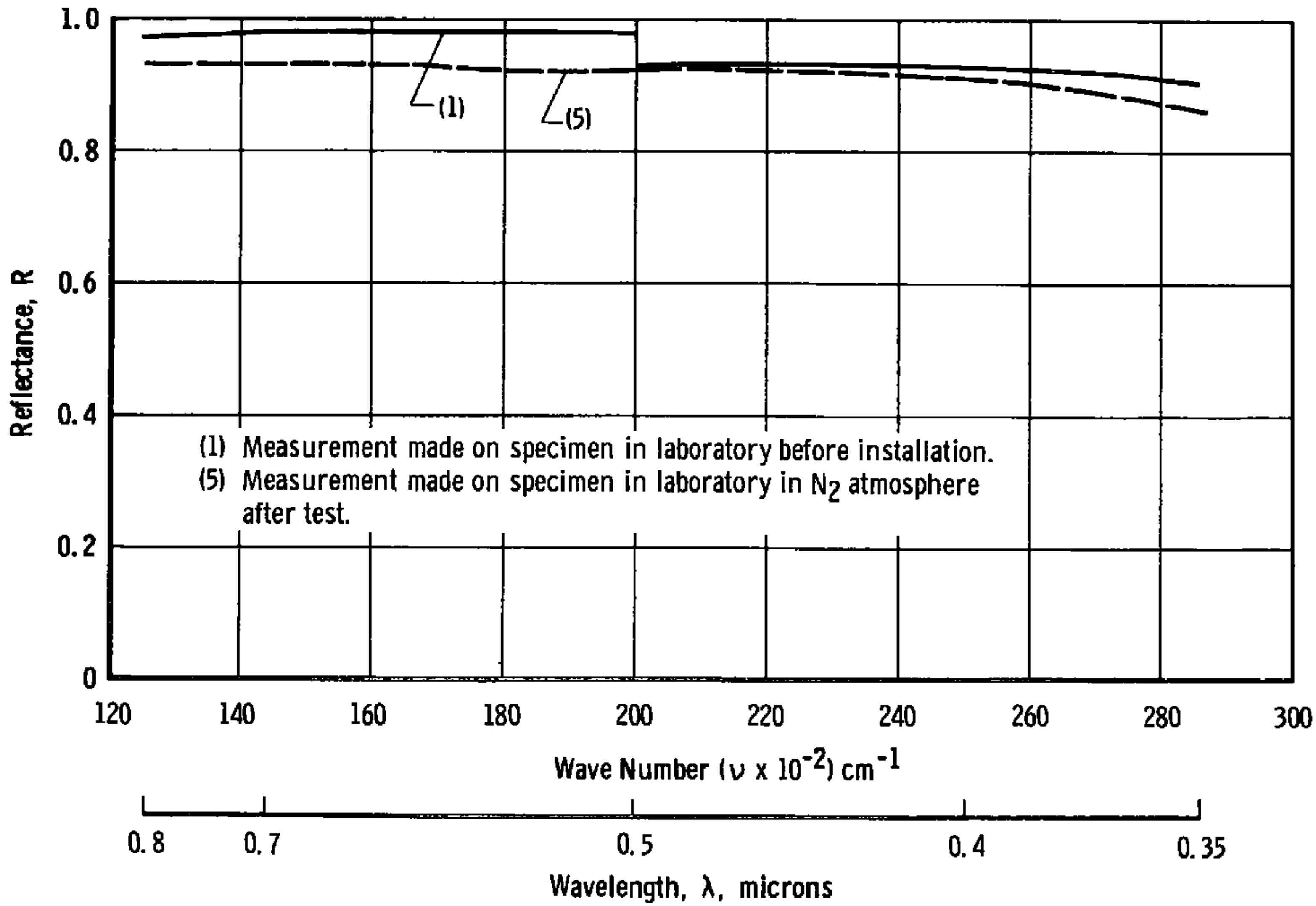

Fig. 61 Test 13—Transmittance Measurements on Specimen, Location G_8, Window

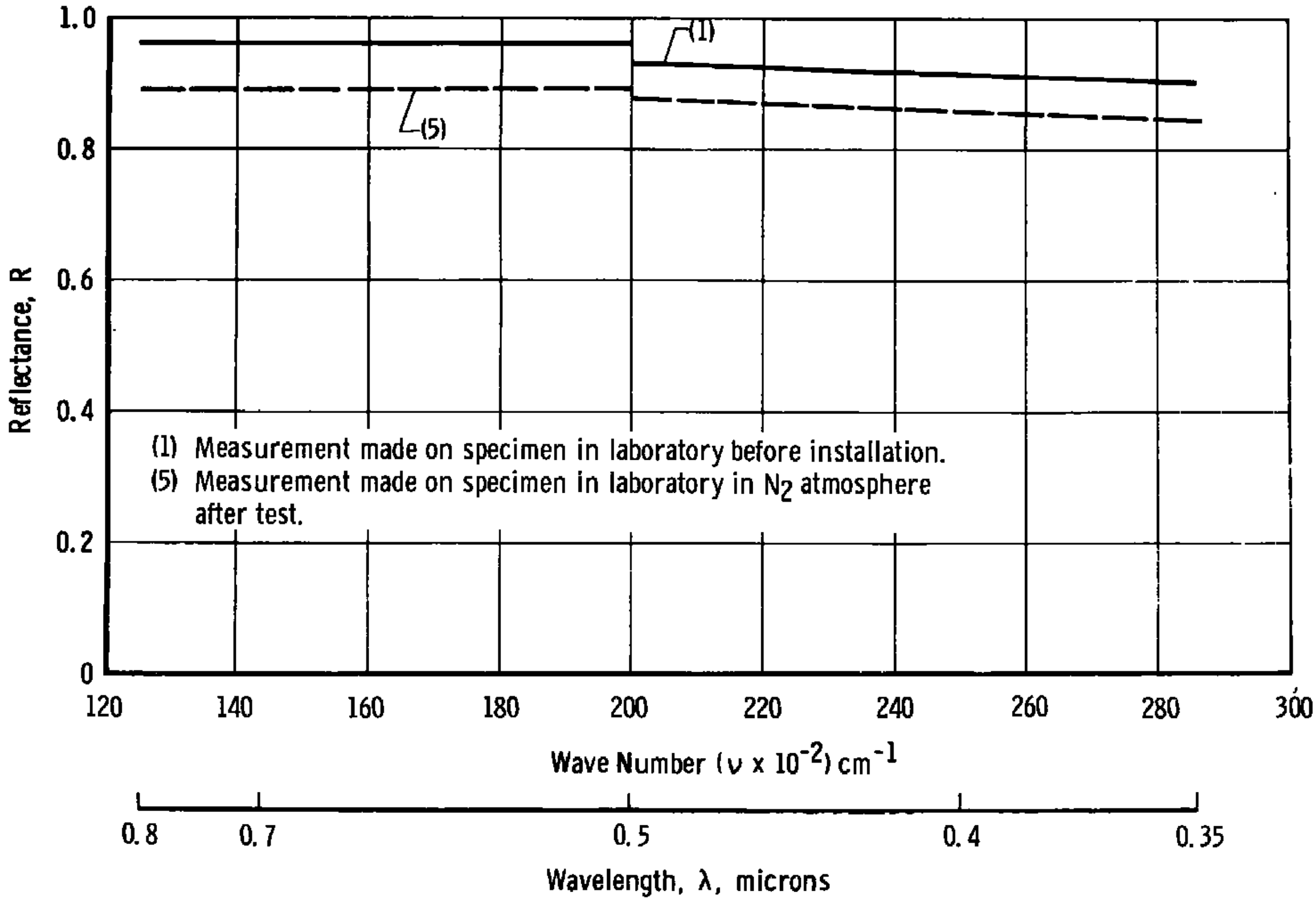

Fig. 62 Test 13—Transmittance Measurements on Specimen, Startracker, Window

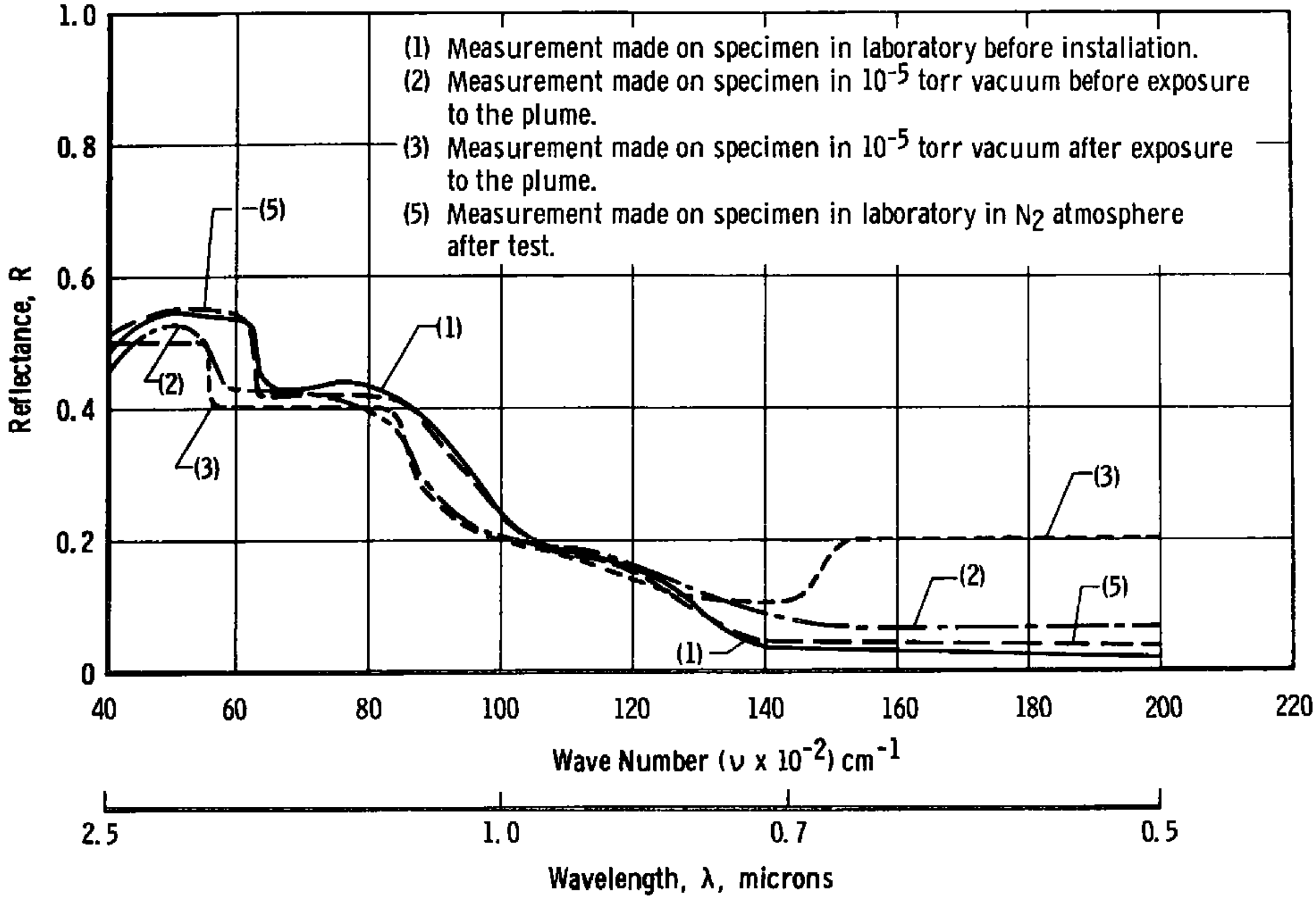

Fig. 63 Test 14—Reflectance Measurements on Specimen, Location S_7, Type K

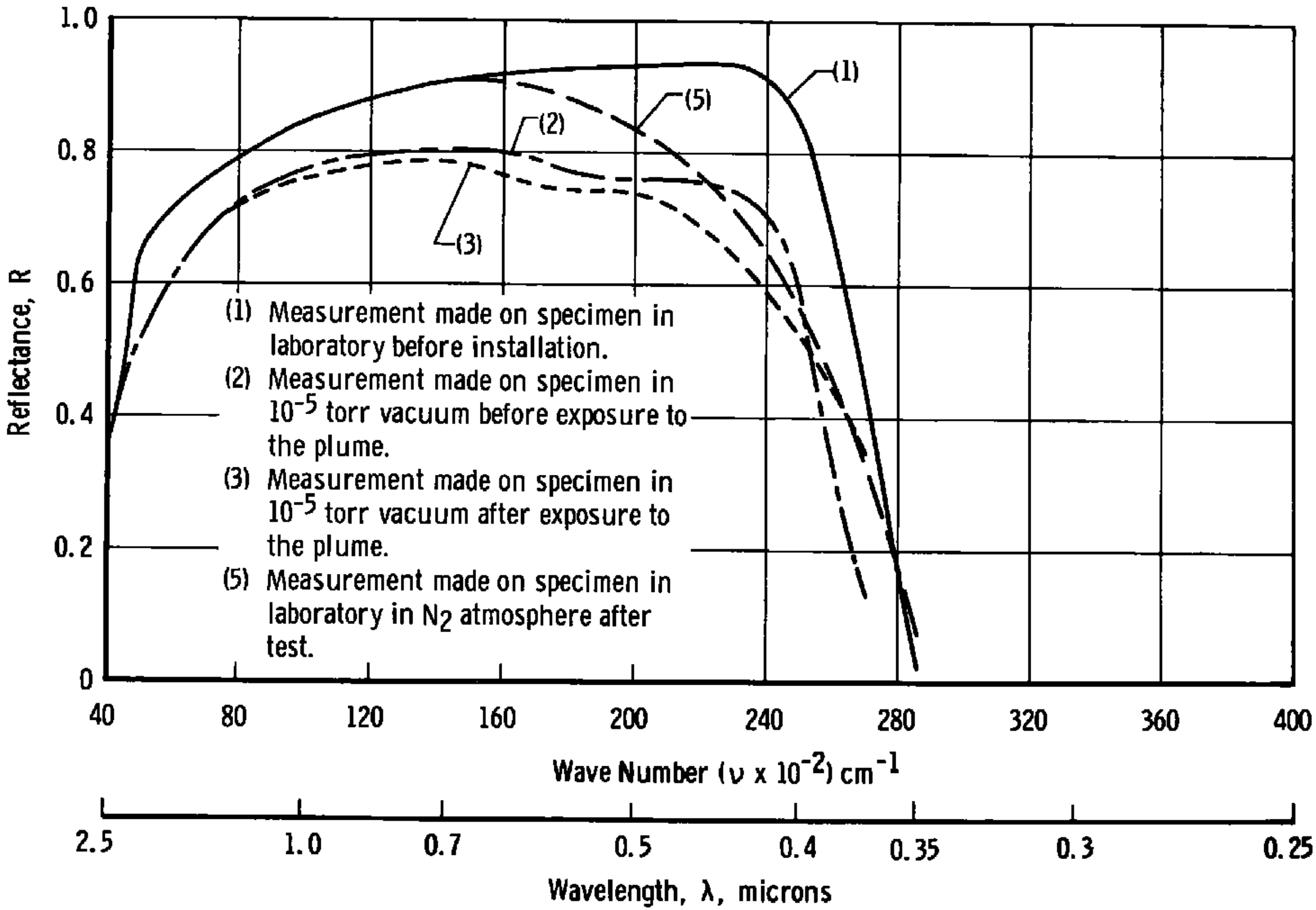

Fig. 64 Test 14—Reflectance Measurements on Specimen, Location S_{10}, Type T_1

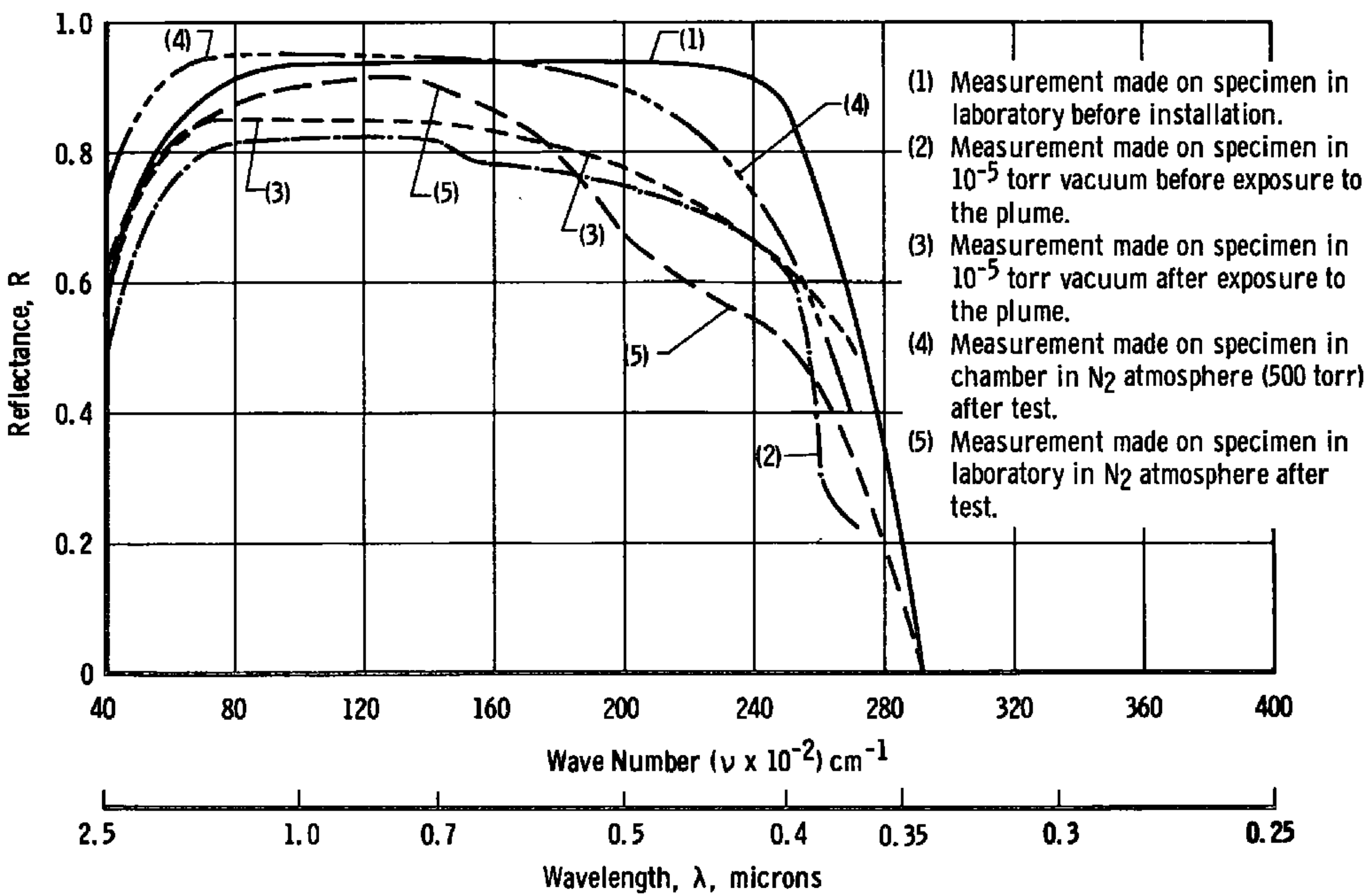

Fig. 65 Test 14—Reflectance Measurements on Specimen, Location S_{11}, Type A

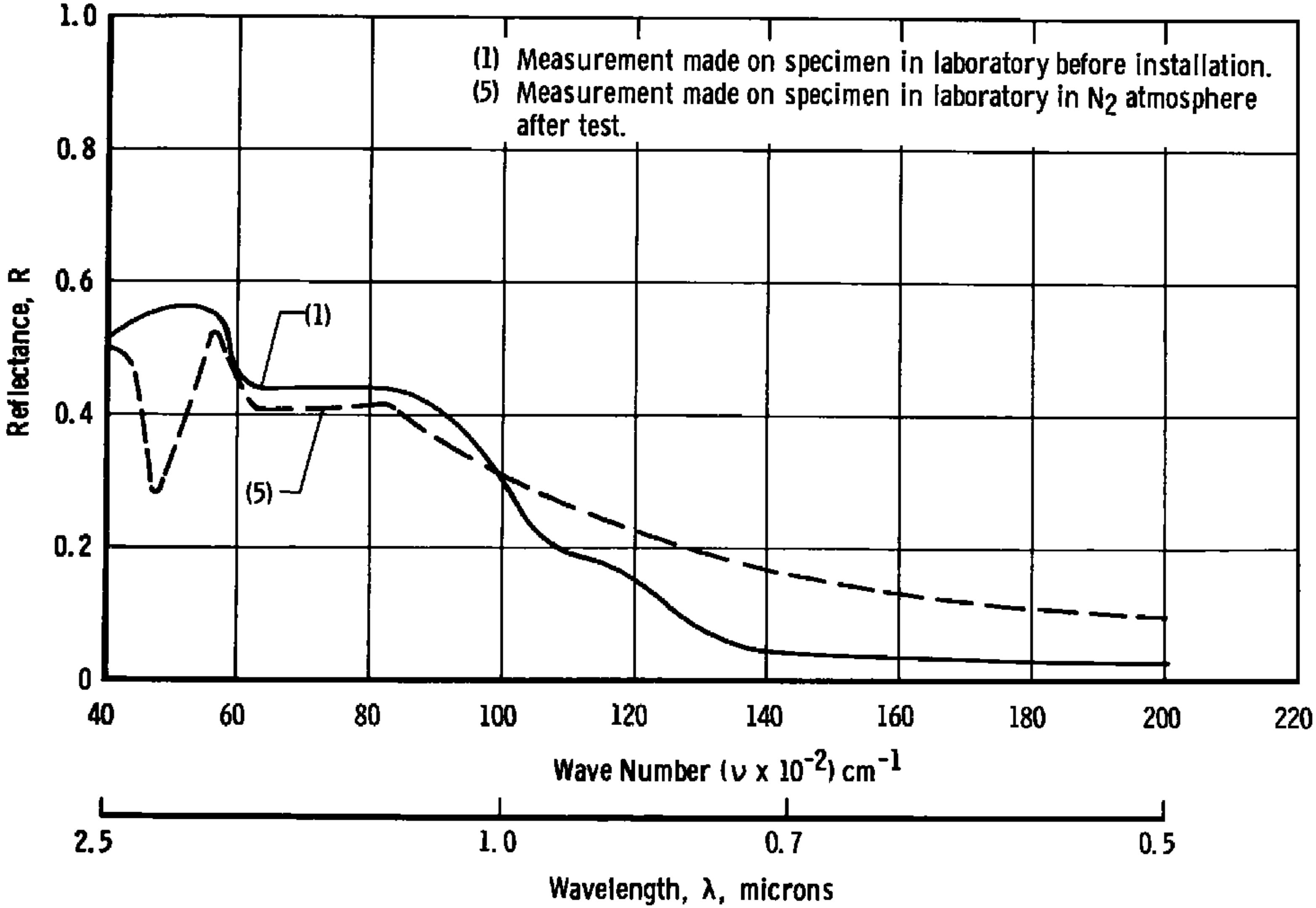

Fig. 66 Test 14—Reflectance Measurements on Specimen, Location S_{13}, Type K

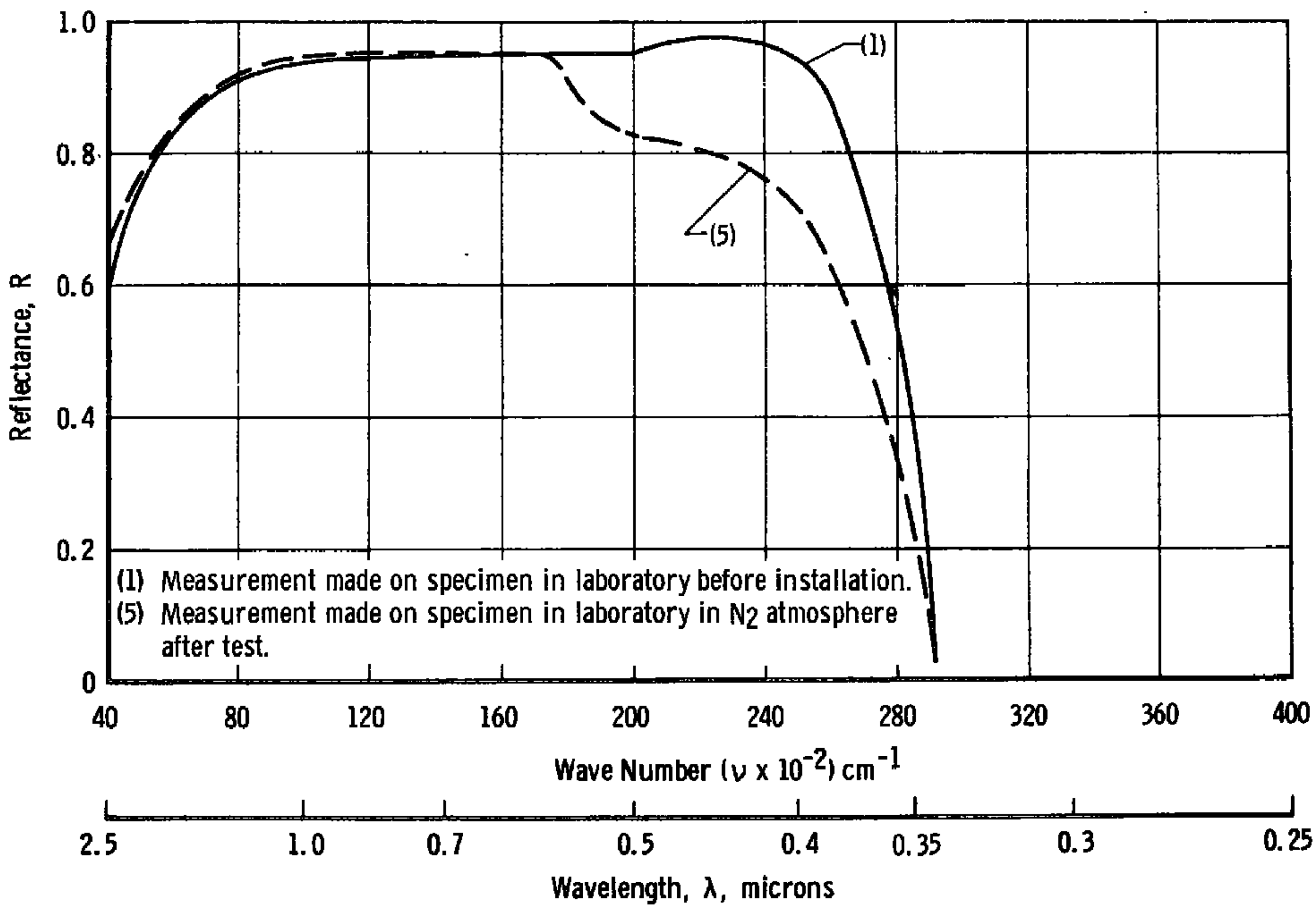

Fig. 67 Test 14—Reflectance Measurements on Specimen, Location S_{14}, Type A

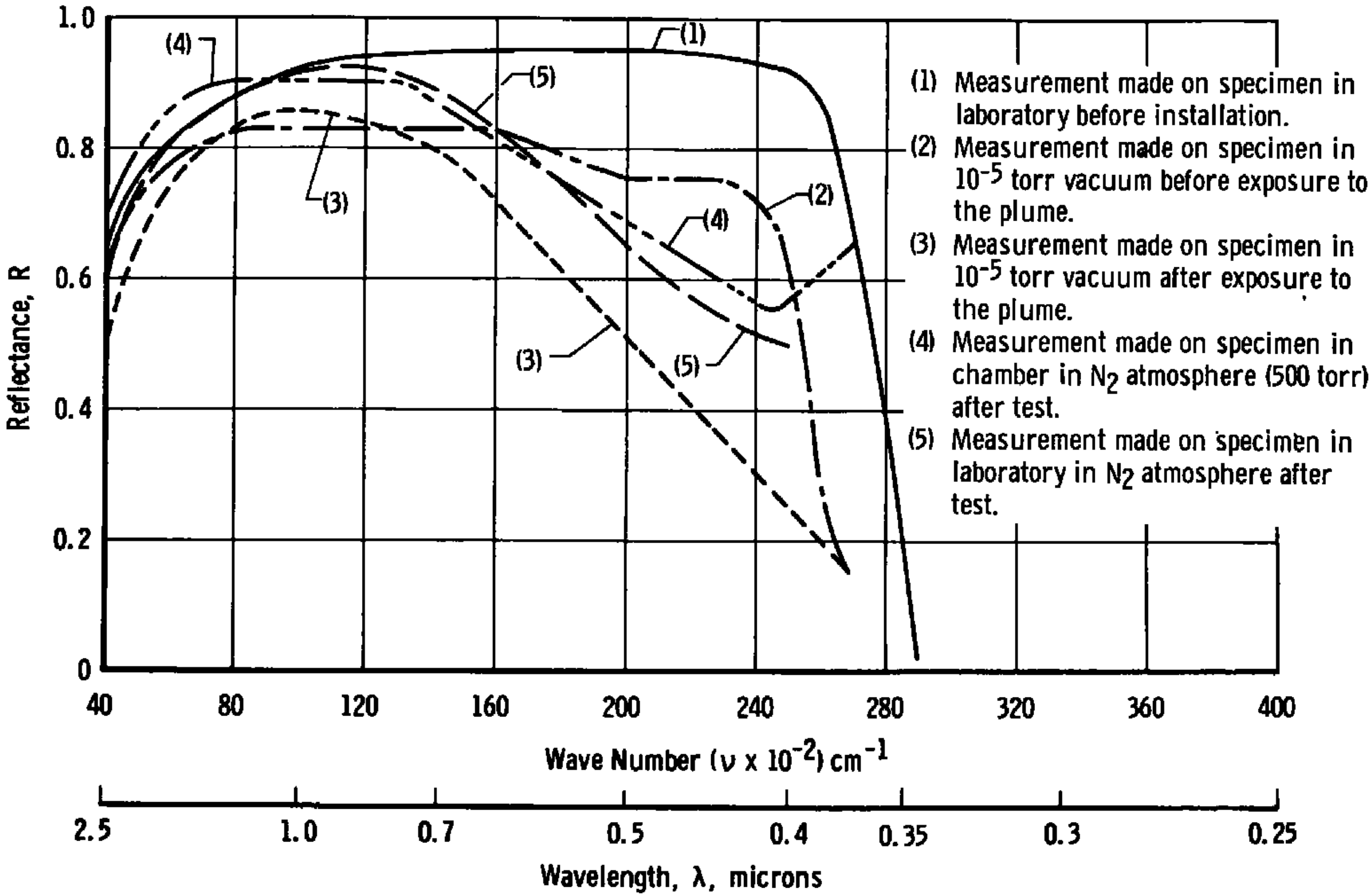

Fig. 68 Test 14—Reflectance Measurements on Specimen, Location S_{15}, Type A

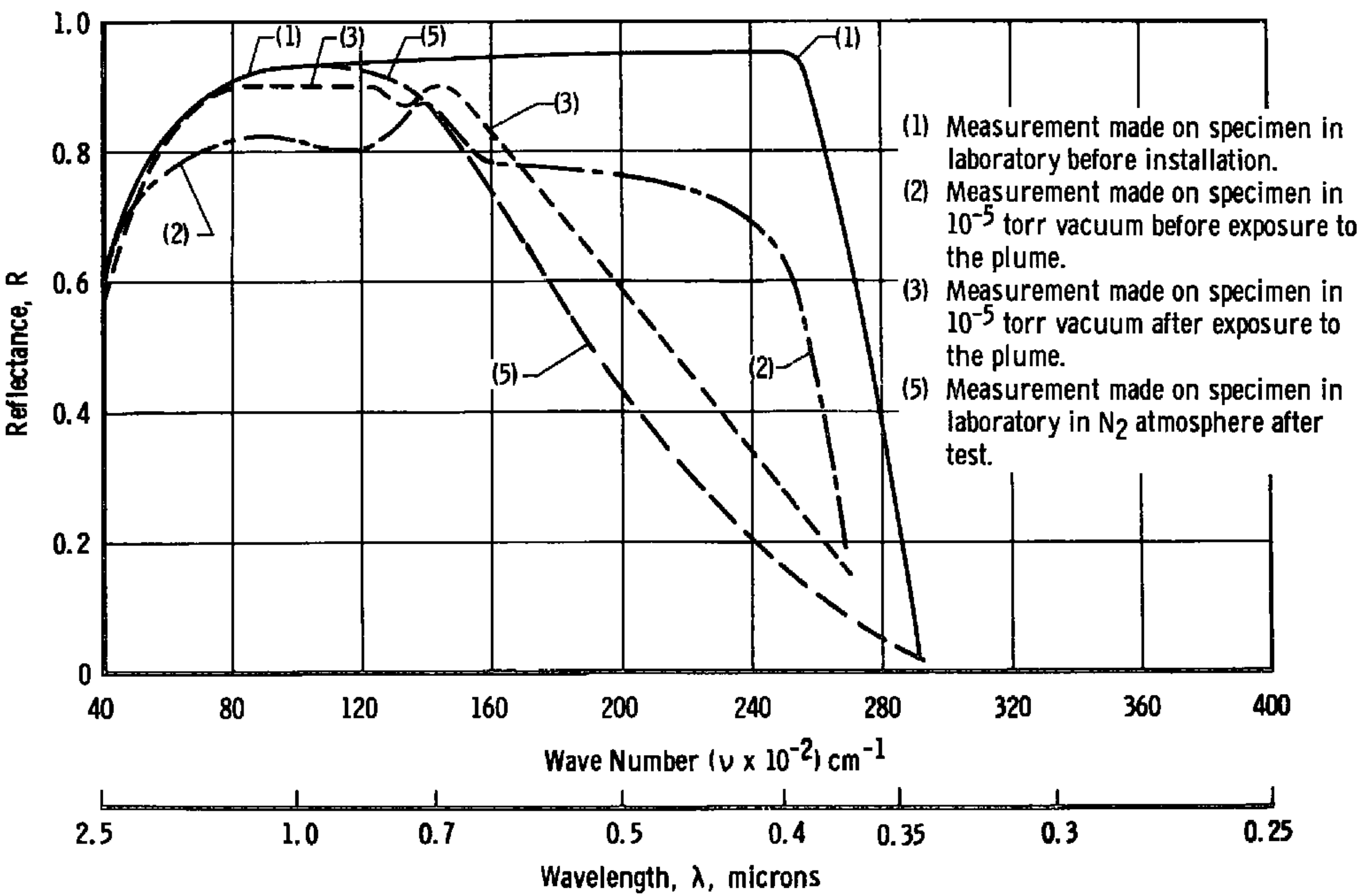

Fig. 69 Test 14—Reflectance Measurements on Specimen, Location S_{16}, Type A

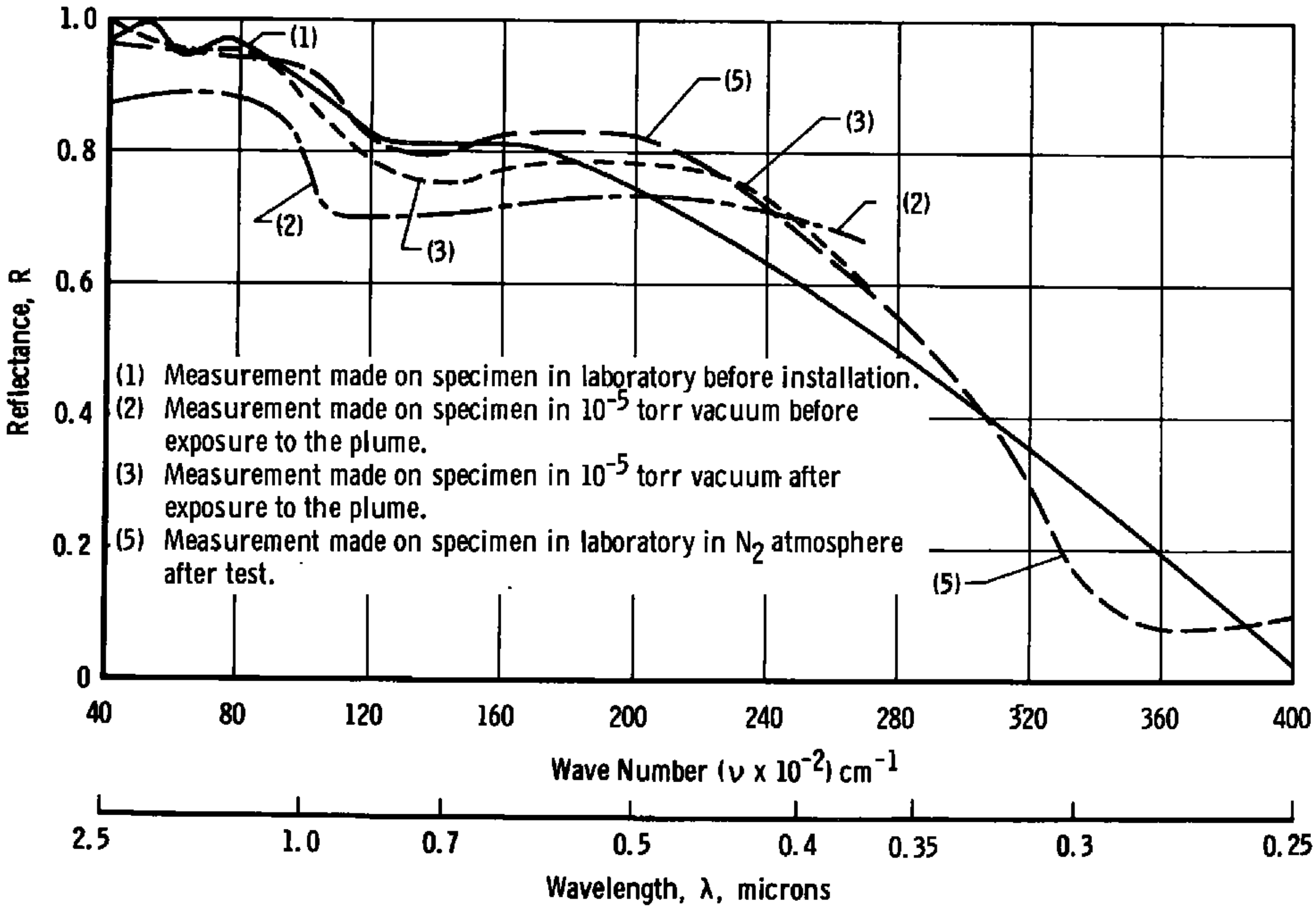

Fig. 70 Test 14—Reflectance Measurements on Specimen, Location S_{18}, Type T_2

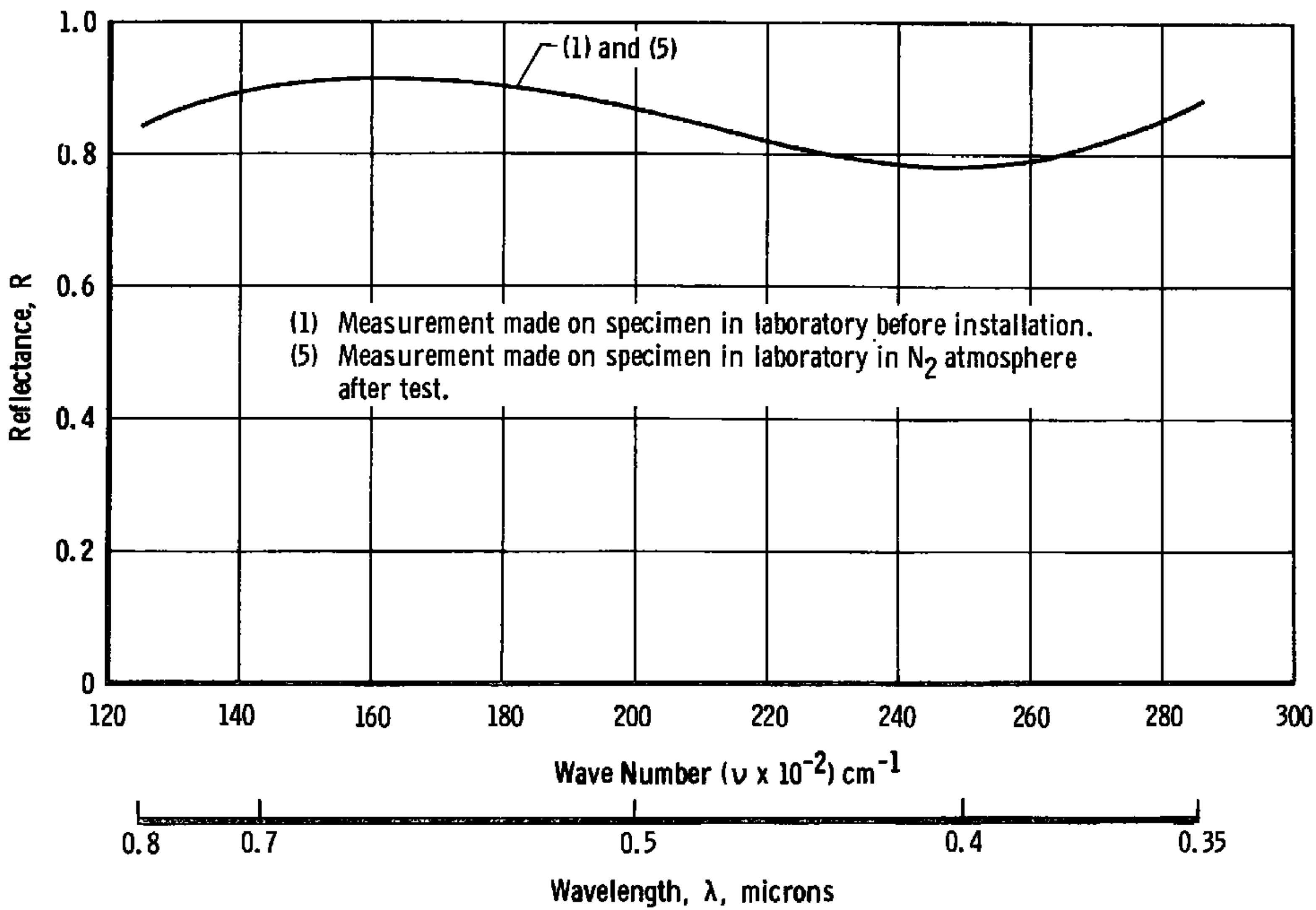

Fig. 71 Test 14—Reflectance Measurements on Specimen, Location G_3, Mirror

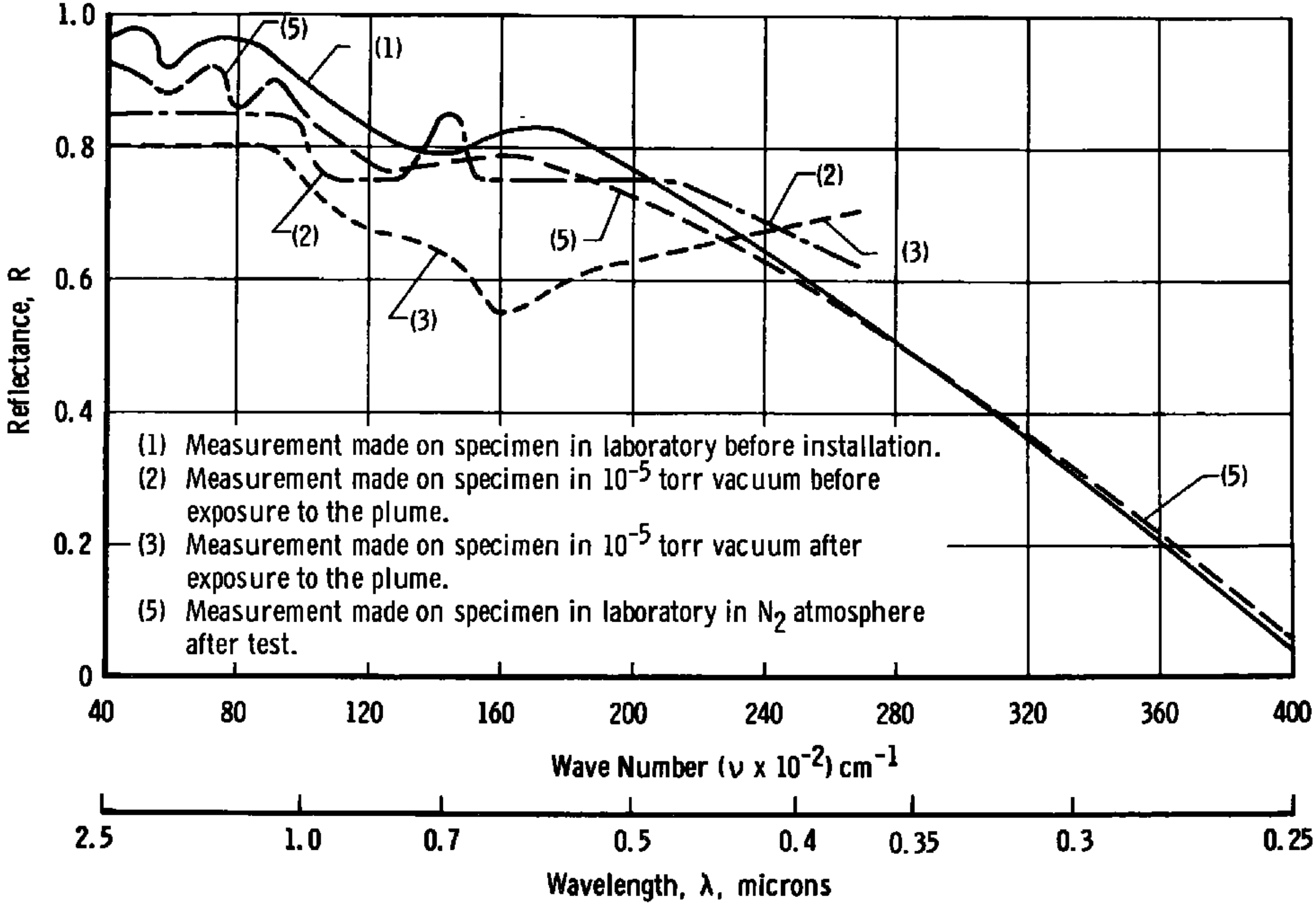

Fig. 72 Test 14--Reflectance Measurements on Specimen, Startracker, Type T_2

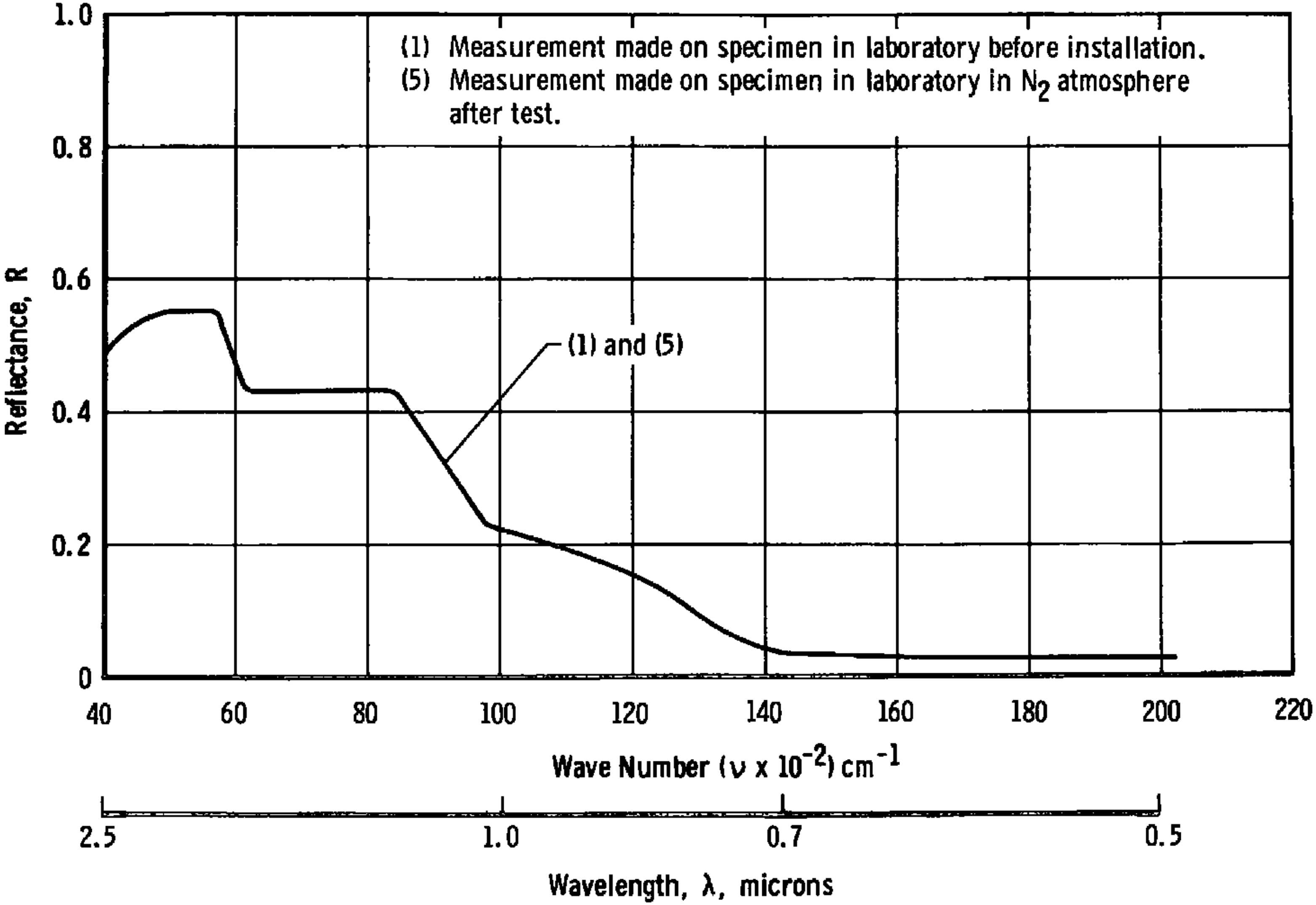

Fig. 73 Test 15—Reflectance Measurements on Specimen, Location S_7, Type K

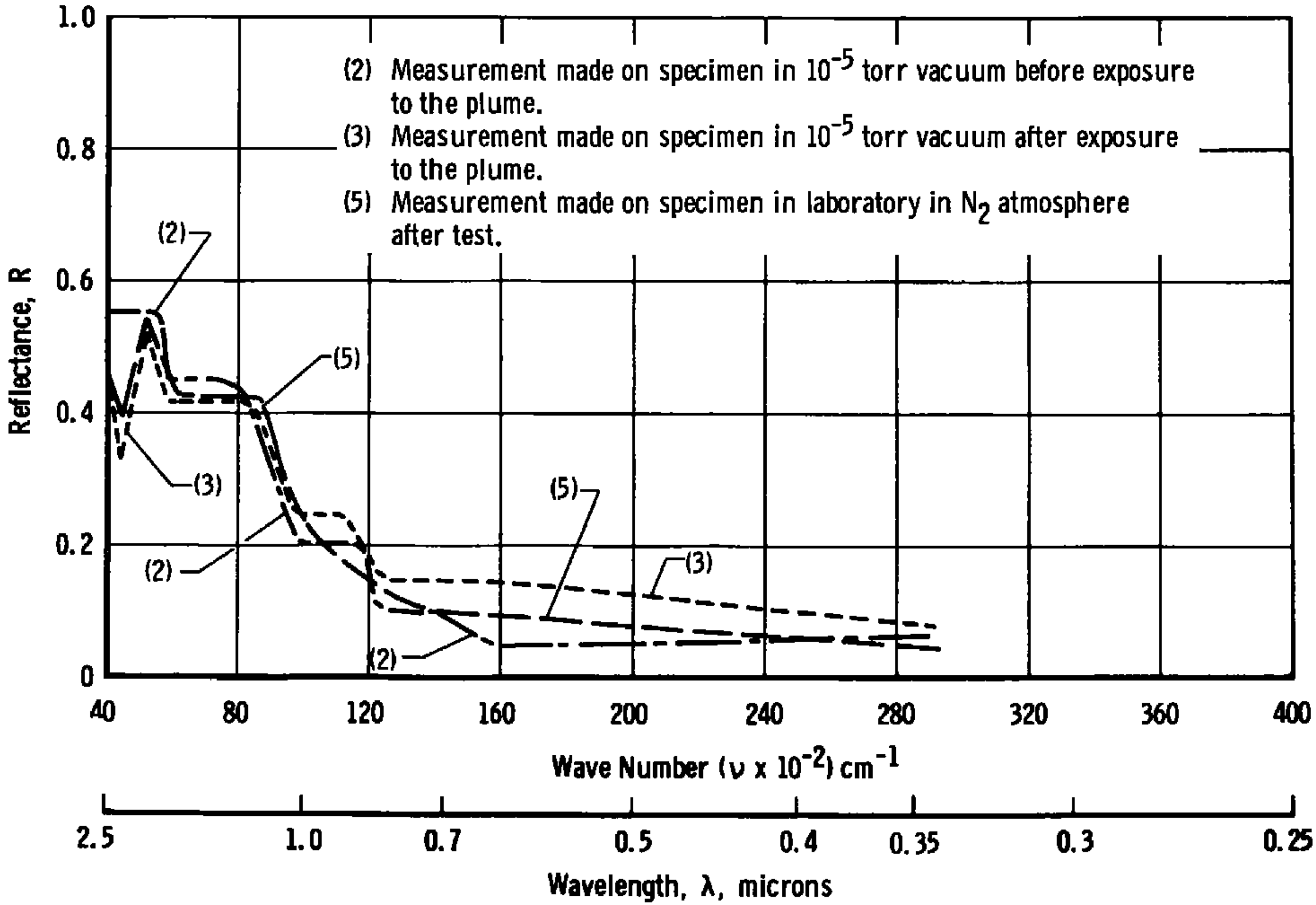

Fig. 74 Test 15—Reflectance Measurements on Specimen, Location S_{13}, Type K

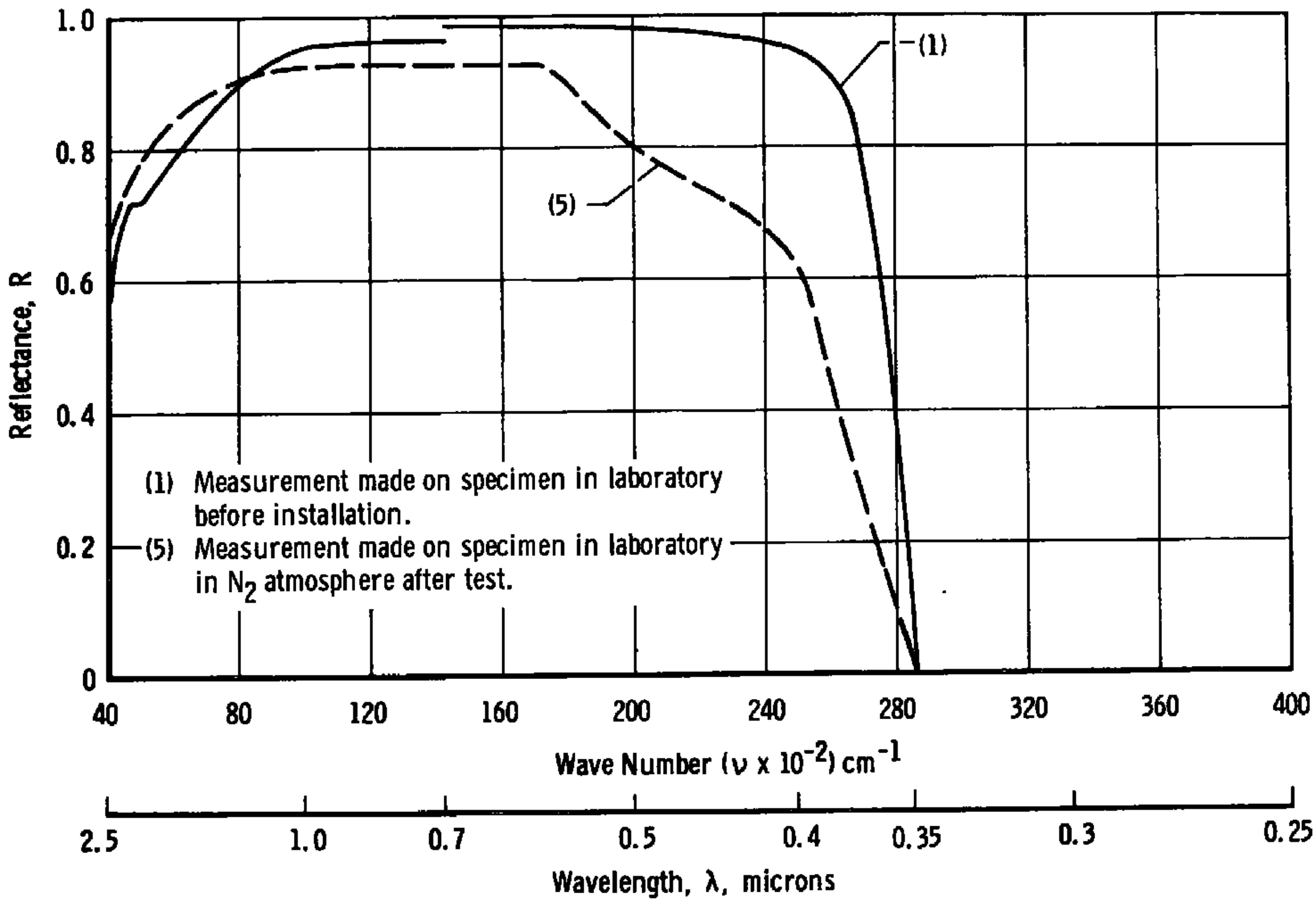

Fig. 75 Test 15—Reflectance Measurements on Specimen, Location S_{15}, Type A

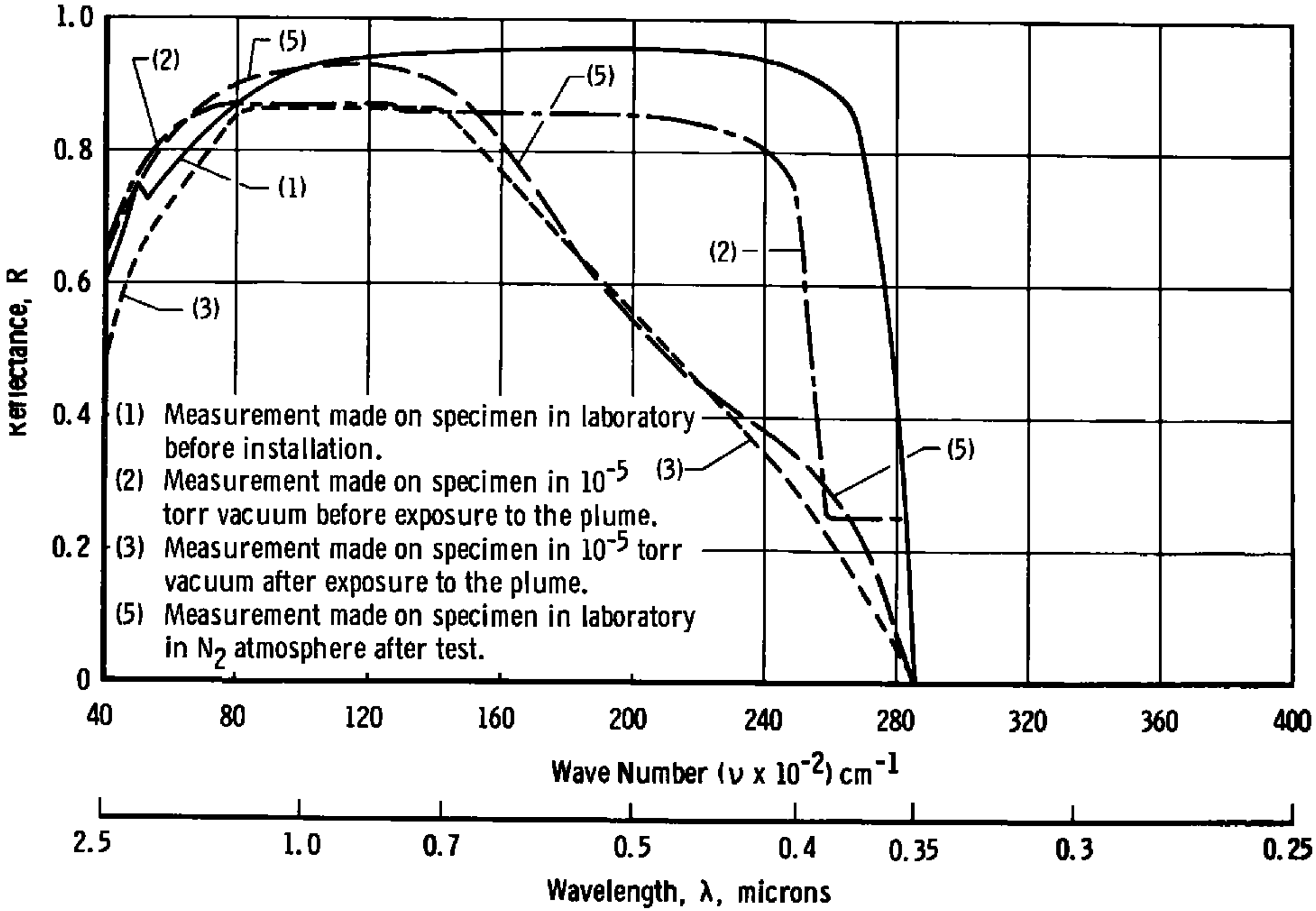

Fig. 76 Test 15—Reflectance Measurements on Specimen, Location S_{16}, Type A

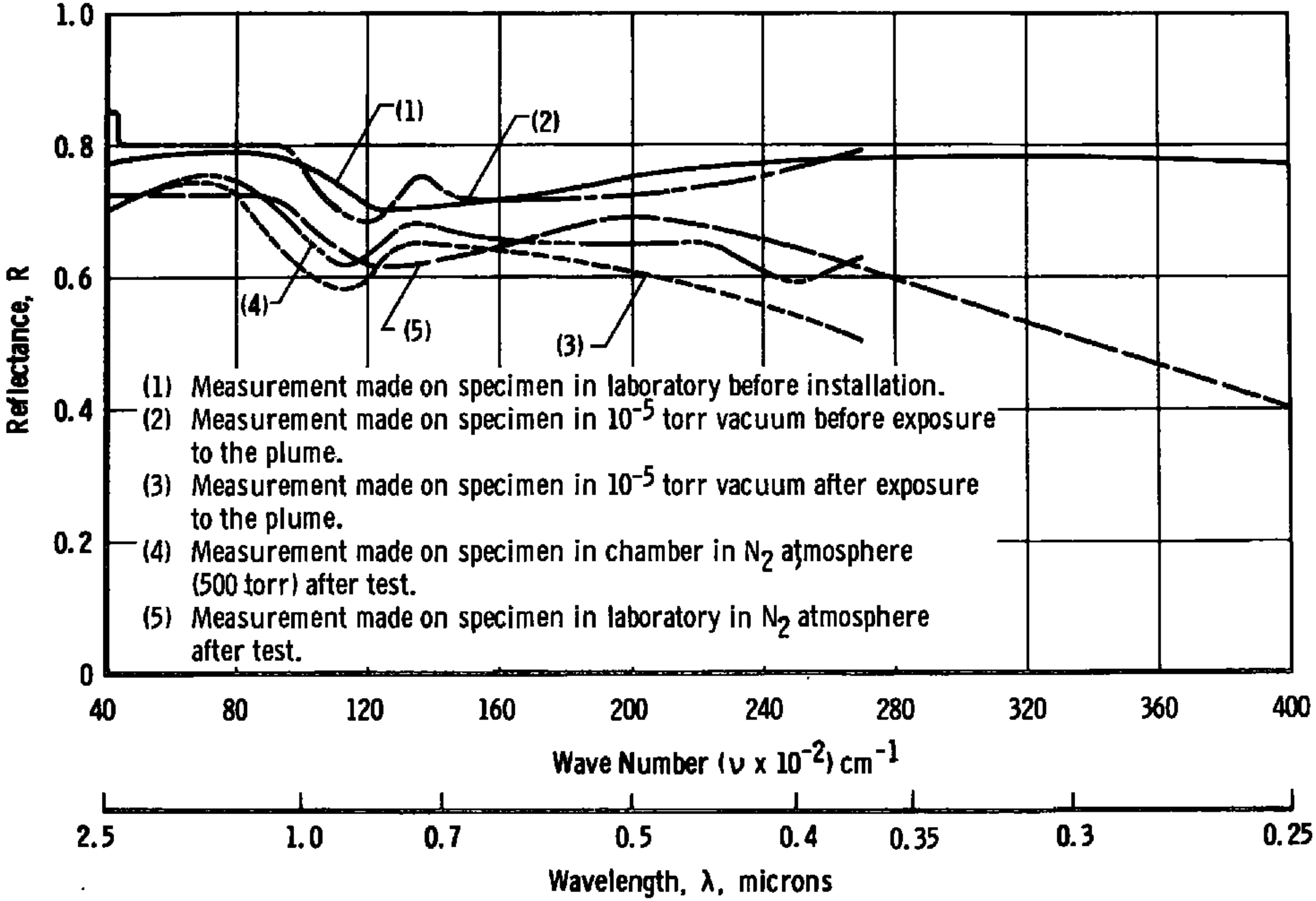

Fig. 77 Test 15—Reflectance Measurements on Specimen, Location S_{19} Type B

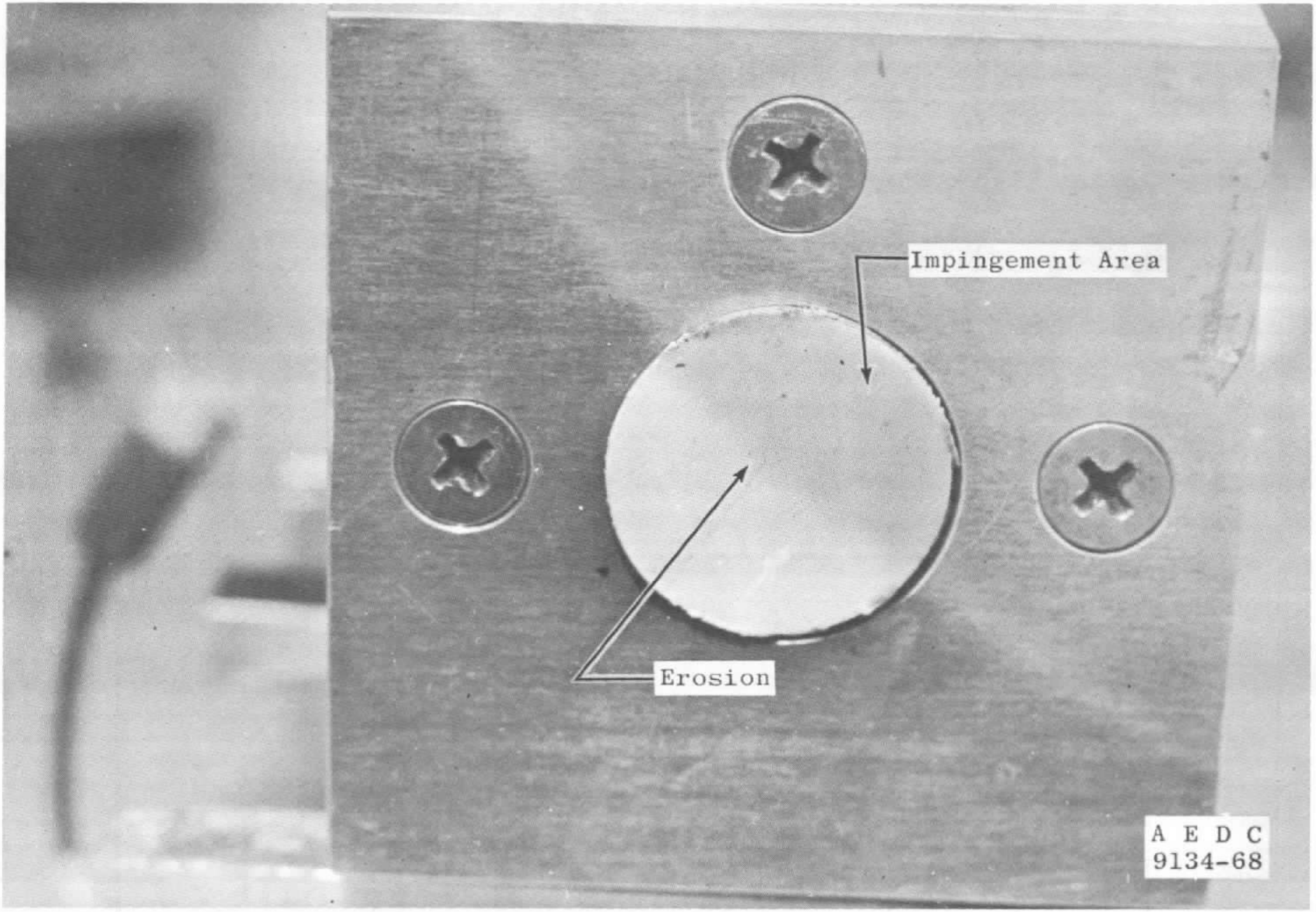

Fig. 78 Erosion of Specimen, Location S_{14}, Cube, Type T_1, after Exposure to Plume—Test 15

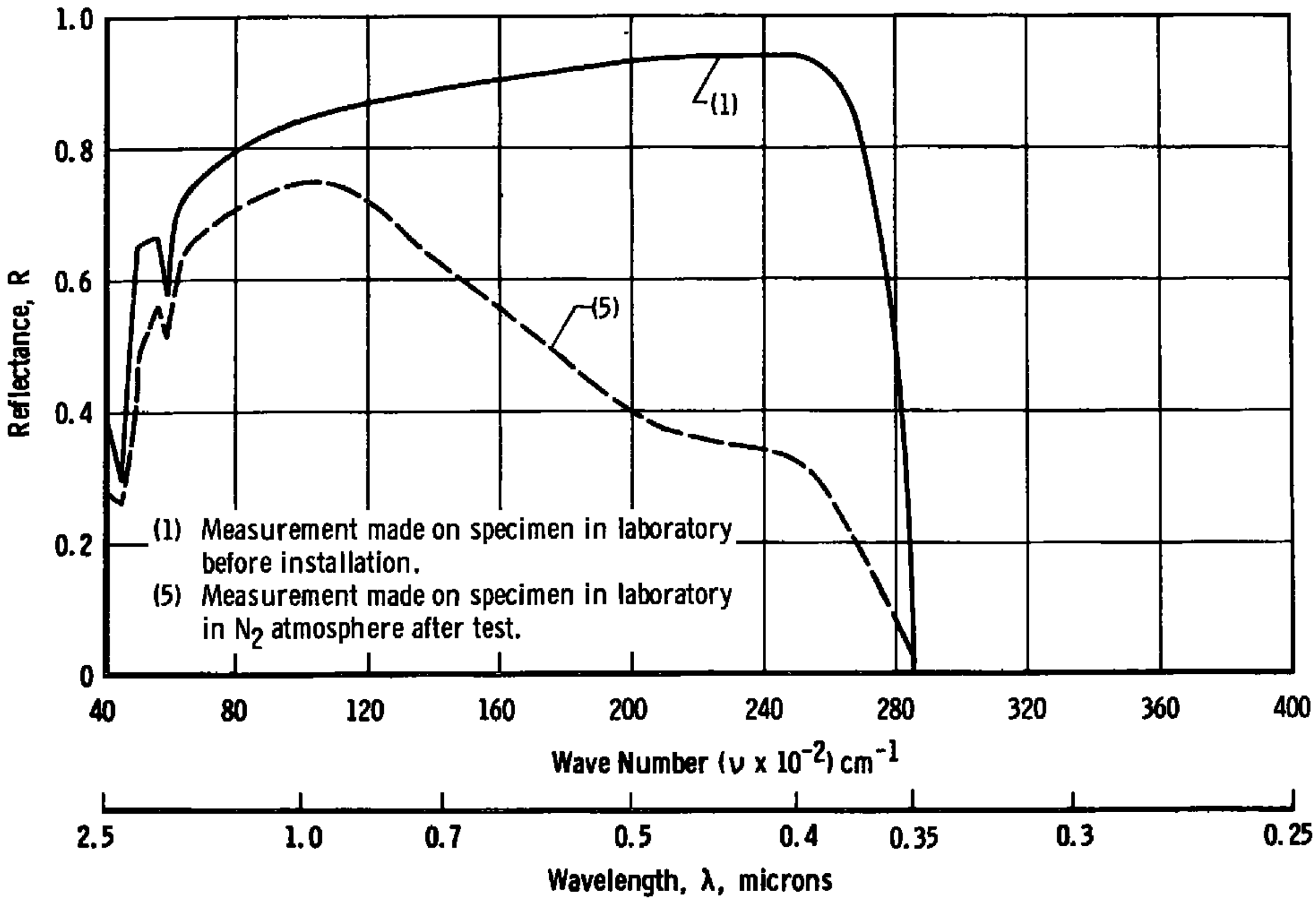

Fig. 79 Test 15—Reflectance Measurements on Specimen, Location S_{14}, Cube, Type T_1

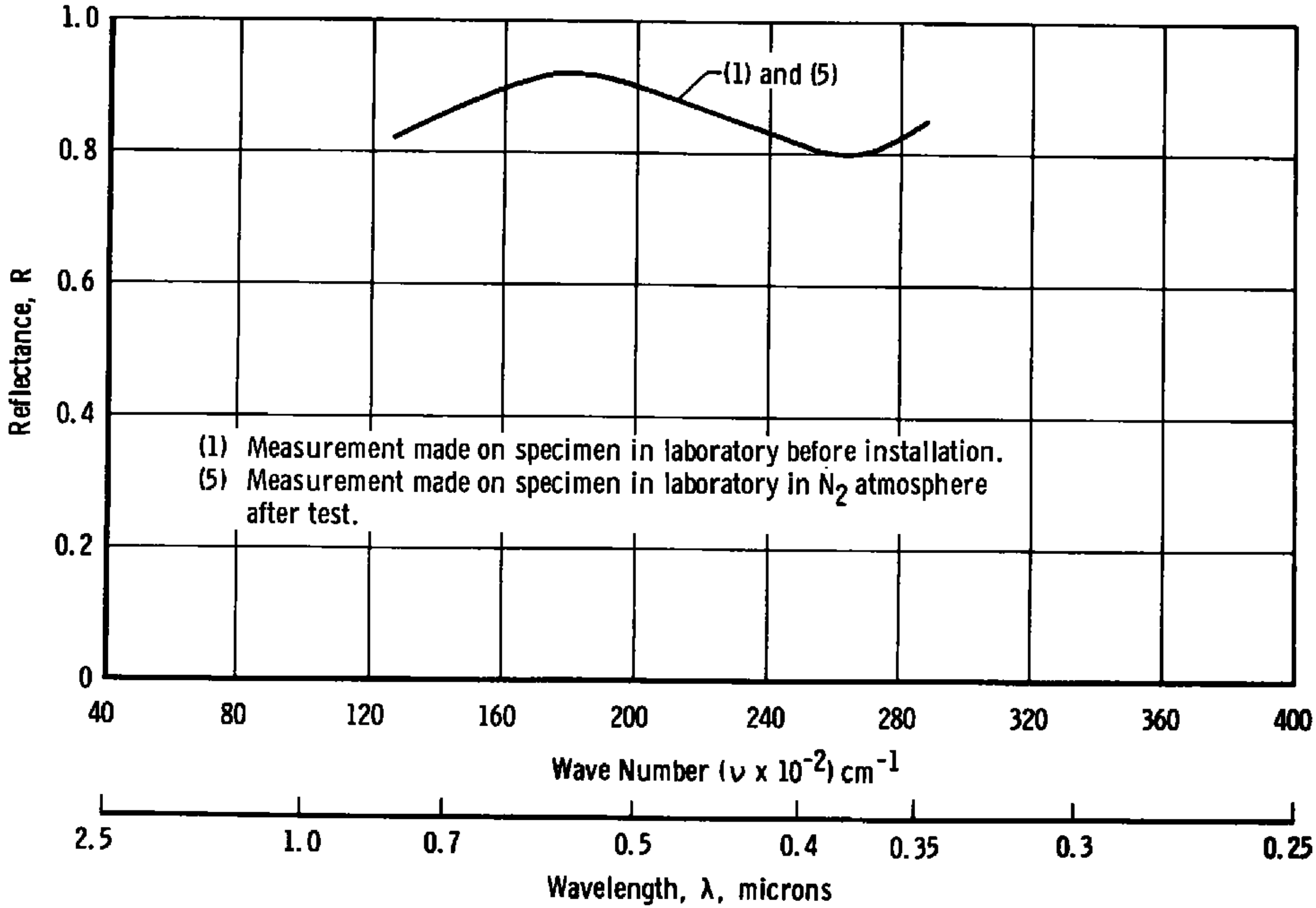

Fig. 80 Test 15—Reflectance Measurements on Specimen, Location C_3, Mirror

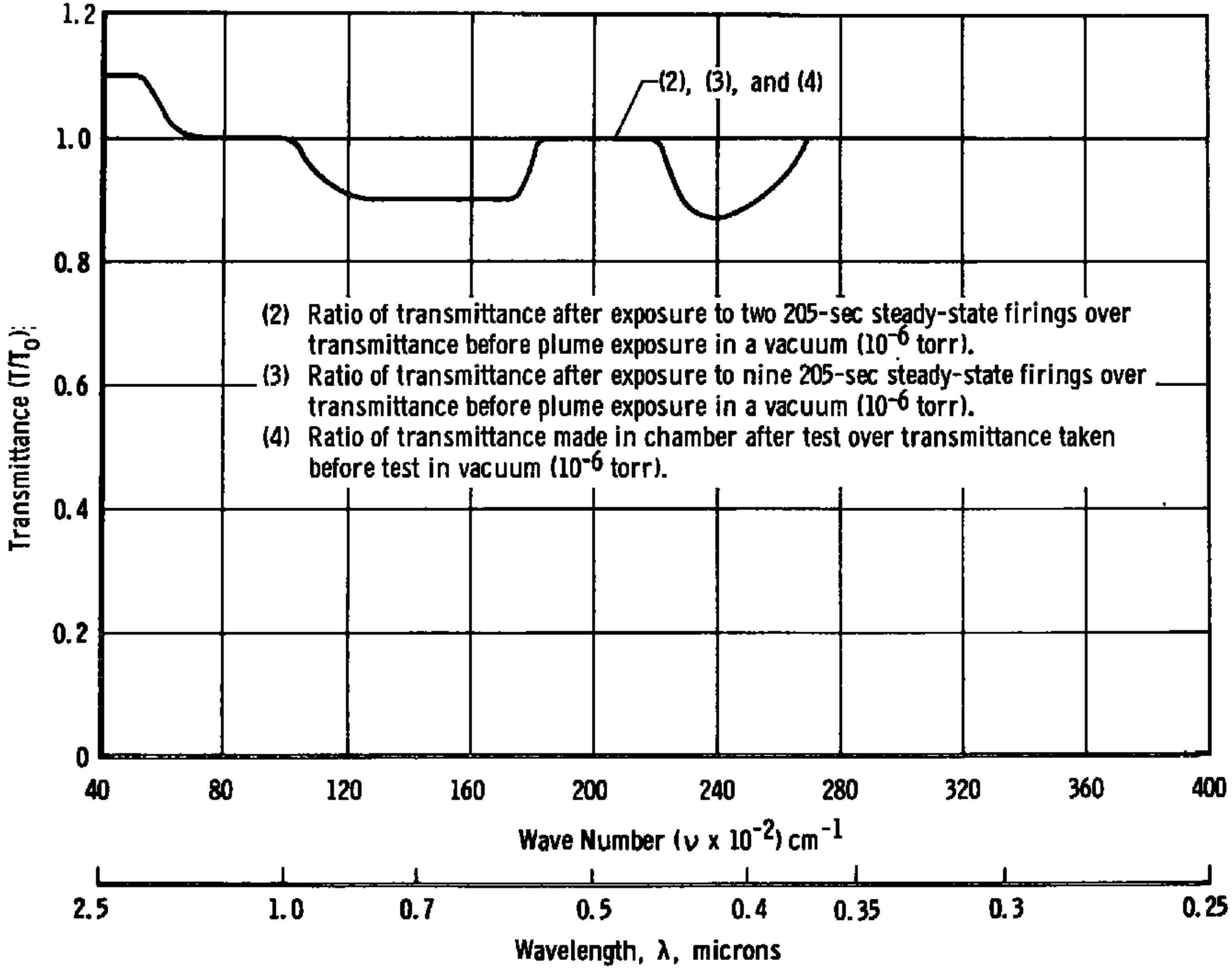

Fig. 81 Test 15—Transmittance Measurements on Specimen, Location V_1, View Port

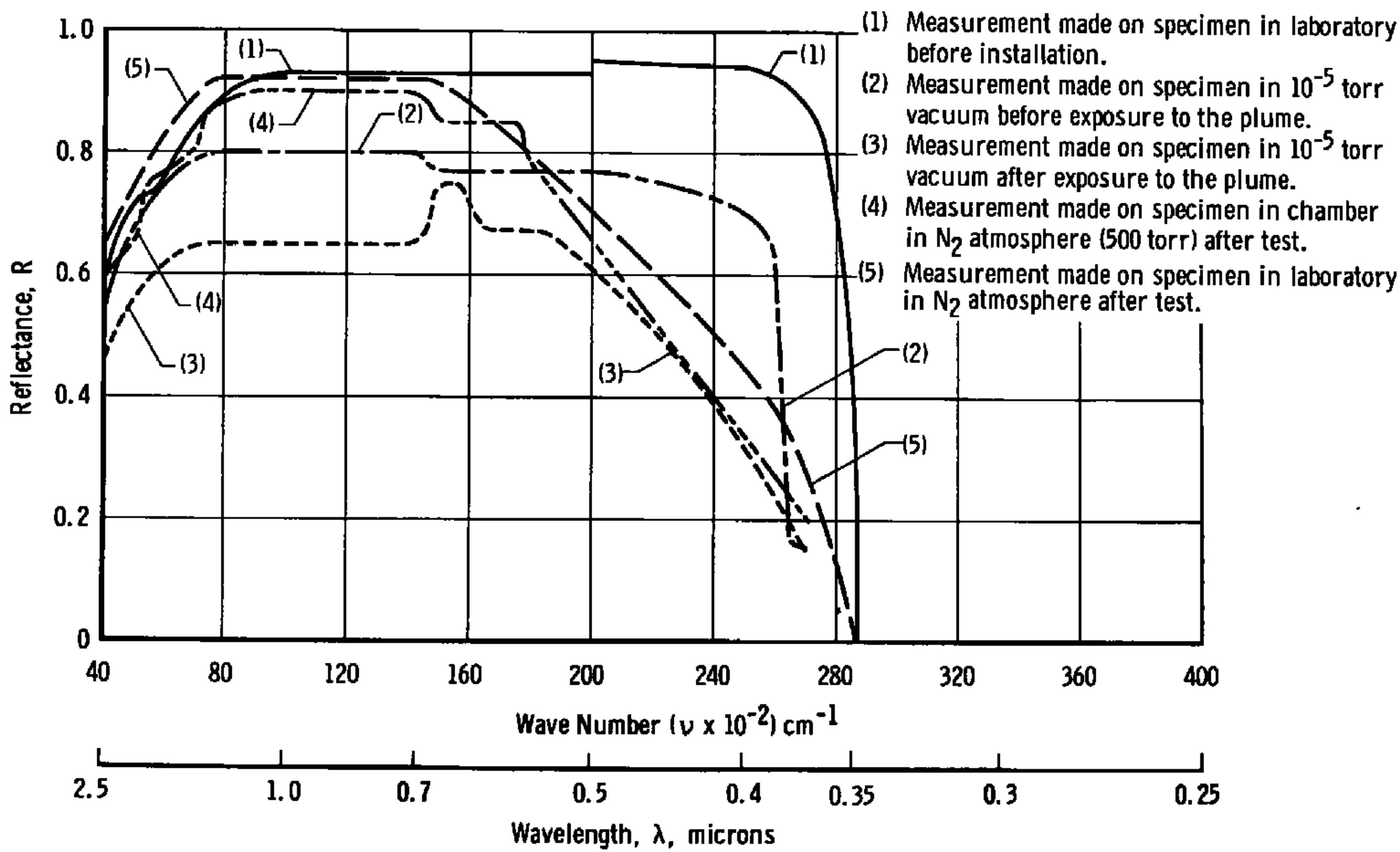

Fig. 82 Test 20—Reflectance Measurements on Specimen, Location S_{11}, Type A

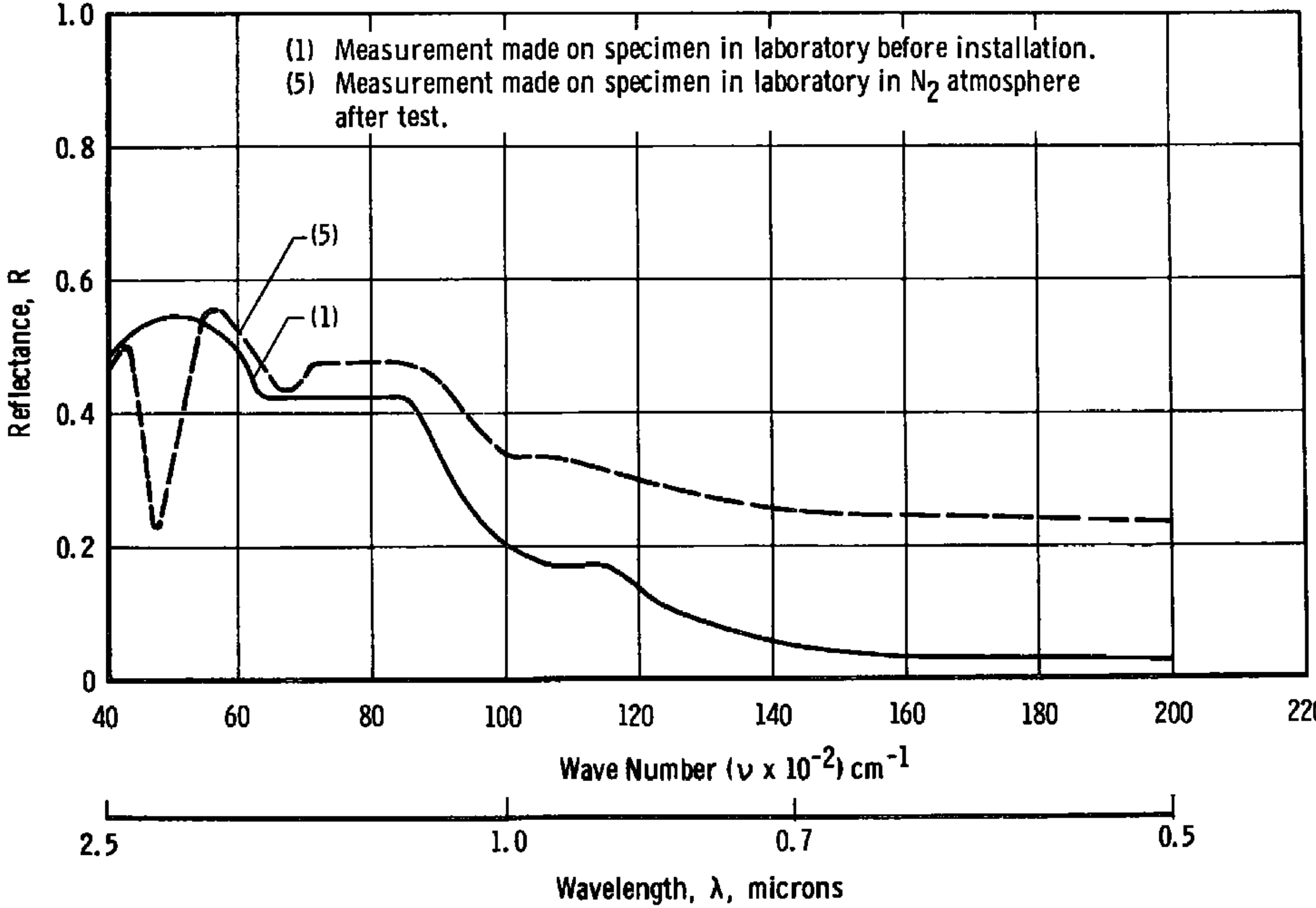

Fig. 83 Test 20—Reflectance Measurements on Specimen, Location S_{13}, Type K

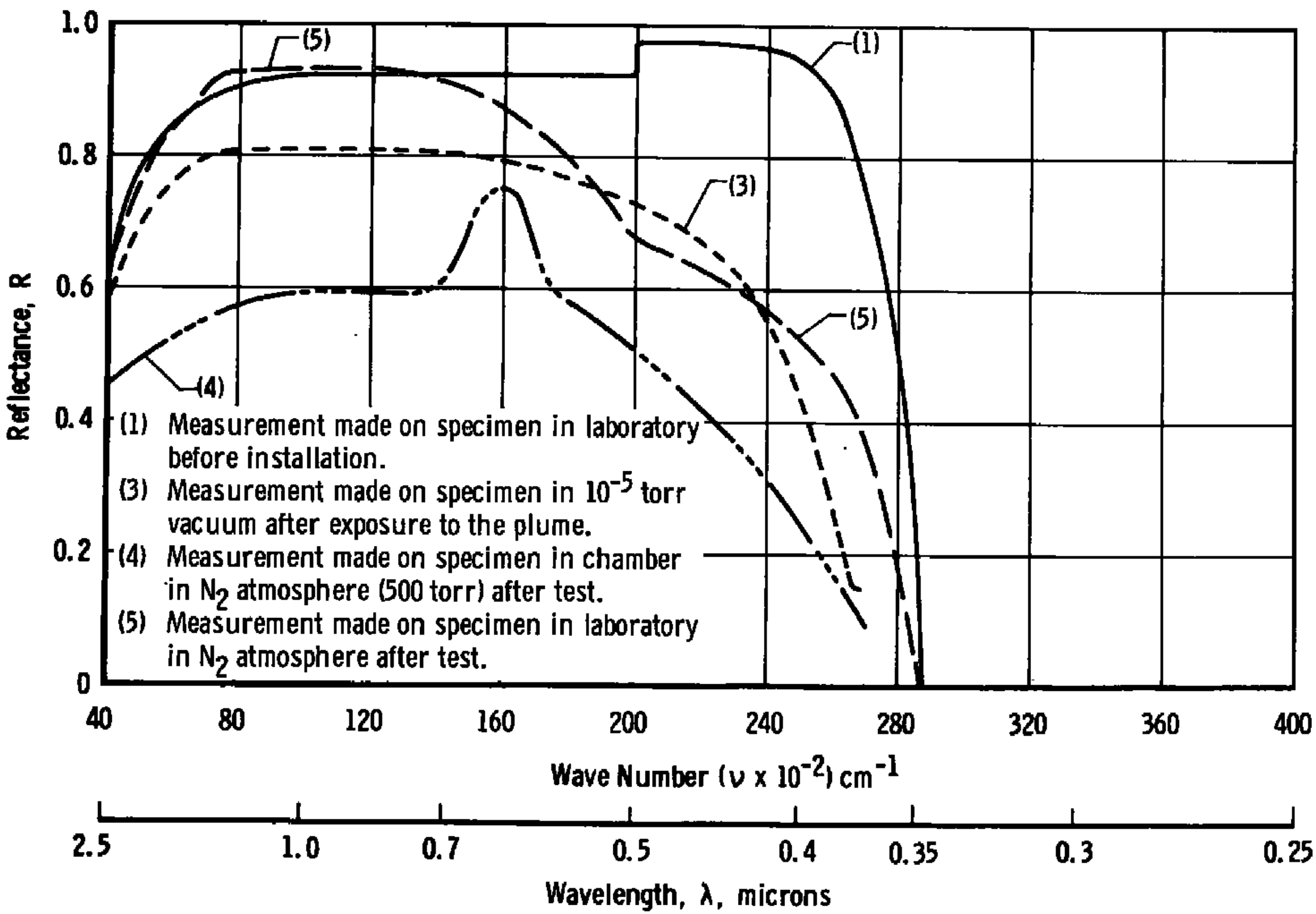

Fig. 84 Test 20—Reflectance Measurements on Specimen, Location S_{15}, Type A

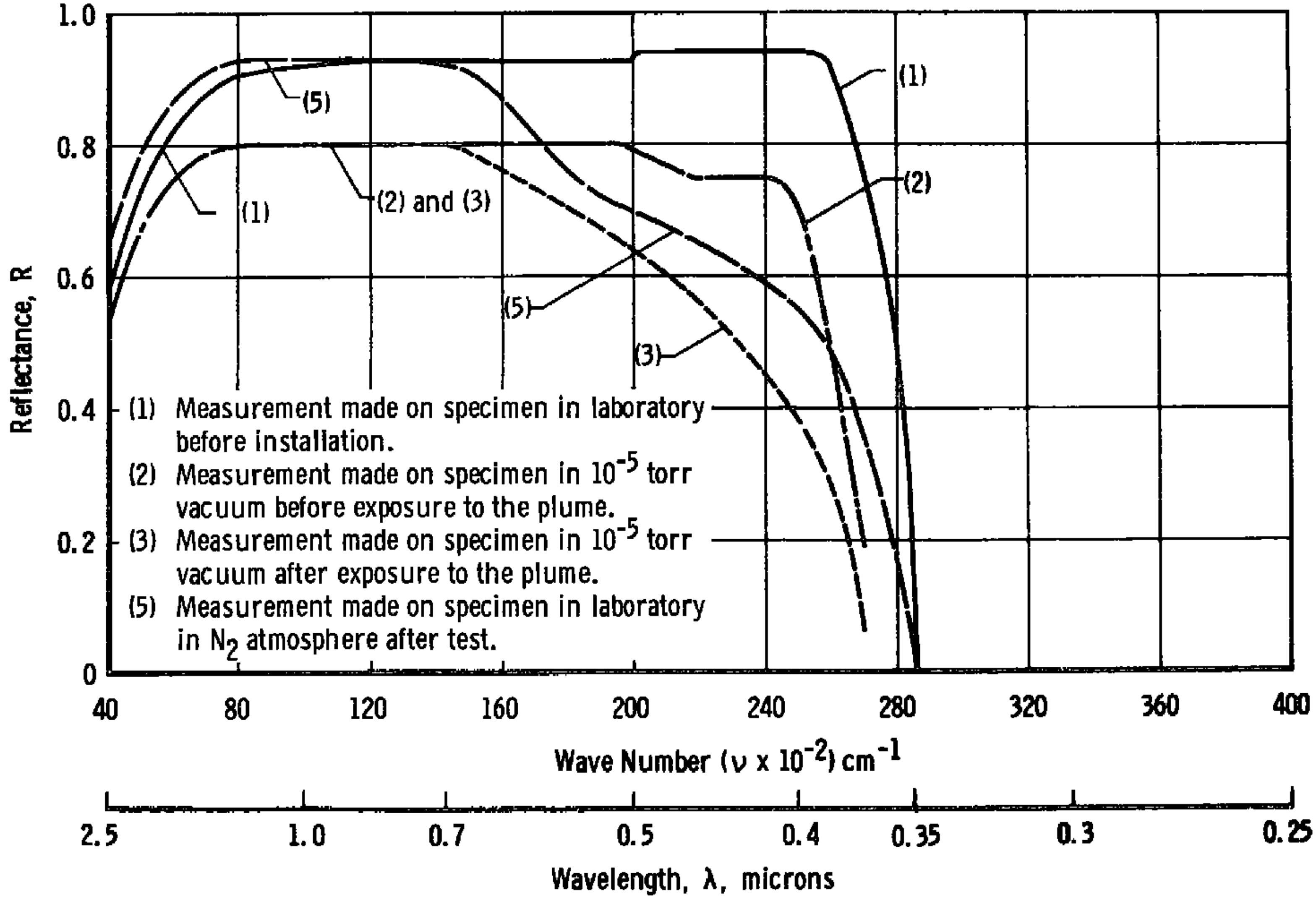

Fig. 85 Test 20—Reflectance Measurements on Specimen, Location S_{16}, Type A

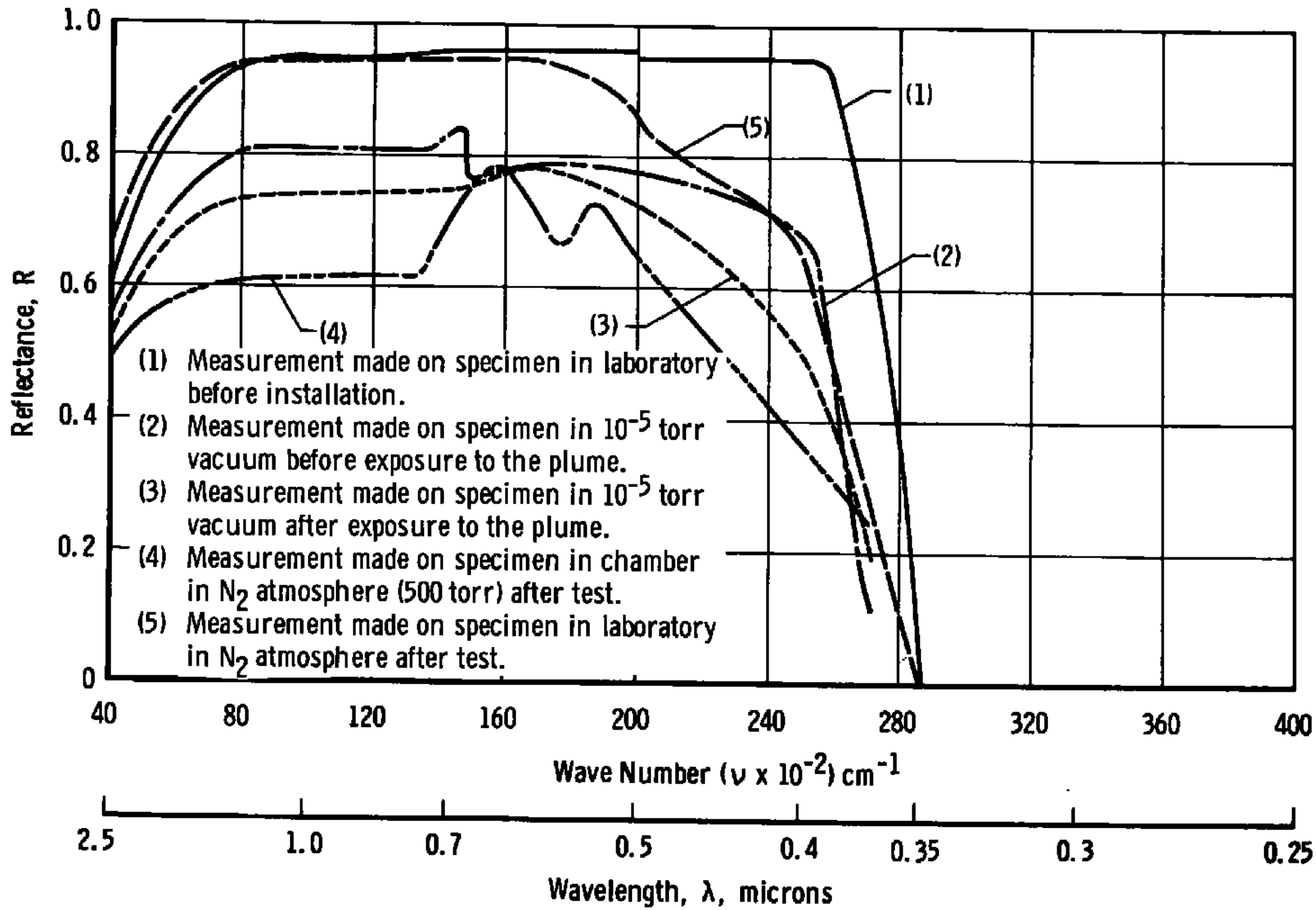

Fig. 86 Test 20—Reflectance Measurements on Specimen, Location S_{19}, Type A

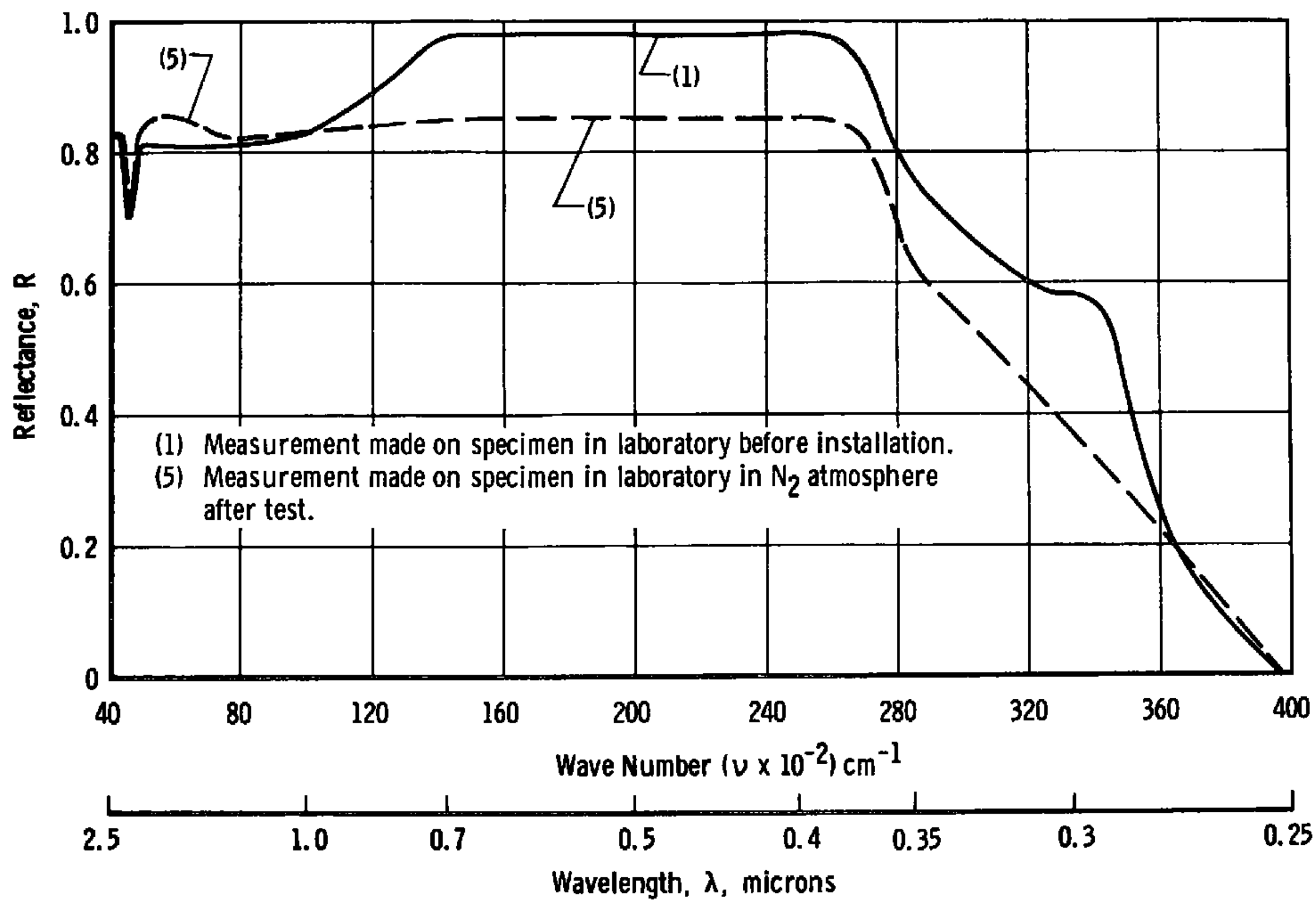

Fig. 87 Test 20—Transmittance Measurements on Specimen, Location V_1, View Port

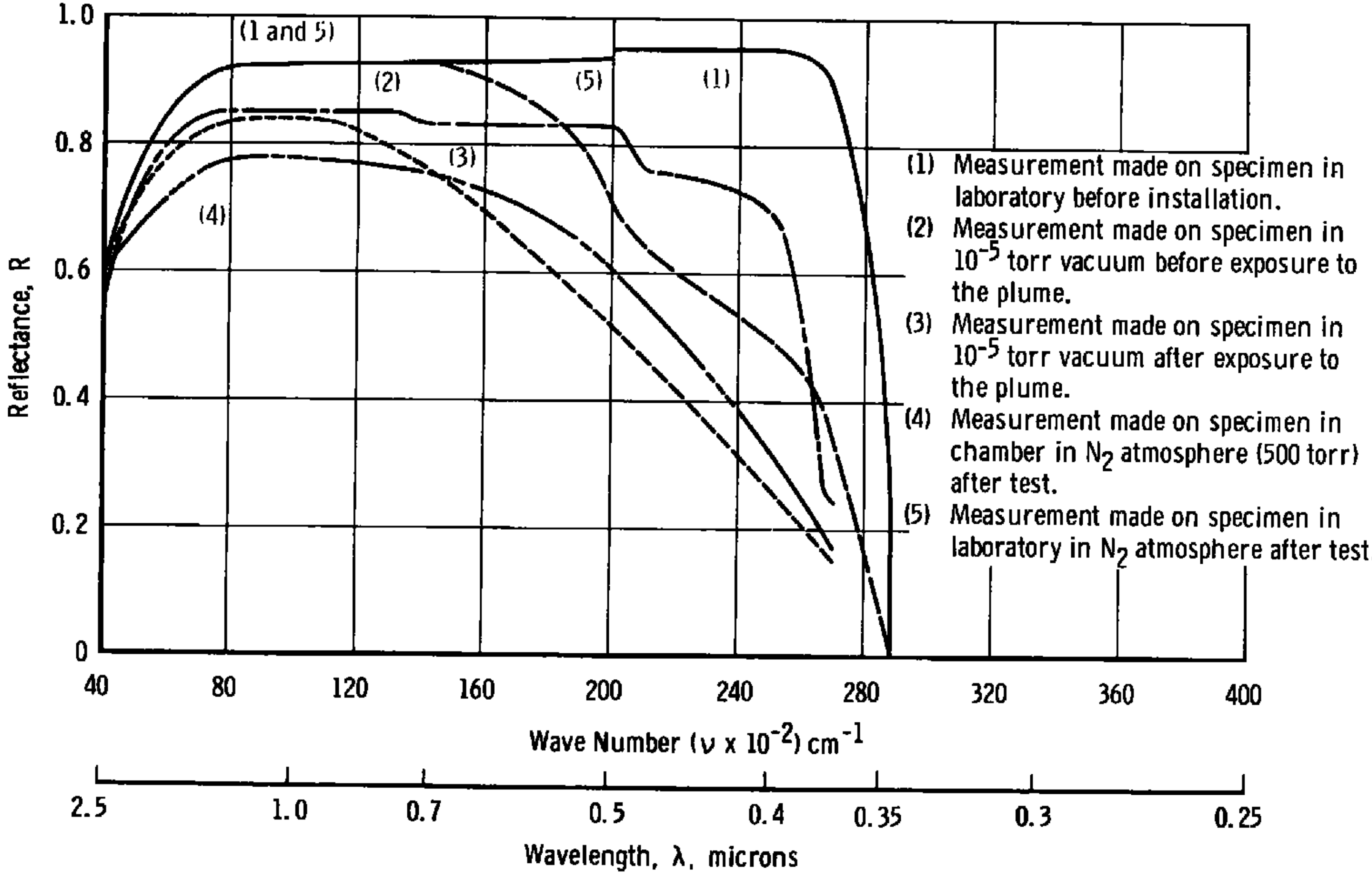

Fig. 88 Test 21—Reflectance Measurements on Specimen, Location S_{11}, Type A

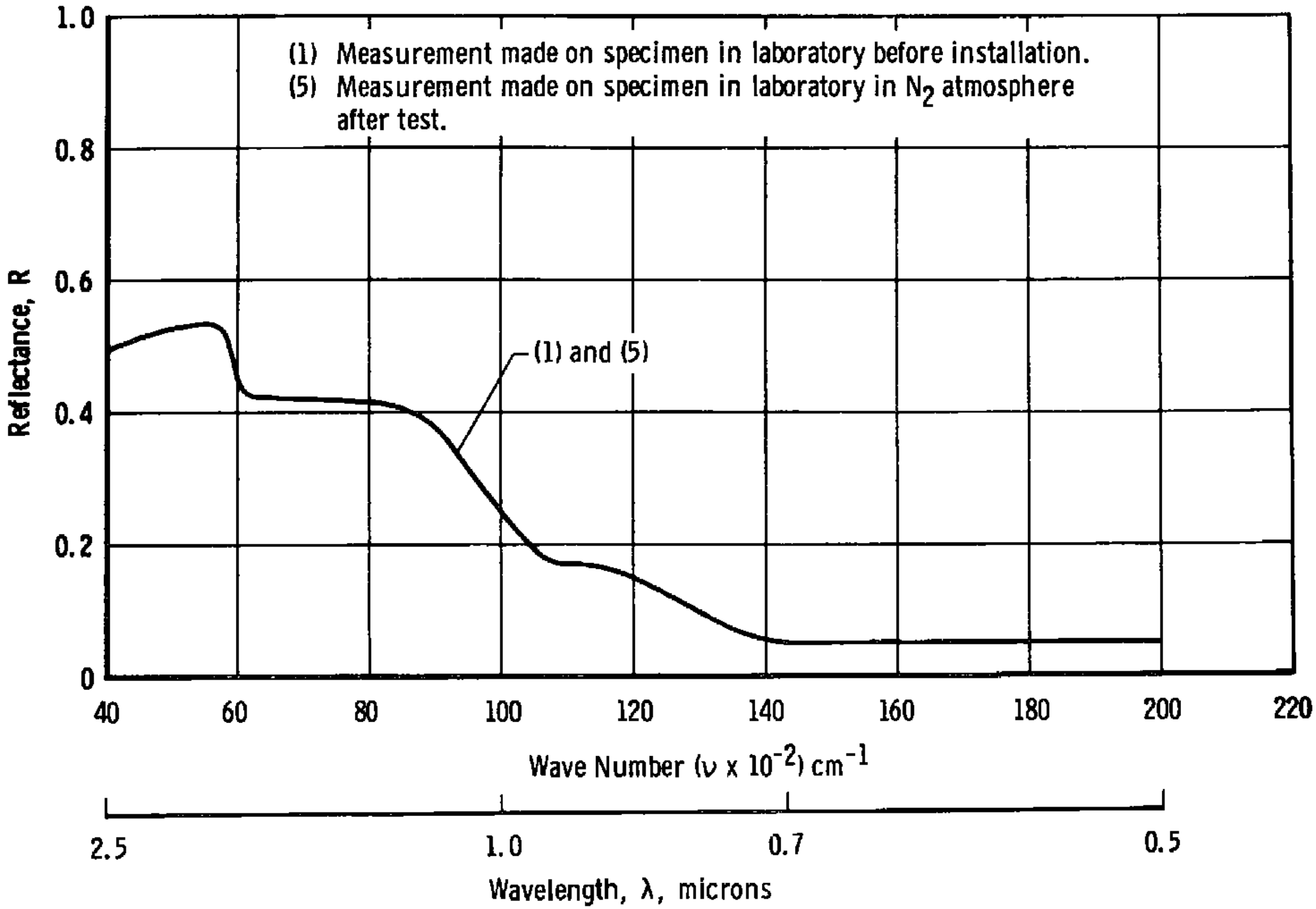

Fig. 89 Test 21—Reflectance Measurements on Specimen, Location S_{13}, Type K

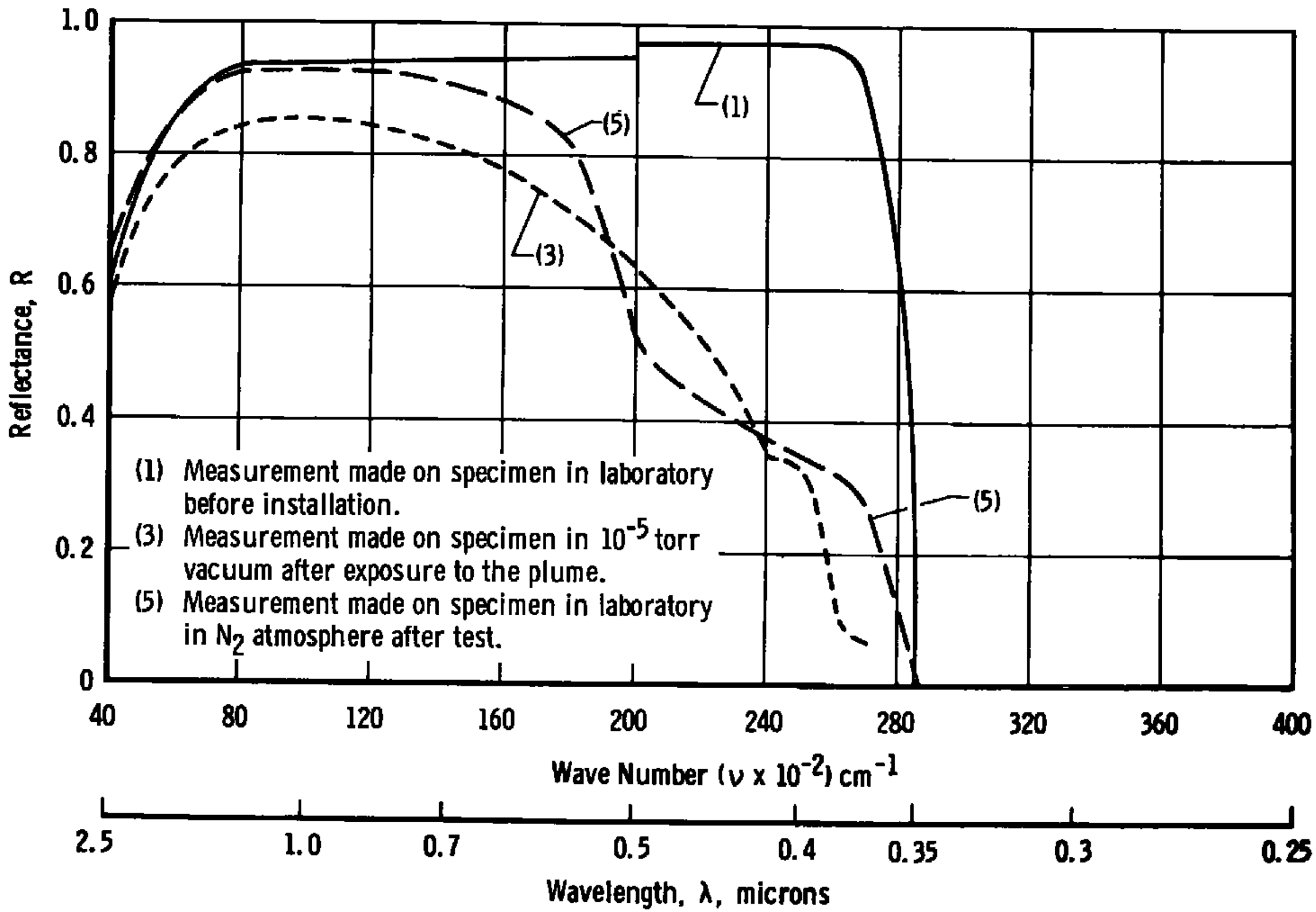

Fig. 90 Test 21—Reflectance Measurements on Specimen, Location S_{15}, Type A

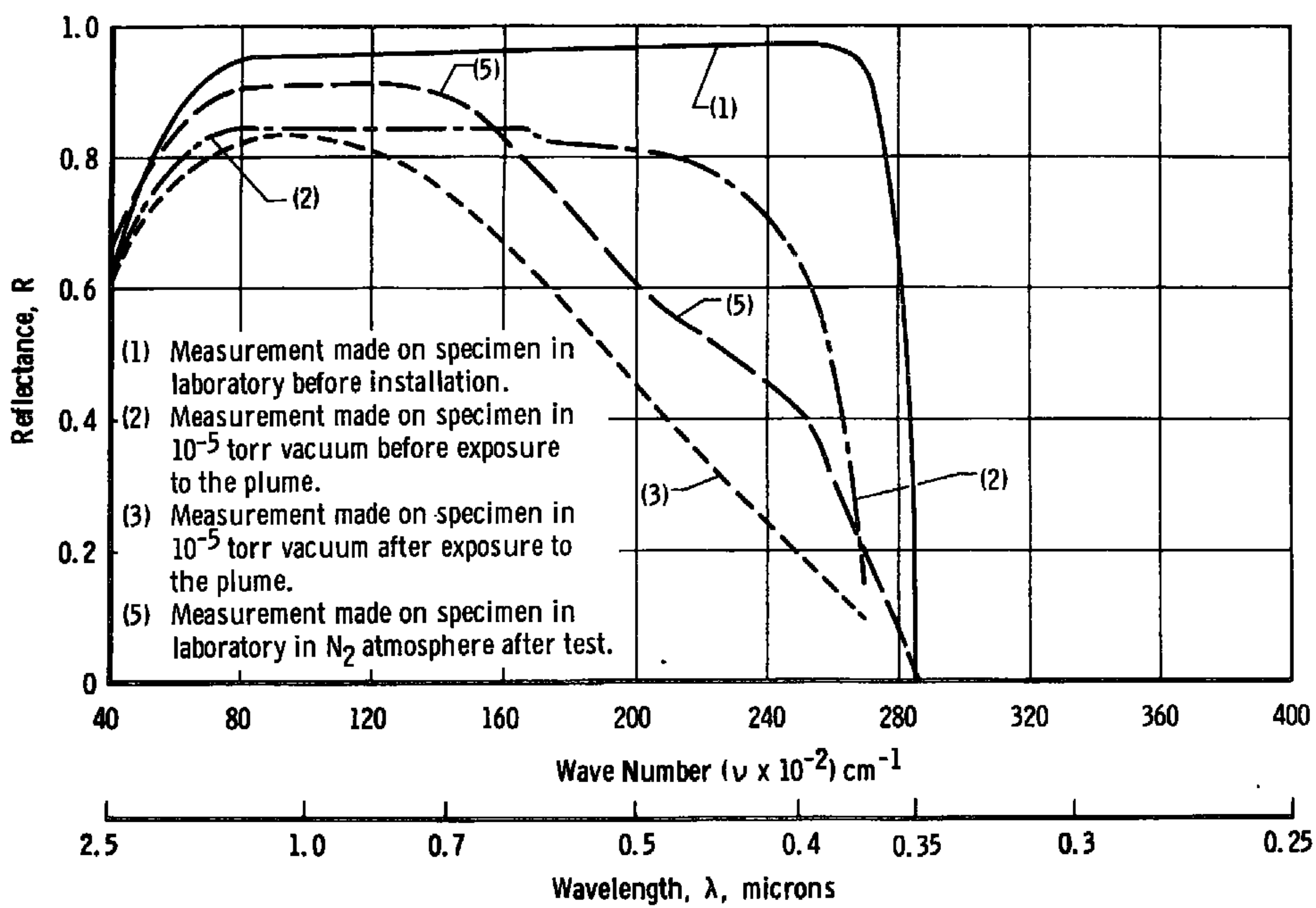

Fig. 91 Test 21—Reflectance Measurements on Specimen, Location S_{16}, Type A

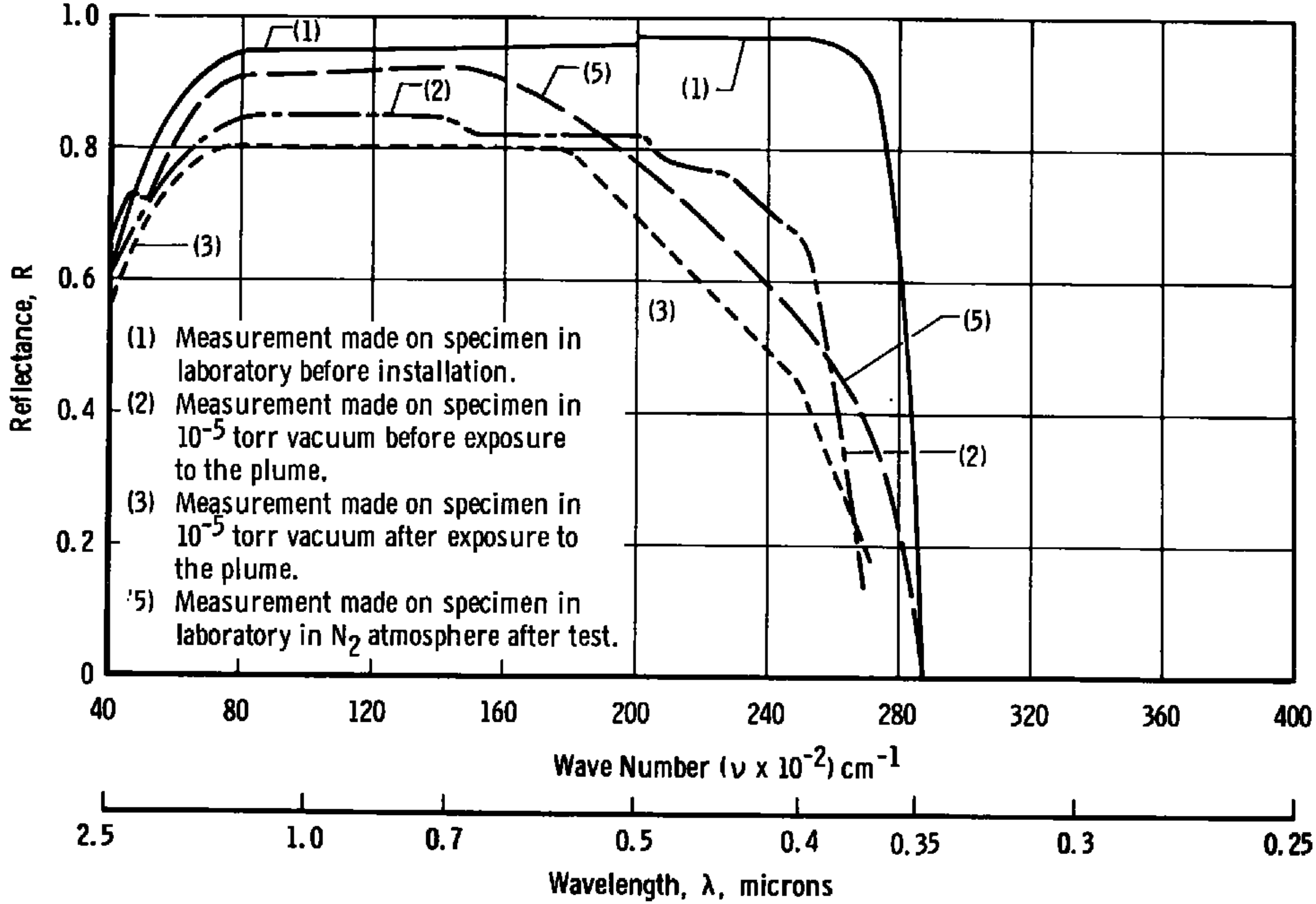

Fig. 92 Test 21—Reflectance Measurements on Specimen, Location S_{19}, Type A

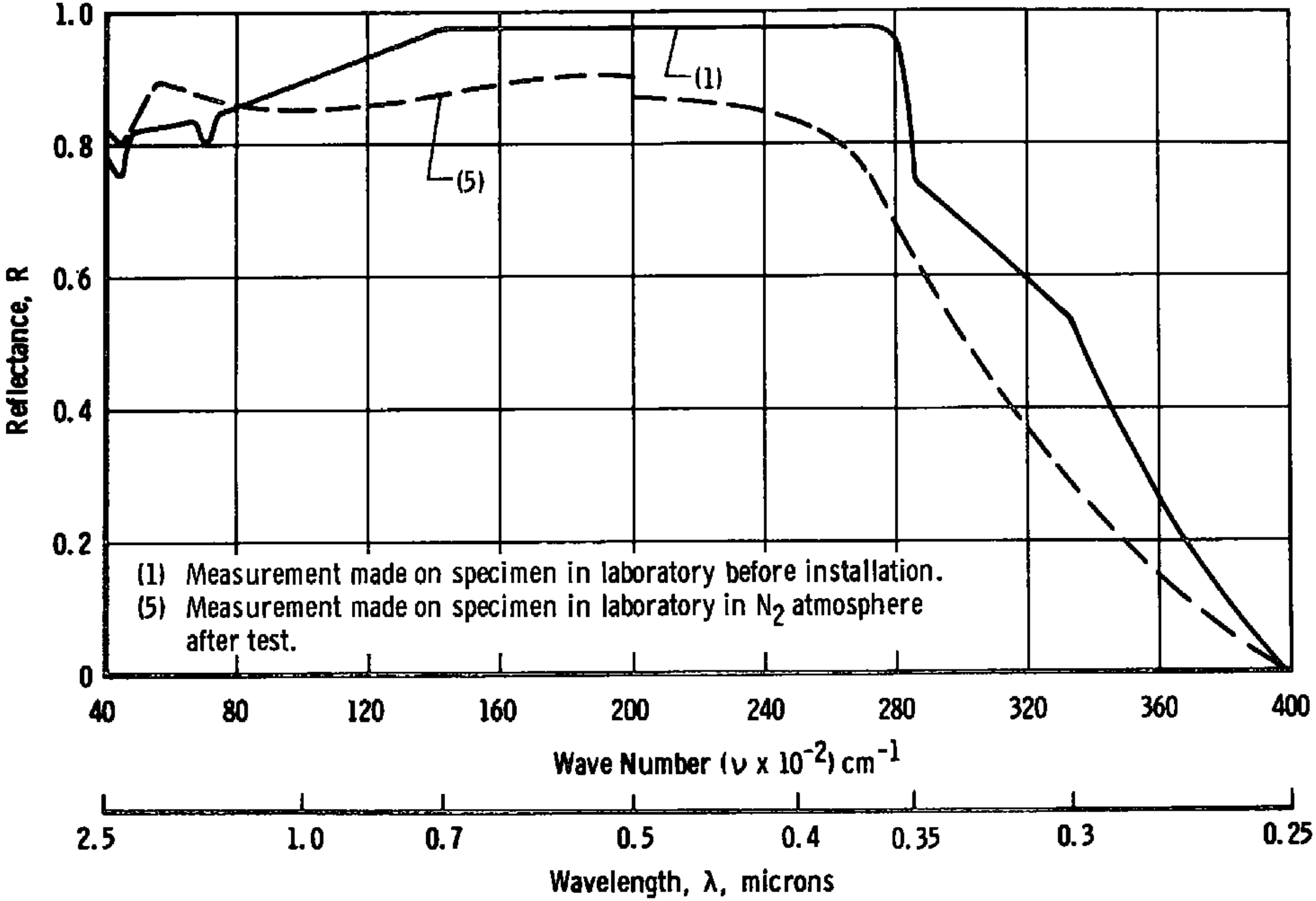

Fig. 93 Test 21—Transmittance Measurements on Specimen, Location V_1, View Port

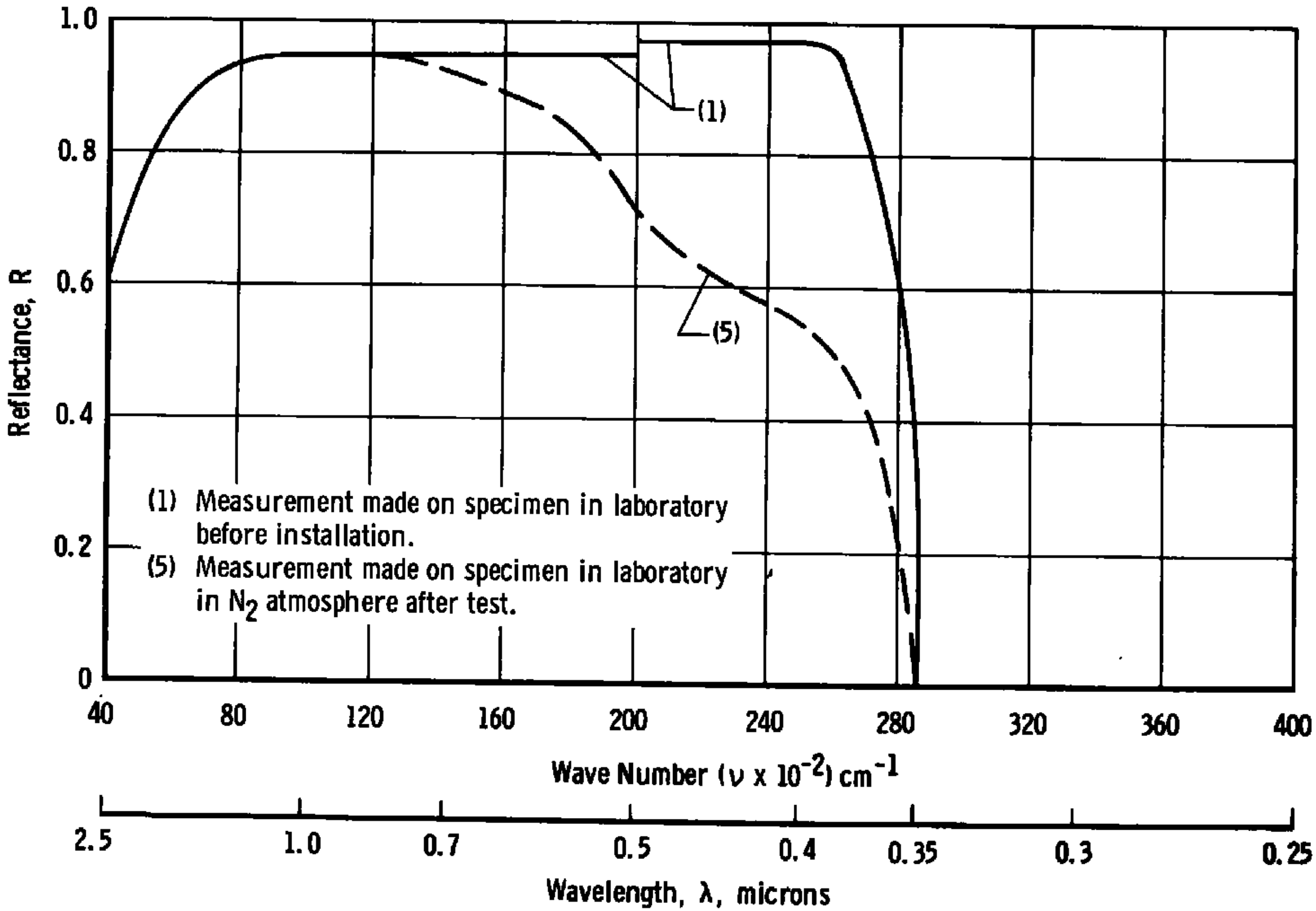

Fig. 94 Test 22—Reflectance Measurements on Specimen, Location S_{11}, Type A

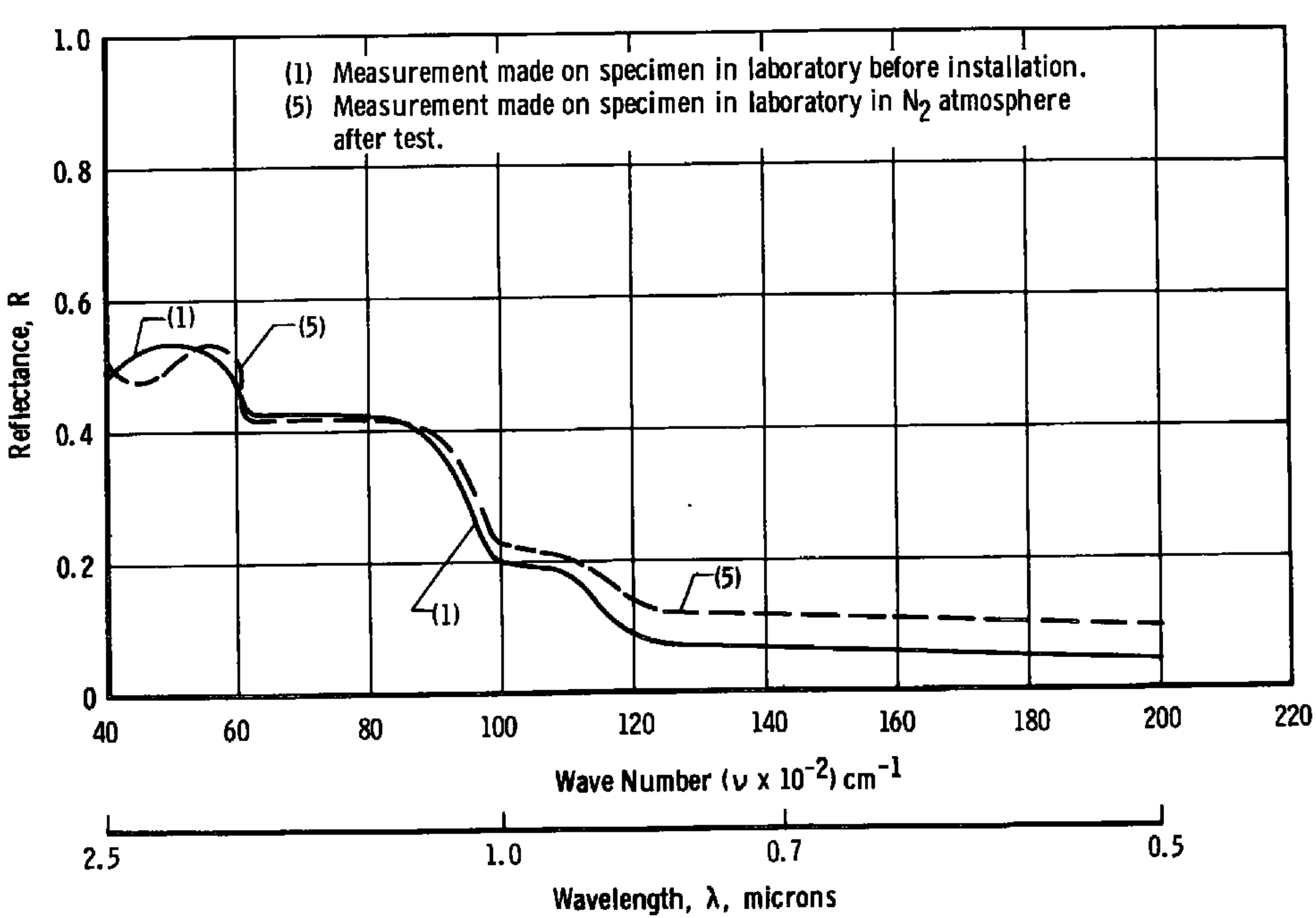

Fig. 95 Test 22—Reflectance Measurements on Specimen, Location S_{13}, Type K

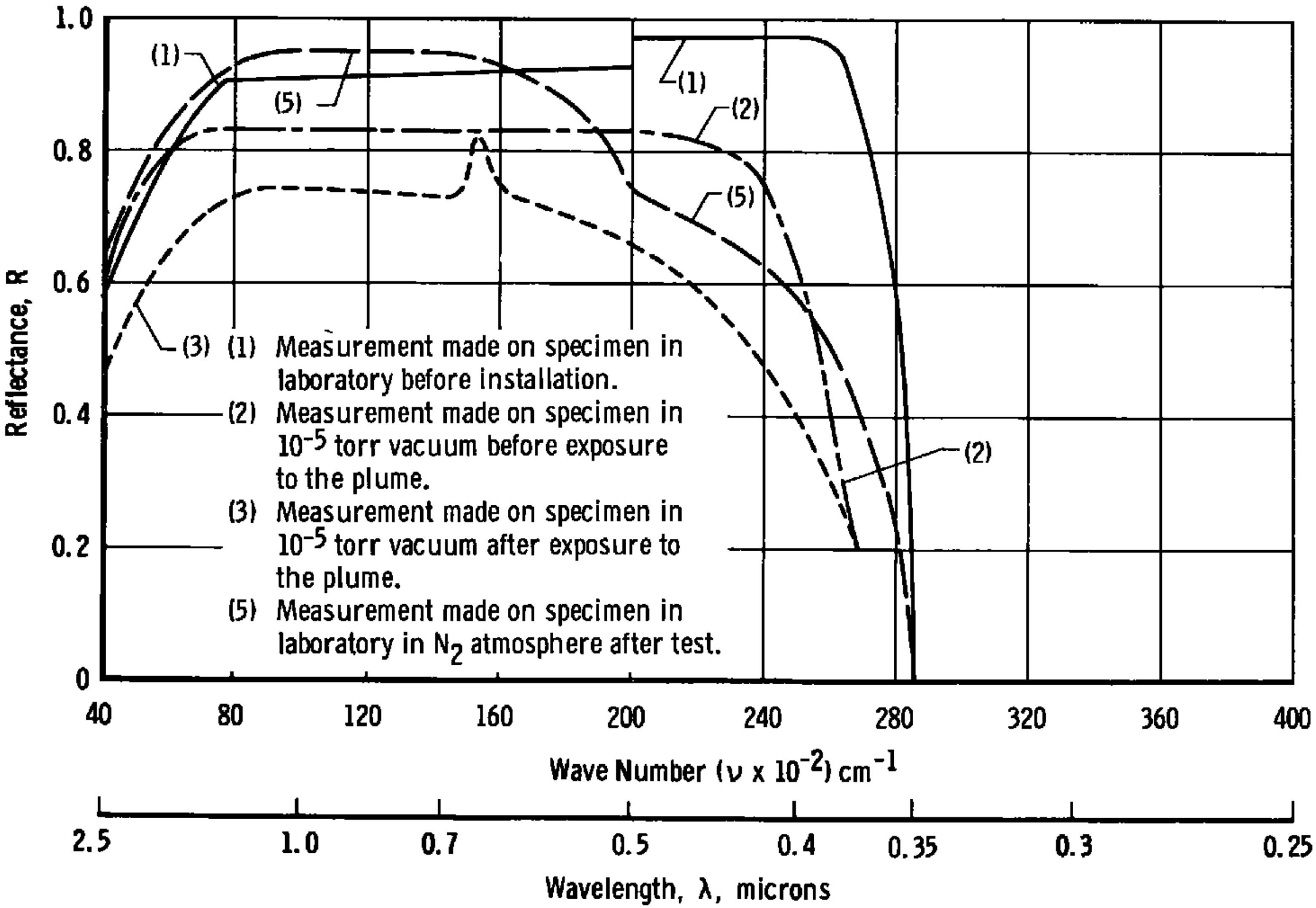

Fig. 96 Test 22—Reflectance Measurements on Specimen, Location S_{15}, Type A

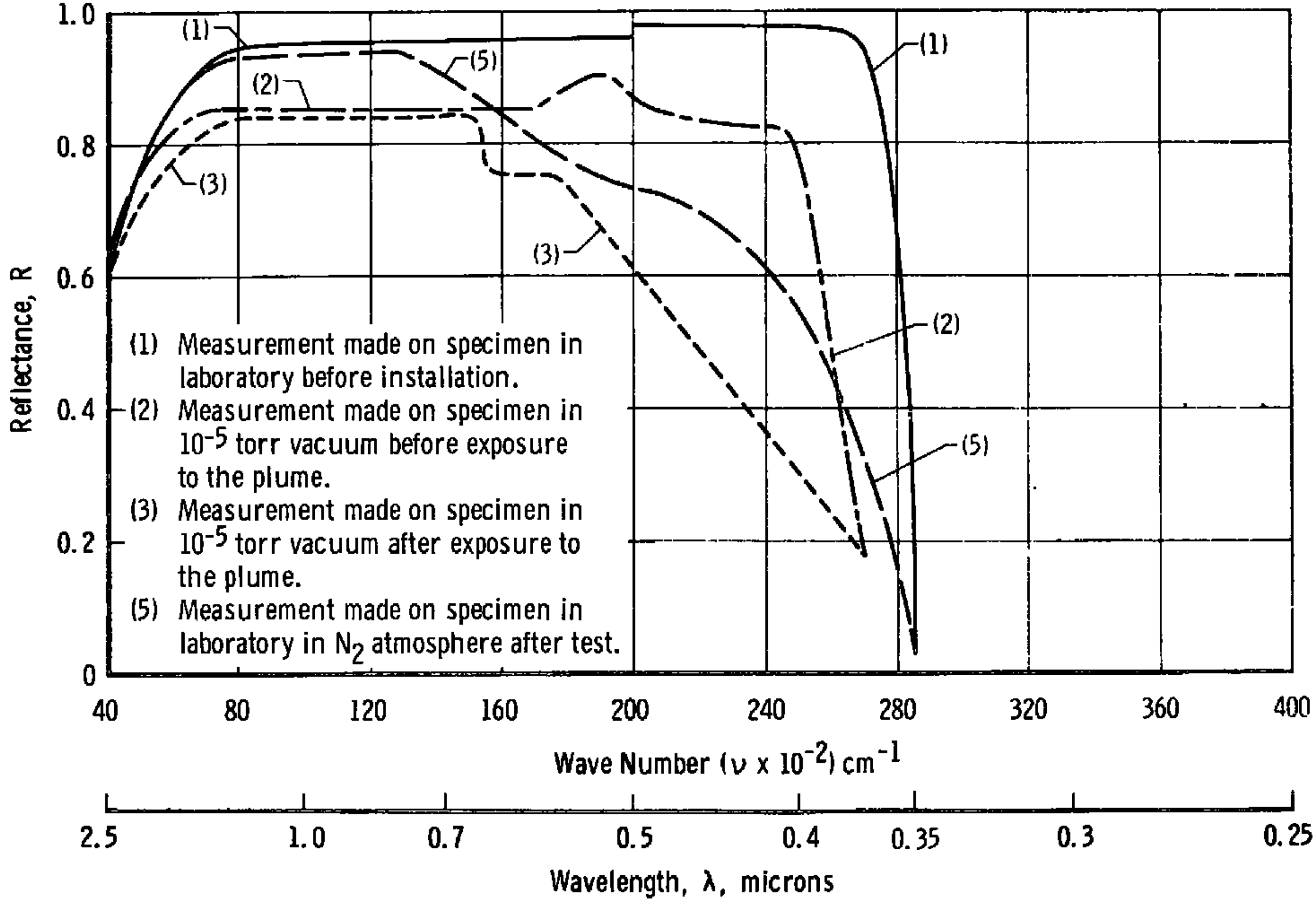

Fig. 97 Test 22—Reflectance Measurements on Specimen, Location S_{16}, Type A

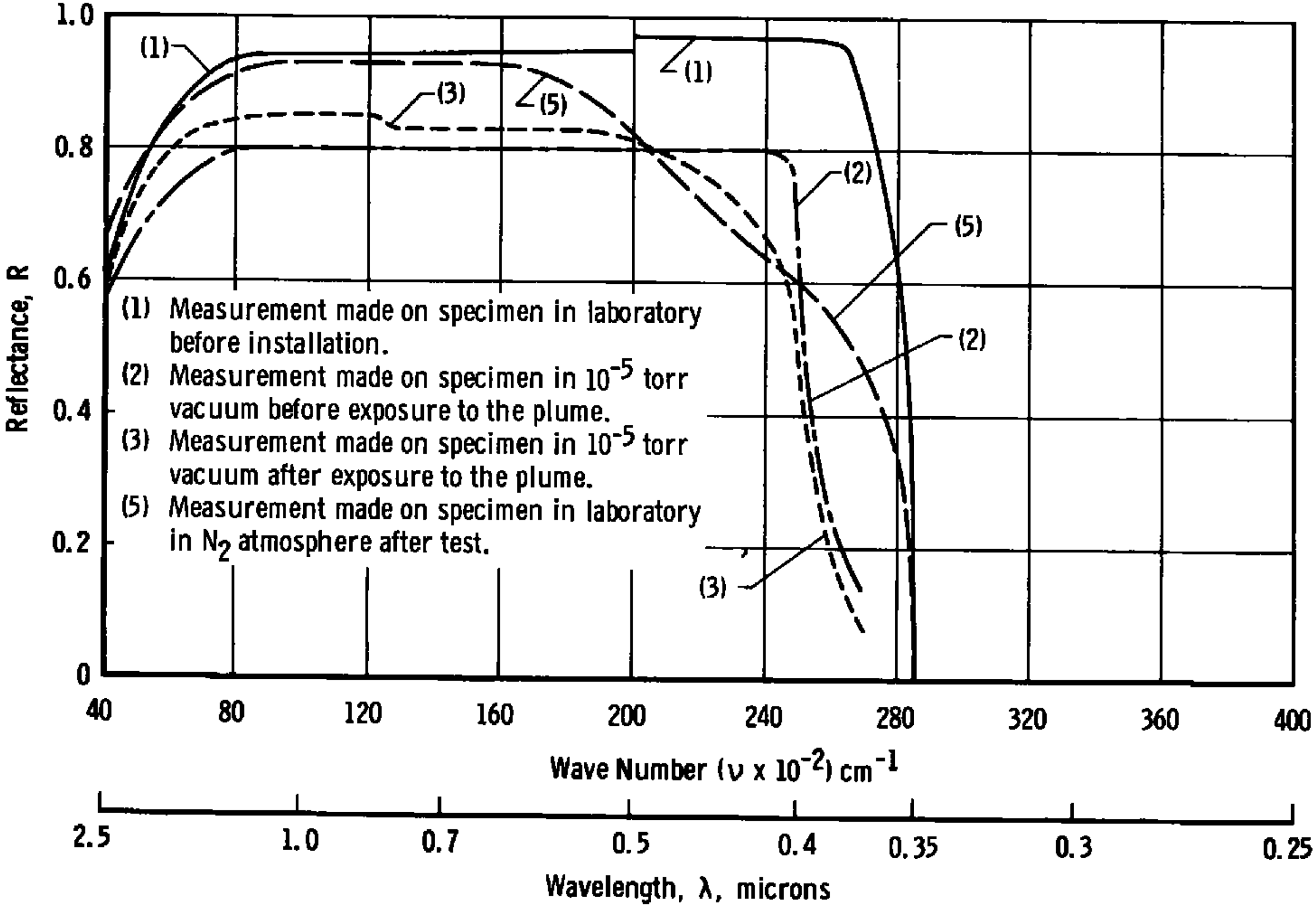

Fig. 98 Test 22—Reflectance Measurements on Specimen, Location S_{19}, Type A

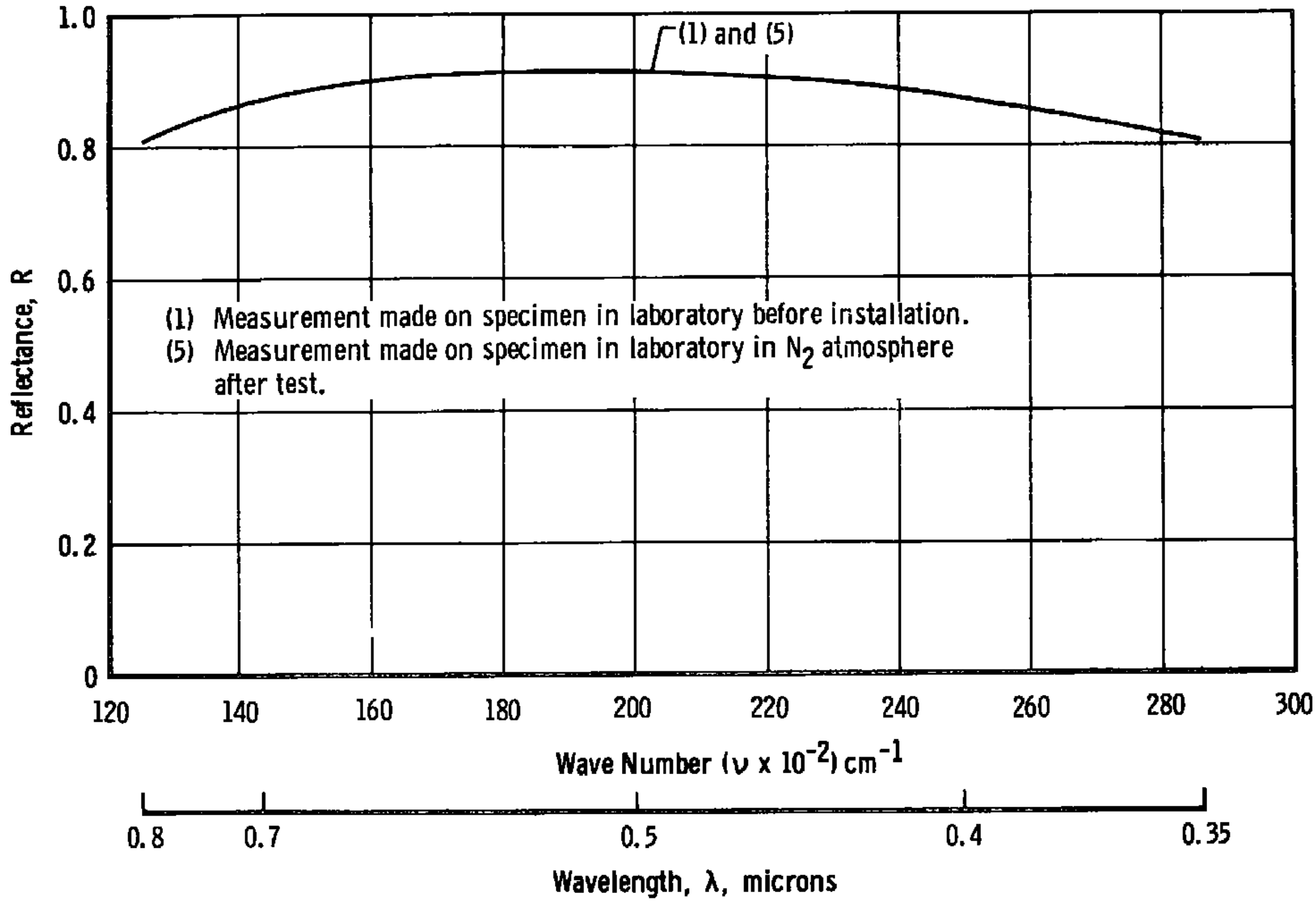

Fig. 99 Test 22—Reflectance Measurements on Specimen, Location C_1, Mirror

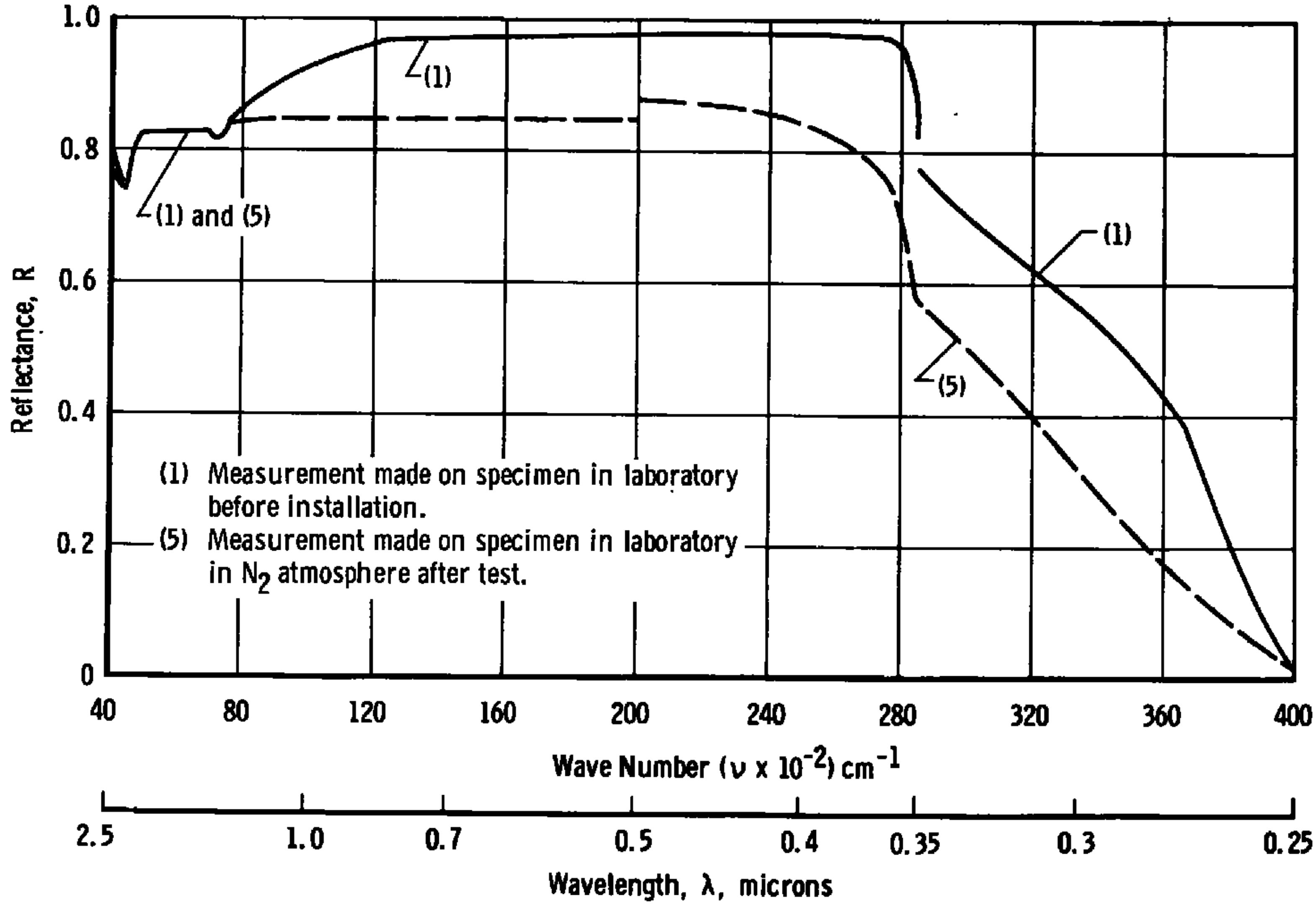

Fig. 100 Test 22—Transmittance Measurements on Specimen, Location V_1, View Port

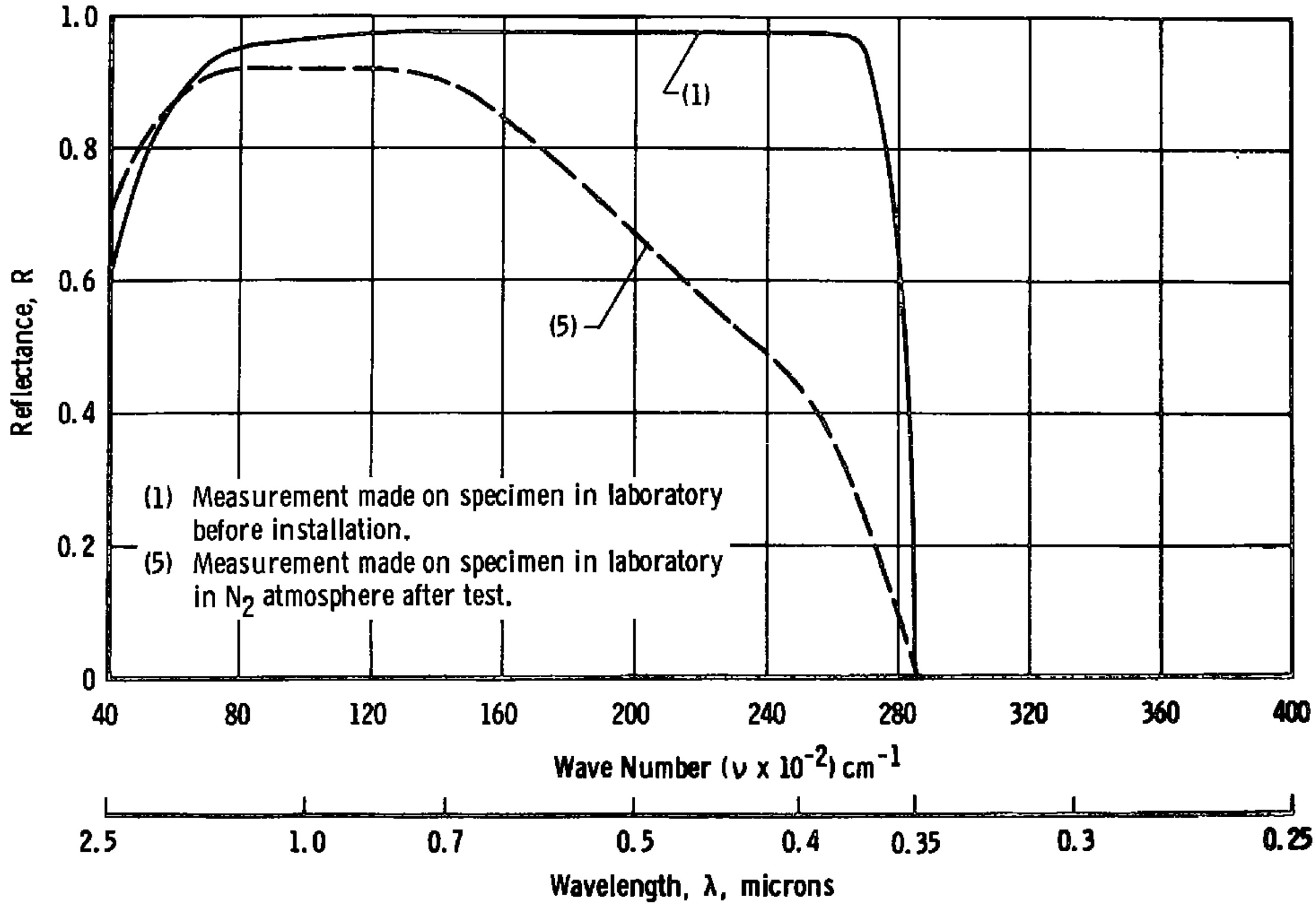

Fig. 101 Test 23—Reflectance Measurements on Specimen, Location H_1, Type A

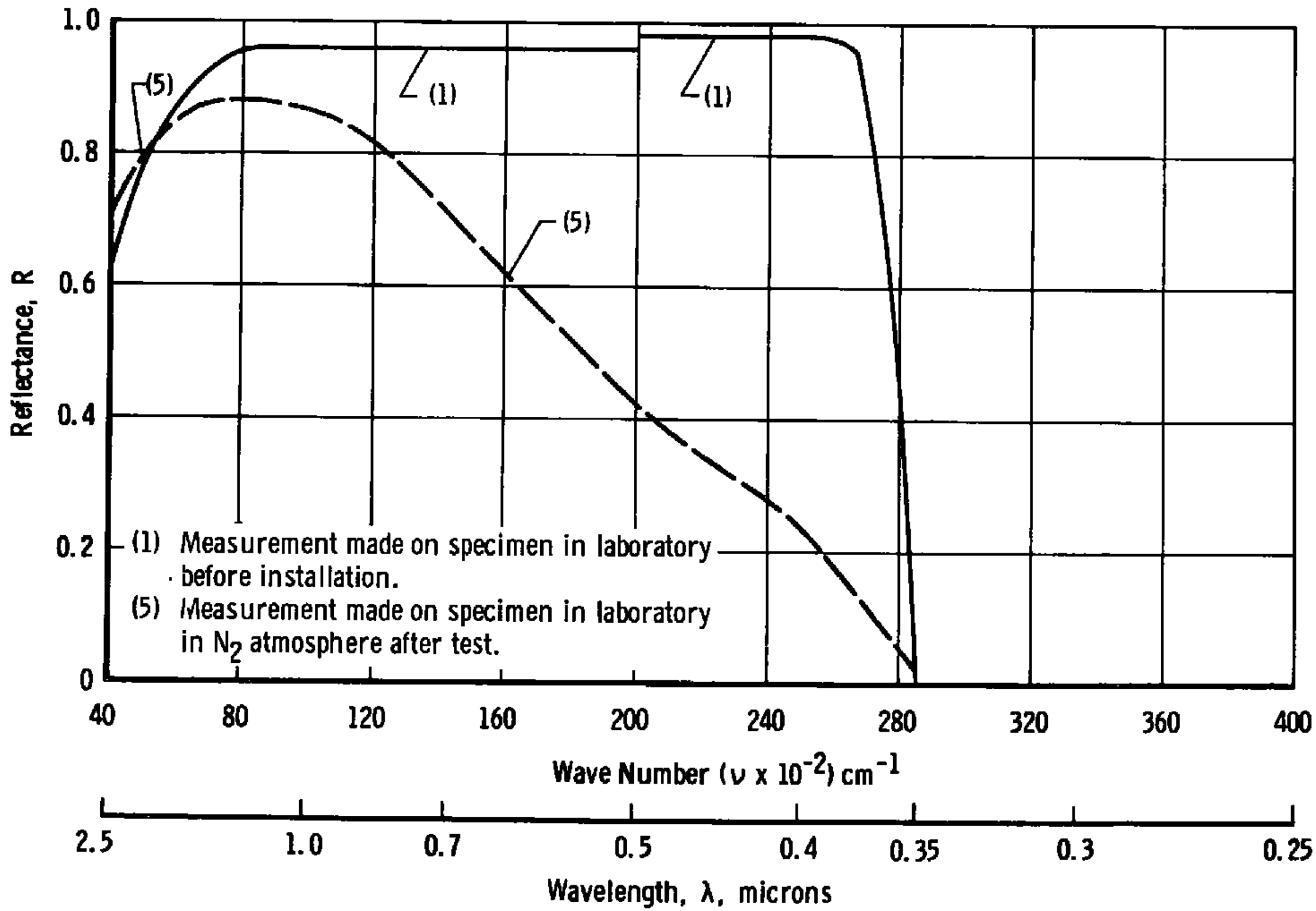

Fig. 102 Test 23—Reflectance Measurements on Specimen, Location S_{12}, Type A

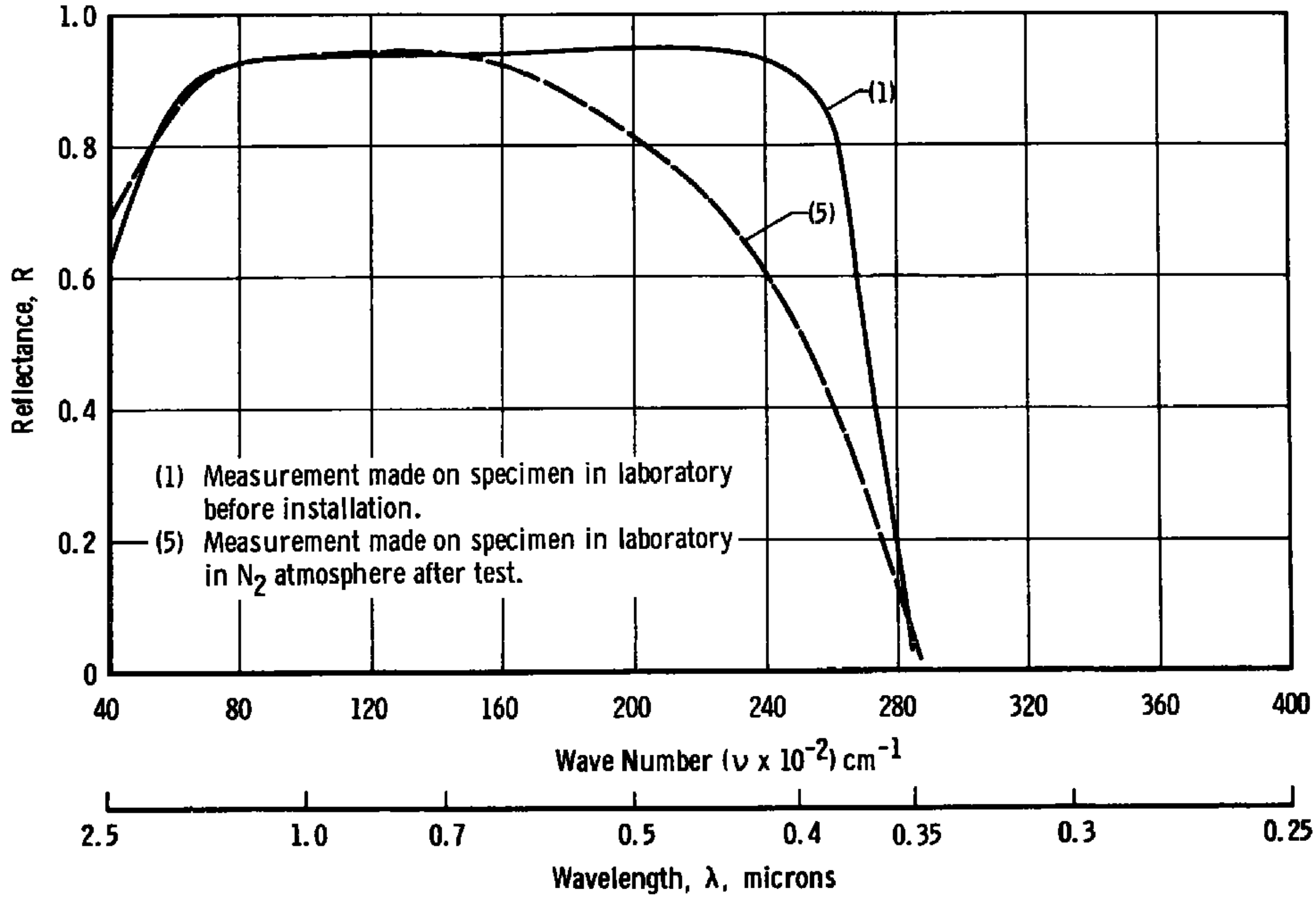

Fig. 103 Test 23—Reflectance Measurements on Specimen, Location S_{13}, Type A

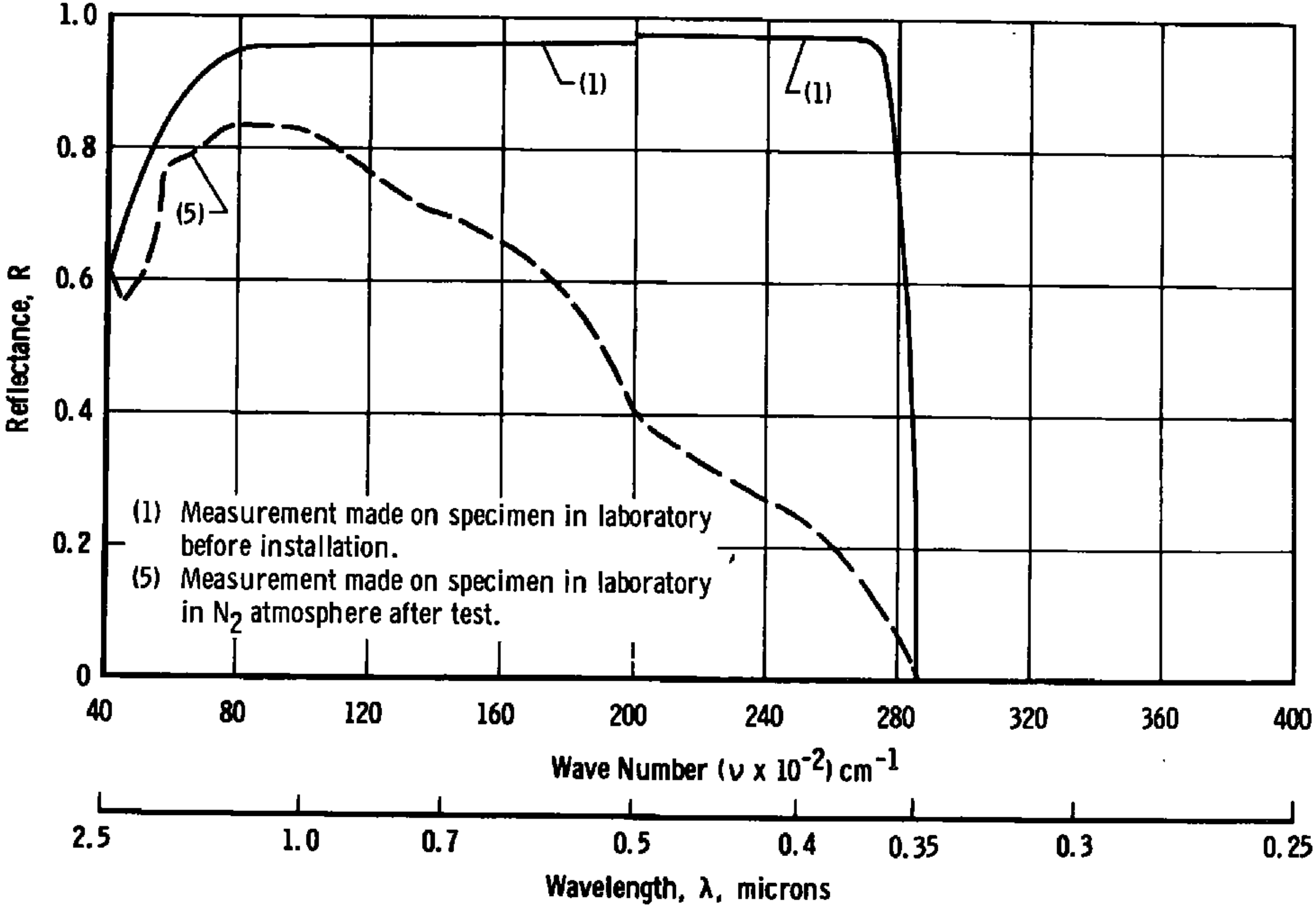

Fig. 104 Test 23—Reflectance Measurements on Specimen, Location S_{15}, Type A

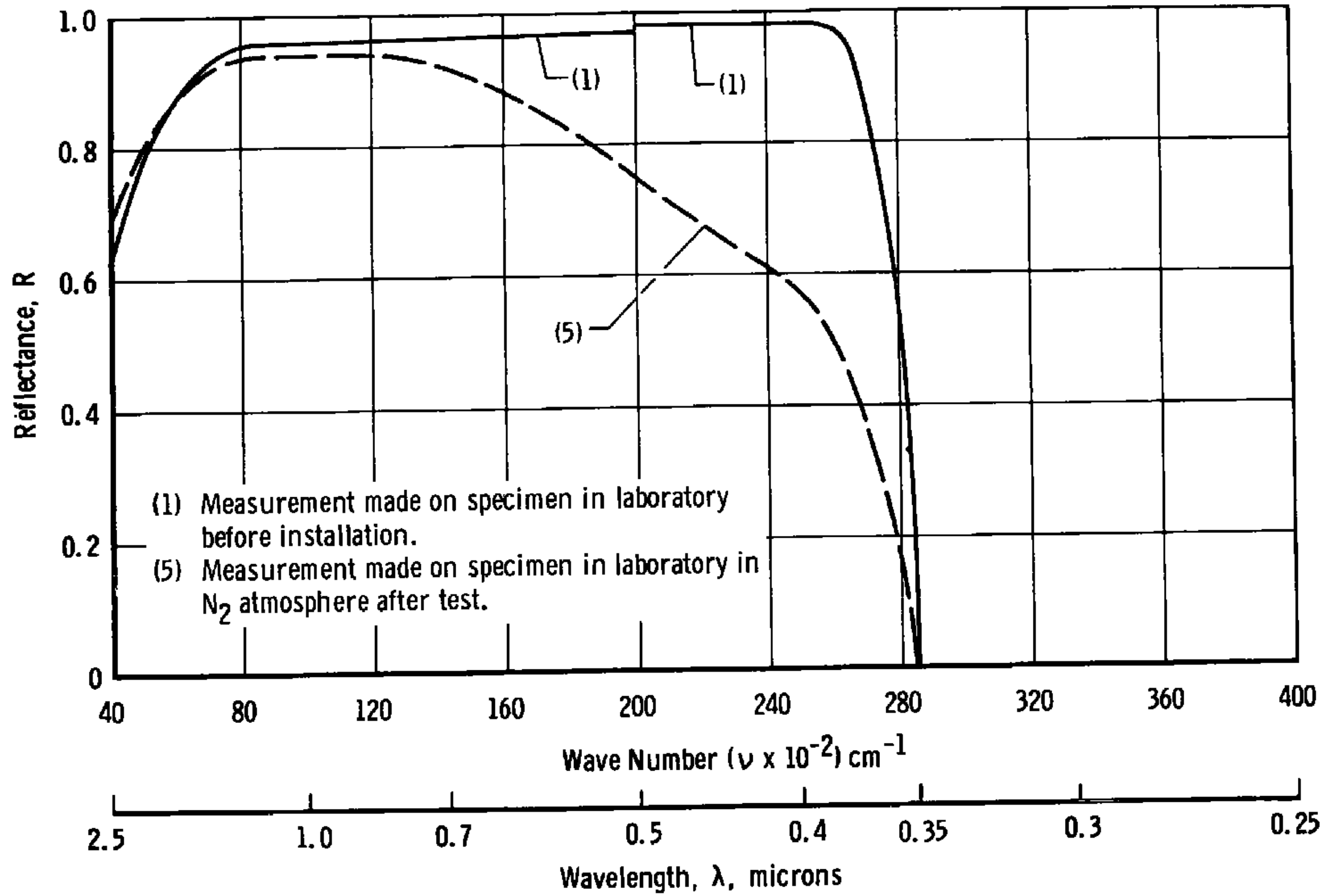

Fig. 105 Test 23—Reflectance Measurements on Specimen, Location S_{16}, Type A

APPENDIX II
TEST LOG

TEST 3

LONGITUDINAL THRUSTER (PULSE-MODE FIRING)

OBJECTIVE: Determine if contamination is produced by the 1-lb thruster in the pulse-mode operation.

RESULTS: Large amounts of contamination produced by thruster. The contamination that accumulated on the thruster exit was blown off onto the test panel.

TEST HARDWARE:
Test Panel 1
Surface Coating Specimens
Mirror and Window Specimens
View Port Specimen
Horizon Sensor Specimen

TEST CONDITIONS: h = 1.14 in., α = 18 deg, P_{ox} = 150 psia, P_F = 125 psia, Altitude = 400,000 ft

Run No.	Run Time, sec	P_c, psia	Specimen Measurement Sequence	Photographic Coverage
	Pulsing Mode (msec)/(msec)/No. of Cycles		Pretest Laboratory Prefire In Situ	
3-1	1000/500/60 1000/50 /10			Black and White High-Speed Motion Pictures
3-2	1000/500/69 1000/50 /10			Colored High-Speed Motion Pictures
3-3	1000/500/60 1000/50 /10		Postfire In Situ	Black and White High-Speed Motion Pictures
3-4	20/3000/300			Black and White High-Speed Motion Pictures
3-5	20/3000/86			Colored High-Speed Motion Pictures
			Sea-Level In Situ Posttest Laboratory	

Test 3

Specimen Location	Type	Pre Lab	In Situ							Post Lab
			Pre	Post 3	Post	Post	Post	Post	Post S. L.	
S1										
S2										
S3										
S4										
S5										
S6	K	R								R
S7	B	R								R
S8	C	R								R
S9	M	R	R	R					R	R
S10										
S11	B	R								R
S12	C	R	R, ϵ	R, ϵ					R	R
S13	A	R								R
S14										
S15	A	R								R
S16	A	R	R, ϵ	R, ϵ					R	R
S17	C	R								R
S18	K	R								R
S19	A	R								R
S20	B	R	R, ϵ	R, ϵ					R	R
S21	B	R								R
S22										
S23										
S24										
S25	M	R	R	R					R	R
S26										
S27										
S28										
H1	H		T	T						T
V1	V		T	T					T	T
H2										
V2										
G1										
G2										
G3										
G4										
G5										
G6										
G7										
G8										
G9										
G10										
G11										
G12										

TEST 4B

LONGITUDINAL THRUSTER (STEADY-STATE FIRING)

OBJECTIVE: Determine if contamination is produced by the 1-lb thruster in the steady-state mode operation. Evaluate the effect of the contamination on the test specimens.

RESULTS: Test aborted after the first two firings. Contamination produced by thruster was less than that of pulse-mode operation.

TEST HARDWARE:
Test Panels 1 and 2
Surface Coating Specimens
Mirror and Window Specimens
View Port Specimen
Horizon Sensor Specimen with Ramp

TEST CONDITIONS: h = 1.14 in., α = 18 deg, P_{ox} = 150 psia,
P_F = 125 psia, Altitude = 400,000 ft

Run No.	Run Time, sec	P_c, psia	Specimen Measurement Sequence	Photographic Coverage
			Pretest Laboratory Prefire In Situ	
4B-1	205	87		Motion Pictures
4B-2	203	87	Postfire In Situ	Motion Pictures of Panel during Warmup
			Posttest Laboratory	

Test 43

Specimen Location	Type	Pre Lab	In Situ: Pre	Post 2	Post	Post	Post	Test	Post S.L.	Post Lab
S1										
S2										
S3										
S4										
S5										
S6										
S7	K	R	R, c	R, c						R
S8	C	R								R
S9										
S10	T	R	R, c	R, c						
S11	A	R	R, c	R, c						R
S12	C	R								R
S13	K	R	R, c	R, c						R
S14	A	R								R
S15	A	R	R, c	R, c						R
S16	A	R	R, c	R, c						R
S17	C	R								R
S18										
S19	B	R	R, c	R, c						R
S20	B	R								R
S21	K	R								R
S22										
S23	W	T	T	T						
S24										
S25										
S26										
S27										
S28										
H1	H		T	T						T
V1	V		T	T						T
H2										
V2										
G1										
G2										
G3	M	R	R							
G4	M	R	R							
G5										
G6										
G7	W		T							
G8	W	T								
G9	M	T	T	T						
G10										
G11										
G12										

TEST 4C

LONGITUDINAL THRUSTER (STEADY-STATE FIRING)

OBJECTIVE: Same as test 4B

RESULTS: Contamination was less than that of pulse-mode operation. Contamination was deposited on test panel and specimens.

TEST HARDWARE: Test Panels 1 and 2
Surface Coating Specimens
Mirror and Window Specimens
View Port Specimen
Horizon Sensor Specimen with Ramp

TEST CONDITIONS: h = 1.14 in., α = 18 deg, P_{ox} = 150 psia,
P_F = 125 psia, Altitude = 400,000 ft

Run No.	Run Time, sec	P_c, psia	Specimen Measurement Sequence	Photographic Coverage
			Pretest Laboratory Prefire In Situ	
4C-1	205	90		
4C-2	145		Postfire In Situ	
4C-3	205			
4C-4	205		Postfire In Situ	
4C-5	205			
4C-6	205			
4C-7	205		Postfire In Situ	
4C-8	205		Postfire In Situ	
4C-9	205	90		Motion Pictures during Warmup
			Sea-Level In Situ Posttest Laboratory	

Test 4C

Specimen Location	Type	Pre Lab	In Situ Pre	In Situ Post 2	In Situ Post 4	In Situ Post 7	In Situ Post 8	In Situ Post	In Situ Post S.I.	Post Lab
S1										
S2										
S3										
S4										
S5										
S6	B	R								R
S7	K	R	R, ε	R, ε	R, ε	R, ε			R	R
S8	C	R							· —	R
S9										
S10	T_1	R	R, ε	R, ε		R, ε			R	R
S11	A	R	R, ε	R, ε	R, ε	R, ε			R	R
S12	C	R								R
S13	K	R	R, ε	R, ε	R, ε	R, ε	R, ε		R	R
S14	A	R								R
S15	A	R	R, ε	R, ε	R, ε	R, ε	R, ε		R	R
S16	A	R	R, ε	R, ε	R, ε	R, ε			R	R
S17	C	R								R
S18	T_2	R	R, ε	R, ε		R, ε	R, ε		R	R
S19	B	R	R, ε	R, ε	R, ε	R, ε			R	R
S20	B	R								R
S21	K	R								R
S22										
S23	W	T	T	T		T			T	T
S24										
S25										
S26										
S27										
S28										
H1	H									T
V1	V		T	T	T	T	T		T	T
H2										
V2										
G1										
G2										
G3	M	R	R		R	R			R	R
G4	M	R	R		R	R			R	R
G5										
G6										
G7	W	T	T		T	T			T	T
G8	W	T								T
G9	M	R	R		R	R			R	R
G10										
G11										
G12										
Control	W	T								R
Control	W	T								T

TEST 5A

LONGITUDINAL THRUSTER (STEADY-STATE FIRING)

OBJECTIVE: Evaluate effect of fence (Fig. II-1) to shield specimens located at V_1, H_1, S_{14}, G_8, and G_3.

RESULTS: Presence of fence did not effectively shield the above specimen locations. Aborted test after firing 5A-3 because of chamber leak.

TEST HARDWARE: Test Panels 1 and 2
Surface Coating Specimens
Mirror and Window Specimens
View Port Specimen
Horizon Sensor Specimen with Ramp
3/4-in.-High Fence Downstream from Thruster

TEST CONDITIONS: h = 1.14 in., α = 18 deg, P_{ox} = 150 psia,
P_F = 125 psia, Altitude = 400,000 ft

Run No.	Run Time, sec	P_c, psia	Specimen Measurement Sequence	Photographic Coverage
			Pretest Laboratory	None
			Prefire In Situ	
5A-1	205	90		
5A-2	205	90	Postfire In Situ	
5A-3	205	90		

Test 5A

Specimen Location	Type	Pre Lab	In Situ Pre	Post 2	Post	Post	Post	Post	Post S.I.	Post Lab
S1										
S2										
S3										
S4										
S5										
S6	B	R								
S7	K	R	R, c	R, c						
S8	C	R								
S9										
S10	M	R	R	R						
S11	C	R								
S12	C	R	R, ε	R, ε						
S13	K	R								
S14	A	R								
S15	J	R	R, ε	R, ε						
S16	J	R	R, ε	R, ε						
S17	C	R								
S18	B	R	R	R, ε						
S19										
S20	B	R	R, ε	R, ε						
S21	K	R								
S22										
S23	W	T	T	T						
S24										
S25										
S26										
S27										
S28										
H1	H									
V1	V		T	T						
H2										
V2										
G1										
G2										
G3	M	R	R	R						
G4	M	R	R							
G5										
G6										
G7	W	T	T	T						
G8	W	T								
G9	M	R	R							
G10										
G11										
G12										

TEST 5B

LONGITUDINAL THRUSTER (STEADY-STATE FIRING)

OBJECTIVE: Same as test 5A

RESULTS: Fence did not reduce the amount of contamination deposited on specimens located at H_1, V_1, S_{14}, G_8, and G_3.

TEST HARDWARE: Test Panels 1 and 2
Surface Coating Specimens
Mirror and Window Specimens
View Port Specimen
Horizon Sensor Specimen with Ramp
3/4-in.-High Fence Downstream from Thruster

TEST CONDITIONS: h = 1.14 in., α = 18 deg, P_{ox} = 150 psia, P_F = 125 psia, Altitude = 400,000 ft

Run No.	Run Time, sec	P_c, psia	Specimen Measurement Sequence	Photographic Coverage
			Pretest Laboratory	None
			Prefire In Situ	
5B-1	83	90		
5B-2	81			
5B-3	41			
5B-4	205		Postfire In Situ	
5B-5	205			
5B-6	205		Postfire In Situ	
5B-7	205			
5B-8	205			
5B-9	205		Postfire In Situ	
5B-10	205			
5B-11	205	90	Postfire In Situ	
			Sea-Level In Situ	
			Posttest Laboratory	

Test 5B

Specimen Location	Type	Pre Lab	In Situ Pre	Post 4	Post 6	Post 9	Post 11	Post	Post S.L.	Post Lab
S1										
S2										
S3										
S4										
S5										
S6	B	R								R
S7	K	R	R	R	R	R			R	R
S8	D	R								R
S9										
S10	M	R	R	R		R			R	R
S11	A	R								R
S12	C	R	R	R	R	R	R		R	R
S13	K	R								R
S14	A	R								R
S15	J	R	R	R			R		R	R
S16	J	R	R	R	R	R	R		R	R
S17	C	R								R
S18	B	R	R	R	R	R	R		R	R
S19	D	R								R
S20	B	R	R	R			R		R	R
S21	K	R								R
S22										
S23	W	T	T	T		T	T		T	T
S24										
S25										
S26										
S27										
S28										
H1	H									T
V1	V		T	T	T	T	T		T	T
H2										
V2										
G1										
G2										
G3	M	R	R		H		R		R	R
G4	M	R	R		R		R		R	R
G5										
G6										
G7	W	T	T		T		T		T	T
G8										
G9	M	R	R		R		R		R	R
G10										
G11										
G12										

TEST 6

LONGITUDINAL THRUSTER (STEADY-STATE AND PULSE-MODE FIRING)

OBJECTIVE: Determine effect of plume on an operational monopole directional antenna (Fig. II-1).

RESULTS: No appreciable effect on antenna performance.
Plume ablated the antenna's Teflon cover. Large amounts of contamination accumulated on antenna in the thruster pulse-mode operation.

TEST HARDWARE: Test Panel 1
Monopole Directional Antenna and
Ground Plate (Was Operated)

TEST CONDITIONS: h = 1.14 in., α = 18 deg, P_{ox} = 150 psia,
P_F = 125 psia, Altitude = 400,000 ft

Run No.	Run Time, sec	P_c, psia	Specimen Measurement Sequence	Photographic Coverage
6-1	20/500/1000		None	
6-2	20/1000/1000			Motion Pictures
6-3	50/500/400			Motion Pictures
6-4	50/1000/800			Motion Pictures
6-5	205	90		Motion Pictures
6-6	205	90		Motion Pictures
6-7	100/500/200			Motion Pictures
6-8	100/1000/200			
6-9	1000/500/100			Motion Pictures
6-10	1000/1000/100			Motion Pictures
6-11	108	90		
6-12	300	90		Color Stills
6-13	0			
6-14	100	90		Color Stills

TEST 13

LONGITUDINAL THRUSTER (STEADY-STATE FIRING)

OBJECTIVE: Investigate effectiveness of 1.5-in.-high by 29-in.-long fence (Fig. II-1) to shield specimens on panel 2. Determine effect of heating panels 1 and 2.

RESULTS: Fence shielded specimens on panel 2 satisfactorily. Contamination on the panels was reduced by heating panels to 105°F.

TEST HARDWARE: Test Panels 1 and 2
Surface Coating Specimens
Mirror and Window Specimens
View Port Specimen
Horizon Sensor Specimen
Cover on Test Panel 2
Startracker with Window Specimen
1.5-in.-High Fence between Panels 1 and 2

TEST CONDITIONS: h = 1.14 in., α = 18 deg, P_{ox} = 150 psia, P_F = 125 psia, Altitude = 400,000 ft

Run No.	Run Time, sec	P_c, psia	Specimen Measurement Sequence	Photographic Coverage
Heated Samples to 105°F and Kept Lights On during Firings to Heat Panel for First Four Runs			Pretest Laboratory Prefire In Situ	
13-1	205	89		Motion Pictures
13-2	↓	↓		↓
13-3	↓	↓		↓
13-4	205	89	Postfire In Situ	↓
Maintain Samples at 70°F and Lights Off for Remaining Runs				↓
13-5	205	89		↓
13-6	↓	↓		↓
13-7	↓	↓		↓
13-8	205	89	Postfire In Situ	↓
			Sea-Level In Situ	
			Posttest Laboratory	

Test 13

Specimen Location	Type	Pre Lab	In Situ Pre	Post 4	Post 8	Post	Post	Post	Post S.T.	Post Lab
S1										
S2										
S3										
S4										
S5										
S6	B	R								R
S7	K	R	R, ε	R, ε	R, ε				R	R
S8	D									
S9										
S10	M	R								R
S11	A	R	R, ε	R, ε	R, ε				R	R
S12	B	R	R, ε	R, ε	R, ε					R
S13	K									R
S14	A	R								R
S15	A		R, ε	R, ε	R, ε					R
S16	A	R	R, ε	R, ε	R, ε					R
S17	B	R								R
S18	B	R								R
S19	D									
S20	B	R	R, ε	R, ε	R, ε					R
S21	K	R								R
S22										
S23										
S24										
S25										
S26										
S27										
S28										
H1	H									T
V1	V		T	T	T				T	T
H2	Emcal									
V2										
G1										
G2	M	R								R
G3	M	R								R
G4										
G5										
G6										
G7	W	T								T
G8	W	T								T
G9	M	R								R
G10										
G11										
G12										
Startracker	W	T								T

TEST 14

LONGITUDINAL THRUSTER (STEADY-STATE FIRING)

OBJECTIVE: Evaluate amount of contamination covered cavity (Fig. II-1), startracker sled, and flush startracker.

RESULTS: Large amounts of contamination was deposited on the above hardware. MMH dumped on test panel because of N_2O_4 propellant line freezing during firing 14-6.

TEST HARDWARE:
Test Panels 1 and 2
Surface Coating Specimens
Mirror and Window Specimens
View Port Specimen
Horizon Sensor Specimen with Ramp
Cover on Test Panel 2
Startracker (Flush) with T_2 Specimen
Bob Sled with Window Specimen

TEST CONDITIONS: h = 1.14 in., α = 18 deg, P_{ox} = 150 psia, P_F = 125 psia, Altitude = 400,000 ft

Run No.	Run Time, sec	P_c, psia	Specimen Measurement Sequence	Photographic Coverage
			Pretest Laboratory Prefire In Situ	
14-1	205	90		Motion Pictures
14-2			Postfire In Situ	
14-3				
14-4			Postfire In Situ	
14-5				
14-6				
14-7				
14-8				
14-9	205	90	Postfire In Situ	Motion Pictures
			Sea-Level In Situ	
			Posttest Laboratory	

Test 14

Specimen Location	Type	Pre Lab	In Situ Pre	Post 2	Post 4	Post 9	Post	Post	Post S.L.	Post Lab
S1										
S2										
S3										
S4										
S5										
S6	B	R								R
S7	K	R	R, ε	R, ε	R, ε	R, ε			R	R
S8	D									
S9										
S10	T_1	R	R, ε	R, ε	R, ε	R, ε			R	R
S11	A	R	R, ε	R, ε	R, ε	R, ε			R	R
S12	D									R
S13	K	R								R
S14	A	R								R
S15	A	R	R, ε	R, ε	R, ε	R, ε			R	R
S16	A	R	R, ε	R, ε	R, ε	R, ε			R	R
S17										
S18	T_2	R	R, ε	R, ε	R, ε	R, ε			R	R
S19	D									
S20										
S21	K									
S22										
S23										
S24										
S25										
S26										
S27										
S28										
H1	H									T
V1	V		T	T	T	T			T	T
H2	Emcal									
V2										
G1										
G2	W	T								T
G3	M	R								R
G4	M	R								R
G5										
G6										
G7										
G8	W	T								T
G9										
G10										
G11										
G12										
Startracker	T_2	R	R, ε	R, ε	R, ε	R, ε			R	R
Bobsled	W	T	T	T	T	T			T	T

TEST 15

LONGITUDINAL THRUSTER (STEADY-STATE FIRING)

OBJECTIVE: Evaluate effect of contamination on short covered cavity and thermal coating cube.

RESULTS: No noticeable contamination on short covered cavity and thermal coating cube. Figure 78 shows erosion of specimen on cube because of plume impingement.

TEST HARDWARE:
Test Panels 1 and 2
Surface Coating Specimens
Mirror and Window Specimens
View Port Specimen
Horizon Sensor Specimen
Short Cavity with Cover on Test Panel 2
Cube with T_1 Specimen in S_{14}

TEST CONDITIONS: h = 1.14 in., α = 18 deg, P_{OX} = 150 psia, P_F = 125 psia, Altitude = 400,000 ft

Run No.	Run Time, sec	P_c, psia	Specimen Measurement Sequence	Photographic Coverage
			Pretest Laboratory	
			Prefire In Situ	
15-1	205	90		Motion Pictures
15-2	↓	↓	Postfire In Situ	↓
15-3				
15-4			Postfire In Situ	
15-5				
15-6				
15-7			Postfire In Situ	
15-8				
15-9	205	90	Postfire In Situ	Motion Pictures
			Sea-Level In Situ	
			Posttest Laboratory	

Test 15

Specimen Location	Type	Pre Lab	In Situ							Post Lab
			Pre	Post 2	Post 4	Post 7	Post 9	Post	Post S.L.	
S1										
S2										
S3										
S4										
S5										
S6	B	R								R
S7	K	R	ε	ε	ε	ε	ε			R
S8										
S9										
S10	Heat Flux Probe									
S11	A	?	ε	ε	ε	ε	ε			
S12										
S13	K		R, ε	R, ε	R, ε	R, ε	R, ε		R	R
S14	Cube T_1									
S15	A	R	ε	ε	ε	ε	ε			R
S16	A	R	R, ε	R, ε	R, ε	R, ε	R, ε		R	R
S17										
S18	W	T	T	T	T	T	T		T	T
S19	B	R	R, ε	R, ε	R, ε	R, ε	R, ε		R	R
S20										
S21	K	R								R
S22										
S23										
S24										
S25										
S26										
S27										
S28										
H1										
V1	V		T	T	T	T	T		T	T
H2	Emcal									
V2										
C1	M	R								R
C2	W	T								T
C3	M	R								R
C4	W	T								T
G5										
G6										
G7										
G8										
G9										
G10										
G11										
G12										

TEST 20

LONGITUDINAL THRUSTER (STEADY-STATE FIRING)

OBJECTIVE: Evaluate amount of contamination on heated horizon sensor hood, H_1.

RESULTS: Horizon sensor hood was contaminated when test chamber V_1 pressure increased to 10^{-1} torr. Only the ramp of the horizon sensor hood was contaminated from the plume.

TEST HARDWARE:
Test Panels 1 and 2
Surface Coating Specimens
Mirrow and Window Specimens
View Port Specimen
Horizon Sensor Specimen with Ramp
Cover on Test Panel 2
Startracker (Flush) with Mirror Specimen
Bobsled with Window Specimen

TEST CONDITIONS: h = 1.14 in., α = 18 deg, P_{ox} = 150 psia, P_F = 125 psia, Altitude = 400,000 ft

Run No.	Run Time, sec	P_c, psia	Specimen Measurement Sequence	Photographic Coverage
			Pretest Laboratory	
			Prefire In Situ	
20-1	205	89		Motion Pictures
20-2			Postfire In Situ	
20-3				
20-4			Postfire In Situ	
20-5				
20-6				
20-7			Postfire In Situ	
20-8				
20-9	205	89	Postfire In Situ	Motion Pictures
			Sea-Level In Situ	
			Posttest Laboratory	

Test 20

Specimen Location	Type	Pre Lab	In Situ Pre	Post 2	Post 4	Post 7	Post 9	Post	Post S. L.	Post Lab
S1										
S2										
S3										
S4										
S5										
S6	A	R								R
S7	K	R	R, ε	R, ε	R, ε	R, ε	R, ε		R	R
S8	D									
S9										
S10										
S11	A	R	R, ε	R, ε	R, ε	R, ε	R, ε		R	R
S12	D									
S13	K	R								R
S14										
S15	A	R	R, ε	R, ε	R, ε	R, ε	R, ε		R	R
S16	A	R	R, ε	R, ε	R, ε	R, ε	R, ε		R	R
S17	A	R								R
S18										
S19	A	R	R, ε	R, ε	R, ε	R, ε	R, ε		R	R
S20	D									
S21	K	R								R
S22										
S23	W	T	T	T	T	T	T		T	T
S24										
S25										
S26										
S27	Emcal									
S28										
H1	H		T	T	T	T	T		T	T
V1	V	T								T
H2										
V2										
G1										
G2	M	R								R
G3	M	R								R
G4	M	R								R
G5										
G6										
G7	W	T								T
G8	W	T								T
G9	M	R								R
G10										
G11										
G12										
Startracker	M	R	R	R	R	R	R		R	R
Bossled	W	T	T	T	T	T	T		T	T

TEST 21

LONGITUDINAL THRUSTER (STEADY-STATE FIRING)

OBJECTIVE: Evaluate amount of contamination on unheated horizon sensor hood, H, and heated panel.

RESULTS: Same as test 20.

TEST HARDWARE: Test Panels 1 and 2
Surface Coating Specimens
Mirror and Window Specimens
View Port Specimen
Horizon Sensor with Ramp
Short Cavity with Cover on Test Panel 2

TEST CONDITIONS: h = 1.14 in., α = 18 deg, P_{ox} = 150 psia, P_F = 125 psia, Altitude = 400,000 ft

Run No.	Run Time, sec	P_c, psia	Specimen Measurement Sequence	Photographic Coverage
			Pretest Laboratory Prefire In Situ	
Heated Panel to 100°F and Maintained during All Runs				
21-1	205	89		Motion Pictures
21-2	↓	↓	Postfire In Situ	↓
21-3				
21-4			Postfire In Situ	
21-5				
21-6				
21-7			Postfire In Situ	
21-8	↓	↓		↓
21-9	205	89	Postfire In Situ	Motion Pictures
			Sea-Level In Situ	
			Posttest Laboratory	

Test 21

Specimen Location	Type	Pre Lab	In Situ Pre	In Situ Post 2	In Situ Post 4	In Situ Post 7	In Situ Post 9	In Situ Post	In Situ Post S. L.	Post Lab
S1										
S2										
S3										
S4										
S5										
S6	A	R								R
S7	K	R	R, ε	R, ε	R, ε	R, ε	R, ε		R	R
S8	D									
S9										
S10										
S11	A	R	R, ε	R, ε	R, ε	R, ε	R, ε		R	R
S12	D									
S13	K	R								R
S14										
S15	A	R	R, ε	R, ε	R, ε	R, ε	R, ε		R	R
S16	A	R	R, ε	R, ε	R, ε	R, ε	R, ε		R	R
S17	A	R								R
S18										
S19	A	R	R, ε	R, ε	R, ε	R, ε	R, ε		R	R
S20	D									
S21	K	R								R
S22										
S23	W	T	T	T	T	T	T		T	T
S24										
S25										
S26										
S27	Emcal									
S28										
H1	H		T	T	T	T	T		T	T
V1	V	T								T
H2										
V2										
C1	M	R								R
C2	W	T								T
C3	M	R								R
C4	W	T								T
G5										
G5										
G7										
G8										
G9										
G10										
G11										
G12										

TEST 22

LONGITUDINAL THRUSTER (STEADY-STATE FIRING)

OBJECTIVE: Evaluate the amount of contamination on covered short cavity with additional baffle.

RESULTS: There was not any noticeable contamination on the covered short cavity with additional baffle.

TEST HARDWARE: Test Panels 1 and 2
Surface Coating Specimens
Mirror and Window Specimens
View Port Specimen
Short Cavity with Cover and Additional Baffle on Test Panel 2
Cube at S_{10}

TEST CONDITIONS: h = 1.14 in., α = 18 deg, P_{ox} = 150 psia, P_F = 125 psia, Altitude = 400,000 ft

Run No.	Run Time, sec	P_c, psia	Specimen Measurement Sequence	Photographic Coverage
			Pretest Laboratory	
			Prefire In Situ	
22-1	205	56		Motion Pictures
22-2	↓	90	Postfire In Situ	↓
22-3	↓	↓		↓
22-4	↓	↓	Postfire In Situ	↓
22-5	↓	↓		↓
22-6	↓	↓		↓
22-7	↓	↓	Postfire In Situ	↓
22-8	↓	↓		↓
22-9	205	90	Postfire In Situ	Motion Pictures
			Sea-Level In Situ	
			Posttest Laboratory	

Test 22

Specimen Location	Type	Pre Lab	In Situ Pre	Post 2	Post 4	Post 7	Post 9	Post	Post S.L.	Post Lab
S1										
S2										
S3										
S4										
S5										
S6	A	R								R
S7	K	R	ε	ε	ε	ε	ε			R
S8	D									
S9										
S10	Cube with calorimeter									
S11	A	R	ε	ε	ε	ε	ε			R
S12	D									
S13	K	R								R
S14	Heat flux probe									
S15	A	R	R, ε	R, ε	R, ε	R, ε	R, ε		R	R
S16	A	R	R, ε	R, ε	R, ε	R, ε	R, ε		R	R
S17	A	R								R
S18										
S19	A	R	R, ε	R, ε	R, ε	R, ε	R, ε		R	R
S20	D									
S21	K	R								R
S22										
S23	W	T	T	T	T	T	T		T	T
S24										
S25										
S26										
S27	Emcal									
S28										
H1										
V1	V	T	T	T	T	T	T		T	T
H2										
V2										
C1	M	R								R
C2	W	T								T
C3	M	R								R
C4	W	T								T
G5										
G6										
G7										
G8										
G9										
G10										
G11										
G12										

TEST 23

LONGITUDINAL THRUSTER (STEADY-STATE FIRING)

OBJECTIVE: Evaluate effect of low altitude on contamination ejected from thruster.

RESULTS: Contamination observed along and near centerline of thruster and on panel 2.

TEST HARDWARE: Test Panel 1
Surface Coating Specimens
Mirror and Window Specimens
View Port Specimen

TEST CONDITIONS: h = 1.14 in., α = 18 deg, P_{ox} = 150 psia,
P_F = 125 psia, Altitude = 250,000 ft

Run No.	Run Time, sec	P_c, psia	Specimen Measurement Sequence	Photographic Coverage
			Pretest Laboratory	
23-1	205	90		Motion Pictures
23-2	↓	↓		↓
23-3				
23-4				
23-5				
23-6				
23-7				
23-8	205			
23-9	500	90		Motion Pictures
			Posttest Laboratory	

Test 23

Specimen Location	Type	Pre Lab	In Situ Pre	Post	Post	Post	Post	Post	Post S.L.	Post Lab
S1										
S2										
S3										
S4										
S5										
S6										
S7										
S8										
S9										
S10										
S11	D									
S12	A	R								R
S13	A	R								R
S14	D									
S15	A	R								R
S16	A	R								R
S17	D									
S18										
S19										
S20										
S21										
S22										
S23	W	T								T
S24										
S25										
S26										
S27										
S28										
H1	A	R								R
V1	V									T
H2										
V2										
G1										
G2										
G3										
G4										
G5										
G6										
G7										
G8										
G9										
G10										
G11										
G12										

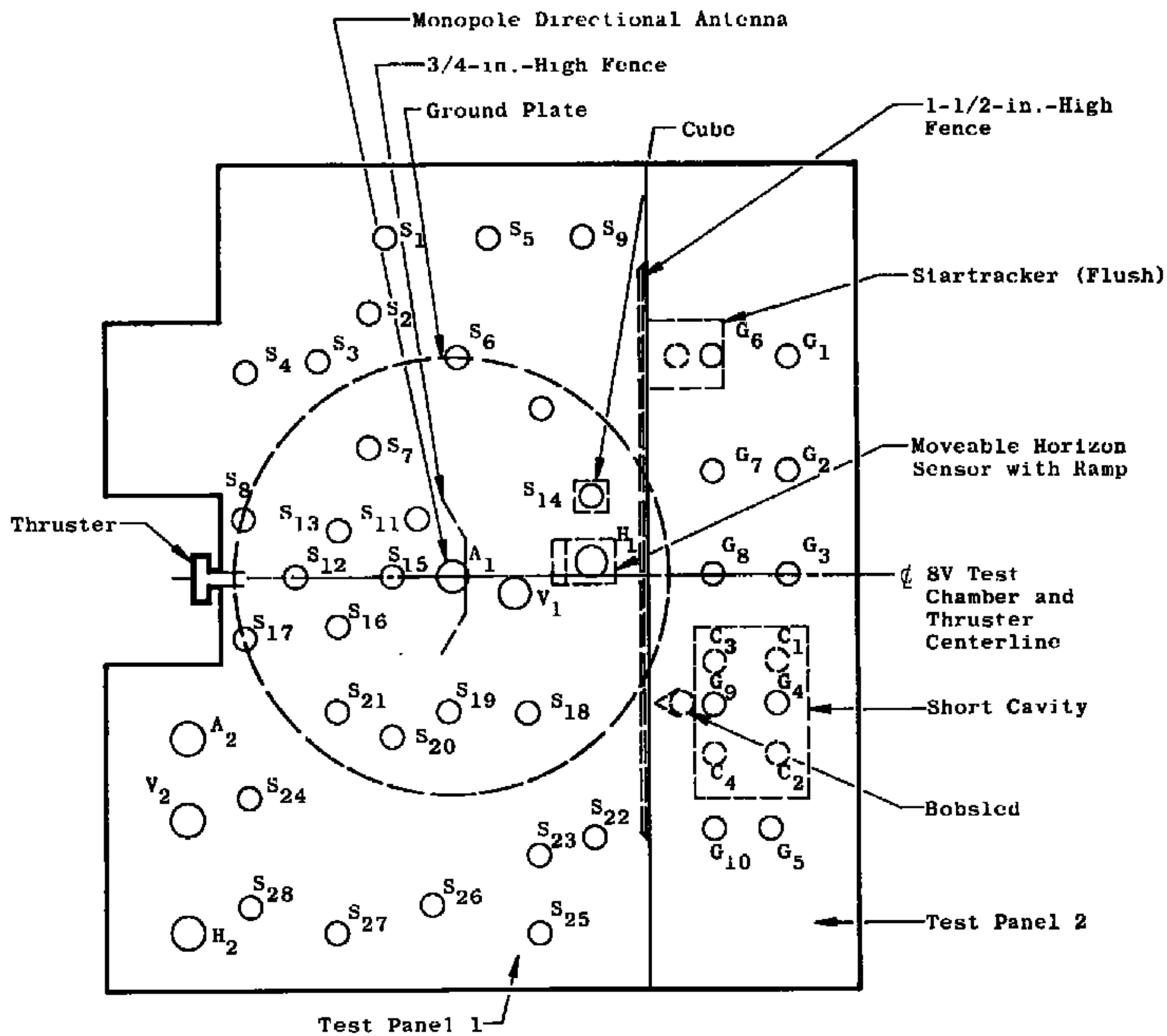

Fig. II-1 Contamination Controls and Antenna with Ground Plate on Test Panels 1 and 2

APPENDIX III
TABLES OF OPTICAL MEASUREMENTS

TABLE I

Primary Test 3

Firing No.	Solar Absorptance, α_s	Emittance, ϵ	α_s/ϵ	Average Visible Reflectance, $\bar{R}$	Specimen Location and Type
0	0.2774	0.9413	0.295	0.7233	S16A
3	0.2187			0.6968	S16A
S.L.	0.2462			0.6346	S16A
0	0.1717	0.3494	0.492	0.8269	S12C
3	0.1868	0.4371	0.427	0.7808	S12C
S.L.	0.2424			0.7689	S12C
0	0.2636	0.2318	1.14	0.7520	S20B
3	0.2892	0.2254	1.27	0.7141	S20B
S.L.	0.2785			0.7260	S20B
0	0.1586			0.8719	S25M
3	0.1956			0.8261	S25M
S.L.	0.1925			0.8170	S25M
0	0.1604			0.8528	S9M
3					S9M
S.L.	0.1798			0.8202	S9M

TABLE II

Primary Test 4B

Firing No.	Solar Absorptance, α_s	Emittance, ϵ	α_s/ϵ	Average Visible Reflectance, $\bar{R}$	Specimen Location and Type
0	0.2238	0.9548	0.234	0.7199	S11A
2	0.2262	0.9629	0.234	0.7015	S11A
0	0.2208	0.9570	0.230	0.7285	S15A
2	0.2639	0.9584	0.275	0.6408	S15A
0	0.2199	0.9454	0.232	0.7304	S16A
2	0.2549	0.9542	0.267	0.6458	S16A
0	0.8413	0.9064	0.928	0.06378	S7K
2	0.8394	0.9153	0.917	0.06525	S7K
0	0.8370	0.8946	0.935	0.06846	S13K
2	0.7902	0.9086	0.869	0.13960	S13K
0	0.2722	0.3513	0.774	0.7350	S19B
2	0.3090	0.2276	1.357	0.6956	S19B
0	0.5263	0.8205	0.641	0.4632	$S10T_1$
2	0.5266	0.8399	0.626	0.4593	$S10T_1$
0	0.1991			0.8108	G3M
0	0.1857			0.8173	G4M
0	0.1864			0.8223	G9M
2					G9M

TABLE II (Concluded)

Primary Test 4B

Firing No.	Relative Solar Transmittance, t_s	Average Visible Relative Transmittance, $\overline{T}$	Specimen Location and Type
0			S23W
2	1.078	1.042	S23W
0			G7W
0			V1
2	0.9042	0.8665	VI

TABLE III

Primary Test 4C

Firing No.	Solar Absorptance, α_s	Emittance, ϵ	α_s/ϵ	Average Visible Reflectance, $\bar{R}$	Specimen Location and Type
0	0.2178	0.9398	0.231	0.7282	S11A
2	0.2146	0.9405	0.228	0.7207	S11A
4	0.2358	0.9214	0.255	0.6907	S11A
7	0.2321	0.9463	0.245	0.6932	S11A
8					S11A
S. L.	0.3042			0.6124	S11A
0	0.2195	0.9401	0.233	0.7247	S15A
2	0.2300	0.9315	0.246	0.7073	S15A
4	0.2780	0.9299	0.298	0.6491	S15A
7	0.2510	0.9234	0.271	0.6829	S15A
8	0.2374	0.9200	0.258	0.7019	S15A
S. L.	0.3202			0.5508	S15A
0	0.1938	0.9261	0.209	0.7517	S16A
2	0.2191	0.9386	0.233	0.7014	S16A
4	0.2258	0.9015	0.250	0.7082	S16A
7	0.2152	0.9034	0.236	0.7245	S16A
S. L.	0.2565			0.6287	S16A
0	0.8467	0.8935	0.947	0.06087	S7K
2	0.8457	0.8991	0.940	0.06255	S7K
4	0.8515	0.8934	0.953	0.05711	S7K
7	0.8408	0.8947	0.939	0.06321	S7K
S. L.	0.8542			0.05531	S7K
0	0.8503	0.8980	0.946	0.05658	S13K
2	0.8053	0.8926	0.902	0.1225	S13K
4	0.8064	0.8923	0.903	0.1282	S13K
7	0.8410	0.8872	0.947	0.08371	S13K
8	0.8395	0.8925	0.940	0.08544	S13K
S. L.	0.8153			0.1128	S13K
0	0.2615	0.2355	1.110	0.7400	S19B
2	0.3693	0.2267	1.629	0.6229	S19B
4	0.3526	0.2469	1.428	0.6490	S19B
7	0.3385	0.2363	1.432	0.6587	S19B
S. L.	0.3303			0.6671	S19B
0	0.5337	0.8152	0.654	0.4502	$S10T_1$
2	0.5318	0.8317	0.639	0.4538	$S10T_1$
7	0.5225	0.8072	0.647	0.4608	$S10T_1$
S. L.	0.5396			0.4373	$S10T_1$

TABLE III Con'd

Primary Test 4C

Firing No.	Solar Absorptance, α_s	Emittance, ϵ	α_s/ϵ	Average Visible Reflectance, $\bar{R}$	Specimen Location and Type
0		0.5736			$S18T_2$
2	0.2695	0.6040	0.476	0.6684'	$S18T_2$
7	0.2453	0.6170	0.397	0.6966	$S18T_2$
8	0.2593	0.6086	0.426	0.6766	$S18T_2$
S.L.	0.2502			0.6853	$S18T_2$
0					G3M
4	0.1631			0.8574	G3M
7	0.2788			0.7177	G3M
S.L.	0.1822			0.8230	G3M
0					G4M
4	0.1703			0.8410	G4M
7	0.1593			0.8595	G4M
S.L.					G4M
0					G9M
4					G9M
7					G9M
8					G9M

TABLE III (Concluded)

Primary Test 4C

Firing No.	Relative Solar Transmittance, t_s	Average Visible Relative Transmittance, $\overline{T}$	Specimen Location and Type
0			V1
2	0.9270	0.8873	V1
4	0.8694	0.8079	V1
7	0.8417	0.7822	V1
8	0.8110	0.7511	V1
S.L.	0.8694	0.860	V1
0			S23W
2	1.024	1.036	S23W
7	0.9943	0.9875	S23W
S.L.	0.9815	0.9780	S23W
0			G7W
4			G7W
7			G7W
S.L.			G7W

TABLE IV

Primary Test 5A

Firing No.	Solar Absorptance, α_S	Emittance, ϵ	α_S/ϵ	Average Visible Reflectance, $\bar{R}$	Specimen Location and Type
0		0.8920			S15J
2	0.2655			0.6581	S15J
0		0.9006			S16J
2	0.2734			0.6943	S16J
0		0.8486			S7K
2	0.8452			0.06505	S7K
0		0.2757			S12C
2	0.1630	0.2542		0.8091	S12C
0					S18B
2	0.3015			0.6906	S18B
0		0.2164			S20B
2	0.2965			0.6989	S20B
0					S10M
2	0.1802			0.8166	S10M
0					G3M
2	0.1794			0.8289	G3M
0					G4M
2					G4M
0					G9M
2					G9M

NOTE: Have tabulated data and curves for all prefire in situ for all above specimen, and they all look good; but for some reason, there are no special values calculated. Also all ϵ data after firing 2 looks bad.

TABLE IV (Concluded)

Primary Test 5A

Firing No.	Relative Solar Transmittance, t_s	Average Visible Relative Transmittance, $\overline{T}$	Specimen Location and Type
0			V1
2	0.9044	0.8669	V1
0			S23W
2	0.9881	0.9824	S23W
0			G7W
2	0.9815	0.9752	G7W

TABLE V

Primary Test 5B

Firing No.	Solar Absorptance, α_s	Average Visible Reflectance, $\bar{R}$	Specimen Location and Type
0	0.2024	0.7961	S15J
2	0.2391	0.7103	S15J
9	0.2818	0.6370	S15J
S.L.	0.5266	0.3263	S15J
0	0.1583	0.7771	S16J
2	0.1907	0.7119	S16J
4	0.2105	0.6700	S16J
7	0.2881	0.5887	S16J
9	0.2500	0.6037	S16J
S.L.	0.2810	0.5696	S16J
0	0.1440	0.8450	S12C
2	0.1659	0.8001	S12C
4	0.1437	0.8286	S12C
7	0.1617	0.8021	S12C
9	0.1434	0.8348	S12C
S.L.	0.1601	0.8126	S12C
0	0.8427	0.05449	S7K
2	0.8391	0.06000	S7K
4	0.7355	0.2113	S7K
7	0.8393	0.05979	S7K
S.L.	0.8448	0.05781	S7K
0	0.2379	0.7683	S18B
2	0.3515	0.6187	S18B
4	0.3402	0.6547	S18B
7	0.3387	0.6487	S18B
9	0.3629	0.6137	S18B
S.L.	0.3339	0.6604	S18B
0	0.2453	0.7479	S20B
2	0.2902	0.6926	S20B
9	0.3346	0.6445	S20B
S.L.	0.2949	0.6861	S20B
0	0.1368	0.8593	S10M
2	0.1468	0.8459	S10M
7	0.1567	0.8263	S10M
S.L.	0.5787	0.3477	S10M

TABLE V (Continued)

Primary Test 5B

Firing No.	Solar Absorptance, α_S	Average Visible Reflectance, $\bar{R}$	Specimen Location and Type
0	0.2787	0.6816	G3M
4	0.1440	0.8594	G3M
9	0.1463	0.8584	G3M
S.L.	0.1747	0.8097	G3M
0	0.1436	0.8501	G4M
4	0.1503	0.8426	G4M
9	0.1407	0.8625	G4M
S.L.	0.1500	0.8486	G4M
0	0.1508	0.8428	G9M
4	0.1426	0.8536	G9M
9	0.1773	0.7992	G9M
S.L.	0.1556	0.8314	G9M

TABLE V (Concluded)

Primary Test 5B

Firing No.	Relative Solar Transmittance, t_s	Average Visible Relative Transmittance, $\overline{T}$	Specimen Location and Type
0			V1
2	0.9682	1.001	V1
4	0.9406	0.9349	V1
7	0.5206	0.4812	V1
9			V1
S.L.	0.9621	1.018	V1
0			S23W
2	1.056	1.044	S23W
7	1.028	1.008	S23W
9	1.011	0.9961	S23W
S.L.	1.001	1.009	S23W
0			G7W
4	1.092	1.132	G7W
9	1.076	1.113	G7W

TABLE VI

Primary Test 13

Firing No.	Solar Absorptance, α_s	Emittance, ϵ	α_s/ϵ	Average Visible Reflectance, $\bar{R}$	Specimen Location and Type
0	0.1218	0.9935	0.122	0.8797	S11A
4		1.027			S11A
8	0.1056	1.007	0.105	0.8829	S11A
S.L.	0.1580			0.7488	S11A
0	0.1447	1.025	0.141	0.8217	S15A
4		1.019			S15A
8	0.2016	1.014	0.198	0.6847	S15A
0	0.1419	0.9919	0.143	0.8392	S16A
4	0.1358	1.021	0.133	0.7321	S16A
8	0.1512	1.008	0.150	0.8307	S16A
0		0.9866			S7K
4	0.7158	0.9965	0.718	0.3153	S7K
8	0.5047	0.9820	0.513	0.5742	S7K
S.L.	0.7116			0.3140	S7K
0	0.2431	0.2162	1.124	0.7668	S12B
4	0.2789	0.2107	1.323	0.7279	S12B
8	0.3123			0.6738	S12B
0		0.2216			S20B
4	0.2446	0.2224	1.099	0.7976	S20B
8		0.2117			S20B

Data on view port window at V-1 invalid.

TABLE VII

Primary Test 14

Firing No.	Solar Absorptance, α_S	Emittance, ϵ	α_S/ϵ	Average Visible Reflectance, $\bar{R}$	Specimen Location and Type
0	0.2349	1.035	0.226	0.6909	S11A
2		1.034			S11A
4		1.053			S11A
9	0.2108	1.037	0.203	0.7064	S11A
S.L.	0.1163			0.7969	S11A
0	0.2129	1.016	0.209	0.7223	S15A
2	0.2616	1.002	0.261	0.6279	S15A
4	0.2665	1.045	0.255	0.5841	S15A
9	0.3105	1.019	0.304	0.5151	S15A
S.L.	0.1851			0.7232	S15A
0	0.2230	0.9981	0.223	0.7074	S16A
2		1.008			S16A
4	0.2653	1.003	0.264	0.6061	S16A
9	0.2593	1.016	0.255	0.5444	S16A
S.L.					S16A
0	0.8249	0.9787	0.842	0.06720	S7K
2	0.7682	0.9685	0.793	0.1851	S7K
4		0.9796			S7K
9	0.8195	0.9873	0.830	0.07784	S7K
S.L.					S7K
0	0.2555	0.9549	0.267	0.7042	$S10T_1$
2	0.2385	0.9582	0.248	0.7239	$S10T_1$
4	0.2626	0.9946	0.264	0.6819	$S10T_1$
9	0.2811	0.9871	0.284	0.6744	$S10T_1$
S.L.					$S10T_1$
0	0.2254	0.3453	0.652	0.7167	$S18T_2$
2		0.3842			$S18T_2$
4	0.1772	0.4246	0.417	0.7508	$S18T_2$
9	0.2145	0.4818	0.445	0.7199	$S18T_2$
S.L.					$S18T_2$
0	0.2162	0.3871	0.558	0.7412	STAR-T_2
2	0.3118	0.3940	0.791	0.6458	STAR-T_2
4	0.1999	0.4171	0.479	0.7682	STAR-T_2
9	0.2008	0.4985	0.402	0.7544	STAR-T_2
S.L.					STAR-T_2

Data on windows located at V-1 and bobsled invalid.

TABLE VIII

Primary Test 15

Firing No.	Solar Absorptance, α_s	Emittance, ϵ	α_s/ϵ	Average Visible Reflectance, $\bar{R}$	Specimen Location and Type
0		1.022			S11A
2		1.010			S11A
4		1.023			S11A
7		1.015			S11A
9		1.014			S11A
0		0.9958			S15A
2		1.001			S15A
4		0.9908			S15A
7		0.9904			S15A
9		0.9797			S15A
0	0.1456	0.9975	0.145	0.7935	S16A
2	0.1961	0.9920	0.197	0.6892	S16A
4		0.9948			S16A
7	0.2419	0.9786	0.247	0.6038	S16A
9	0.2659	0.9821	0.271	0.5610	S16A
S.L.	0.2614			0.5715	S16A
0		0.9200			S7K
2		0.9673			S7K
4		0.9791			S7K
7		0.9778			S7K
9		0.9569			S7K
0	0.8213	0.9565	0.858	0.06956	S13K
2		0.9558			S13K
4	0.8202	0.9552	0.858	0.08679	S13K
7		0.9602			S13K
9	0.8109	0.9552	0.848	0.1082	S13K
S.L.	0.7934			0.1169	S13K
0	0.2508	0.2171	1.155	0.7433	S19B
2	0.2868	0.2153	1.332	0.6867	S19B
4	0.3108	0.2230	1.393	0.6698	S19B
7	0.3428	0.2550	1.344	0.6273	S19B
9	0.3526	0.2620	1.345	0.6102	S19B
S.L.	0.3296			0.6424	S19B

TABLE VIII (Concluded)

Primary Test 15

Firing No.	Relative Solar Transmittance, t_s	Average Visible Relative Transmittance, $\overline{T}$	Specimen Location and Type
0			V1
2	0.9647	0.9443	V1
4	0.9425	0.9158	V1
7	0.9463	0.9295	V1
9	0.9515	0.9061	V1
S. L.	0.9651	0.9771	V1
0			S18W
2	0.9208	0.9798	S18W
4	0.9218	0.9713	S18W
7	0.9020	0.9430	S18W
9	0.9129	0.9400	S18W
S. L.			S18W

TABLE IX

Primary Test 20

Firing No.	Solar Absorptance, α_S	Emittance, ϵ	α_S/ϵ	Average Visible Reflectance, $\bar{R}$	Specimen Location and Type
0	0.2382	0.9703	0.245	0.7001	S11A
2		0.9608			S11A
4	0.3090	0.9712	0.318	0.6150	S11A
7	0.3066	0.9595	0.319	0.5780	S11A
9	0.3856			0.5224	S11A
S. L.	0.2332			0.5985	S11A
0		0.9439			S15A
2	0.2552	0.9707	0.262	0.6341	S15A
4	0.3130	0.9570	0.327	0.6023	S15A
7	0.3803	0.8577	0.443	0.5338	S15A
9	0.3692	0.9292	0.397	0.5356	S15A
S. L.	0.4447			0.4801	S15A
0	0.2250	0.9714	0.231	0.7194	S16A
2	0.3605	0.9527	0.378	0.5967	S16A
4	0.2938	0.9589	0.306	0.5876	S16A
7	0.2830	0.9677	0.292	0.5861	S16A
9	0.2720			0.5759	S16A
S. L.	0.3190			0.5400	S16A
0A	0.1990	0.9535	0.208	0.7265	S19A
0B		0.9506			S19A
0C	0.1919	0.9553	0.200	0.7388	S19A
0	0.2283	0.9652	0.236	0.7019	S19A
2	0.1843	0.9506	0.193	0.6674	S19A
4	0.2473	0.9547	0.259	0.6945	S19A
7		0.9672			S19A
9	0.2872	0.9599	0.299	0.6492	S19A
S. L.	0.3748			0.5908	S19A
0	0.8294	0.9583	0.865	0.07374	S7K
2	0.8317	0.9557	0.870	0.07358	S7K
4	0.8205	0.9604	0.854	0.09788	S7K
7		0.9530			S7K
9	0.8280	0.9552	0.866	0.08204	S7K
S. L.	0.7425			0.2089	S7K
0	0.1716			0.8088	STAR-M
2	0.2620			0.6528	STAR-M
4	0.2150			0.8339	STAR-M
7					STAR-M
9	0.2062			0.7969	STAR-M
S. L.	0.1602			0.8280	STAR-M

TABLE IX (Concluded)

Primary Test 20

Firing No.	Relative Solar Transmittance, t_s	Average Visible Relative Transmittance, $\overline{T}$	Specimen Location and Type
0A			S23W
0B			S23W
0C			S23W
2	0.9811	0.9720	S23W
4			S23W
7			S23W
9	0.8929	0.8890	S23W
S.L.	0.9715	0.9506	S23W
0			BOB-W
2	1.0065	1.039	BOB-W
4			BOB-W
7			BOB-W
9			BOB-W
S.L.			BOB-W

TABLE X

Primary Test 21

Firing No.	Solar Absorptance, α_s	Emittance, ϵ	α_s/ϵ	Average Visible Reflectance, $\bar{R}$	Specimen Location and Type
0	0.1942	0.9669	0.200	0.7391	S11A
2		0.9725			S11A
4	0.2284	0.9678	0.235	0.6481	S11A
7	0.2769			0.5563	S11A
9	0.3252	0.9565	0.339	0.4874	S11A
S.L.	0.3250			0.5514	S11A
0					S15A
2	0.3593	0.7970	0.450	0.4940	S15A
4	0.2779	0.9644	0.288	0.5619	S15A
7		0.9407			S15A
9		0.8920			S15A
S.L.					S15A
0	0.1974	0.9607	0.205	0.7312	S16A
2		0.9584			S16A
4	0.4201	0.9616	0.436	0.4125	S16A
7	0.3137	0.9584	0.327	0.5167	S16A
9	0.3415	0.9526	0.358	0.4635	S16A
S.L.	0.3292			0.4987	S16A
0	0.1992	0.9644	0.206	0.7290	S19A
2	0.2145	1.069	0.200	0.6971	S19A
4		0.9685			S19A
7		0.9686			S19A
9	0.2596	0.9576	0.271	0.6358	S19A
S.L.					S19A
0	0.8267	0.9547	0.865	0.07672	S7K
2	0.8218	0.9603	0.855	0.08027	S7K
4	0.8247	0.9639	0.855	0.07757	S7K
7		0.9491			S7K
9	0.7735	0.9502	0.814	0.1618	S7K
S.L.	0.8144			0.1065	S7K

TABLE X (Concluded)

Primary Test 21

Firing No.	Relative Solar Transmittance, t_s	Average Visible Relative Transmittance, $\overline{T}$	Specimen Location and Type
0			S23W
2	0.9515	0.9493	S23W
4			S23W
7			S23W
9			S23W
S. L.			S23W

TABLE XI

Primary Test 22

Firing No.	Solar Absorptance, α_s	Emittance, ϵ	α_s/ϵ	Average Visible Reflectance, $\bar{R}$	Specimen Location and Type
0		0.9572			S11A
2		0.9647			S11A
4		0.9442			S11A
7		0.9456			S11A
9		0.9470			S11A
0	0.1875	0.9216	0.203	0.7557	S15A
2	0.2501	0.8802	0.284	0.6575	S15A
4	0.2547	0.8927	0.285	0.6287	S15A
7	0.2771	0.9236	0.300	0.5882	S15A
9	0.3202	0.9516	0.336	0.5900	S15A
S.L.					S15A
0	0.1631	0.9537	0.171	0.7840	S16A
2	0.1900	0.9533	0.199	0.7198	S16A
4	0.2446	0.9554	0.256	0.6307	S16A
7	0.2615	0.9469	0.276	0.6017	S16A
9	0.2686	0.9558	0.281	0.5907	S16A
S.L.					S16A
0		0.9474			S19A
2	0.1761	0.9340	0.188	0.7760	S19A
4	0.1981	0.9452	0.209	0.7267	S19A
7	0.2064	0.9550	0.216	0.7063	S19A
9	0.2146	0.9442	0.227	0.6825	S19A
S.L.					S19A
0		0.9335			S7K
2		0.9456			S7K
4		0.9416			S7K
7		0.9450			S7K
9					S7K

TABLE XI (Concluded)

Primary Test 22

Firing No.	Relative Solar Transmittance, t_s	Average Visible Relative Transmittance, $\overline{T}$	Specimen Location and Type
0			V1
2	0.8536	0.7681	V1
4	0.8281	0.7391	V1
7	0.8438	0.7488	V1
9	0.8262	0.7195	V1
S. L.			V1
0			S23W
2	0.8714	0.7956	S23W
4	0.8608	0.7803	S23W
7	0.8730	0.7894	S23W
9	0.8147	0.7393	S23W
S. L.			S23W

UNCLASSIFIED
Security Classification

DOCUMENT CONTROL DATA - R & D

(Security classification of title, body of abstract and indexing annotation must be entered when the overall report is classified)

1. ORIGINATING ACTIVITY (Corporate author) Arnold Engineering Development Center ARO, Inc., Operating Contractor Arnold Air Force Station, Tennessee	2a. REPORT SECURITY CLASSIFICATION UNCLASSIFIED 2b. GROUP N/A

3. REPORT TITLE

EFFECTS AND CONTROL OF CONTAMINATION FROM A SCALED MOL TRANSLATIONAL THRUSTER IN A LONGITUDINAL ORIENTATION

4. DESCRIPTIVE NOTES (Type of report and inclusive dates)

May through December 21, 1968 - Final Report

5. AUTHOR(S) (First name, middle initial, last name)

David W. Hill, Jr. and Dale K. Smith, ARO, Inc.

6. REPORT DATE October 1969	7a. TOTAL NO. OF PAGES 181	7b. NO. OF REFS 12
8a. CONTRACT OR GRANT NO. F40600-69-C-0001 b. Program Element 35121F c. Program Area 632A d.	9a. ORIGINATOR'S REPORT NUMBER(S) AEDC-TR-69-152 9b. OTHER REPORT NO(S) (Any other numbers that may be assigned this report) N/A	

10. DISTRIBUTION STATEMENT This document may be further distributed by any holder only with specific prior approval of MOL Project Office (SAFSL-3), AF Unit Post Office, Los Angeles, California 90045.

11. SUPPLEMENTARY NOTES Available in DDC	12. SPONSORING MILITARY ACTIVITY MOL Project Office (SAFSL-3) AF Unit Post Office Los Angeles, California 90045

13. ABSTRACT A test was conducted to determine the effects and control of contamination produced by a 1-lb scaled Manned Orbital Laboratory thruster. The test required firing the 1-lb translational thruster for 205 sec continuously and pulsing in its longitudinal position and determining the effects of contaminates from the thruster impinging on optical and thermal control surface test specimens located on a flat plate exposed to the thruster exhaust plume. The contamination ejected from the thruster in steady-state operation was much less than that of pulse-mode operation. Fences were used on the test plate to shield specimens from the thruster exhaust plume. In situ reflectance, emittance, and transmittance measurements were made on the optical and thermal control surface test specimens surfaces under vacuum conditions and at atmospheric pressure. Pretest and posttest laboratory measurements were made at atmospheric conditions. Contamination deposited on the plate was focused along and near the axis of the thruster. Contamination was ejected from the thruster at the startup of the engine in the steady-state operation. A 1.5-in.-high by 24-in.-long fence shielded specimens on the panel satisfactorily as opposed to a 0.75-in.-high fence. The in situ reflectance and transmittance measurements on the specimens at the simulated altitude were more realistic of the contamination encountered by the specimens from the thruster exhaust than the atmospherical posttest laboratory measurements.

This document may be further distributed by any holder only with specific prior approval of MOL Project Office Office (SAFSL-3), AF Unit Post Office, Los Angeles, California 90045.

DD FORM 1 NOV 65 1473

UNCLASSIFIED
Security Classification

14. KEY WORDS	LINK A		LINK B		LINK C	
	ROLE	WT	ROLE	WT	ROLE	WT
Manned Orbital Laboratory						
thrusters						
contamination						
control						
steady state						
pulse spacing modulation						
reflectance						
emittance						
transmittance						

AFSC
Arnold AFS Tenn